Mapping the Structure of the Oxytocinergic System in the Prairie Vole Brain: Implications for Modes of Neuropeptide Release and Modulation of Social Behaviors

Erin Nicole Ramos

M.A. University of Virginia, 2022
B.A., University of Wisconsin-Madison, 2018

A Dissertation Presented to the Faculty of the University of Virginia in Candidacy for the Degree of Doctor of Philosophy

Department of Psychology
University of Virginia
August, 2024

Alev Erisir, M.D., Ph.D.
Jessica J. Connelly, Ph.D.
Wendy J. Lynch, Ph.D.
Ali D. Guler, Ph.D.
Allison M. Perkeybile, Ph.D.

ABSTRACT

Interactions with others are a fundamental aspect of mammalian life. While multiple biological processes underpin normal mammalian behaviors, oxytocin is a well-studied neuropeptide hormone notable for its role in modulating neural pathways and influencing behavior. Acting within both the viscera and central nervous system, oxytocin regulates a variety of physiological and behavioral functions. Centrally, the oxytocinergic system modulates social behaviors such as bonding, aggression, and complex cognitive functions like empathy. Prairie voles (*Microtus ochrogaster*), known for their unique social behaviors resembling those of humans, provide an excellent model for studying these processes due to their biparental and socially monogamous nature, which is heavily influenced by the oxytocinergic system.

This dissertation investigates the neuroanatomical circuitry of the prairie vole, focusing on three specific oxytocin systems. In Chapter 1, I review oxytocin's roles as a hormone in the viscera, a neuropeptide in central regions containing oxytocin axons, and a paracrine molecule in regions with oxytocin dendrites. I discuss how these systems may independently regulate specific behaviors through subcortical circuitry or cortical signaling. I also address a critical question in the field: how does oxytocin exert its effects in the cerebral cortex despite the apparent scarcity of oxytocin axons in this region?

Chapter 2 details the design and development of The Histochemical Brain Atlas of the Prairie Vole. Previous research on prairie voles has relied on brain atlases of other rodents, such as mice and rats. To address this gap, we created a comprehensive histochemical atlas specific to the prairie vole brain, providing a valuable resource for future studies and supporting the aims of Chapter 3.

In Chapter 3, I explore the oxytocinergic system in the prairie vole brain. Using immunohistochemistry, RNAScope in-situ hybridization, and advanced microscopy techniques (electron, confocal, and light-sheet), I map the distribution of oxytocin cells and axons across the whole brain and correlate these with the expression of oxytocin receptor transcripts. My findings reveal a lack of correlation between oxytocin axons and *Oxtr* expression, particularly in the cerebral cortex, where few oxytocin axons coincide with numerous *Oxtr*-expressing cells. Electron microscopy studies indicate that dendrites of the paraventricular nucleus extend into the third ventricle, releasing oxytocin directly into the cerebrospinal fluid (CSF). This suggests that oxytocin in the CSF travels to the cerebral cortex to bind to oxytocin receptors.

This dissertation elucidates the intricate roles of oxytocin within the prairie vole brain, highlighting the diverse mechanisms by which oxytocin influences social behaviors through its action in different neuroanatomical regions. The development of the prairie vole brain atlas provides a critical tool for future research, facilitating more precise investigations into the neurochemical bases of behavior. The discovery of oxytocin's diffusion into the cerebrospinal fluid and its subsequent action in the cerebral cortex offers novel insights into oxytocinergic modulation of higher-order cognitive functions.

For my nana, Nancy Sandstrom, one of the strongest women I know who has always believed in me and my potential.

Acknowledgments

This dissertation would not have been possible without the immense support and assistance I have received throughout each project. I am profoundly grateful for the exceptional mentorship at UVA. First and foremost, I extend my deepest gratitude to Alev Erisir, whose guidance and encouragement have consistently driven me to grow as a scientist. I also wish to thank Jessica Connelly and Allison Perkeybile for their invaluable help and advice on the genetic, epigenetic, and prairie vole behavioral aspects of my research. Additionally, I am thankful to my additional committee members, Wendy Lynch and Ali Guler, for their insightful questions and constructive feedback on my results.

I am deeply appreciative of my parents, Kimberly Kastar and Jay Kastar, who have always supported me and my pursuits. Finally, my heartfelt thanks go to my wife, Estefhania Ramos. Her unwavering love and support have been my cornerstone throughout this journey. She has been my rock and best friend, ensuring that even in the most stressful times, I found moments of joy and laughter.

Table of Contents

CHAPTER 1

A Review of Oxytocin's Role on Mammalian Behavior, and the Evidence for Three Distinct Oxytocinergic Systems

I. Introduction

Oxytocin (OXT) is a nonapeptide that is highly conserved across mammalian species and plays a role in various complex functions, from stimulating birth to regulating social bonding (Leng et al. 2005; Quintana et al. 2019; Brown et al. 2020; Carter et al. 2020). Since its discovery as a molecule that can cause uterine contractions by Henry H. Dale in 1906 and the identification of its synthesis by Vincent du Vigneaud in 1953, OXT has been extensively studied for its actions as a hormone on the viscera, specifically, during labor (Dale 1906; Vigneaud et al. 1953). However, more recent studies have focused on oxytocin's actions in the central nervous system (CNS) (Hurlemann and Grinevich 2018; Quintana et al. 2019; Brown et al. 2020; Carter et al. 2020; Menon and Neumann 2023) and revealed a large list of behaviors oxytocin may be involved in. Vast and complex are oxytocin's role in the body and the brain, and dysfunctions of the oxytocinergic system have been linked to many disorders in humans such as autism, schizophrenia, anxiety, and post-partum depression (Hurlemann and Grinevich 2018; Carter et al. 2020). In this chapter, I review the literature regarding oxytocin and propose three distinct roles oxytocin may have in the nervous and visceral systems, each associated with a different mode of oxytocin release: 1) The peripheral/visceral functions associated with humoral release of oxytocin, 2) modulation of reward-related behaviors such as bonding, via oxytocin's release from the axons in subcortical brain regions and 3) regulation of social behaviors such as aggression via parenchymal oxytocin in the cortical regions.

II. Oxytocin as a peptide hormone vs. a neurohormone – utilization in the visceral vs. central nervous system

Oxytocin can act as a typical hormone, traveling long distances in the blood to reach targets containing its receptor (OXTR) (Brownstein et al. 1980; Fuchs et al. 1984a; Caldwell et al. 2017). Oxytocin also acts as a neuropeptide, which can be directly released from axons in distinct brain regions (Knobloch and Grinevich 2014; Marlin et al. 2015; Carcea et al. 2021). Interestingly, a third mechanism for its function has been demonstrated: it can be released from the soma or the dendrites of the oxytocin-producing cells into the extracellular space presumably playing a paracrine function. This paracrine function was suggested through volume transmission, mediating a signaling mechanism among neighboring cells, potentially synchronizing their firing or other metabolic processes (Ludwig and Leng 2006; Chini et al. 2017). Since oxytocin is synthesized through one primary pathway and interacts with one specific receptor, I will begin this section by discussing its synthesis and receptor. I will also summarize the neuroanatomy of the oxytocinergic systems and outline the specific modes of release associated with its actions as a hormone, as a neuropeptide, and as a paracrine factor.

a. Where and how is oxytocin *synthesized*?

Induction of Oxytocin Synthesis: The synthesis of oxytocin is induced by several intracellular mechanisms that involve hormonal, peptidergic, and steroidal systems regulating parturition and lactation. A major factor is estrogen, through binding to estrogen-responsive elements in the promoter region of the OXT gene (Richard and Zingg 1990). Activation of estrogen receptors (Estrogen Receptor β, ERβ) in OXT+ hypothalamic cells is crucial for stimulating the synthesis and enhancing the gene expression of OXT, highlighting the importance of the interaction between these hormonal systems for the proper production and functioning of oxytocin **(Fig 1a)** (Patisaul and Scordalakes 2003; Nishimura et al. 2022). Estrogen enters the plasma membrane to bind to ERβ, forming a complex translocated into the nucleus (**Fig 1a**) (Fuentes and Silveyra 2019). This translocation directly induces transcriptional changes to estrogen-responsive genes via estrogen-responsive elements in the promoter region of a gene, such as the promoter of the OXT gene (Richard and Zingg 1990; Fuentes and Silveyra 2019). Other hormonal systems also likely induce OXT production, but these have not yet been studied in depth (Burbach et al., 2006).

Oxytocin synthesis: Peptides are synthesized in fundamentally different ways than small molecule neurotransmitters in neurons. The synthesis of neurotransmitters occurs within presynaptic terminals that contain the specific precursors and enzymes (Masson et al. 1999). The neurotransmitters are then taken into small vesicles and released at the synaptic active zone into the synaptic cleft as a result of action potential arrival to the axonal terminal (Patri 2019; Masson et al.). In contrast, propeptides and peptides are synthesized in the cell body and the Golgi apparatus, and then transported to neuronal processes. The oxytocin gene is transcribed within the nucleus into mRNA and then translocated out of the nucleus (Richard and Zingg 1990; Westover et al. 2004). At the rough endoplasmic reticulum (RER), ribosomes translate the signal sequence and begin the process of translation to form the peptide chain (**Fig 1b**) (Davidovich et al. 2009). The preprohormone of oxytocin consists of the signal peptide, the neuropeptide (i.e. OXT) on the N-terminus, and neurophysin I (Brownstein 1983; Lee et al. 2009). As a result, the prepropeptide is bigger than the final nine-amino acid peptide oxytocin (Lee et al. 2009). Within the RER of the cell body, the preprohormone is cleaved, removing the signal peptide, and trafficked to the Golgi apparatus as the propeptide containing OXT and neurophysin I (**Fig 1b**) (Brownstein 1983). In the Golgi apparatus, the entire propeptide is packaged into large dense-core vesicles (DCVs) and transported down the axon via microtubule tracks or to the dendrites (**Fig 1c**) (Chini et al. 2017; Jurek and Neumann 2018). Axonal transport is typically stimulated through the activation of protein kinase A, which will increase the association of kinesin-2 and ANXA1 and move OXT from the cell body to the distal portions of the axon (Makani et al. 2013). While activation of protein kinase C interferes with the association of these two motor proteins, resulting in increased dendritic OXT accumulation (Makani et al. 2013). The propeptide is further cleaved in large DCVs, yielding the peptide OXT and neurophysin I (Gainer et al. 1977).

Oxytocin-producing neurons: The primary OXT-producing cell bodies in the mouse and rat brain reside in the paraventricular hypothalamus (PVH) and the supraoptic nucleus (SON), as well as other accessory nuclei of the hypothalamus and bed nucleus of the stria terminalis (BNST) (Zhang et al. 2021a; Li et al. 2024, Rhodes et al 1981). The

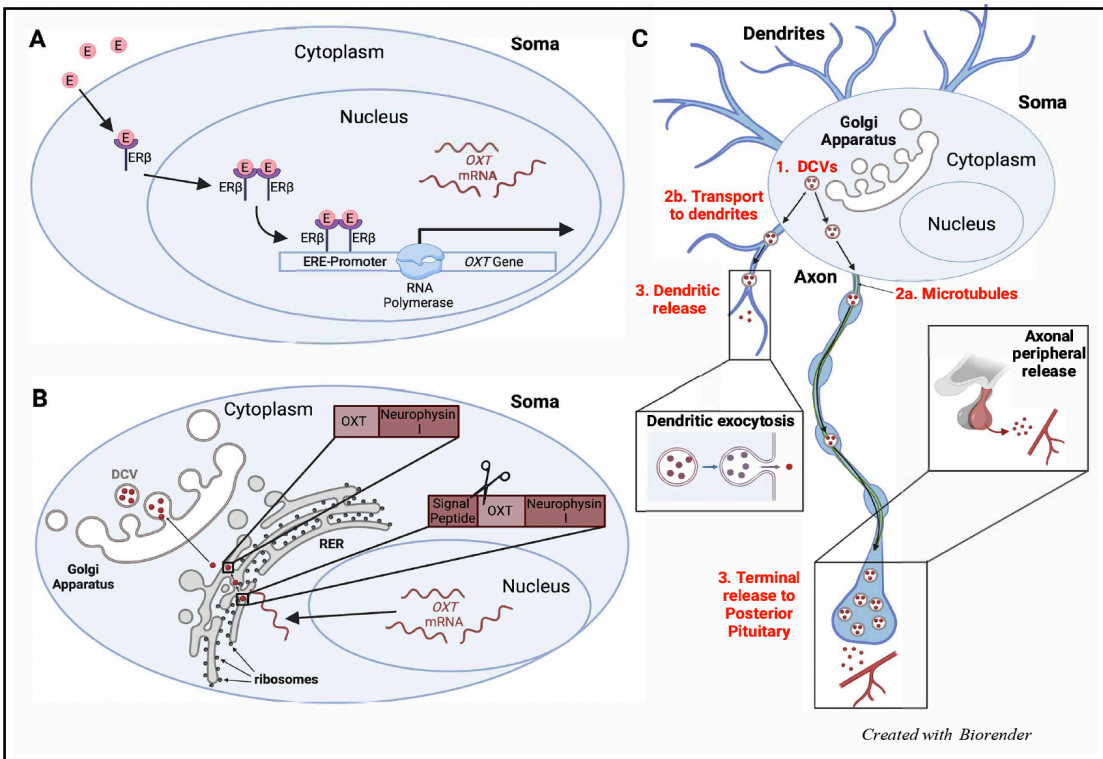

Figure 1: Graphical depiction of the stimulation, synthesis, and transport of OXT in an OXT cell. **A**) Estrogen (pink E) binding to its receptor, Estrogen Receptor β (purple ERβ receptor), dimerizing, and translocating into the nucleus and binds to estrogen-responsive elements (ERE's) in the promoter region of the *OXT* gene. This binding induces transcriptional changes, causing RNA polymerase to transcribe the DNA into mRNA, increasing *OXT* mRNA (red transcripts) in the cell. **B**) Following transcription, the *OXT* mRNA is translocated out of the nucleus and travels to the rough endoplasmic reticulum (RER) (gray) that contains ribosomes (dark gray on the RER). The ribosomes translate the mRNA into the prepropeptide of OXT (red circles). The prepropeptide contains the signal peptide, OXT, and neurophysin I, and within the RER the signal peptide is cleaved. The propeptide, containing OXT and neurophysin I, travels to the Golgi apparatus where it is packaged into dense core vesicles (DCVs) (white circles containing OXT). **C**) Once OXT is packaged into DCVs (1) it travels to either the axon (2a) or dendrite (2b). 2a. DCVs are transported through the axon via microtubules (green), and cluster in varicosities (swellings along the axon), eventually, they are released at the axon terminal in the posterior pituitary to travel in the periphery (3). 2b. DCVs travel to the dendrites and are released via dendritic exocytosis to act locally (3).

oxytocinergic cells in the PVH are classified as either magnocellular or parvocellular based on several cellular characteristics including size, location within the PVH, electrophysiological activity, and projection targets (Swanson and Sawchenko 1983; Althammer and Grinevich 2018; Grinevich and Ludwig 2021). Magnocellular cells are large, 20-30 mm in diameter, while parvocellular cells display smaller soma diameter, 10-20 um (Brown et al. 2013; Althammer and Grinevich 2018, Rhodes et al 1981). Magnocellular cells of the PVH viewed in a coronal section are typically more lateral, while the parvocellular are primarily medial (Swanson and Sawchenko 1983; Roy et al. 2018) (Swanson and Sawchenko 1983; Roy et al. 2018). However, this clear division is not seen in all rodent models, including in prairie voles, which do not display a clear distinction between the magnocellular and parvocellular cell populations (**Fig 2a-d**)

(Kelly et al. 2018; Kenkel et al. 2021). Further, all SON OXT cells are magnocellular and display the same characteristics as PVH magnocellular cells (Swanson and Sawchenko 1983; Brown et al. 2013).

Inputs to oxytocin-producing neurons: Inputs to oxytocin-producing neurons are varied. The strongest input to both the magnocellular and parvocellular OXT cells comes from regions of the hypothalamus (Tang et al. 2020). Other regions across the brain such as the prelimbic cortex, Acb, amygdala, and the periaqueductal gray also project to the OXT cells of the PVH (Tang et al. 2020). Excitatory input from these regions can depolarize the cell and lead to an action potential.

Intrinsic properties of oxytocin-producing neurons: Magnocellular and parvocellular cells display distinct differences in their electrophysiological activity (Brown et al. 2013; Althammer et al. 2021, Luther and Tasker 2000). The magnocellular OXT cells display transient outward rectification, increasing the membrane potential of the cell, and the A-type potassium current, a voltage-gated calcium-independent potassium current (Luther & Tasker, 2000). A-type potassium currents display rapid activation during an action potential (AP) and rapid inactivation following the AP. Further, activity patterns can change under specific conditions such as parturition and lactation, some magnocellular OXT cells before parturition may be silent or continuously firing, but following parturition these cells exhibit synchronized high-frequency bursting patterns of activity, inducing the release of OXT (Summerlee 1981; Stern and Armstrong 1998; Wang and Hatton 2004; Rossoni et al. 2008; Brown et al. 2013). On the other hand, parvocellular OXT cells lack transient outward rectification and express T-type calcium current, these are low-voltage gated calcium channels that require smaller membrane depolarizations for opening (Iftinca and Zamponi 2009; Althammer and Grinevich 2018; Althammer et al. 2021; Chen et al. 2022). While the magnocellular cells of the PVH and SON project axons via the median eminence to the posterior pituitary (Brown et al. 2013; Althammer and Grinevich 2018; Zhang et al. 2021a; Li et al. 2024), the parvocellular cells of the PVH project to magnocellular OXT neurons of the SON, brainstem regions, and the spinal cord (Eliava et al. 2016; Grinevich and Dobolyi 2022). However, which cells are projecting to the forebrain regions remains a topic of debate.

Outputs of oxytocin-producing cells: To examine where the OXT axons in the forebrain originate from, Zhang and colleagues injected the retrogradely transported adeno-associated virus (AAV) coupled to an enhanced green fluorescent protein (EGFP) in the posterior pituitary of the rat (Zhang et al. 2021a). They demonstrated that the magnocellular cells of the hypothalamus, primarily in the PVH and SON but in many accessory nuclei as well, project to the posterior pituitary (PPi), as expected. Interestingly, using an *Oxt-Cre* rat line in conjunction with these AAV injections, they also found that the axons of these magnocellular cells (primarily PVH cells) that project to the PPi gave off many collaterals and projected to far-reaching forebrain regions such as the nucleus accumbens (Acb), lateral septum (LS), and caudate putamen (CPu) (**Fig 3A**) (Zhang et al. 2021a). This would suggest that the OXT+ axons found throughout the forebrain regions are collaterals of the axons projecting to the PPi. As a result, the activity at the cell body can lead to OXT release both humorally and centrally, thus, these two pathways are not independent. The researchers found that using Designer Receptors Activated Only by Designer Drugs (DREADDs) to stimulate OXT neurons did, indeed, increase OXT in the periphery and modulate the social behaviors of male rats. Animals

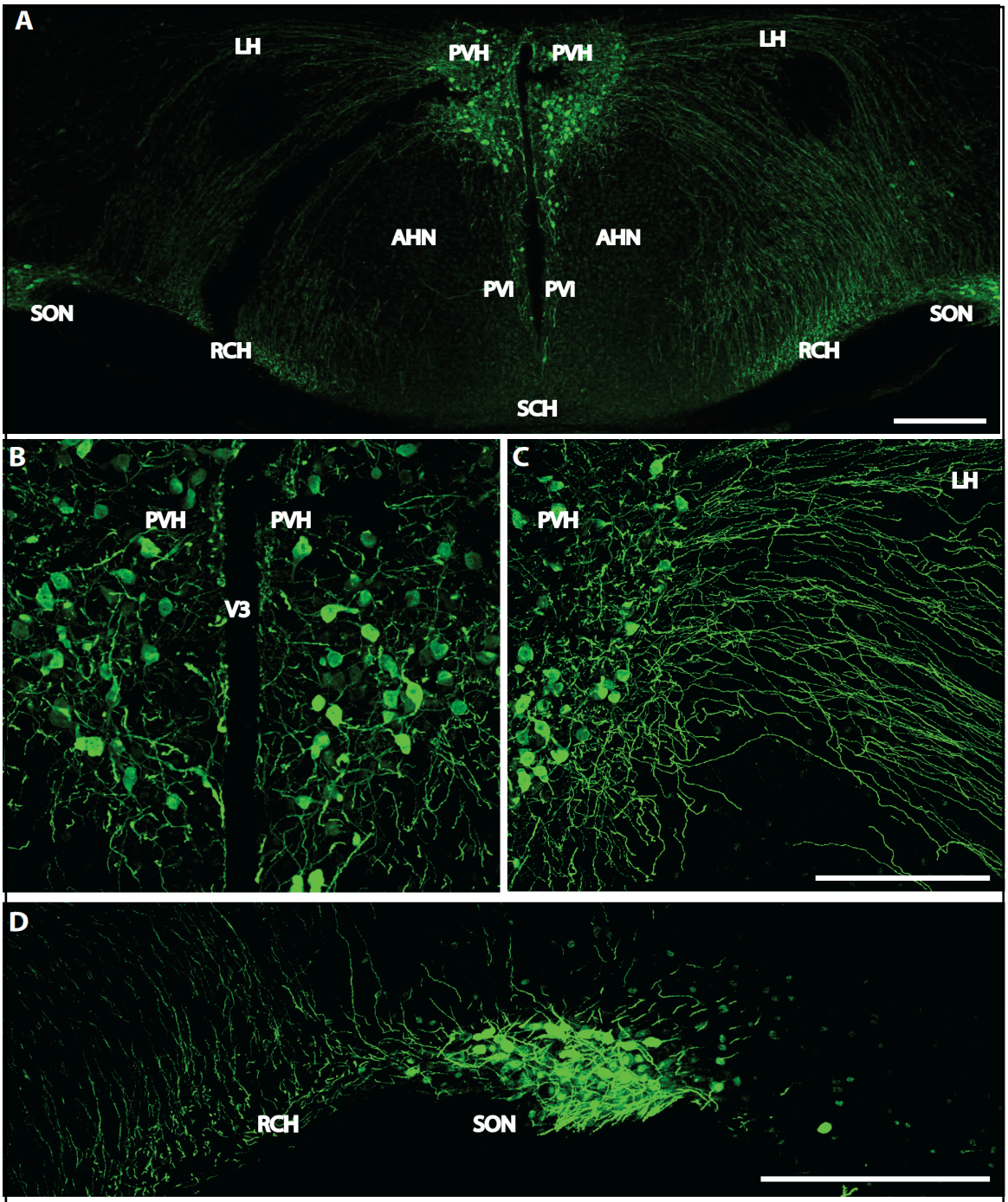

Figure 2: Immunohistochemical staining of oxytocin in the hypothalamus of the prairie vole. **A**) A low magnification image of a coronal section of the hypothalamus illustrating two primary OXT expressing regions, the PVH and SON, and the axonal projections to the ventral portion of the brain, scale bar = 300 µm. **B**) A higher magnification view of the same section in A, illustrating PVH cells and dendrites extending towards the third ventricle (V3). **C**) Higher magnification view of the same section in A, displaying axons projecting from the PVH towards the lateral hypothalamus (LH), scale bar for B & C = 150 µm. **D**) 10x objective magnification of the SON in section A, scale bar = 500 µm.

with increased activation of these magnocellular OXT cells spent more time socially investigating a juvenile male rat, suggesting OXT is modulating a social behavior (investigation) through specific circuitries in the brain via OXT release from the axons. Further, the observation that OXT+ axons in forebrain structures are collaterals from PPi projections has been seen in other studies of rats and prairie voles (Ross et al. 2009; Knobloch et al. 2012). In contrast to this recent finding, a study done in the mouse found that the axons projecting to major forebrain regions originate from cells other than the magnocellular cells projecting to the PPi (Li et al. 2024). In this study, using a Cre-dependent recombinant AAV that expresses yellow fluorescent protein for energy transfer (YPet) in an *Oxt-Ires-Cre* mouse line, researchers found first that 90% of the labeling was co-localized, indicating sufficient specificity of the created rAAV (Li et al. 2024). Researchers then traced the projections of 264 neurons individually and revealed 2 clusters: Cluster 1 (C1) contained neurons that terminated in the ME and Cluster 2 (C2) comprised neurons that terminated in the forebrain, midbrain, pons, cerebellum, and medulla but had no termination sites in the ME (Li et al. 2024). Further, a previous study using fluorescent-activated cell sorting (FACS), uncovered 181 differentially expressed genes between magnocellular and parvocellular cell types (Lewis et al. 2020). Li et al., injected Fluorogold intraperitoneally to label the C1 cell type, and cholera toxin B (CTB) to label the C2 cell type, and then examined 9 of the differentially expressed genes that were determined by Lewis et al. 2020, using *in situ* hybridization. They found that these two clusters are primarily independent populations comprising the magnocellular and parvocellular cell types, respectively. Li et al. 2024, suggest that the C1 cluster comprises the magnocellular OXT cells the C2 cluster comprises the parvocellular population, and the C2 cluster is the primary cell type projecting to the forebrain (**Fig 3A**). This study directly opposes the previously mentioned rat study and would indicate that the peripheral release of OXT is independent of central release. That is, activity-dependent release of OXT into the periphery would not inherently stimulate release within the central nervous system from axons in forebrain regions. The differences observed from these two studies may be a species-specific difference, or both studies may be correct. Some axon collaterals from magnocellular PPi-projecting cells may extend to distant forebrain regions, while parvocellular cells may also project to these regions. Methodological differences could explain why each study might miss one of the populations. Although many studies support coordinated peripheral and central release (Landgraf et al. 1988; Ross et al. 2009; Zhang et al. 2021a), others do not (Amico et al. 1990; Li et al. 2024), and some only find a link after intranasal administration or stress (Valstad et al. 2017; Quintana et al. 2021).

b. Where is OXT released?

The most robust release of oxytocin occurs at the posterior pituitary. It is important to note, that unlike neurotransmitters which may be released following a single action potential, oxytocin is released following spike train stimulation (Neumann et al. 1988). Once sufficiently stimulated, the oxytocinergic cells generate brief spike trains of action potentials (Armstrong et al. 1994), leading to oxytocin release from axons in the PPi from dense core vesicles (Grinevich and Ludwig 2021). Particularly, the axons that arrive at the median eminence release oxytocin onto fenestrated capillaries, and thus into

the blood, which carries the hormone to viscera (**Fig3A**) (Zhang et al. 2021a; Grinevich and Ludwig 2021). The oxytocin in the plasma acts on OXTR in organs including the uterus, mammary glands, the heart, and the kidney (Jankowski et al. 1998, 2020; Loichot et al. 2001; Carter et al. 2020). There is some evidence for local oxytocin synthesis in viscera as well, but the bulk of OXT within the periphery is derived from the hypothalamus and secreted through the hypothalamo-neurohypophysial system (Einspanier and Ivell 1997; Jankowski et al. 1998; Carter et al. 2020).

Oxytocin is also released within forebrain regions that contain OXT+ axons, Again, sufficient stimulation is required for OXT release from the axons. Additionally, OXT is not the only molecule present in OXT+ axons. The vesicular glutamate transporter 2 (VgluT2) is co-expressed and glutamate is often co-released with OXT (Knobloch et al. 2012; Hasan et al. 2019; Grinevich and Ludwig 2021). These axons display primarily asymmetric synapses, which is a characteristic morphological feature of

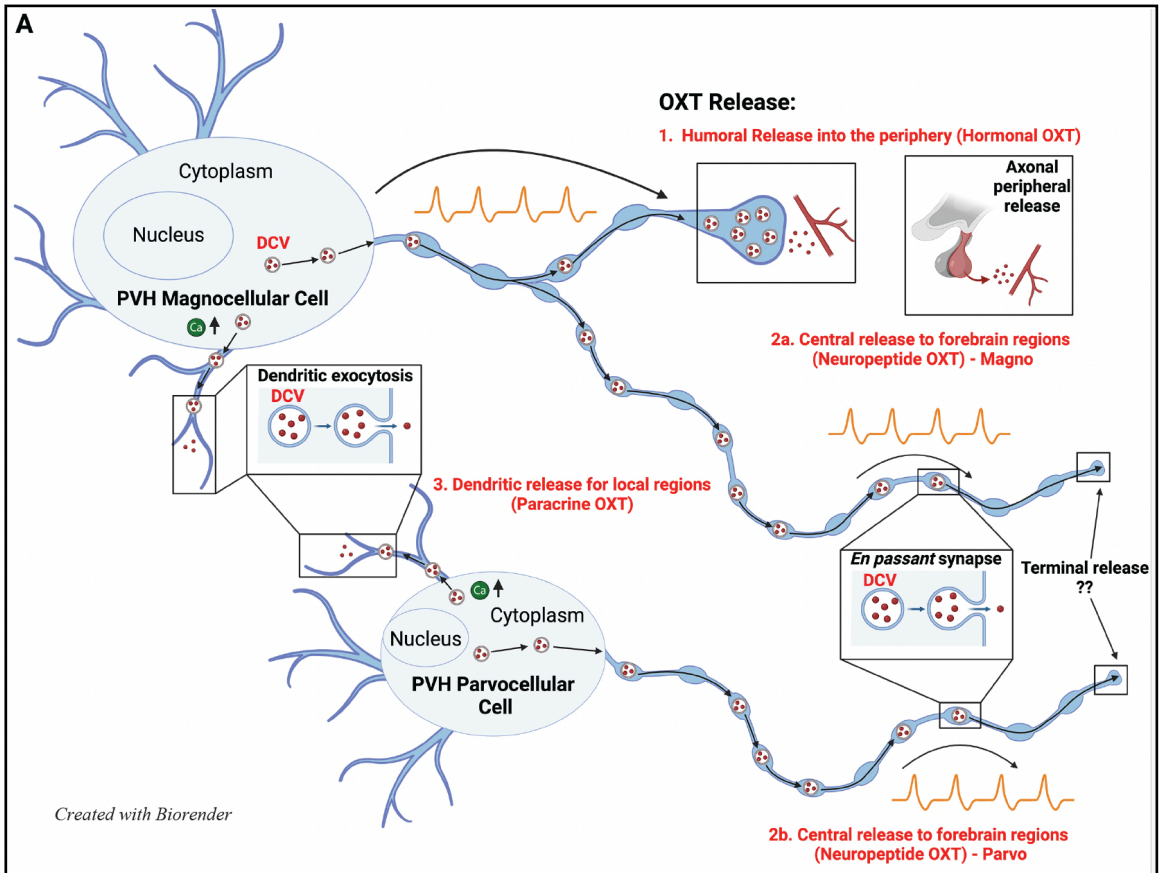

Figure 3: A graphical depiction of the three modes of oxytocin (red circles) release. **1**) The first pathway is the humoral release from the magnocellular cells that project to the posterior pituitary (PPi). Depicted here is a PVH cell, however many magnocellular cells of other hypothalamic regions project to the PPi. DCVs (large white circles) from the cell are transported through the axon, and with spike train action potentials OXT is released from axonal terminals into the blood capillaries. **2**) The second mode of release is central release to forebrain regions. (2a) There is evidence that the projections to forebrain regions are derived from axon collaterals of the magnocellular cells. (2b) There is also evidence that OXT+ projections to forebrain regions emanate from an independent population of cells. Oxytocin may be released from en passant terminals, however there is no clear evidence supporting this possibility. Likewise, OXT may be released at a synaptic terminal, but evidence for this release is lacking as well. **3**) Finally, dendrites release OXT following mobilization of Ca2+ (green circles) from intracellular stores, this OXT acts as a paracrine signaling molecule for local OXTR.

a glutamatergic synapse on target post-synaptic cells (Colonnier 1968; Peters and Palay 1996). However, there is not sufficient evidence that OXT is being released from these synaptic sites along with glutamate. OXT may also be released via exocytosis from axonal swellings, also called varicosities, along the axon (**Fig 3A**) (Buma et al. 1984; Morris and Pow 1988; Grinevich and Ludwig 2021). Once released from the axon, OXT diffuses in the extracellular space and acts as a neuropeptide, binding to OXTR in regions close to the site of release (Chini et al. 2017). The lack of OXT release in an active zone has made the study of OXT's central release difficult. If OXT were released in an active zone, like other neurotransmitters, researchers could use electron microscopy to observe vesicles docking and releasing at a synapse and this would be direct evidence for release in a specific region. Instead, researchers have utilized tools such as intracerebral microdialysis to monitor local extracellular concentrations (Neumann et al. 1993; Veenema and Neumann 2008). Using microdialysis allows researchers to observe OXT changes over time, but this technique lacks spatial specificity. The presence of both OXT+ axons and dense core vesicles (DCVs) can be used as a proxy to determine the exact location where OXT is released (Chini et al. 2017; Oti et al. 2021; Althammer et al. 2021). Recently, Otero-Garcia et al., 2016 and Son et al., 2022 have examined the oxytocinergic projectome across the mouse brain to examine potential OXT release sites. Both studies found that the primary axonal projections of OXT cells are in sub-cortical regions, indicating these regions likely utilize OXT released from these axons. However, examination of DCVs in these axons is lacking and the release of OXT is assumed solely based on the presence of the axons. Many of these axons may be simply axons of passage, indicating the need for studies examining the presence or absence of DCVs. Finally, a recent study has developed a $GRAB_{OT1.0}$ sensor (Qian et al. 2023), this allows for the detection of oxytocin release from both axons and dendrites of OXT+ cells. This tool has indicated that although both axonal and dendritic release are activity-dependent, the mechanisms triggering release from axons vs. dendrites are different. Specifically, N-type calcium channels mediate axonal release while L-type calcium channels mediate the somato-dendritic release (Qian et al. 2023), again leading to the conclusion that these systems are functionally independent.

The third release mode of OXT is its somato-dendritic release (Morris and Pow 1988; Pow and Morris 1989; Ludwig et al. 2002; Bergquist and Ludwig 2008) that is, OXT's action via paracrine signaling (**Fig 3A**). This mode of release illustrates the OXT neuron's unique characteristics that lie between neurotransmitter and peptide hormone. Dendritic exocytosis is stimulated via calcium release from intracellular stores (Ludwig et al. 2002; Ludwig and Leng 2006; Qian et al. 2023), which can be triggered by GPCR signaling to increase intracellular calcium, for example, OXT binding to OXTR on these cells. Dendritically released OXT can then bind locally to OXTR through this paracrine signaling mechanism, akin to endocrine cells' paracrine signaling in the periphery (Ozawa and Sand 1986). This mechanism is assumed to be important for the pulsatile nature of OXT at parturition and during lactation and allows for the synchronized firing of OXT cells in the same region (Crowley and Armstrong 1992; Carter et al. 2020, Neumann et al. 1994) Using an oxytocin antagonist in the SON, Neumann et al., 1994, found that OXT-OXTR binding is essential for the rise in OXT and sufficient milk transfer to pups during suckling. Indicating that this positive feedback loop acting within the SON is mediated by OXT binding and it is assumed that this feedback is from the

dendritically released OXT, not axonal OXT (Neumann et al., 1994). There have been suggestions that the OXT released from the somata and dendrites may also travel through the extracellular space to reach regions of the brain with OXTR besides local hypothalamic cells, such as regions of the cerebral cortex that lack OXT+ axons (Ludwig and Leng 2006). Researchers agree that it is improbable for OXT released through dendritic exocytosis in the hypothalamus to traverse the extracellular space and reach distant regions to bind to OXTR (Chini et al. 2017). Still, other researchers have proposed that peripheral OXT may cross the blood-brain barrier to reach OXTR in the cerebral cortex (Lee et al. 2018; Yamamoto et al. 2019). This is also an unlikely mechanism and will be discussed further in section V.

c. The oxytocin receptor: structure, regulation, and signaling cascades

OXTR is a G protein-coupled receptor (GPCR) and is oxytocin's only receptor (Gimpl and Fahrenholz 2001, Busnelli and Chini, 2018) unlike a structurally similar peptide vasopressin which has 3 receptors (Busnelli & Chini 2018; Gimpl & Fahrenholz, 2001). These receptors are
a subfamily of GPCRs and OXT can bind to all four of them, but with different affinities, displaying the highest affinity to OXTR (Busnelli & Chini, 2018; Gimpl & Fahrenholz, 2001). Moreover, isoforms of OXTR can interact with vasopressin receptors and other GPCRs, such as dopamine 2 receptors, to form heterodimers (Terrillon et al. 2003; Hernández-Mondragón et al. 2023). The formation of these heterodimers and their interactions with one another can modulate the recognition, signaling, and trafficking of their GPCRs and will influence the subsequent intracellular signaling (Fuxe et al. 2012; Borroto-Escuela et al. 2013; Hernández-Mondragón et al. 2023).

GPCRs are seven transmembrane-domain proteins that couple to specific G-protein families: Gi/o, Gs, Gq/11, and G12/13, to activate signaling cascades within the cell (Hilger et al. 2018). All GPCRs are bound to heterotrimeric G-proteins and contain a Gα, and a β/γ subunit (Hilger et al. 2018; Tuteja 2009). Following the binding of the ligand to the receptor, the activated receptor catalyzes the exchange of GTP for GDP on the Gα subunit, causing a conformational change and leading to the dissociation of the β/γ subunit (Tuteja, 2009). Which G-protein family the Gα subunit belongs to will affect the following intracellular cascade. OXTR belongs to the class-A/rhodopsin GPCR family, and just recently the crystal structure of the human OXTR protein has been elucidated (Inoue et al. 1994; Waltenspühl et al. 2020). OXT binds to OXTR within the transmembrane core (Busnelli & Chini, 2018) and once OXT is bound, the GPCR will be activated and can be coupled to either Gαq/11 or Gαi/o. (**Fig 4A**). If OXTR is coupled to Gαq/11, this subunit will stimulate phospholipase C-β (PLCβ) and further hydrolyze phosphatidylinositol 4,5-biphosphate (PIP2) into inositol 1,4,5-triphosphate (IP3) and 1,2-diacylglycerol (DAG) (**Fig 4A**) (Busnelli & Chini, 2018; Tuteja 2009). IP3 will increase the release of intracellular calcium stores, while DAG activates protein kinase C (PKC) and phosphorylates downstream proteins (Busnelli & Chini, 2018; Tuteja 2009). Activation of the Ca^{2+} second messenger system, which can influence various enzymes, intracellular receptors, or transcription factors, will affect gene expression within the cell. (Tuteja 2009). However, OXTR can also couple to the Gαi/o subunit, typically with higher concentrations of OXT present (**Fig 4A**) (Busnelli & Chini, 2018). If this pathway

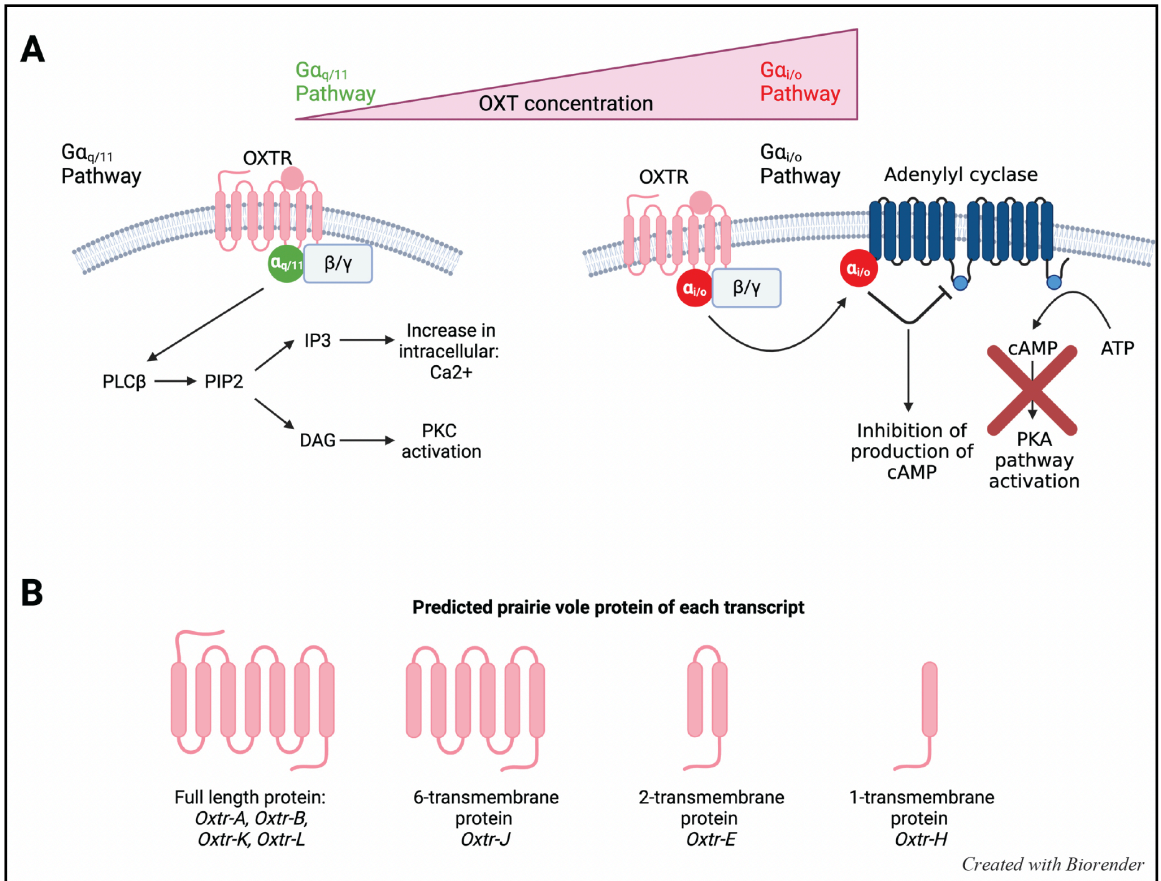

Figure 4: The oxytocin receptor (OXTR), a GPCR, expresses at least 7 RNA transcripts in the prairie vole. **A**) OXTR couples either the Gq/11 or Gi/o pathways, one determinant of which pathway it couples to is OXT concentration. At low OXT concentrations, Gαq /11 signaling is activated. The α subunit dissociates and activates PLCβ which hydrolzyes PIP2 into IP3 and DAG. IP3 increases intracellular calcium and DAG activates PKC. At high OXT concentrations, the Gαi /o signal transduction pathway is activated. This signaling inhibits adenylyl cyclase, and inhibits cAMP production so there is no activation of PKA. **B**) Recently (Danoff, Page et al., 2023), seven Oxtr transcripts have been found in the prairie vole. Displayed here are the predicted protein structures if these transcripts are translated into proteins (adapted from Danoff, Page et al., 2023). Four of these have the ability to make the full-length seven-transmembrane protein, one would make a six-transmembrane protein, one a two-transmembrane protein, and one would create a one-transmembrane protein.

is activated, adenylate cyclase activity is inhibited which in turn inhibits cyclic adenosine monophosphate (cAMP) production; this path inhibits downstream intracellular signaling (**Fig 4A**) (Busnelli & Chini, 2018). OXTR binding in a specific region can then modulate the output of that region through these G-protein coupled cascades. Individual differences in OXTR expression are important because if one individual has higher OXTR expression than another, they will have a stronger post-synaptic response to the same amount of released OXT. This is because higher OXTR expression allows more OXT to bind to the available receptors, resulting in a greater response. Many studies have found that *Oxtr* transcript expression, which is often positively correlated to the amount of protein expression, is regulated through epigenetic means (Gregory and Connelly et al. 2009; Puglia et al. 2015; Perkeybile et al. 2019; Kenkel et al. 2019; Danoff and Page et al. 2023a).

Oxytocin receptors are expressed throughout the brain (Quintana et al. 2019; Inoue et al. 2022; Son et al. 2022). Many studies have focused on the individual variability in *Oxtr* expression (Puglia et al. 2015; Perkeybile et al. 2015; Ahern et al. 2021; Inoue et al. 2022; Danoff et al. 2023b). Studies suggest that many of the individual differences seen in the display of behavior, particularly social vs non-social behaviors, can be linked to differences in the expression of the oxytocin receptor (Keebaugh and Young 2011; Jurek and Neumann 2018; Carter 2022). Further, the expression of OXTR has been a focus of study due to some of the difficulties with studying the OXT peptide itself such as the lack of an active zone indicating release, and difficulties accurately measuring OXT because of its pulsatile nature and differences in methodology (Kagerbauer et al. 2013; Leng and Ludwig 2016; Lefevre et al. 2017; Carter et al. 2020).

i. Epigenetic regulation of the oxytocin receptor (OXTR)

In animal models, early life experience plays an essential role in regulating gene expression later in life (Weaver et al. 2004; Perkeybile et al. 2019). Gene expression can be controlled through epigenetic regulation such as methylation of a cytosine followed by a guanine, typically called a CpG (cytosine-phosphate-guanine) site (Perkeybile et al. 2019; Kenkel et al. 2019). The seminal work on how early life care impacts the epigenetic regulation of genes via methylation was done by Weaver et al. in 2004. This study illustrated that maternal care in a rat model can impact the expression levels of the glucocorticoid receptor (GR) gene in the hippocampus of adult animals (as late in life as post-natal day 90, PND90) (Weaver et al. 2004). Using cross-fostering, bisulfite conversion, and western blots for immunoreactivity, researchers found that offspring of high-licking and grooming mothers have significantly lower methylation in the promoter region of the GR gene, which correlated with an increase in GR immunoreactivity (IR). This finding was independent of the genetic background of the offspring. Such that offspring from a low-licking and grooming dam cross-fostered to a high-licking and grooming dam displayed the same lower methylation and high expression seen in animals raised and genetically related to high-licking and grooming dams. Thus, this epigenetic regulation is, at least in part, driven by maternal care. This increase in GR protein expression later in life will impact the regulation of the stress response in adulthood.

The relationship between methylation and expression of many genes follows the same pattern described above, higher methylation is related to lower gene expression (Moore 2017). The OXTR gene, in both human and animal models, also displays this relationship (Gregory and Connelly et al. 2009; Perkeybile et al. 2019; Danoff et al. 2021, Danoff and Page et al. 2023a). In work done by Perkeybile et al. 2019, researchers found that like the GR gene in rats, *Oxtr* methylation and expression in the prairie vole (Microtus ochrogaster) nucleus accumbens (Acb) can be regulated by maternal care. Using a handling method to experimentally increase maternal behavior, this study found that higher maternal care in the first week of life was related to lower *Oxtr* methylation and higher expression in the Acb at adolescence. An increase in the availability of OXTR in the Acb has been correlated with a multitude of prosocial behaviors in this animal such as alloparental care (Olazábal and Young 2006b; Ross and Young 2009; Keebaugh and Young 2011), pair-bonding in females (Ross et al. 2009; Kenkel et al. 2021), and maternal care (Keebaugh et al. 2015). OXTR in the prairie vole Acb plays an important

role in driving these behaviors, and although OXT only has the singular receptor this receptor has many transcripts (Danoff and Page et al. 2023a).

ii. Transcriptional diversity of the OXTR

Recent work in the prairie vole has uncovered at least seven unique *Oxtr* transcripts (Danoff and Page et al. 2023a). Through 5′ rapid amplification of cDNA ends (RACE), tissue from the Acb, and uterine samples were examined to identify all *Oxtr* transcripts present in the vole. Unsurprisingly, the canonical "main" transcript was observed consisting of four exons and three introns, but six other transcripts were also found (Danoff and Page et al. 2023a). Four of the transcripts, if translated into a protein would create the full seven-transmembrane protein (*Oxtr*-A, *Oxtr*-B, *Oxtr*-K, and *Oxtr*-L), one would create a truncated version of OXTR containing six transmembrane domains (*Oxtr*-J), another would contain two transmembrane domains (*Oxtr*-E), and finally one would create a single transmembrane protein (*Oxtr*-H) (**Fig 4B**). If any or all of these transcripts are translated into a protein, they could regulate the binding capacity of OXT to the full-length protein (Meyerowitz et al. 2022; Danoff and Page et al. 2023a). These truncated forms could also interact with other G proteins at the membrane or cytoplasm making these proteins unavailable for heterodimerization or homodimerization to the full-length protein. Interestingly, *Oxtr*-H may play a particularly important role in the regulation of the full-length transcript. Previous work has found that *Oxtr*-H expression is positively correlated to *Oxtr*-A (the full-length transcript) only when an animal is an A allele carrier at a specific single-nucleotide polymorphism (SNP) (Danoff et al. 2021). Suggesting an interesting genetic x epigenetic regulation of OXTR in prairie voles.

III. Animal models used for studying OXT and OXTR signaling

Work on the oxytocinergic system, including both the peptide and its receptor, has been examined in a litany of animal models including mice, rats, prairie voles, primates, and humans (Kimura et al. 1992; Domes et al. 2007; Lee et al. 2009; Arias Del Razo et al. 2020; Carter et al. 2020; Son et al. 2022). There are benefits to using each model to answer specific questions, and these will be summarized below.

a. The oxytocinergic system in mice and rats and its behavioral impact

Early studies began by examining OXT in the periphery (Dale 1906; Crowley and Armstrong 1992). Once OXT was discovered and its role in the periphery was described, researchers began examining where OXT is synthesized and released. Later research uncovered the major role that OXT plays in inducing maternal behavior in the rat model, indicating that OXT is not only important in the periphery but also must play a role in the CNS (Pedersen and Prange 1979; Pedersen et al. 1982). Researchers found that by administering OXT intracerebroventricularly, virgin rats will display the full repertoire of maternal behaviors when previously they were averse to pups (Pedersen and Prange 1979). This discovery laid the foundation for OXT research and its involvement in parental behaviors, as well as social behaviors. Further work by Francis, Champagne, and Meaney 2000, found that OXTR levels in rats also drive differences in maternal behavior. Rat dams that display high levels of pup licking/grooming and arched-back nursing (LG-

ABN), behaviors that are appetitive and show a concerted effort on the part of the dam, have increased levels of OXTR in brain regions that mediate the expression of maternal care (Francis et al. 2000). These studies indicate that OXT plays a role in mother-infant bonding and the stimulation of maternal care. Rats were initially used for these studies because they are physiologically similar to humans, easy to maintain, have larger brains than mice, and exhibit distinct maternal behaviors that can be observed and measured.

Later research included both mice and rats, as mice exhibit similar maternal behaviors. This allowed for species comparisons, which helped highlight important evolutionary characteristics of maternal behavior. The main advantage of using mice and rats in current research is the comprehensive annotation of their genomes and the availability of molecular/genetic tools like knock-out and *Cre*-driver lines. In mouse models, oxytocin has been demonstrated to facilitate and promote maternal behavior by signaling through various subcortical and cortical circuits (Marlin et al. 2015; Carcea et al. 2021). Indicating that signaling through OXT-OXTR binding in the brain to drive maternal behavior is evolutionarily preserved. OXT also plays an important role in other kinds of social behaviors ranging from aggression in the rat (Bosch et al. 2005; Calcagnoli et al. 2014), juvenile social play behavior in the rat (Bredewold et al. 2014), pro-social/social avoidance behaviors in both mice and rats (Winslow and Insel 2002; Lukas et al. 2011), and even autism-like behaviors in the mouse (Teng et al. 2013). Much of this research has used knock-out models and *Cre*-lines to study OXT signaling in the brain, allowing for causal conclusions about OXT's role in these behaviors. While mice and rats are crucial for understanding the circuitry and causal links between OXT release and specific behaviors, they lack many complex social behaviors related to oxytocinergic functioning.

b. The prairie vole as an animal model, behavioral links to OXT

Since the 1980's prairie voles have emerged as a unique animal model for studying social behaviors seen in humans, such as pair-bonding and alloparenting (Getz et al. 1981; Aragona and Wang 2004; Carter et al. 2020; Danoff et al. 2021). The earliest studies of prairie voles focused on social monogamy, and the observation that in the wild most prairie vole mates preferred to spend time with their familiar partner (Getz et al. 1981). This pair-bonding behavior was then subsequently assessed in a lab setting by the creation of the partner preference test (PPT), where a pair-bonded vole (male or female) has the choice to spend time with its mate, a stranger, or alone in a neutral cage (Williams et al. 1994; Kenkel et al. 2021). The strength of the pair bond can be measured by the amount of time the test animal spends with its mate vs. in the other cages. Social monogamy is a typical aspect of human social behavior, and exploring its biological basis can reveal evolutionarily conserved systems crucial for normal human social interactions (Lukas and Clutton-Brock 2013). Since social monogamy is rare among rodents and absent in mice and rats, prairie voles are particularly useful for studying the biological underpinnings of monogamy (Getz et al. 1981; Aragona and Wang 2004; Kenkel et al. 2021). OXT was found to be an important driver of monogamy, especially in female voles (Williams et al. 1994; Aragona and Wang 2004; Kenkel et al. 2021). Through osmotic mini-pumps releasing OXT intracerebroventricularly, but not peripherally, females formed a partner preference after only 6 hours of co-habitation with a male without mating, which is not a sufficient amount of time to form a pair-bond in control

animals (Williams et al. 1994). Indicating that central OXT regulates the formation of pair bonds in females. In males, vasopressin (AVP) appears to drive male pair-bonding behavior (Winslow et al. 1993). However, both peptides can modulate and drive social contact and partner preference in either sex, likely through binding to either the AVP receptors or OXTR (Cho et al. 1999). This seminal work done in the prairie vole has uncovered that social bonding between partners is driven by oxytocinergic signaling centrally, which led researchers to examine whether OXT plays a role in other prairie vole-specific behaviors, such as alloparenting.

Before ever giving birth, prairie voles engage in alloparenting behaviors such as licking, grooming, and huddling over offspring (Carter et al. 2020; Kenkel et al. 2021). This behavior, commonly seen in the wild as older siblings caring for younger ones, is unique to prairie voles and is found in only about 3% of mammals (Kenkel et al. 2017; Rogers and Bales 2019; Carter et al. 2020). In most rodent species, males do not participate in offspring care, and females generally exhibit maternal behaviors only after giving birth (Kenkel et al. 2017; Rogers and Bales 2019). While most adolescent prairie voles will care for pups, there is individual variability in the amount of time spent with them, but very few will attack the pups (Perkeybile et al. 2015; Finton et al. 2022). Infanticidal behavior is often seen in males and nulliparous females of other species (Rogers and Bales, 2019). Interestingly, alloparental care in virgin adult males is common but virgin adult females show wide variability in alloparental care, where some adult females no longer display alloparental care and will attack pups (Lonstein and De Vries 1999; Olazábal and Young 2006b). Alloparental care at any age in females is facilitated via OXT signaling while interfering with this system through OXT agonists/antagonists early in life can impact alloparental care in males in adulthood (Olazábal and Young 2006b, a; Bales et al. 2007). Highlighting the importance of OXT in a second unique prairie vole behavior that is also displayed by humans. Intimating that OXT in humans likely also drives many of these gregarious social behaviors.

There are many benefits to using the prairie vole for research, as opposed to a traditional animal model. The first, described above, is many social behaviors we are interested in determining the biological basis for in humans are natural behaviors in prairie voles. Another advantage of using the prairie vole model is the extensive research conducted not only in laboratory settings but also in naturalistic field environments (Carter and Perkeybile 2018; Kenkel et al. 2021). Most traditional model studies are confined to lab settings. This has sparked ongoing debates regarding the validity of lab-based behavioral studies and whether the observed behaviors are natural for the animals, particularly since most lab mice and rats are inbred and several generations removed from their wild counterparts. In contrast, prairie voles consistently exhibit pair-bonding and alloparental behaviors in both field and lab settings (Kenkel et al., 2021; Getz et al., 1981). In addition, prairie vole colonies are generally outbred, mirroring the genetic diversity found in the wild. This allows researchers to study behavioral variations across populations (Kenkel et al., 2021). For instance, there are differences in behaviors like genetic monogamy, biparental care, and aggression among prairie voles from Illinois, Indiana, and Kansas (Mabry et al. 2011; Kenkel et al. 2021). Researchers can leverage these differences to explore the biological factors underlying these behavioral variations (Kenkel et al., 2021).

c. OXT in non-human and human primates, implications for dysfunction in the system

While rodents are a great model for studying social behaviors, and the underlying circuitry directing that behavior, they often fall short of addressing the primary purpose of using these models, which is to inform human biology, behavior, and development. Thus, utilizing non-human primates (NHPs), due to their evolutionary closeness to humans is an ideal animal model, but does pose some challenges such as costs (Kenkel et al., 2021). However, many studies have utilized NHPs to examine OXT's impact on social behaviors, to build on the previous rodent literature, and to uncover the evolutionarily conserved aspects of this system (Chang et al. 2012; Chang and Platt 2014; Freeman et al. 2016; Putnam et al. 2018; Arias Del Razo et al. 2020).

NHPs are typically very social animals, and they can perform cognitively demanding tasks, like humans (Putnam et al., 2018). In marmosets, a socially monogamous NHP, researchers used intranasal OXT (IN-OXT) and an orally administered OXT antagonist (L-368,899) to determine OXT's role in pair-bonding over 3 weeks of cohabitation (Smith et al. 2010). They found that following IN-OXT marmosets initiated more huddling behaviors compared to controls and after the antagonist treatment, they decreased proximity to their partner (Smith et al., 2010). Interestingly, marmosets that received IN-OXT treatment facilitated partner seeking in a PPT over initial contact with a stranger while control animals interacted with both the partner and stranger equally. These results indicate that OXT may facilitate bonding in this species, consistent with what was seen in the vole literature. Further observations have been done on circulating levels of OXT in cerebrospinal fluid (CSF) and plasma in animals that appear to have social deficits (Winslow et al. 2003). The CSF contains OXT, typically at levels higher than is seen in the plasma (Kagerbauer et al. 2013; Martin et al. 2018), suggesting independent mechanisms of release from the peripheral OXT release, which will be discussed further in Section V. Researchers have also utilized nursery rearing (NR) vs. mother rearing (MR) to examine if early life experience impacts social behaviors later in life and if circulating basal OXT is affected (Winslow et al. 2003). OXT was lower in CSF of NR animals, but not different in the plasma, demonstrating further evidence that central OXT release is likely independent from the peripheral OXT release. NR animals also display more abnormal repetitive behaviors, and less social contact behaviors than MR animals (Winslow et al., 2003).

Both repetitive locomotor behaviors and disinterest in social contact are autism-like characteristics, and OXT levels in the plasma of children with autism may be lower than control children (Modahl et al. 1998; John and Jaeggi 2021). The literature on the relationship between autism and OXT has been conflicting, but a recent meta-analysis of 31 studies has found strong evidence for differences in OXT levels in children (John & Jaeggi, 2021). To date, only one study appears to have examined OXT in the CSF, a central measure of OXT, and has not found a difference in CSF OXT in autistic children compared to neurotypical children (Oztan et al. 2018). This study did find a difference in AVP which was significantly lower in the autism group (Oztan et al., 2018). Illustrating again the interplay and importance of these two systems, OXT and AVP, to potentially regulate species-typical behaviors. Research on the oxytocin receptor has also found differences in OXTR in individuals with autism (Yrigollen et al. 2008; Gregory and Connelly et al. 2009), including a genomic deletion containing the OXTR gene that is

implicated in autism spectrum disorder (ASD). Further, work from Gregory and Connelly et al. found increases in the methylation status of a CpG island in individuals with ASD, which correlated with decreases in *OXTR* mRNA transcript expression (Gregory and Connelly et al., 2009). One interesting note, some CpG sites in this CpG island are conserved in the prairie vole and have also been found to regulate *Oxtr* expression yet are not conserved in the mouse or rat, further underscoring the advantages of investigating the oxytoincergic system in the vole (Perkeybile et al. 2019). OXT in ASD patients may be regulated through both the peptide release and at the receptor level, however, work done in humans has many drawbacks such as the lack of random assignment, large heterogeneity across the population, and relatively small sample sizes. Therefore, there is a great benefit to using animal models to study OXT and behavior, and which animal model is best depends on the question.

IV. Three oxytocinergic systems: hormonal, neuropeptide, and paracrine signaling regulating reproduction, hedonics (bonding), and other social behaviors (complex cognitive functions, aggression)

Oxytocin's different actions in the visceral and central nervous system point to three distinct signaling pathways. The first is oxytocin's utilization in the periphery, primarily responsible for regulating reproduction (Brownstein et al. 1980; Fuchs et al. 1984b; Caldwell et al. 2017), the second is oxytocin's utilization centrally in limbic regions to play a role in hedonics and bonding behaviors (Carter 1992; Bale et al. 2001; Olff et al. 2013; Borland et al. 2019; Liu et al. 2020; Giannotti et al. 2022), and finally, it's actions in cortical regions control aspects of complex cognitive functions and aggressive social behaviors. This section will examine the role of OXT in each of these pathways and the circuitries involved in the central oxytocinergic modulation of these behaviors.

a. Hormonal OXT: Humoral release into the periphery for reproduction

The first and most studied of the oxytocinergic systems is the peripheral release and its' physiological effects on the body, particularly the initiation of contractions at birth and milk letdown during lactation (Soloff et al. 1979; Perkinson et al. 2021). From PVH and SON axons, the oxytocin is released into the bloodstream from dense core vesicles (DCV) to reach peripheral targets containing oxytocin receptors (OXTR), including regions such as the uterus, the mammary glands, and the corpus luteum to regulate parturition, lactation, and ovulation, respectively (**Fig 5A**) (Gimpl and Fahrenholz 2001; Vanderwall et al. 2012).

b. Neuropeptide OXT: Central release via axons for hedonics

The second system is linked to hedonics and reward-related behaviors (Carter 1992; Bale et al. 2001; Olff et al. 2013; Borland et al. 2019; Liu et al. 2020; Giannotti et al. 2022) as well as behaviors related to bonding and the stress response (**Fig 5B**) (Dabrowska et al. 2011; Bosch et al. 2016). This system involves oxytocin release in limbic regions, including the nucleus accumbens (Acb), the amygdala, and the bed nucleus of the stria terminalis (BNST). The oxytocin-releasing axons in these regions originate primarily from the PVH, (Zhang et al. 2021b; Freda et al. 2022; Li et al. 2024) and they release oxytocin that is transported in DCVs likely from axonal varicosities

(Armstrong et al. 1982; Tweedle et al. 1989; Knobloch et al. 2012). These regions contain OXTR protein and *Oxtr* transcripts, detected by autoradiography and RNAScope

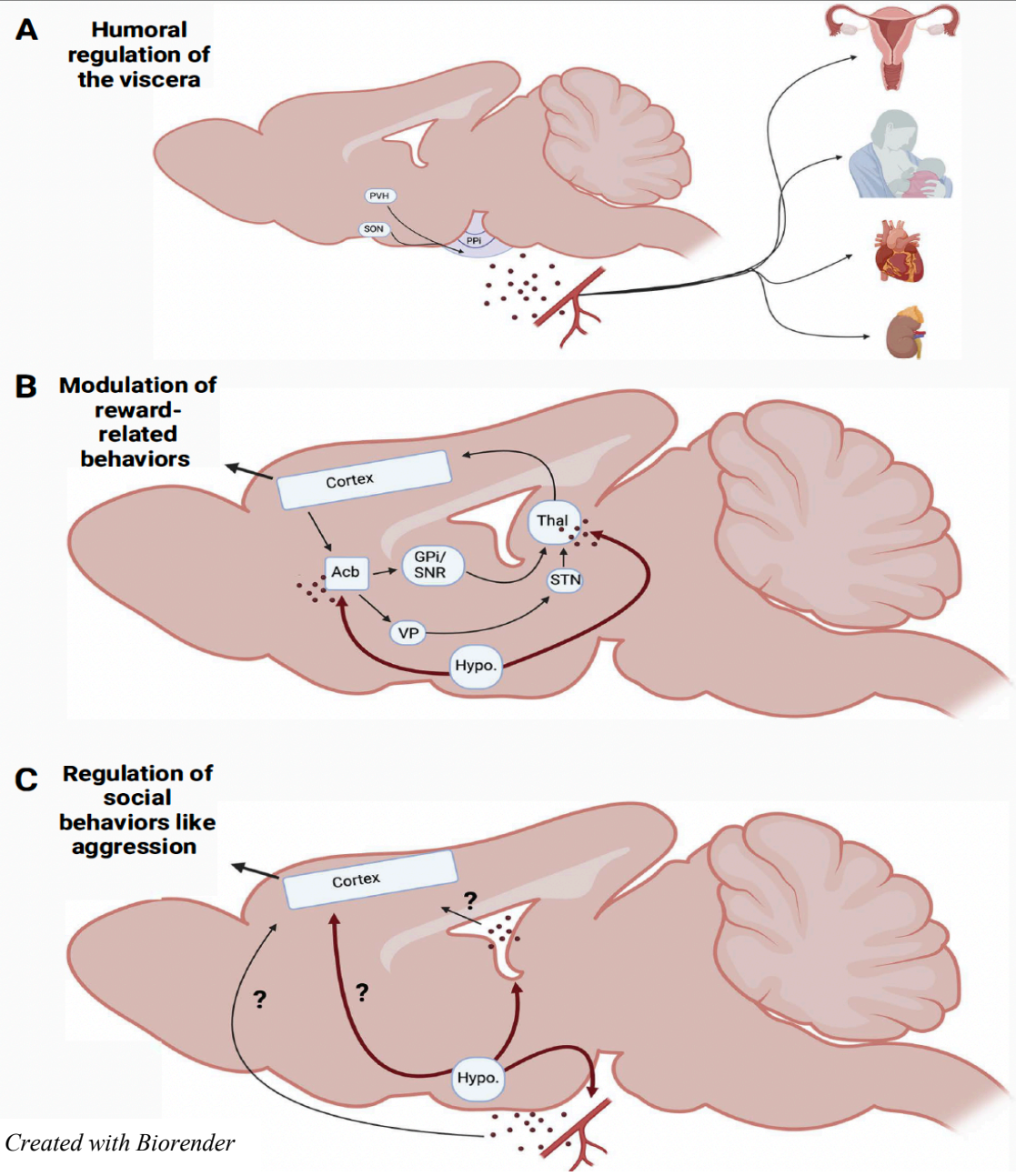

Created with Biorender

Figure 5: There are likely three distinct roles of OXT in the viscera and central nervous system. **A**) The first role is OXT's release from the magnocellular cells of the hypothalamus, primarily the PVH and SON, into the into the posterior pituitary (PPi). From the PPi, OXT travels through the blood capillaries into the viscera. In the periphery OXT binds to the oxytocin receptor in the uterus, mammary tissue, heart, and kidney. **B**) OXT axons of the hypothalamus also project centrally to regions such as the nucleus accumbens (Acb) and thalamus (Thal), through this circuitry OXT modulates reward-related behaviors such as social bonding. **C**) Finally, OXT binds within cortical regions to regulate social behaviors like aggression. However, how OXT reaches the cortical regions is still unknown. Likely, OXT travels throughout the CSF within the ventricles and subarachnoid space to bind OXTR in cortical regions.

in-situ hybridization, and display unique patterns associated with individual differences in behavior, as such they likely bind to oxytocin directly released from axons (**Fig 5B**) (Insel and Shapiro 1992; Olazábal and Young 2006b; Jurek and Neumann 2018; Smith et al. 2019; Inoue et al. 2022). As previously mentioned, central OXT drives maternal behavior, this is modulated through circuitry that primarily utilizes the medial preoptic area of the hypothalamus (MPOA), the Acb, and the ventral tegmental area (VTA) (Numan 2007; Numan and Stolzenberg 2009). Within this circuitry, OXT interacts with the dopaminergic (DA) system to drive appetitive maternal behaviors such as licking/grooming and retrieval behaviors (Numan and Stolzenberg 2009). OXT and DA signaling through this circuitry indicates these behaviors are rewarding and motivated. In the rat model, OXT binding in the VTA increases DA release from the VTA to the Acb (Shell), and higher DA in the AcbSh is related to higher licking and grooming behavior in high-care mothers (Champagne 2004; Shahrokh et al. 2010). In prairie voles, blocking OXT-OXTR interactions in the AcbSh reduces spontaneous alloparental behavior in virgin female adults, whereas increasing OXTR expression via viral-vector gene transfer enhances this behavior (Olazábal and Young 2006b; Keebaugh and Young 2011). Enhancing OXTR expression in the Acb of female prairie voles also promotes partner preference formation (Keebaugh & Young, 2011). The Acb circuitry and regulation of oxytocinergic and dopaminergic signaling seem to mediate both maternal care in rats and these unique behaviors in prairie voles. This implies that such behaviors are motivated and rewarding, and notably, these regions contain OXT+ axons in mice (Otero-García et al. 2016; Son et al. 2022), rats (Moaddab et al. 2015), and prairie voles (Ross et al. 2009; Bosch et al. 2016). Consequently, OXT released from OXT+ axons likely binds to OXTR, modulating neuronal firing in the Acb and influencing downstream signaling and subsequent behavior.

c. Paracrine OXT: Central release for complex cognitive functioning and aggression

The third system involves oxytocin action in cortical areas, playing a role in aggressive behaviors, learning, and other more complex cognitive functions that require the involvement of sensory and association cortices (**Fig 5C**) (Bales and Carter 2003; Hurlemann et al. 2010; Marlin et al. 2015; Jurek and Neumann 2018). For example, prairie voles exhibit consoling behavior after their partners experience stress and separation (Burkett et al. 2016), which is linked to OXTR binding in the anterior cingulate cortex (Cg), highlighting the importance of oxytocin availability to the cortex (Burkett et al., 2016). Burkett and colleagues, separated pair-bonded animals and had the test animal observe their partner undergoing a stressor, such as a shock or loud tone, and noted increased allogrooming, which is the grooming of another animal, following the stressor (Burkett et al., 2016). Compared to animals that were only separated, the test animal spent significantly more time allogrooming their partner. This consoling behavior was not observed if OXT binding was blocked by an antagonist (OXT-A) injected intracerebroventricularly. Further autoradiography and FOS immunoreactivity showed that this behavior is mediated by the Cg, and injecting OXT-A in the Cg reduced partner-directed grooming after separation and stress (Burkett et al., 2016). Consolation behavior, previously considered a higher-order cognitive ability seen only in animals like primates, canids, and elephants, appears to also occur in rodents and can be driven by OXT in the

cerebral cortex. OXT in the cortex also impacts anxiety-like and aggressive behaviors, particularly through the top-down control from prefrontal cortical regions to regions of the amygdala (Bosch et al. 2005). In rodent models, the resident-intruder test (RIT) is commonly used to evaluate aggressive responsiveness. In studies involving rats, heightened aggression has been associated with decreased expression of OXT axons in males and reduced activation of OXT neurons in females (Jong and Neumann, 2017). The medial prefrontal cortex (mPFC) plays a crucial role in regulating top-down control of the amygdala to either enhance or reduce aggressive behavior; OXT binding to OXTR in this region modulates mPFC output and influences aggression levels (Jong and Neumann, 2017). Regarding maternal aggression in rats, injecting an OXTR antagonist into the mPFC has been shown to increase aggression toward intruders, suggesting that OXT in the mPFC affects aggression across different contexts (Sabihi et al. 2014b). Furthermore, injecting an OXTR antagonist in this region enhances anxiety-like behaviors in postpartum rats but decreases such behaviors in male and female virgin rats (Sabihi et al. 2014b, a). Overall, OXT in the cerebral cortex appears to regulate aggressive and anxiety-like responses in a context-dependent manner, in addition to its roles in promoting prosocial behaviors mediated through limbic regions. Although these circuitries involved in bonding vs. more complex behaviors are discussed as separate systems, there is overlap between all circuitries. While several cortical regions exhibit abundant OXTR presence (Bosch et al. 2016; Newmaster et al. 2020; Inoue et al. 2022; Son et al. 2022), and oxytocin in cortical areas has demonstrated behavioral impacts, these regions generally lack a high density of oxytocin-containing fibers (Mitre et al. 2018; Liao et al. 2020; Manjila et al. 2022; Son et al. 2022). This suggests that oxytocin's effects in the cortex operate independently of axonal or humoral oxytocin release (Veening et al. 2010a; Ferris et al. 2015; Mitre et al. 2018; Son et al. 2022), which has led to a long-standing debate within the field: where is the oxytocin in the cerebral cortex coming from (**Fig 5C**)?

V. How does OXT reach the cerebral cortex? Implications for cerebrospinal fluid (CSF) OXT vs. plasma OXT

a. Is OXT in the CSF plasma-derived?

One suggestion has been that CSF OXT may be responsible for bringing OXT to the cerebral cortex (Leng and Ludwig 2008; Chini et al. 2017; Jirikowski 2019), but how the OXT gets to the CSF has also been a matter of debate. Some work has shown that OXT from the periphery can pass the blood-brain barrier (BBB) (Lee et al. 2018; Yamamoto et al. 2019) and may be responsible for the OXT in the CSF, however, OXT's ability to pass the BBB at endogenous levels is unclear. Further, OXT is present in the CSF at higher concentrations than in the periphery (Kagerbauer et al. 2013), and the two are not correlated (Kagerbauer et al. 2013; Martin et al. 2018). In addition, plasma oxytocin has a significantly shorter half-life (about 2-5 minutes) than CSF oxytocin (about 20-30 minutes)(Mens et al. 1983; Leng and Ludwig 2008; Veening et al. 2010a) suggesting that plasma clearance rate poses a bottleneck for sustaining the CSF oxytocin

concentration. It is unlikely that plasma OXT is the primary source of OXT to the CSF. So how does OXT reach the CSF?

b. CSF flow and peptidergic signaling

First, I will describe what is CSF and what role it plays in the brain. Cerebrospinal fluid (CSF) resides within the brain's ventricles and the subarachnoid space of the brain and spinal cord, providing a protective barrier between the brain and its external environment (Sakka et al. 2011). It acts as a 'shock absorber,' mitigating the risk of brain tissue injury upon head impact (Czarniak et al. 2023). CSF is primarily produced by ependymal cells lining the ventricular surfaces, forming a single layer of cuboidal epithelium with tight junctions (Sakka et al. 2011; Brinker et al. 2014; Deng et al. 2023). These cells are equipped with cilia and numerous microvilli to monitor the extracellular space and CSF content (Sakka et al., 2011; Brinker et al., 2014). Microvilli increase surface area for sensing CSF composition, while motile cilia circulate CSF throughout the brain (Brinker et al. 2014). Ependymal cells play a crucial role in maintaining homeostasis by clearing toxins and regulating concentrations of regulatory peptides (Deng et al. 2023). They may actively transport signals from brain parenchyma into the CSF, influencing broader brain regions through ventricular flow. The presence of numerous peptides in CSF suggests its role in distributing these molecules to receptor sites throughout the brain (Post et al. 1982). The dynamic exchange between CSF and brain parenchyma underscores its significance in regulating neural signaling pathways and maintaining overall brain function.

c. Is the source of OXT in the CSF dendritically released neuropeptide OXT?

Previous studies have suggested that somatodendritic release mechanisms may contribute to oxytocin (OXT) presence in cerebrospinal fluid (CSF) (Leng and Ludwig 2008; Chini et al. 2017), although direct evidence for this process remains limited. Observations indicate that OXT-positive dendrites extend proximally to, and possibly through, the ependymal cell layer (Knobloch and Grinevich 2014), suggesting a potential pathway for OXT release directly into the CSF. Recent investigations have also identified OXT axons traversing along major ventricular pathways in mice; given the likely ability of OXT to be released from axonal varicosities, it is plausible that OXT could enter the CSF through this mechanism as well (Veening et al. 2010b; Ma et al. 2017).

Studies have demonstrated rapid distribution of CSF throughout the brain via ventricular flow and the subarachnoid space along capillaries (Ma et al. 2017). These findings collectively underscore potential pathways through which OXT may influence broader neural circuits and behavior, highlighting the intricate interplay between central OXT release and its distribution within the brain (Ma et al., 2017). Within as little as 10 minutes CSF can reach various regions of the brain, and within 30 minutes, it permeates extensively throughout the subarachnoid space, including areas surrounding cerebral cortex capillaries (Ma et al., 2017). If oxytocin (OXT) is released directly into the CSF, this fluid circulation may enable OXT to bind to receptors in these cortical regions through volume transmission (Veening et al. 2010; Jirikowski 2019). Likely, the OXTR is binding to this OXT that is directly released into the CSF from dendritic and axonal

release. This release would also be activity-dependent but would be involved in a kind of "broadcasting message" (Veening et al. 2010) of OXT. Thus, large fluctuations of OXT, say at birth or during lactation, would have vast non-specific effects on many regions at one time. This system may be essential for "priming" the brain for birth and motherhood. As mentioned, female rodents are typically not maternal before giving birth so dramatic plastic changes happen following parturition and this broadcasting of OXT may be an essential part of that process.

In this chapter, I review the literature on oxytocin and propose three distinct roles for this hormone within the nervous and visceral systems, each linked to a specific mode of release. First, I discuss the peripheral and visceral functions associated with the humoral release of oxytocin. Second, I explore how oxytocin released from axons in subcortical brain regions modulates reward-related behaviors, such as bonding. Lastly, I examine the regulation of social behaviors, including aggression, via parenchymal oxytocin release in cortical regions.

Aims of this Dissertation:

1. The first aim of this dissertation was to create an essential tool to study the neuroanatomical cytoarchitecture of the prairie vole brain. Previously, prairie vole researchers have utilized a rat or mouse brain atlas for their studies which has been sufficient. However, as mentioned in this introduction, the oxytocinergic system of mice and rats has been well studied and described. The oxytocinergic system of the prairie vole has not, even though many prairie vole unique behaviors rely on OXT-OXTR signaling. To examine this system, I first needed to map out each brain region of the prairie vole brain. The Histochemical Brain Atlas of the Prairie Vole (*Microtus ochrogaster*) is a tool created and included in chapter 2.
2. My second aim was to determine the oxytocinergic system of the prairie vole. Utilizing the brain atlas tool, immunohistochemistry, RNAScope in situ hybridization, and a variety of microscopy techniques, we have fully mapped out OXT+ cell and axonal regions of the prairie vole brain. Finally, I examine the potential for OXT released to reach the cerebral cortex through the cerebrospinal fluid (CSF) through electron microscopy.

References:

Ahern TH, Olsen S, Tudino R, Beery AK (2021) Natural variation in the oxytocin receptor gene and rearing interact to influence reproductive and nonreproductive social behavior and receptor binding. Psychoneuroendocrinology 128:105209. https://doi.org/10.1016/j.psyneuen.2021.105209

Althammer F, Eliava M, Grinevich V (2021) Chapter 3 - Central and peripheral release of oxytocin: Relevance of neuroendocrine and neurotransmitter actions for physiology and behavior. In: Swaab DF, Kreier F, Lucassen PJ, et al. (eds) Handbook of Clinical Neurology. Elsevier, pp 25–44

Althammer F, Grinevich V (2018) Diversity of oxytocin neurones: Beyond magno- and parvocellular cell types? J Neuroendocrinology 30:e12549. https://doi.org/10.1111/jne.12549

Amico JA, Challinor SM, Cameron JL (1990) Pattern of Oxytocin Concentrations in the Plasma and Cerebrospinal Fluid of Lactating Rhesus Monkeys (Macaca mulatto,): Evidence for Functionally Independent Oxytocinergic Pathways in Primates*. The Journal of Clinical Endocrinology & Metabolism 71:1531–1535. https://doi.org/10.1210/jcem-71-6-1531

Aragona BJ, Wang Z (2004) The Prairie Vole (Microtus ochrogaster): An Animal Model for Behavioral Neuroendocrine Research on Pair Bonding. ILAR Journal 45:35–45. https://doi.org/10.1093/ilar.45.1.35

Arias Del Razo R, Berger T, Conley AJ, et al (2020) Effects of chronic intranasal oxytocin on behavior and cerebral glucose uptake in juvenile titi monkeys. Psychoneuroendocrinology 113:104494. https://doi.org/10.1016/j.psyneuen.2019.104494

Armstrong WE, Scho¨ler J, McNeill TH (1982) Immunocytochemical, Golgi and electron microscopic characterization of putative dendrites in the ventral glial lamina of the rat supraoptic nucleus. Neuroscience 7:679–694. https://doi.org/10.1016/0306-4522(82)90074-4

Armstrong WE, Smith BN, Tian M (1994) Electrophysiological characteristics of immunochemically identified rat oxytocin and vasopressin neurones in vitro. The Journal of Physiology 475:115–128. https://doi.org/10.1113/jphysiol.1994.sp020053

Bale TL, Davis AM, Auger AP, et al (2001) CNS Region-Specific Oxytocin Receptor Expression: Importance in Regulation of Anxiety and Sex Behavior. J Neurosci 21:2546–2552. https://doi.org/10.1523/JNEUROSCI.21-07-02546.2001

Bales KL, Carter CS (2003) Sex differences and developmental effects of oxytocin on aggression and social behavior in prairie voles (Microtus ochrogaster). Hormones and Behavior 44:178–184. https://doi.org/10.1016/S0018-506X(03)00154-5

Bales KL, Van Westerhuyzen JA, Lewis-Reese AD, et al (2007) Oxytocin has dose-dependent developmental effects on pair-bonding and alloparental care in female prairie voles. Hormones and Behavior 52:274–279. https://doi.org/10.1016/j.yhbeh.2007.05.004

Bergquist F, Ludwig M (2008) Dendritic Transmitter Release: A Comparison of Two Model Systems. J Neuroendocrinology 20:677–686. https://doi.org/10.1111/j.1365-2826.2008.01714.x

Borland JM, Rilling JK, Frantz KJ, Albers HE (2019) Sex-dependent regulation of social reward by oxytocin: an inverted U hypothesis. Neuropsychopharmacol 44:97–110. https://doi.org/10.1038/s41386-018-0129-2

Borroto-Escuela DO, Romero-Fernandez W, Garriga P, et al (2013) G Protein–Coupled Receptor Heterodimerization in the Brain. In: Methods in Enzymology. Elsevier, pp 281–294

Bosch OJ, Dabrowska J, Modi ME, et al (2016) Oxytocin in the nucleus accumbens shell reverses CRFR2-evoked passive stress-coping after partner loss in monogamous male prairie voles. Psychoneuroendocrinology 64:66–78. https://doi.org/10.1016/j.psyneuen.2015.11.011

Bosch OJ, Meddle SL, Beiderbeck DI, et al (2005) Brain Oxytocin Correlates with Maternal Aggression: Link to Anxiety. J Neurosci 25:6807–6815. https://doi.org/10.1523/JNEUROSCI.1342-05.2005

Bredewold R, Smith CJW, Dumais KM, Veenema AH (2014) Sex-specific modulation of juvenile social play behavior by vasopressin and oxytocin depends on social context. Front Behav Neurosci 8:. https://doi.org/10.3389/fnbeh.2014.00216

Brinker T, Stopa E, Morrison J, Klinge P (2014) A new look at cerebrospinal fluid circulation. Fluids Barriers CNS 11:10. https://doi.org/10.1186/2045-8118-11-10

Brown CH, Bains JS, Ludwig M, Stern JE (2013) Physiological Regulation of Magnocellular Neurosecretory Cell Activity: Integration of Intrinsic, Local and Afferent Mechanisms. J Neuroendocrinology 25:678–710. https://doi.org/10.1111/jne.12051

Brown CH, Ludwig M, Tasker JG, Stern JE (2020) Somato-dendritic vasopressin and oxytocin secretion in endocrine and autonomic regulation. J Neuroendocrinol 32:e12856. https://doi.org/10.1111/jne.12856

Brownstein MJ (1983) Biosynthesis of Vasopressin and Oxytocin. Annu Rev Physiol 45:129–135. https://doi.org/10.1146/annurev.ph.45.030183.001021

Brownstein MJ, Russell JT, Gainer H (1980) Synthesis, Transport, and Release of Posterior Pituitary Hormones. Science 207:373–378. https://doi.org/10.1126/science.6153132

Buma P, Roubos EW, Buijs RM (1984) Ultrastructural demonstration of exocytosis of neural, neuroendocrine and endocrine secretions with an in vitro tannic acid (TARI-) method. Histochemistry 80:247–256. https://doi.org/10.1007/BF00495773

Burbach, J. P., Young, L. J., & Russell, J. (2006) Oxytocin: synthesis, secretion, and reproductive functions. Knobil and Neill's physiology of reproduction, 2:3055-3128.

Burkett JP, Andari E, Johnson ZV, et al (2016) Oxytocin-dependent consolation behavior in rodents. Science 351:375–378. https://doi.org/10.1126/science.aac4785

Busnelli, M., & Chini, B. (2018) Molecular basis of oxytocin receptor signalling in the brain: what we know and what we need to know. Behavioral pharmacology of neuropeptides: Oxytocin 3-29.

Calcagnoli F, De Boer SF, Beiderbeck DI, et al (2014) Local oxytocin expression and oxytocin receptor binding in the male rat brain is associated with aggressiveness. Behavioural Brain Research 261:315–322. https://doi.org/10.1016/j.bbr.2013.12.050

Caldwell HK, Aulino EA, Freeman AR, et al (2017) Oxytocin and behavior: Lessons from knockout mice. Developmental Neurobiology 77:190–201. https://doi.org/10.1002/dneu.22431

Carcea I, Caraballo NL, Marlin BJ, et al (2021) Oxytocin neurons enable social transmission of maternal behaviour. Nature 596:553–557. https://doi.org/10.1038/s41586-021-03814-7

Carter CS (2022) Sex, love and oxytocin: Two metaphors and a molecule. Neuroscience & Biobehavioral Reviews 143:104948. https://doi.org/10.1016/j.neubiorev.2022.104948

Carter CS (1992) Oxytocin and sexual behavior. Neuroscience & Biobehavioral Reviews 16:131–144. https://doi.org/10.1016/S0149-7634(05)80176-9

Carter CS, Kenkel WM, MacLean EL, et al (2020) Is Oxytocin "Nature's Medicine"? Pharmacol Rev 72:829–861. https://doi.org/10.1124/pr.120.019398

Carter CS, Perkeybile AM (2018) The Monogamy Paradox: What Do Love and Sex Have to Do With It? Front Ecol Evol 6:202. https://doi.org/10.3389/fevo.2018.00202

Champagne FA (2004) Variations in Nucleus Accumbens Dopamine Associated with Individual Differences in Maternal Behavior in the Rat. Journal of Neuroscience 24:4113–4123. https://doi.org/10.1523/JNEUROSCI.5322-03.2004

Chang SWC, Barter JW, Ebitz RB, et al (2012) Inhaled oxytocin amplifies both vicarious reinforcement and self reinforcement in rhesus macaques (*Macaca mulatta*). Proc Natl Acad Sci USA 109:959–964. https://doi.org/10.1073/pnas.1114621109

Chang SWC, Platt ML (2014) Oxytocin and social cognition in rhesus macaques: Implications for understanding and treating human psychopathology. Brain Research 1580:57–68. https://doi.org/10.1016/j.brainres.2013.11.006

Chen S, Xu H, Dong S, Xiao L (2022) Morpho-Electric Properties and Diversity of Oxytocin Neurons in Paraventricular Nucleus of Hypothalamus in Female and Male Mice. J Neurosci 42:2885–2904. https://doi.org/10.1523/JNEUROSCI.2494-21.2022

Chini B, Verhage M, Grinevich V (2017) The Action Radius of Oxytocin Release in the Mammalian CNS: From Single Vesicles to Behavior. Trends in Pharmacological Sciences 38:982–991. https://doi.org/10.1016/j.tips.2017.08.005

Cho MM, DeVries AC, Williams JR, Carter CS (1999) The effects of oxytocin and vasopressin on partner preferences in male and female prairie voles (Microtus ochrogaster). Behavioral Neuroscience 113:1071–1079. https://doi.org/10.1037/0735-7044.113.5.1071

Colonnier M (1968) Synaptic patterns on different cell types in the different laminae of the cat visual cortex. An electron microscope study. Brain Research 9:268–287. https://doi.org/10.1016/0006-8993(68)90234-5

Crowley WR, Armstrong WE (1992) Neurochemical Regulation of Oxytocin Secretion in Lactation. 13:

Czarniak N, Kamińska J, Matowicka-Karna J, Koper-Lenkiewicz O (2023) Cerebrospinal Fluid–Basic Concepts Review. Biomedicines 11:1461. https://doi.org/10.3390/biomedicines11051461

Dabrowska J, Hazra R, Ahern TH, et al (2011) Neuroanatomical evidence for reciprocal regulation of the corticotrophin-releasing factor and oxytocin systems in the hypothalamus and the bed nucleus of the stria terminalis of the rat: Implications for balancing stress and affect. Psychoneuroendocrinology 36:1312–1326. https://doi.org/10.1016/j.psyneuen.2011.03.003

Dale HH (1906) On some physiological actions of ergot. The Journal of Physiology 34:163–206. https://doi.org/10.1113/jphysiol.1906.sp001148

Danoff JS, Page EA, Perkeybile AM, et al (2023a) Transcriptional diversity of the oxytocin receptor in prairie voles: mechanistic implications for behavioral neuroscience and maternal physiology. Front Genet 14:. https://doi.org/10.3389/fgene.2023.1225197

Danoff JS, Ramos EN, Hinton TD, et al (2023b) Father's care uniquely influences male neurodevelopment. Proc Natl Acad Sci USA 120:e2308798120. https://doi.org/10.1073/pnas.2308798120

Danoff JS, Wroblewski KL, Graves AJ, et al (2021) Genetic, epigenetic, and environmental factors controlling oxytocin receptor gene expression. Clin Epigenet 13:23. https://doi.org/10.1186/s13148-021-01017-5

Davidovich C, Belousoff M, Bashan A, Yonath A (2009) The evolving ribosome: from non-coded peptide bond formation to sophisticated translation machinery. Research in Microbiology 160:487–492. https://doi.org/10.1016/j.resmic.2009.07.004

Deng S, Gan L, Liu C, et al (2023) Roles of Ependymal Cells in the Physiology and Pathology of the Central Nervous System. Aging Dis 14:468–483. https://doi.org/10.14336/AD.2022.0826-1

Domes G, Heinrichs M, Michel A, et al (2007) Oxytocin Improves "Mind-Reading" in Humans. Biological Psychiatry 61:731–733. https://doi.org/10.1016/j.biopsych.2006.07.015

Einspanier A, Ivell R (1997) Oxytocin and Oxytocin Receptor Expression in Reproductive Tissues of the Male Marmoset Monkey1. Biology of Reproduction 56:416–422. https://doi.org/10.1095/biolreprod56.2.416

Eliava M, Melchior M, Knobloch-Bollmann HS, et al (2016) A New Population of Parvocellular Oxytocin Neurons Controlling Magnocellular Neuron Activity and Inflammatory Pain Processing. Neuron 89:1291–1304. https://doi.org/10.1016/j.neuron.2016.01.041

Ferris CF, Yee JR, Kenkel WM, et al (2015) Distinct BOLD Activation Profiles Following Central and Peripheral Oxytocin Administration in Awake Rats. Frontiers in Behavioral Neuroscience 9:

Finton CJ, Kelly AM, Ophir AG (2022) Support for the parental practice hypothesis: Subadult prairie voles exhibit similar behavioral and neural profiles when alloparenting kin and non-kin. Behavioural Brain Research 417:113571. https://doi.org/10.1016/j.bbr.2021.113571

Francis DD, Champagne FC, Meaney MJ (2000) Variations in Maternal Behaviour are Associated with Differences in Oxytocin Receptor Levels in the Rat. J Neuroendocrinology 12:1145–1148. https://doi.org/10.1046/j.1365-2826.2000.00599.x

Freda SN, Priest MF, Badong D, et al (2022) Brainwide input-output architecture of paraventricular oxytocin and vasopressin neurons. 2022.01.17.476652

Freeman SM, Samineni S, Allen PC, et al (2016) Plasma and CSF oxytocin levels after intranasal and intravenous oxytocin in awake macaques. Psychoneuroendocrinology 66:185–194. https://doi.org/10.1016/j.psyneuen.2016.01.014

Fuchs A-R, Fuchs F, Husslein P, Soloff MS (1984a) Oxytocin receptors in the human uterus during pregnancy and parturition. American Journal of Obstetrics and Gynecology 150:734–741. https://doi.org/10.1016/0002-9378(84)90677-X

Fuchs A-R, Fuchs F, Husslein P, Soloff MS (1984b) Oxytocin receptors in the human uterus during pregnancy and parturition. American Journal of Obstetrics and Gynecology 150:734–741. https://doi.org/10.1016/0002-9378(84)90677-X

Fuentes N, Silveyra P (2019) Estrogen receptor signaling mechanisms. In: Advances in Protein Chemistry and Structural Biology. Elsevier, pp 135–170

Fuxe K, O. Borroto-Escuela D, Marcellino D, et al (2012) GPCR Heteromers and their Allosteric Receptor-Receptor Interactions. CMC 19:356–363. https://doi.org/10.2174/092986712803414259

Gainer H, Sarne Y, Brownstein MJ (1977) Biosynthesis and axonal transport of rat neurohypophysial proteins and peptides. The Journal of cell biology 73:366–381. https://doi.org/10.1083/jcb.73.2.366

Getz LL, Carter CS, Gavish L (1981) The mating system of the prairie vole, Microtus ochrogaster: Field and laboratory evidence for pair-bonding. Behav Ecol Sociobiol 8:189–194. https://doi.org/10.1007/BF00299829

Giannotti G, Mottarlini F, Heinsbroek JA, et al (2022) Oxytocin and orexin systems bidirectionally regulate the ability of opioid cues to bias reward seeking. Transl Psychiatry 12:432. https://doi.org/10.1038/s41398-022-02161-z

Gimpl G, Fahrenholz F (2001) The Oxytocin Receptor System: Structure, Function, and Regulation. Physiological Reviews 81:629–683. https://doi.org/10.1152/physrev.2001.81.2.629

Gregory SG, Connelly JJ, Towers AJ, et al (2009) Genomic and epigenetic evidence for oxytocin receptor deficiency in autism. BMC Med 7:62. https://doi.org/10.1186/1741-7015-7-62

Grinevich V, Dobolyi Árpád (2022) Neuroanatomy of Neuroendocrine Systems. Springer International Publishing AG, Cham

Grinevich V, Ludwig M (2021) The multiple faces of the oxytocin and vasopressin systems in the brain. J Neuroendocrinology 33:e13004. https://doi.org/10.1111/jne.13004

Hasan MT, Althammer F, Silva Da Gouveia M, et al (2019) A Fear Memory Engram and Its Plasticity in the Hypothalamic Oxytocin System. Neuron 103:133-146.e8. https://doi.org/10.1016/j.neuron.2019.04.029

Hernández-Mondragón JC, Hernández-Hernández DA, Crespo-Ramírez M, et al (2023) Evidence for the existence of facilitatory interactions between the dopamine D2 receptor and the oxytocin receptor in the amygdala of the rat. Relevance for anxiolytic actions. Front Pharmacol 14:1251922. https://doi.org/10.3389/fphar.2023.1251922

Hilger D, Masureel M, Kobilka BK (2018) Structure and dynamics of GPCR signaling complexes. Nat Struct Mol Biol 25:4–12. https://doi.org/10.1038/s41594-017-0011-7

Hurlemann R, Grinevich V (eds) (2018) Behavioral Pharmacology of Neuropeptides: Oxytocin. Springer International Publishing, Cham

Hurlemann R, Patin A, Onur OA, et al (2010) Oxytocin Enhances Amygdala-Dependent, Socially Reinforced Learning and Emotional Empathy in Humans. J Neurosci 30:4999–5007. https://doi.org/10.1523/JNEUROSCI.5538-09.2010

Iftinca MC, Zamponi GW (2009) Regulation of neuronal T-type calcium channels. Trends in Pharmacological Sciences 30:32–40. https://doi.org/10.1016/j.tips.2008.10.004

Inoue K, Ford CL, Horie K, Young LJ (2022) Oxytocin receptors are widely distributed in the prairie vole (Microtus ochrogaster) brain: Relation to social behavior, genetic polymorphisms, and the dopamine system. Journal of Comparative Neurology 530:2881–2900. https://doi.org/10.1002/cne.25382

Inoue T, Kimura T, Azuma C, et al (1994) Structural organization of the human oxytocin receptor gene. Journal of Biological Chemistry 269:32451–32456. https://doi.org/10.1016/S0021-9258(18)31656-9

Insel TR, Shapiro LE (1992) Oxytocin receptor distribution reflects social organization in monogamous and polygamous voles. Proc Natl Acad Sci USA 89:5981–5985. https://doi.org/10.1073/pnas.89.13.5981

Jankowski M, Broderick TL, Gutkowska J (2020) The Role of Oxytocin in Cardiovascular Protection. Front Psychol 11:2139. https://doi.org/10.3389/fpsyg.2020.02139

Jankowski M, Hajjar F, Kawas SA, et al (1998) Rat heart: A site of oxytocin production and action. Proc Natl Acad Sci USA 95:14558–14563. https://doi.org/10.1073/pnas.95.24.14558

Jirikowski GF (2019) Diversity of central oxytocinergic projections. Cell Tissue Res 375:41–48. https://doi.org/10.1007/s00441-018-2960-5

John S, Jaeggi AV (2021) Oxytocin levels tend to be lower in autistic children: A meta-analysis of 31 studies. Autism 25:2152–2161. https://doi.org/10.1177/13623613211034375

de Jong, T. R., & Neumann, I. D. (2018) Oxytocin and aggression. Behavioral pharmacology of neuropeptides: oxytocin, 175-192.

Jurek B, Neumann ID (2018) The Oxytocin Receptor: From Intracellular Signaling to Behavior. Physiological Reviews 98:1805–1908. https://doi.org/10.1152/physrev.00031.2017

Kagerbauer SM, Martin J, Schuster T, et al (2013) Plasma Oxytocin and Vasopressin do not Predict Neuropeptide Concentrations in Human Cerebrospinal Fluid. Journal of Neuroendocrinology 25:668–673. https://doi.org/10.1111/jne.12038

Keebaugh AC, Barrett CE, Laprairie JL, et al (2015) RNAi knockdown of oxytocin receptor in the nucleus accumbens inhibits social attachment and parental care in monogamous female prairie voles. Social Neuroscience 10:561–570. https://doi.org/10.1080/17470919.2015.1040893

Keebaugh AC, Young LJ (2011) Increasing oxytocin receptor expression in the nucleus accumbens of pre-pubertal female prairie voles enhances alloparental responsiveness and partner preference formation as adults. Hormones and Behavior 60:498–504. https://doi.org/10.1016/j.yhbeh.2011.07.018

Kelly AM, Hiura LC, Ophir AG (2018) Rapid nonapeptide synthesis during a critical period of development in the prairie vole: plasticity of the paraventricular nucleus of the hypothalamus. Brain Struct Funct 223:2547–2560. https://doi.org/10.1007/s00429-018-1640-2

Kenkel WM, Gustison ML, Beery AK (2021) A Neuroscientist's Guide to the Vole. Current Protocols 1:e175. https://doi.org/10.1002/cpz1.175

Kenkel WM, Perkeybile AM, Carter CS (2017) The neurobiological causes and effects of alloparenting. Developmental Neurobiology 77:214–232. https://doi.org/10.1002/dneu.22465

Kenkel WM, Perkeybile A-M, Yee JR, et al (2019) Behavioral and epigenetic consequences of oxytocin treatment at birth. Sci Adv 5:eaav2244. https://doi.org/10.1126/sciadv.aav2244

Kimura T, Tanizawa O, Mori K, et al (1992) Structure and expression of a human oxytocin receptor. Nature 356:526–529. https://doi.org/10.1038/356526a0

Knobloch HS, Charlet A, Hoffmann LC, et al (2012) Evoked Axonal Oxytocin Release in the Central Amygdala Attenuates Fear Response. Neuron 73:553–566. https://doi.org/10.1016/j.neuron.2011.11.030

Knobloch HS, Grinevich V (2014) Evolution of oxytocin pathways in the brain of vertebrates. Front Behav Neurosci 8:. https://doi.org/10.3389/fnbeh.2014.00031

Landgraf R, Neumann I, Schwarzberg H (1988) Central and peripheral release of vasopressin and oxytocin in the conscious rat after osmotic stimulation. Brain Research 457:219–225. https://doi.org/10.1016/0006-8993(88)90689-0

Lee H-J, Macbeth AH, Pagani J, Young WS (2009) Oxytocin: The Great Facilitator of Life. Progress in Neurobiology S030100820900046X. https://doi.org/10.1016/j.pneurobio.2009.04.001

Lee MR, Scheidweiler KB, Diao XX, et al (2018) Oxytocin by intranasal and intravenous routes reaches the cerebrospinal fluid in rhesus macaques: determination using a novel oxytocin assay. Mol Psychiatry 23:115–122. https://doi.org/10.1038/mp.2017.27

Lefevre A, Mottolese R, Dirheimer M, et al (2017) A comparison of methods to measure central and peripheral oxytocin concentrations in human and non-human primates. Sci Rep 7:17222. https://doi.org/10.1038/s41598-017-17674-7

Leng G, Caquineau C, Sabatier N (2005) Regulation of Oxytocin Secretion. In: Vitamins & Hormones. Elsevier, pp 27–58

Leng G, Ludwig M (2016) Intranasal Oxytocin: Myths and Delusions. Biological Psychiatry 79:243–250. https://doi.org/10.1016/j.biopsych.2015.05.003

Leng G, Ludwig M (2008) Neurotransmitters and peptides: whispered secrets and public announcements. The Journal of Physiology 586:5625–5632. https://doi.org/10.1113/jphysiol.2008.159103

Lewis EM, Stein-O'Brien GL, Patino AV, et al (2020) Parallel Social Information Processing Circuits Are Differentially Impacted in Autism. Neuron 108:659-675.e6. https://doi.org/10.1016/j.neuron.2020.10.002

Li H, Jiang T, An S, et al (2024) Single-neuron projectomes of mouse paraventricular hypothalamic nucleus oxytocin neurons reveal mutually exclusive projection patterns. Neuron 112:1081-1099.e7. https://doi.org/10.1016/j.neuron.2023.12.022

Liao P-Y, Chiu Y-M, Yu J-H, Chen S-K (2020) Mapping Central Projection of Oxytocin Neurons in Unmated Mice Using Cre and Alkaline Phosphatase Reporter. Frontiers in Neuroanatomy 14:

Liu CM, Hsu TM, Suarez AN, et al (2020) Central oxytocin signaling inhibits food reward-motivated behaviors and VTA dopamine responses to food-predictive cues in male rats. Hormones and Behavior 126:104855. https://doi.org/10.1016/j.yhbeh.2020.104855

Loichot C, Krieger J-P, De Jong W, et al (2001) High concentrations of oxytocin cause vasoconstriction by activating vasopressin V 1A receptors in the isolated perfused rat kidney. Naunyn-Schmiedeberg's Archives of Pharmacology 363:369–375. https://doi.org/10.1007/s002100000372

Lonstein, De Vries (1999) Sex Differences in the Parental Behaviour of Adult Virgin Prairie Voles: Independence From Gonadal Hormones and Vasopressin. Journal of Neuroendocrinology 11:441–449. https://doi.org/10.1046/j.1365-2826.1999.00361.x

Ludwig M, Leng G (2006) Dendritic peptide release and peptide-dependent behaviours. Nat Rev Neurosci 7:126–136. https://doi.org/10.1038/nrn1845

Ludwig M, Sabatier N, Bull PM, et al (2002) Intracellular calcium stores regulate activity-dependent neuropeptide release from dendrites. Nature 418:85–89. https://doi.org/10.1038/nature00822

Lukas D, Clutton-Brock TH (2013) The Evolution of Social Monogamy in Mammals. Science 341:526–530. https://doi.org/10.1126/science.1238677

Lukas M, Toth I, Reber SO, et al (2011) The Neuropeptide Oxytocin Facilitates Pro-Social Behavior and Prevents Social Avoidance in Rats and Mice. Neuropsychopharmacol 36:2159–2168. https://doi.org/10.1038/npp.2011.95

Luther, J. A., & Tasker, J. G. (2000) Voltage-gated currents distinguish parvocellular from magnocellular neurones in the rat hypothalamic paraventricular nucleus. The Journal of Physiology, 523:193-209. https://doi.org/10.1111/j.1469-7793.2000.t01-1-00193.x

Ma Q, Ineichen BV, Detmar M, Proulx ST (2017) Outflow of cerebrospinal fluid is predominantly through lymphatic vessels and is reduced in aged mice. Nat Commun 8:1434. https://doi.org/10.1038/s41467-017-01484-6

Mabry KE, Streatfeild CA, Keane B, Solomon NG (2011) avpr1a length polymorphism is not associated with either social or genetic monogamy in free-living prairie voles. Animal Behaviour 81:11–18. https://doi.org/10.1016/j.anbehav.2010.09.021

Makani V, Sultana R, Sie KS, et al (2013) Annexin A1 Complex Mediates Oxytocin Vesicle Transport. J Neuroendocrinology 25:1241–1254. https://doi.org/10.1111/jne.12112

Manjila SB, Betty R, Kim Y (2022) Missing pieces in decoding the brain oxytocin puzzle: Functional insights from mouse brain wiring diagrams. Frontiers in Neuroscience 16:

Marlin BJ, Mitre M, D'amour JA, et al (2015) Oxytocin enables maternal behaviour by balancing cortical inhibition. Nature 520:499–504. https://doi.org/10.1038/nature14402

Martin J, Kagerbauer SM, Gempt J, et al (2018) Oxytocin levels in saliva correlate better than plasma levels with concentrations in the cerebrospinal fluid of patients in neurocritical care. J Neuroendocrinology 30:e12596. https://doi.org/10.1111/jne.12596

Masson J, Sagne C, Hamon M, Mestikawy SE Neurotransmitter Transporters in the Central Nervous System

Menon R, Neumann ID (2023) Detection, processing and reinforcement of social cues: regulation by the oxytocin system. Nature Reviews Neuroscience 24:

Mens WBJ, Witter A, Van Wimersma Greidanus TB (1983) Penetration of neurohypophyseal hormones from plasma into cerebrospinal fluid (CSF): Half-times of disappearance of these neuropeptides from CSF. Brain Research 262:143–149. https://doi.org/10.1016/0006-8993(83)90478-X

Meyerowitz JG, Robertson MJ, Barros-Álvarez X, et al (2022) The oxytocin signaling complex reveals a molecular switch for cation dependence. Nat Struct Mol Biol 29:274–281. https://doi.org/10.1038/s41594-022-00728-4

Mitre M, Minder J, Morina EX, et al (2018) Oxytocin Modulation of Neural Circuits. In: Hurlemann R, Grinevich V (eds) Behavioral Pharmacology of Neuropeptides: Oxytocin. Springer International Publishing, Cham, pp 31–53

Moaddab M, Hyland BI, Brown CH (2015) Oxytocin excites nucleus accumbens shell neurons in vivo. Molecular and Cellular Neuroscience 68:323–330. https://doi.org/10.1016/j.mcn.2015.08.013

Modahl C, Green LA, Fein D, et al (1998) Plasma oxytocin levels in autistic children. Biological Psychiatry 43:270–277. https://doi.org/10.1016/S0006-3223(97)00439-3

Moore DS (2017) Behavioral epigenetics. WIREs Mechanisms of Disease 9:e1333. https://doi.org/10.1002/wsbm.1333

Morris JF, Pow DV (1988) Capturing and Quantifying the Exocytotic Event. Journal of Experimental Biology 139:81–103. https://doi.org/10.1242/jeb.139.1.81

Neumann, I. N. G. A., Koehler, E. L. L. E. N., Landgraf, R. A. I. N. E. R., & Summy-Long, J. O. A. N. (1994) An oxytocin receptor antagonist infused into the supraoptic nucleus attenuates intranuclear and peripheral release of oxytocin during suckling in conscious rats. Endocrinology 134:141-148. https://doi.org/10.1210/en.134.1.141

Neumann I, Russell JA, Landgraf R (1993) Oxytocin and vasopressin release within the supraoptic and paraventricular nuclei of pregnant, parturient and lactating rats: A microdialysis study. Neuroscience 53:65–75. https://doi.org/10.1016/0306-4522(93)90285-N

Neumann I, Schwarzberg H, Landgraf R (1988) Measurement of septal release of vasopressin and oxytocin by the push-pull technique following electrical stimulation of the paraventricular nucleus of rats. Brain Research 462:181–184. https://doi.org/10.1016/0006-8993(88)90603-8

Newmaster KT, Nolan ZT, Chon U, et al (2020) Quantitative cellular-resolution map of the oxytocin receptor in postnatally developing mouse brains. Nat Commun 11:1885. https://doi.org/10.1038/s41467-020-15659-1

Nishimura K, Yoshino K, Ikeda N, et al (2022) Oestrogen-dependent hypothalamic oxytocin expression with changes in feeding and body weight in female rats. Commun Biol 5:912. https://doi.org/10.1038/s42003-022-03889-6

Numan M (2007) Motivational systems and the neural circuitry of maternal behavior in the rat. Developmental Psychobiology 49:12–21. https://doi.org/10.1002/dev.20198

Numan M, Stolzenberg DS (2009) Medial preoptic area interactions with dopamine neural systems in the control of the onset and maintenance of maternal behavior in rats. Frontiers in Neuroendocrinology 30:46–64. https://doi.org/10.1016/j.yfrne.2008.10.002

Olazábal DE, Young LJ (2006a) Species and individual differences in juvenile female alloparental care are associated with oxytocin receptor density in the striatum and the lateral septum. Hormones and Behavior 49:681–687. https://doi.org/10.1016/j.yhbeh.2005.12.010

Olazábal DE, Young LJ (2006b) Oxytocin receptors in the nucleus accumbens facilitate "spontaneous" maternal behavior in adult female prairie voles. Neuroscience 141:559–568. https://doi.org/10.1016/j.neuroscience.2006.04.017

Olff M, Frijling JL, Kubzansky LD, et al (2013) The role of oxytocin in social bonding, stress regulation and mental health: An update on the moderating effects of context and interindividual differences. Psychoneuroendocrinology 38:1883–1894. https://doi.org/10.1016/j.psyneuen.2013.06.019

Otero-García M, Agustín-Pavón C, Lanuza E, Martínez-García F (2016) Distribution of oxytocin and co-localization with arginine vasopressin in the brain of mice. Brain Struct Funct 221:3445–3473. https://doi.org/10.1007/s00429-015-1111-y

Oti T, Satoh K, Uta D, et al (2021) Oxytocin Influences Male Sexual Activity via Non-synaptic Axonal Release in the Spinal Cord. Current Biology 31:103-114.e5. https://doi.org/10.1016/j.cub.2020.09.089

Ozawa S, Sand O (1986) Electrophysiology of excitable endocrine cells. Physiological Reviews 66:887–952. https://doi.org/10.1152/physrev.1986.66.4.887

Oztan O, Garner JP, Partap S, et al (2018) Cerebrospinal fluid vasopressin and symptom severity in children with autism. Annals of Neurology 84:611–615. https://doi.org/10.1002/ana.25314

Patisaul HB, Scordalakes EM (2003) Oxytocin, But Not Oxytocin Receptor, is Regulated by Oestrogen Receptor b in the Female Mouse Hypothalamus. Journal of Neuroendocrinology

Patri M (2019) Synaptic Transmission and Amino Acid Neurotransmitters. In: Heinbockel T, B. Csoka A (eds) Neurochemical Basis of Brain Function and Dysfunction. IntechOpen

Pedersen CA, Ascher JA, Monroe YL, Prange AJ (1982) Oxytocin Induces Maternal Behavior in Virgin Female Rats. Science 216:648–650. https://doi.org/10.1126/science.7071605

Pedersen CA, Prange AJ (1979) Induction of maternal behavior in virgin rats after intracerebroventricular administration of oxytocin. Proceedings of the National Academy of Sciences 76:6661–6665. https://doi.org/10.1073/pnas.76.12.6661

Perkeybile AM, Carter CS, Wroblewski KL, et al (2019) Early nurture epigenetically tunes the oxytocin receptor. Psychoneuroendocrinology 99:128–136. https://doi.org/10.1016/j.psyneuen.2018.08.037

Perkeybile AM, Delaney-Busch N, Hartman S, et al (2015) Intergenerational transmission of alloparental behavior and oxytocin and vasopressin receptor distribution in the prairie vole. Front Behav Neurosci 9:. https://doi.org/10.3389/fnbeh.2015.00191

Perkinson MR, Kim JS, Iremonger KJ, Brown CH (2021) Visualising oxytocin neurone activity in vivo: The key to unlocking central regulation of parturition and lactation. J Neuroendocrinology 33:e13012. https://doi.org/10.1111/jne.13012

Peters A, Palay SL (1996) The morphology of synapses. J Neurocytol 25:687–700. https://doi.org/10.1007/BF02284835

Post RM, Gold P, Rubinow DR, et al (1982) PEPTIDES IN THE CEREBROSPINAL FLUID OF NEUROPSYCHIATRIC PATIENTS: AN APPROACH m CENTRAL NERVOUS SYSTEM PEPTIDE FUNCTION. 31:

Pow DV, Morris JF (1989) Dendrites of hypothalamic magnocellular neurons release neurohypophysial peptides by exocytosis. Neuroscience 32:435–439. https://doi.org/10.1016/0306-4522(89)90091-2

Puglia MH, Lillard TS, Morris JP, Connelly JJ (2015) Epigenetic modification of the oxytocin receptor gene influences the perception of anger and fear in the human brain. Proc Natl Acad Sci USA 112:3308–3313. https://doi.org/10.1073/pnas.1422096112

Putnam PT, Young LJ, Gothard KM (2018) Bridging the gap between rodents and humans: The role of non-human primates in oxytocin research. American J Primatol 80:e22756. https://doi.org/10.1002/ajp.22756

Qian T, Wang H, Wang P, et al (2023) A genetically encoded sensor measures temporal oxytocin release from different neuronal compartments. Nat Biotechnol 41:944–957. https://doi.org/10.1038/s41587-022-01561-2

Quintana DS, Lischke A, Grace S, et al (2021) Advances in the field of intranasal oxytocin research: lessons learned and future directions for clinical research. Mol Psychiatry 26:80–91. https://doi.org/10.1038/s41380-020-00864-7

Quintana DS, Rokicki J, Van Der Meer D, et al (2019) Oxytocin pathway gene networks in the human brain. Nat Commun 10:668. https://doi.org/10.1038/s41467-019-08503-8

Rhodes, C. H., Morriell, J. I., Pfaff, D. W. (1981) Immunohistochemical analysis of magnocellular elements in rat hypothalamus: distribution and numbers of cells containing neurophysin, oxytocin, and vasopressin. Journal of Comparative Neurology 198:45-64. https://doi.org/10.1002/cne.901980106

Richard S, Zingg HH (1990) The human oxytocin gene promoter is regulated by estrogens. Journal of Biological Chemistry 265:6098–6103. https://doi.org/10.1016/S0021-9258(19)39297-X

Rogers FD, Bales KL (2019) Mothers, Fathers, and Others: Neural Substrates of Parental Care. Trends in Neurosciences 42:552–562. https://doi.org/10.1016/j.tins.2019.05.008

Ross HE, Freeman SM, Spiegel LL, et al (2009) Variation in Oxytocin Receptor Density in the Nucleus Accumbens Has Differential Effects on Affiliative Behaviors in Monogamous and Polygamous Voles. J Neurosci 29:1312–1318. https://doi.org/10.1523/JNEUROSCI.5039-08.2009

Ross HE, Young LJ (2009) Oxytocin and the neural mechanisms regulating social cognition and affiliative behavior. Frontiers in Neuroendocrinology 30:534–547. https://doi.org/10.1016/j.yfrne.2009.05.004

Rossoni E, Feng J, Tirozzi B, et al (2008) Emergent Synchronous Bursting of Oxytocin Neuronal Network. PLoS Comput Biol 4:e1000123. https://doi.org/10.1371/journal.pcbi.1000123

Roy RK, Augustine RA, Brown CH, Schwenke DO (2018) Activation of oxytocin neurons in the paraventricular nucleus drives cardiac sympathetic nerve activation following myocardial infarction in rats. Commun Biol 1:160. https://doi.org/10.1038/s42003-018-0169-5

Sabihi S, Dong SM, Durosko NE, Leuner B (2014a) Oxytocin in the medial prefrontal cortex regulates maternal care, maternal aggression and anxiety during the postpartum period. Front Behav Neurosci 8:. https://doi.org/10.3389/fnbeh.2014.00258

Sabihi S, Durosko NE, Dong SM, Leuner B (2014b) Oxytocin in the prelimbic medial prefrontal cortex reduces anxiety-like behavior in female and male rats. Psychoneuroendocrinology 45:31–42. https://doi.org/10.1016/j.psyneuen.2014.03.009

Sakka L, Coll G, Chazal J (2011) Anatomy and physiology of cerebrospinal fluid. European Annals of Otorhinolaryngology, Head and Neck Diseases 128:309–316. https://doi.org/10.1016/j.anorl.2011.03.002

Shahrokh DK, Zhang T-Y, Diorio J, et al (2010) Oxytocin-Dopamine Interactions Mediate Variations in Maternal Behavior in the Rat. Endocrinology 151:2276–2286. https://doi.org/10.1210/en.2009-1271

Smith AS, Ågmo A, Birnie AK, French JA (2010) Manipulation of the oxytocin system alters social behavior and attraction in pair-bonding primates, Callithrix penicillata. Hormones and Behavior 57:255–262. https://doi.org/10.1016/j.yhbeh.2009.12.004

Smith CJW, DiBenedictis BT, Veenema AH (2019) Comparing vasopressin and oxytocin fiber and receptor density patterns in the social behavior neural network: Implications for cross-system signaling. Frontiers in Neuroendocrinology 53:100737. https://doi.org/10.1016/j.yfrne.2019.02.001

Soloff MS, Alexandrova M, Fernstrom MJ (1979) Oxytocin Receptors: Triggers for Parturition and Lactation? Science 204:1313–1315. https://doi.org/10.1126/science.221972

Son S, Manjila SB, Newmaster KT, et al (2022) Whole-Brain Wiring Diagram of Oxytocin System in Adult Mice. J Neurosci 42:5021–5033. https://doi.org/10.1523/JNEUROSCI.0307-22.2022

Stern JE, Armstrong WE (1998) Reorganization of the Dendritic Trees of Oxytocin and Vasopressin Neurons of the Rat Supraoptic Nucleus during Lactation. J Neurosci 18:841–853. https://doi.org/10.1523/JNEUROSCI.18-03-00841.1998

Summerlee AJ (1981) Extracellular recordings from oxytocin neurones during the expulsive phase of birth in unanaesthetized rats. The Journal of Physiology 321:1–9. https://doi.org/10.1113/jphysiol.1981.sp013967

Swanson LW, Sawchenko PE (1983) Hypothalamic Integration: Organization of the Paraventricular and Supraoptic Nuclei. Annu Rev Neurosci 6:269–324. https://doi.org/10.1146/annurev.ne.06.030183.001413

Tang Y, Benusiglio D, Lefevre A, et al (2020) Social touch promotes interfemale communication via activation of parvocellular oxytocin neurons. Nat Neurosci 23:1125–1137. https://doi.org/10.1038/s41593-020-0674-y

Teng BL, Nonneman RJ, Agster KL, et al (2013) Prosocial effects of oxytocin in two mouse models of autism spectrum disorders. Neuropharmacology 72:187–196. https://doi.org/10.1016/j.neuropharm.2013.04.038

Terrillon S, Durroux T, Mouillac B, et al (2003) Oxytocin and Vasopressin V1a and V2 Receptors Form Constitutive Homo- and Heterodimers during Biosynthesis. Molecular Endocrinology 17:677–691. https://doi.org/10.1210/me.2002-0222

Tuteja, N. (2009) Signaling through G protein coupled receptors. Plant signaling & behavior 4: 942-947. https://doi.org/10.4161/psb.4.10.9530

Tweedle CD, Smithson KG, Hatton GI (1989) Neurosecretory endings in the rat neurohypophysis are *en passant*. Experimental Neurology 106:20–26. https://doi.org/10.1016/0014-4886(89)90140-4

Valstad M, Alvares GA, Egknud M, et al (2017) The correlation between central and peripheral oxytocin concentrations: A systematic review and meta-analysis. Neuroscience & Biobehavioral Reviews 78:117–124. https://doi.org/10.1016/j.neubiorev.2017.04.017

Vanderwall DK, Rasmussen DM, Carnahan KG, Davis TL (2012) Effect of Administration of Oxytocin During Diestrus on Corpus Luteum Function and Endometrial Oxytocin Receptor Concentration in Cycling Mares. Journal of Equine Veterinary Science 32:536–541. https://doi.org/10.1016/j.jevs.2011.12.011

Veenema A, Neumann I (2008) Central vasopressin and oxytocin release: regulation of complex social behaviours. In: Progress in Brain Research. Elsevier, pp 261–276

Veening JG, de Jong T, Barendregt HP (2010a) Oxytocin-messages via the cerebrospinal fluid: Behavioral effects; a review. Physiology & Behavior 101:193–210. https://doi.org/10.1016/j.physbeh.2010.05.004

Vigneaud VD, Ressler C, Swan CJM, et al (1953) THE SYNTHESIS OF AN OCTAPEPTIDE AMIDE WITH THE HORMONAL ACTIVITY OF OXYTOCIN. J Am Chem Soc 75:4879–4880. https://doi.org/10.1021/ja01115a553

Waltenspühl, Y., Schöppe, J., Ehrenmann, J., et al. (2020). Crystal structure of the human oxytocin receptor. Science Advances 6. DOI: 10.1126/sciadv.abb5419

Wang Y-F, Hatton GI (2004) Milk Ejection Burst-Like Electrical Activity Evoked in Supraoptic Oxytocin Neurons in Slices From Lactating Rats. Journal of Neurophysiology 91:2312–2321. https://doi.org/10.1152/jn.00697.2003

Weaver ICG, Cervoni N, Champagne FA, et al (2004) Epigenetic programming by maternal behavior. Nat Neurosci 7:847–854. https://doi.org/10.1038/nn1276

Westover KD, Bushnell DA, Kornberg RD (2004) Structural Basis of Transcription: Separation of RNA from DNA by RNA Polymerase II. 303:

Williams JR, Insel TR, Harbaugh CR, Carter CS (1994) Oxytocin Administered Centrally Facilitates Formation of a Partner Preference in Female Prairie Voles (*Microtus ochrogaster*). J Neuroendocrinology 6:247–250. https://doi.org/10.1111/j.1365-2826.1994.tb00579.x

Winslow JT, Insel TR (2002) The social deficits of the oxytocin knockout mouse. Neuropeptides 36:221–229. https://doi.org/10.1054/npep.2002.0909

Winslow JT, Noble PL, Lyons CK, et al (2003) Rearing Effects on Cerebrospinal Fluid Oxytocin Concentration and Social Buffering in Rhesus Monkeys. Neuropsychopharmacol 28:910–918. https://doi.org/10.1038/sj.npp.1300128

Winslow JT, Sue C, Harbaugh CR (1993) A role for central vasopressin in pair bonding in monogamous prairie voles. 365:

Yamamoto Y, Liang M, Munesue S, et al (2019) Vascular RAGE transports oxytocin into the brain to elicit its maternal bonding behaviour in mice. Commun Biol 2:76. https://doi.org/10.1038/s42003-019-0325-6

Yrigollen CM, Han SS, Kochetkova A, et al (2008) Genes Controlling Affiliative Behavior as Candidate Genes for Autism. Biological Psychiatry 63:911–916. https://doi.org/10.1016/j.biopsych.2007.11.015

Zhang B, Qiu L, Xiao W, et al (2021a) Reconstruction of the Hypothalamo-Neurohypophysial System and Functional Dissection of Magnocellular Oxytocin Neurons in the Brain. Neuron 109:331-346.e7. https://doi.org/10.1016/j.neuron.2020.10.032

Zhang B, Qiu L, Xiao W, et al (2021b) Reconstruction of the Hypothalamo-Neurohypophysial System and Functional Dissection of Magnocellular Oxytocin Neurons in the Brain. Neuron 109:331-346.e7. https://doi.org/10.1016/j.neuron.2020.10.032

CHAPTER 2

A Histochemical Brain Atlas of the Prairie Vole (*Microtus ochrogaster*): Development and Application

This chapter is published on UVA Dataverse as Ramos, Erin and Erisir, Alev, "The Histochemical Brain Atlas of the Prairie Vole (Microtus ochrogaster)", https://doi.org/10.18130/V3/LSAONY, University of Virginia Dataverse, V1 (2024)

Introduction

The prairie vole animal model has become more popular since the 1980's for its unique social behaviors that mirror human social behaviors (Carter et al. 2020; Kenkel et al. 2021). The prairie vole is biparental, socially monogamous, and participates in alloparental care, the care of a pup that is not one's own (Carter and Getz 1993; Williams et al. 1994; Kenkel et al. 2021). The early work done in the prairie vole focused on these unique behaviors, and the relation of these behaviors to the neuropeptides oxytocin (OXT) and vasopressin (AVP) (Carter and Getz 1993; Sue Carter et al. 1995). These studies discovered the significance of OXT in driving pair-bonding in females (Williams et al. 1994). AVP plays an important role in stimulating pair-bonding in males, however, interference with either the AVP or OXT system can modulate male pair-bonding behavior. Alloparental care is also driven through OXT binding to its receptor (OXTR) in females in adolescence (Olazábal and Young 2006), and virgin adults (Olazábal and Young 2006). Again, AVP and OXT appear to influence male alloparental behavior (Bales et al. 2004).

Following these early discoveries, many researchers have focused on the availability of the OXTR and AVP receptors and found significant differences related to the amount of the receptors expressed and behaviors exhibited (Insel and Shapiro 1992; Ross et al. 2009; Johnson et al. 2016). However, researchers have always utilized a mouse or rat brain atlas to examine the neuroanatomical differences in OXTR. Although mice, rats, and prairie voles are all rodents, it is inaccurate to assume that their neuroanatomical structure is completely evolutionarily conserved. In recent years, technology has advanced in ways that allow the automated processing of tissue, for cell counting (Bjerke et al. 2023), tract tracing (Zhang et al. 2008; Ypma and Bullmore 2016) etc., to use these advanced methods one must have a reliable atlas. Therefore, our lab created the histochemical atlas of the prairie vole brain, to advance both our understanding of the vole brain cytoarchitecture and so researchers can begin to utilize more advanced methods to advance our current understanding of the prairie vole brain. We hope this will be a useful tool and can further elucidate the underlying neuroanatomical structure that drives their unique species-typical behaviors.

Materials and Methods:

Animal model:

One adult (postnatal day 65, PND65) male prairie vole was used. The vole was a descendant of wild-caught stock captured near Champaign, Illinois, and bred at Indiana

University. The animal was pair-housed in polycarbonate cages (27cm x 16cm x 16cm) from the time of weaning on PND21. He was given food (high-fiber Purina rabbit chow) and water ad libitum, cotton nestlets for nesting material, and was maintained on a 14:10 light:dark cycle. He was sexually inexperienced. All procedures involved in generating tissue for the prairie vole atlas were approved by the Institutional Animal Care and Use Committees (IACUC) at Indiana University Bloomington.

Tissue Preparation:

The prairie vole was deeply anesthetized with an overdose of sodium pentobarbital or isofluorane, and transcardially perfused with Tyrode's solution (137 mm NaCl, 2 mm KCl, 0.9 mm CaCl2, 1.2 mm MgCl2, 11.9 mm NaHCO3, 0.4 mm NaH2PO4, 5.5 mm glucose, 281 mOsm, pH 7.4) for 1-2 mins, followed by 10-15 ml of 4% paraformaldehyde (for light microscopy) in 0.1 M phosphate buffer (pH7.4). After 24 hours of post-fixation in the same aldehyde solution, the brain was extracted and sectioned coronally on a vibratome at 50μm and collected in four series. The second and fourth series were mounted on glass slides and stained for Myelin and Nissl, respectively. The first and third series were rinsed in 1% sodium borohydride and stored in 0.05% sodium azide in 0.01 M PBS at 4oC until immunostaining experiments.

Histochemistry for Myelin and Nissl:

For myelin visualization, sections that were mounted on gelatine-subbed slides were rehydrated in 0.02M PBS for 2 min and incubated in 0.2% HAuCl4 for 10-15 min at 60°C, following a modified myelin staining protocol (Corson et al. 2012). After fine myelination was differentiated, slides were then transferred into an intensification solution of 0.2% KAuCl4 for 2-3 min at 60oC, followed by two rinses in 0.02M PBS for 2 min each. Sections were incubated in sodium thiosulfate for 3 min and rinsed three times in 0.02M PBS. Slides were air-dried overnight, dehydrated through a series of ETOH, delipidated in xylenes, and coverslipped with DPX mounting media.

For Nissl visualization, sections were mounted on subbed slides and airdried. The sections were then rehydrated in 100%, 90%, and 70% EtOH solutions, followed by 0.5% cresyl violet in dH2O with 0.3% acetic acid. Slides were then dehydrated in a series of ETOH and xylenes, and coverslipped with DPX mounting media.

Immunohistochemistry for Oxytocin:

For visualization of oxytocin, the sections were pre-incubated for 30 min in 1% BSA, 0.1% Triton-X, 1% BSA in 0.01 M PB, and then transferred to primary antibody rabbit anti-oxytocin (Millipore, CAT#AB911) at 1:20,000 dilution in 0.1M PBS containing 1% BSA, 0.05% sodium azide and 0.3% TritonX (for light microscopy) for 48 hours at room temperature on a shaker Triton-X was omitted from the antibody incubation buffer for electron microscopy experiments. All sections were then rinsed in 0.01 M PBS and transferred to anti-rabbit secondary antibody conjugated to biotin for 2 hours, followed by treatment with avidin-biotin-complex (ABC; Vector) solution for 2 hours. The sections were then rinsed with 0.01 M PBS and incubated in a solution of 0.02% hydrogen peroxide and 0.05% diaminobenzidine for 2-5 min. The sections

prepared for light microscopy were mounted onto subbed slides and coverslipped with DPX mounting media

Imaging and Construction of the Prairie Vole Atlas

To construct an annotated atlas of the prairie vole brain as an open resource tool, all Nissl, Myelin and oxytocin-stained series from one male prairie vole brain were imaged using a Leica MC170 HD microscope at 1.6x and 20x magnifications. The higher magnification images of Nissl or Myelin-stained sections were tiled to make composites of each brain section, using Adobe Photoshop. The Adobe Illustrator software was used to make aligned sets of Nissl, Myelin, and oxytocin labeled sections, representing 200 µm thick coronal planes. The Nissl images were used to outline the section boundaries and the cytoarchitectural borders of all major brain nuclei. These outlines were superimposed on the images of the myelin-stained section in the set, and the outlines of myelinated axon bundles and other differentiated structures were added (**Fig 1**). Demarcated brain regions were annotated using the terminology adopted in the Prairie Vole MRI Brain Atlas (Yee et al. 2016), the Allen Mouse Brain Atlas (Allen Institute for Brain Science, 2004), or the Paxinos and Watson Rat Brain Atlas (Paxinos & Watson, 2007). Thirty-three series extending from the olfactory bulb to the pons were compiled in an anterior-posterior coordinate plane using the anterior-most coronal section that contained the optic chiasm (oc) as the AP zero coordinate. All sections anterior and posterior to the oc are designated as 'oc-' and 'oc+', respectively (**Fig 2A-C**). A pdf version of the prairie vole atlas (The Histochemical Brain Atlas of The Prairie Vole (*Microtus ochrogaster*) is accessible at https://doi.org/10.18130/V3/LSAONY, and in Appendix A.

Conclusions

Although prairie voles are not as widely used as the mouse or rat model, they are an incredibly unique and powerful tool for examining the biological basis of many gregarious social behaviors (Rogers and Bales 2019; Carter et al. 2020; Kenkel et al. 2021). The development of the prairie vole brain atlas enables researchers to employ a broader range of techniques with increased confidence in the accuracy of the brain regions under investigation. Further, the use of automated technology in conjunction with the vole atlas will permit more whole-brain analyses and drastically cut down on the amount of time analysis takes.

For our purposes, we created this atlas to inform Chapter 3 of this dissertation, where I examine the whole brain and determine the regions containing all OXT+ cells and axons. Further, I define their ultrastructural characteristics utilizing electron microscopy. Both endeavors would not have been possible using a mouse brain atlas. I hope that this will be a beneficial tool for prairie vole researchers. Further, an MRI-histology atlas that uses this atlas as a reference is in progress. This will be a beneficial tool to correlate prairie vole MRI work with human fMRI studies and the neural circuitry that may be evolutionarily conserved.

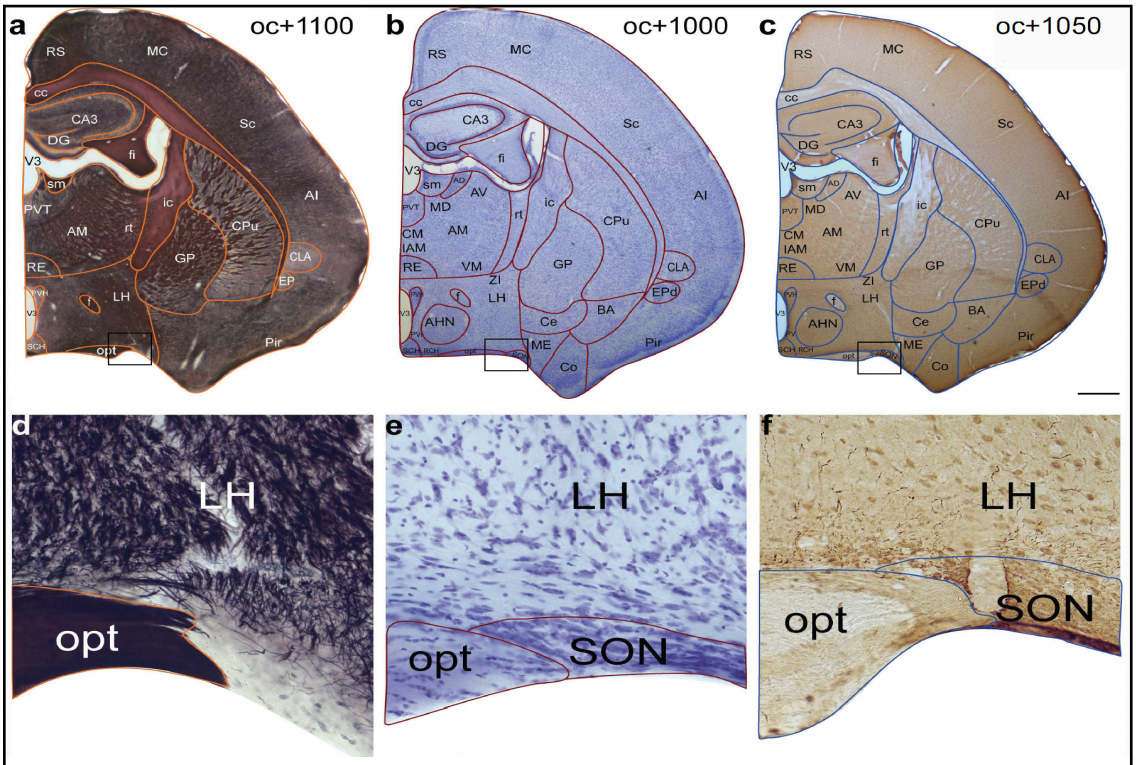

Figure 1: Illustration of the creation of the vole brain atlas. **A**) A myelin-stained section at oc +1100 µm with areas that were able to be demarcated by using the myelin section outlined and labeled, black boxed region is magnified to 20x in D. **B**) The Nissl section 100 µm anterior to the myelin stain with the areas that were outlined in the myelin stain and regions that could be further outlined using the Nissl stain, such as the SON, again magnified region shown in E. **C**) The OXT-stained section that lies between the myelin and Nissl stain with the combined outlines overlaid, magnified region shown in F. **A-C**) Scale bar = 500 µm, D-F) scale bar = 50 µm.

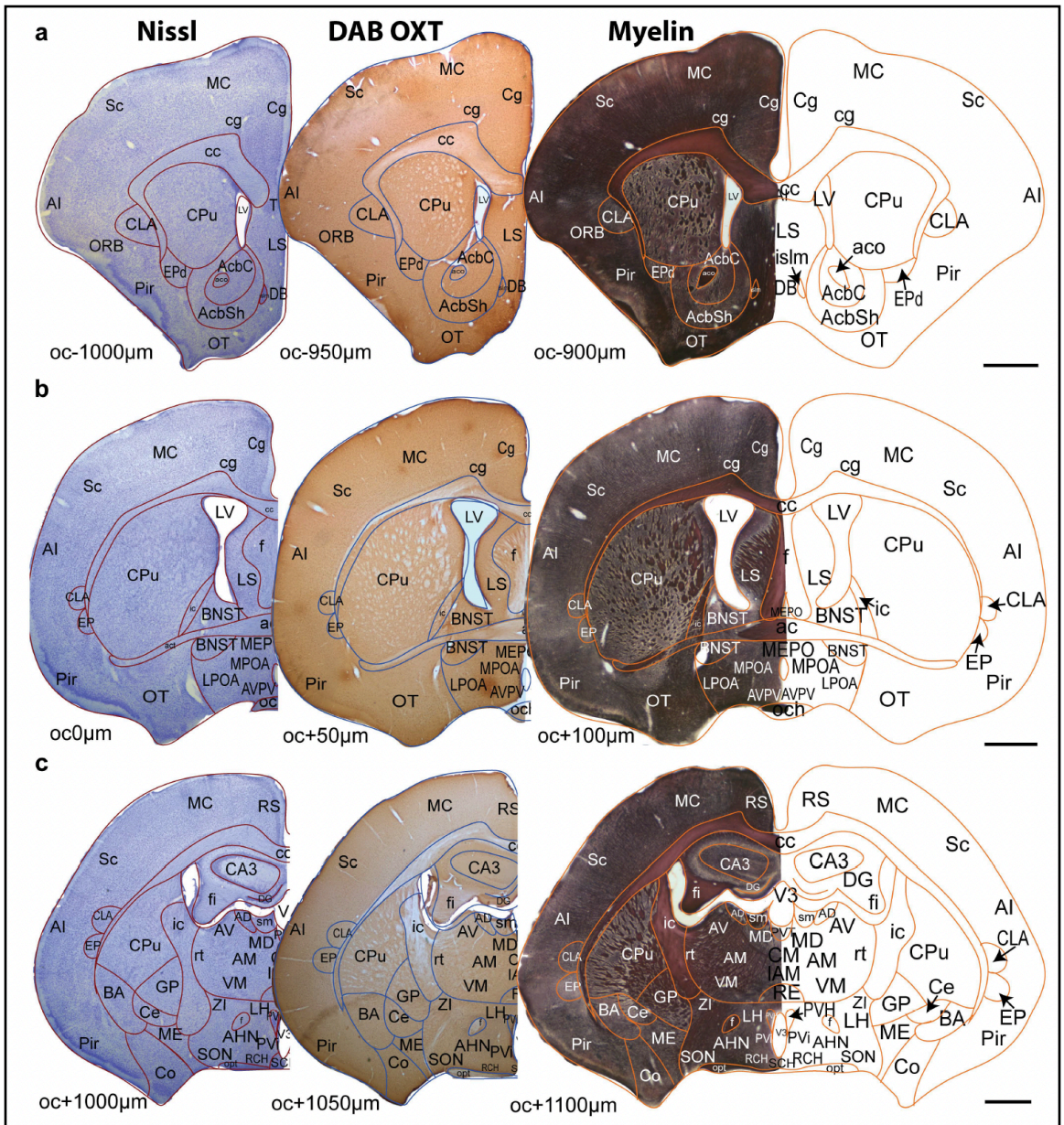

Figure 2: Adjacent coronal sections that are 50µm apart were stained with Nissl, Oxytocin, or Myelin, and annotated to create the prairie vole brain atlas (**A-C**) Three series that are 1000µm apart are illustrated. The anterior-most section of the optic chiasm (**B**) is denoted as the oc0 coordinate, and the sections anterior and posterior to oc0 are marked as oc- and oc+, respectively. Scale bar = 1mm

References:

Allen Reference Atlas – Mouse Brain [Coronal Reference Atlas]. Available from atlas.brain-map.org.

Bales KL, Pfeifer LA, Carter CS (2004) Sex differences and developmental effects of manipulations of oxytocin on alloparenting and anxiety in prairie voles. Developmental Psychobiology 44:123–131. https://doi.org/10.1002/dev.10165

Bjerke IE, Yates SC, Carey H, et al (2023) Scaling up cell-counting efforts in neuroscience through semi-automated methods. iScience 26:107562. https://doi.org/10.1016/j.isci.2023.107562

Carter CS, Getz LL (1993) Monogamy and the Prairie Vole. Scientific American 268:100–106

Carter CS, Kenkel WM, MacLean EL, et al (2020) Is Oxytocin "Nature's Medicine"? Pharmacol Rev 72:829–861. https://doi.org/10.1124/pr.120.019398

Corson J, Aldridge A, Wilmoth K, Erisir A (2012) A survey of oral cavity afferents to the rat nucleus tractus solitarii. Journal of Comparative Neurology 520:495–527. https://doi.org/10.1002/cne.22715

Insel TR, Shapiro LE (1992) Oxytocin receptor distribution reflects social organization in monogamous and polygamous voles. Proc Natl Acad Sci USA 89:5981–5985. https://doi.org/10.1073/pnas.89.13.5981

Johnson ZV, Walum H, Jamal YA, et al (2016) Central oxytocin receptors mediate mating-induced partner preferences and enhance correlated activation across forebrain nuclei in male prairie voles. Hormones and Behavior 79:8–17. https://doi.org/10.1016/j.yhbeh.2015.11.011

Kenkel WM, Gustison ML, Beery AK (2021) A Neuroscientist's Guide to the Vole. Current Protocols 1:e175. https://doi.org/10.1002/cpz1.175

Olazábal DE, Young LJ (2006) Oxytocin receptors in the nucleus accumbens facilitate "spontaneous" maternal behavior in adult female prairie voles. Neuroscience 141:559–568. https://doi.org/10.1016/j.neuroscience.2006.04.017

Paxinos, G. and Watson, C. (1998) The Rat Brain in Stereotaxic Coordinates. Academic Press, San Diego.

Ramos, Erin; Erisir, Alev, 2024, "The Histochemical Brain Atlas of the Prairie Vole (Microtus ochrogaster)", https://doi.org/10.18130/V3/LSAONY, University of Virginia Dataverse, V1

Rogers FD, Bales KL (2019) Mothers, Fathers, and Others: Neural Substrates of Parental Care. Trends in Neurosciences 42:552–562. https://doi.org/10.1016/j.tins.2019.05.008

Ross HE, Freeman SM, Spiegel LL, et al (2009) Variation in Oxytocin Receptor Density in the Nucleus Accumbens Has Differential Effects on Affiliative Behaviors in Monogamous and Polygamous Voles. J Neurosci 29:1312–1318. https://doi.org/10.1523/JNEUROSCI.5039-08.2009

Sue Carter C, Courtney Devries A, Getz LL (1995) Physiological substrates of mammalian monogamy: The prairie vole model. Neuroscience & Biobehavioral Reviews 19:303–314. https://doi.org/10.1016/0149-7634(94)00070-H

Williams JR, Insel TR, Harbaugh CR, Carter CS (1994) Oxytocin Administered Centrally Facilitates Formation of a Partner Preference in Female Prairie Voles (Microtus ochrogaster). J Neuroendocrinol 6:247–250. https://doi.org/10.1111/j.1365-2826.1994.tb00579.x

Yee JR, Kenkel WM, Kulkarni P, et al (2016) BOLD fMRI in awake prairie voles: A platform for translational social and affective neuroscience. NeuroImage 138:221–232. https://doi.org/10.1016/j.neuroimage.2016.05.046

Ypma RJF, Bullmore ET (2016) Statistical Analysis of Tract-Tracing Experiments Demonstrates a Dense, Complex Cortical Network in the Mouse. PLoS Comput Biol 12:e1005104. https://doi.org/10.1371/journal.pcbi.1005104

Zhang W, Olivi A, Hertig SJ, et al (2008) Automated fiber tracking of human brain white matter using diffusion tensor imaging. NeuroImage 42:771–777. https://doi.org/10.1016/j.neuroimage.2008.04.241

CHAPTER 3

The Central Oxytocinergic System in the Prairie Vole (*Microtus ochrogaster*): Pathways, Receptor Interactions, and CSF Release

The study reported in this chapter is accepted for publication in Brain Structure & Function on July7 2024 as, Ramos, E.N., Jiron, G.M., Danoff, J.S., Anderson, Z., Carter, C.S., Perkeybile, A.M., Connelly, J.J., Erisir, A., The Central Oxytocinergic System of the Prairie Vole.

Abstract

Oxytocin (OXT) is a peptide hormone and a neuropeptide that regulates various peripheral physiological processes and modulates behavioral responses in the central nervous system. While the humoral release occurs from the axons arriving at the median eminence, the neuropeptide is also released from oxytocinergic cell axons in various brain structures that contain its receptor, and from their dendrites in hypothalamic nuclei and potentially into the cerebrospinal fluid (CSF). Understanding oxytocin's complex functions requires the knowledge on patterns of oxytocinergic projections in relationship to its receptor (OXTR). This study provides the first comprehensive examination of the oxytocinergic system in the prairie vole (*Microtus ochrogaster*), an animal exhibiting social behaviors that mirror human social behaviors linked to oxytocinergic functioning. Using light and electron microscopy, we characterized the neuroanatomy of the oxytocinergic system in this species. OXT+ cell bodies were found primarily in the hypothalamus, and axons were densest in subcortical regions. Examination of the OXT+ fibers and their relationship to oxytocin receptor transcripts (*Oxtr*) revealed that except for some subcortical structures, the presence of axons was not correlated with the amount of *Oxtr* across the brain. Of particular interest, the cerebral cortex that had high expression of *Oxtr* transcripts contained little to no fibers. Electron microscopy is used to quantify dense cored vesicles (DCV) in OXT+ axons and to identify potential axonal release sites. The ependymal cells that line the ventricles were frequently permissive of DCV-containing OXT+ dendrites reaching the third ventricle. Our results highlight a mechanism in which oxytocin is released directly into the ventricles and circulates throughout the ventricular system, may serve as the primary source for oxytocin that binds to OXTR in the cerebral cortex.

Brain Region Abbreviations

AcbC nucleus accumbens core
AcbSh nucleus accumbens shell
aco anterior commissure, olfactory limb
act anterior commissure, temporal limb
AD anterodorsal nucleus of the thalamus
AHN anterior hypothalamic nucleus
AI agranular insular area
AM anteromedial nucleus of the thalamus
Amy amygdala

aq	cerebral aqueduct
AV	anteroventral nucleus of the thalamus
AVPV	anteroventral periventricular nucleus
BA	basomdeial/basolateral amygdalar nucleus
BNST	bed nucleus of the stria terminalis
CA1	hippocampal area 1
CA2	hippocampal area 2
CA3	hippocampal area 3
cc	corpus callosum
Ce	central amygdalar nucleus
cg	cingulum bundle
Cg	cingulate cortex
CLA	claustrum
CM	central medial thalamic nucleus
Co	cortical amygdaloid nucleus
CPu	caudate putamen
DB	diagonal band of Broca
DG	dentate gyrus
DR	dorsal raphe
EPd	endopiriform dorsal part
f	fornix
GL	glomerular layer of the olfactory bulb
GP	globus pallidus
GrO	granular cell layer olfactory limb
islm	major island of Calleja
LA	lateral amygdalar nucleus
LPOA	lateral preoptic area
LS	lateral septum
LSd	lateral septum - dorsal
LSi	lateral septum - intermediate
LSv	lateral septum - ventral
LV	lateral ventricle
MC	motor cortex
ME	median eminence
Me	medial amygdalar nucleus
MEPO	median preoptic nucleus
MM	mammillary nucleus
MPOA	medial preoptic area
MS	medial septal nucleus
och	optic chiasm
opt	optic tract
ORB	orbital area
OT	olfactory tubercle
PAG	periaqueductal gray
PH	posterior hypothalamic nucleus
Pir	piriform cortex

Pons	Pons
PrL	prelimbic cortex
PVH	paraventricular hypothalamic nucleus
PVi	periventricular hypothalamic nucleus -intermediate
PVpo	periventricular hypothalamic preoptic part
PVT	paraventricular nucleus of the thalamus
RCH	retrochiasmatic area
RE	nucleus of reuniens
RH	rhomboid nucleus
RS	retrosplineal area
rt	reticular nucleus of the thalamus
RTm	reticular nucleus -midbrain
Sc	somatosensory cortex
SC	superior colliculus
SCH	suprachiasmatic nucleus
sm	stria medularis
SN	substantia nigra
SNR	substantia nigra reticular part
SON	supraoptic nucleus
st	stria terminalis
SUB	subiculum
TT	taenia tecta
Tu	tuberal nucleus
V3	third ventricle
VLPO	ventrolateral preoptic area
VM	ventral medial thalamic nucleus
VMH	ventromeidal hypothalamus
VMPO	ventromedial preoptic area
VP	ventral pallidum
VTA	ventral tegmental area
ZI	zona incerta

Introduction

The peptide hormone oxytocin has been widely studied for its action in various physiological processes including the initiation of uterine contractions at birth and milk letdown during lactation (Dale 1906; Soloff et al. 1979; Crowley and Armstrong 1992; Perkinson et al. 2021). However, oxytocin as a neuropeptide, also has multifaceted roles in facilitating social bonding, regulating emotional responses and stress, and impacting more complex cognitive functions including aggression, learning, and empathy (Carter 1992; Bale et al. 2001; Bales and Carter 2003; Olff et al. 2013; Marlin et al. 2015; Jurek and Neumann 2018; Borland et al. 2019; Liu et al. 2020; Giannotti et al. 2022). These behavioral outcomes imply that centrally available oxytocin should have direct effects on various cortical and subcortical brain nuclei, including those in the limbic system, reward pathways, and sensory and association cortices. In support of this idea, the axons of oxytocin-producing hypothalamic cells are found scattered across many subcortical

structures and a few cortical areas in several mammalian species studied so far (Marlin et al. 2015; Otero-García et al. 2016; Son et al. 2022). The brain nuclei that contain oxytocin-producing cell bodies are considered among the sites where oxytocin signaling is expected because the neuropeptide can also be released from dendrites containing dense cored vesicles (DCV) (Ludwig et al. 2002; Ludwig and Leng 2006). Similarly, the transcript for the oxytocin receptor (OXTR) has been found in many brain regions (Olazábal and Young 2006; Bosch et al. 2016; Duchemin et al. 2017; Newmaster et al. 2020; Inoue et al. 2022; Son et al. 2022), including the cerebral cortex where oxytocinergic fibers are sparse. Therefore, understanding the patterns of oxytocinergic innervation across the brain nuclei harboring its receptor is crucial for studying oxytocin's function in the central nervous system.

As an alternative to the most extensively studied rat and mouse species, the prairie vole (Microtus ochrogaster) has emerged as a valuable animal model for the study of oxytocin due to its behavioral characteristics that closely resemble human behavior such as pair bonding and alloparenting, which heavily rely on oxytocinergic signaling (Carter and Getz 1993; Perkeybile et al. 2015; Bosch et al. 2016; Hiura and Ophir 2018; Carter et al. 2020; Loth and Donaldson 2021). Research on the prairie vole model has focused on the expression and variability of OXTR (Insel and Shapiro 1992; Perkeybile et al. 2015; Hiura and Ophir 2018; Inoue et al. 2022) but the sources of oxytocin that bind to these receptors remain understudied. The current study uses a combination of brightfield, light-sheet, confocal, and electron microscopy to characterize oxytocin projections, their ultrastructural morphology, and the relationship between oxytocin fibers and *Oxtr* transcript expression. Importantly, oxytocin is often released from axons via en passant boutons without an active zone, making the observations of oxytocin release sites difficult to study (Chini et al. 2017; Oti et al. 2021). At the ultrastructural resolution, potential release sites of oxytocin can be identified by high incidences of DCVs, that is, large vesicles that pack oxytocin in the cell body and transport to its release sites (Lemos and Dayanithi 2020; Oti et al. 2021). The current study uses electron microscopy to quantify the presence of DCVs as a proxy for the neuropeptide release. We further define and elucidate the different modes of oxytocin release in the central nervous system of prairie voles.

Materials and Methods:

Animals:

A total of 18 adult prairie voles (Microtus ochrogaster) between postnatal days 60 to 90 (PND60-PND90) were used. The voles were descendants of wild-caught stock captured near Champaign, Illinois, and bred at Indiana University (8 animals) and the University of Virginia (10 animals). The animals were pair-housed in polycarbonate cages (27cm x 16cm x 16cm) from the time of weaning on PND21. Animals were given food (high-fiber Purina rabbit chow) and water ad libitum, cotton nestlets for nesting material, and were maintained on a 14:10 light:dark cycle. All animals were nulliparous and sexually inexperienced. All procedures involved in generating tissue for the prairie vole atlas, and in analyzing the oxytocin localization and receptor expression were

reviewed and approved by the Institutional Animal Care and Use Committees (IACUC) at Indiana University Bloomington and the University of Virginia. The animals from Indiana University were used for light and electron microscopy studies. Three animals from the University of Virginia were used for light and electron microscopy studies, 2 were used for whole brain clearing and light-sheet microscopy, and the remaining 5 were used for RNAscope in situ hybridization.

Tissue preparation for light and electron microscopy:

For light and electron microscopy studies, 5 male and 6 female prairie voles were deeply anesthetized with an overdose of sodium pentobarbital or isofluorane, and transcardially perfused with Tyrode's solution (137 mm NaCl, 2 mm KCl, 0.9 mm CaCl2, 1.2 mm MgCl2, 11.9 mm NaHCO3, 0.4 mm NaH2PO4, 5.5 mm glucose, 281 mOsm, pH 7.4) for 1-2 mins, followed by 10-15 ml of 4% paraformaldehyde (for light microscopy), or 4% paraformaldehyde and 0.5% glutaraldehyde (for electron microscopy) in 0.1 M phosphate buffer (pH7.4). After 24 hours of post-fixation in the same aldehyde solution, the brains were extracted and sectioned coronally on a vibratome at 50µm and collected in four series. The second and fourth series were mounted on glass slides and stained for Myelin and Nissl, respectively. The first and third series were rinsed in 1% sodium borohydride and stored in 0.05% sodium azide in 0.01 M PBS at 4oC until immunostaining experiments.

Tissue preparation for RNAScope:

5 female prairie voles were anesthetized with an overdose of sodium pentobarbital. The brains were immediately extracted on dry ice and stored at -80°C until sectioning. For cryostat sectioning, the brains were acclimated at -20°C for at least 2 hours, sliced at 15µm thickness, and mounted onto Superfrost plus slides (Fisherbrand; Pittsburg, Pennsylvania), and stored in slide boxes at -80°C until fluorescent RNAScope staining.

Immunohistochemistry for Oxytocin:

For visualization of oxytocin, the sections were pre-incubated for 30 min in 1% BSA, 0.1% Triton-X, 1% BSA in 0.01 M PB, and then transferred to primary antibody rabbit anti-oxytocin (Millipore, CAT#AB911) at 1:20,000 dilution in 0.1M PBS containing 1% BSA, 0.05% sodium azide and 0.3% TritonX (for light microscopy) for 48 hours at room temperature on a shaker Triton-X was omitted from the antibody incubation buffer for electron microscopy experiments. All sections were then rinsed in 0.01 M PBS and transferred to anti-rabbit secondary antibody conjugated to biotin for 2 hours, followed by treatment with avidin-biotin-complex (ABC; Vector) solution for 2 hours. The sections were then rinsed with 0.01 M PBS and incubated in a solution of 0.02% hydrogen peroxide and 0.05% diaminobenzidine for 2-5 min. The sections prepared for light microscopy were mounted onto subbed slides and coverslipped with DPX mounting media; the other series embedded for electron microscopy.

For pre-embedding gold enhancement staining of OXT fibers, sections were first pre-incubated for 2 hours in a solution of 5% BSA in 0.01 M PBS and 0.05% Triton-X,

and then incubated in anti-oxytocin antibody, as described above. The sections were then rinsed in 0.01M PBS and incubated in anti-rabbit IgG conjugated to 1.4nm gold particles (1:100) in 1% BSA in 0.01M PBS for 2 hours. The tissue was then rinsed in PBS and post-fixed in 1% glutaraldehyde in PBS for 45 minutes, followed by rinses with 1% BSA in 0.01M PBS and distilled water. Sections were then treated in GoldEnhance EM enhancement reagent (Nanoprobes, Yaphank, NY) up to 10 minutes until fiber labeling was detectable by eye. Finally, the sections were rinsed in distilled water, and embedded for electron microscopy as described below.

Electron microscopy tissue preparation:

Resin embedding for electron microscopy followed standard protocols. The sections were treated with 1% osmium tetroxide in 0.1M PB for 1 hour. then transferred into 50% EtOH and counterstained with filtered 4% uranyl acetate in 70% alcohol overnight. The sections were dehydrated through a series of ethanol and acetone solutions and infiltrated with EMbed 812 resin (EMS, Hatfield, PA) overnight. They were then flat-embedded between Aclar sheets (EMS, Hatfield), and placed in a 60ºC oven overnight. Sections containing areas of interest (such as the PVH, SON, NAcc, etc.) were excised and placed in BEEM capsules (EMS, Hatfield). The capsules were filled with resin and were cured in the 60ºC oven overnight, or until polymerized. Areas of interest were traced with a camera lucida and trimmed down to a 1mm x 2mm trapezoid-shaped blockface containing labeled neurons or axons. Ultrathin sections (~60nm thin) were cut and collected on 200 mesh copper grids (Ted Pella, Redding, CA) using an ultramicrotome (Ultracut UCT7; Leica, Buffalo Grove, IL). Ultrathin sections of tissue that were visualized with gold-enhanced were counterstained with uranyl acetate, or UranyLess (EMS, Hatfield, PA) and lead nitrate.

Fluorescent RNAScope for visualizing Oxtr transcripts:

Slides containing 2 coronal sections of the forebrain, including nucleus accumbens (Acb) and the anterior cingulate cortex (Cg), and directly posterior to the genu of the corpus callosum were selected for RNAScope in situ hybridization for the mapping of *Oxtr* transcripts. These regions were selected based on previous literature indicating they are regions high in OXTR expression (Inoue et al. 2022). An RNAScope Multiplex Fluorescent Reagent Kit version 2 (Advanced Cell Diagnostics; Newark, California) was used for fluorescent staining of *Oxtr* transcripts, according to the manufacturer's instructions. Briefly, slides were fixed in 4% paraformaldehyde in 4°C for 1 hour, and then dehydrated through a series of ethanol solutions of 50%, 70%, and two 100%, 5 minutes each. The slides were then stored for up to one week at -20°C. On day 2 of staining, the slides were blocked in hydrogen peroxide, incubated in protease reagents, the *Oxtr* probe (CAT. No. 500721), and three amplification reagents. The hybridized probes were visualized using OPAL 690 and counterstained using DAPI. Finally, slides were coverslipped with ProLong Gold Antifade Mountant (ThermoFisher Scientific; Waltham, Massachusetts). A negative, bacterial DapB (Cat. No. 320871), and a positive, PPIB (Cat. No. 533491) control probes were run in parallel. For the negative control, there was no specific labeling, and for the positive, there were > 15 puncta per cell.

Whole-brain tissue clearance using CLARITY and light-sheet microscopy:

Two prairie vole brains (1 male, 1 female) were cleared using the CLARITY clearance method. The animals were perfused as described above and post-fixed for 24 hours. Then, the whole-brain samples were preserved using SHIELD reagent (LifeCanvas Technologies & Folorunso et al., 2023). Brains then cleared using the delipidation buffer for 24 hours followed by SmartBatch+ Delipidation for 30 hours (LifeCanvas Technologies). For immunolabeling, the cleared brains were incubated in the primary antibody, anti-rabbit OXT, in 5% normal donkey serum (1:5000) for 18 hours. Samples were then washed and fixed in 4% PFA overnight and treated with fluorescent-conjugated anti-rabbit secondary antibody (donkey anti-Rabbit IgG Alexa Fluor 488; Invitrogen, CAT#A32790; 1: 200).

Imaging and analysis of OXT+ cells and fibers:

For mapping the location of oxytocinergic cells and the fibers on the atlas, we examined all OXT-stained sections (every other 50 µm coronal section) of the brain used for the Histochemical Brain atlas of the Prairie Vole (Chapter 2) on the Zeiss Axio Imager M2 microscope with 20x and 40x objectives. When an OXT+ fiber or cell was encountered, we switched to a low magnification objective to identify its location in reference to the brain atlas (Chapter 2) outlines drawn on adjacent Nissl and Myelin sections. Every fourth coronal section from 5 other brains (2 males and 3 females) was also examined using the same strategy to map the location of cells and axons.

All encounters of labeled cell bodies within an identified brain region were evaluated to allocate a semi-quantitative staining density score: regions with 0 cells received a score of 0; 1-6 cells received a score of 1; 6-12 cells received a score of 2; and 12 or more cells received a score of 3. The same staining density quantification strategy was used to map the locations of OXT+ axons: a score of 0 was given when no axon was encountered in the section; + for 1 axon in a small region or 2-4 axons in a large cross-section of a region, such as caudate/putamen; ++ for when neither + or +++ criteria was met; and +++ for when the fibers are unquantifiably dense, such as in lateral septum, or completely filling a small region, such as in s. nigra.

Because staining density scores varied across sections that contain a brain region, and sparsely labeled regions may display no fibers or cells on some sections, it was important to normalize the staining densities to the size of each brain region. For that purpose, a Staining Density Index (SDI) was calculated by using the formula (3N3+2N2+N1)/3NT, where N3, N2, and N1 are the number of sections with a +++, ++, or + score, respectively, and NT is the number of sections the region spans, including the sections with no fibers or cells.

Imaging and Analysis of Oxtr transcripts via RNAScope:

For RNAScope imaging of *Oxtr* transcripts, a STELLARIS 5 (Leica Microsystems) confocal microscope with a 10x objective was used for whole section fluorescence imaging, and a 40x objective for high-magnification z-stack imaging of sections containing the Acb and Cg. Identical settings of the gain and intensity were used for each brain and image. The publicly available software QuPath was used to calculate

the percentage of cells and *Oxtr* puncta in the nucleus accumbens shell (AcbSh), core (AcbC), and cingulate cortex (Cg). The "Cell Detection" tool was used to outline all DAPI nuclei and further expanded by 5 μm to account for cytoplasm. All brains were analyzed using the same threshold parameters, and the subcellular detection tool was further used to automatically count the *Oxtr* puncta.

A publicly available comprehensive dataset of *Oxtr* transcripts in prairie vole brain (Inoue et al. 2022) was used for comparing with our OXT+ fiber quantification data. This dataset is a semi-quantitative assessment of the quantity of *Oxtr* transcripts across the entire prairie vole brain and provides a score between 1-4 for each brain nuclei. To align two datasets, the lists of brain regions included in the two studies are compared, and discrepancies are noted. If a region in *Oxtr* dataset had more subregions than our OXT fiber dataset, such as the BNST, the *Oxtr* score was averaged across subregions to yield one score. Any region included in our dataset that could not be matched to the *Oxtr* regions was excluded. The regions that were in the OXT dataset yet no corresponding *Oxtr* score was provided were also excluded. For a full list of regions included in the OXT/*Oxtr* comparison analysis, see Appendix B, Table 3. All regions were further categorized into the thalamus, hypothalamus, midbrain, striatum/pallidum, and cerebral cortex, based on the classification of these regions within the Allen Mouse Brain Atlas. For a full list of regions included in the OXT/Oxtr comparison analysis, as well as their classification, pooled OXT SDI scores from all female and all male brains, and *Oxtr* scores, see Appendix B, Table 3. OXT SDI scores were pooled because subsequent analysis revealed few sex differences. Data were analyzed using a linear regression model and the lm function in R, and further analyzed through the emmeans package and emtrends function in R to determine estimated linear trends of each sub-region.

Imaging and Analysis of OXT+ neuropil and DCVs via Electron Microscopy:

Electron microscopy images were captured on a JEOL 1010 EM with a 16-megapixel CCD camera (SIA) at 15,000X magnification, yielding 0.8nm/pixel resolution. Cross-sections of dendrites were identified by the presence of microtubules and lack of neurotransmitter vesicles. The presence of myelin sheets is an identifier for myelinated axons. Unmyelinated axons display uniform calibers in longitudinal cross-sections, neurofilaments and fewer microtubules, and they do not receive synapses. Axon terminals may display presynaptic zones, and contain vesicles, including dense cored vesicles. DCVs are membrane-bound round structures with dark centers. DCVs can be in various sizes but they are larger than neurotransmitter vesicles, which have clear centers. We used the presence of DCVs as a proxy for OXT release. Because OXT is not the only peptide packaged into DCVs, nor is OXT the only molecule present in OXT+ cells, we characterized OXT+ DCVs by their unique sizes (Makani et al. 2013). To determine the prototypical size of DCVs in OXT+ and OXT- profiles, we examined OXT+ cell bodies within the PVH and unstained (OXT-) regions displaying DCV's, used the freehand selection tool in ImageJ to draw borders along all DCVs, and measured their areas. This analysis revealed size differences between OXT+ and OXT- DCVs and yielded a cutoff size criterion for OXT+ DCVs. The cutoff size was determined as the intersection of the

density plots between OXT+ DCV's and OXT- DCV's, where the density of OXT+ DCVs falling below the cutoff value was less that 5% of the measured OXT+ DCV's.

Imaging and Analysis of Whole-Brain CLARITY tissue:

For 3D imaging of cleared and OXT-stained brains, a Zeiss Lightsheet 7 microscope at 5x magnification was used. Whole-brain 3D images were examined using Imaris Imaging Software.

Statistical Analysis and Figures:

All statistical analysis was done using R Studio and the ggplot package for data visualization. For comparisons of labeling density across animals, Welch's t-test was used. *Oxtr* vs OXT+ fiber density data were analyzed using a linear regression model and the lm function in R, and further analyzed through the emmeans package and emtrends function in R to determine estimated linear trends of each sub-region. Graphs were made on R Studio. Adobe Illustrator and Adobe Photoshop were used for constructing all figures.

Results

Brain regions containing OXT+ cell bodies and dendrites.

We used The Histochemical Atlas of Prairie Vole Brain as a reference template to map the locations of oxytocin-producing cell bodies in the prairie vole brain. In DAB-labeled sections, oxytocin immunostain (OXT+) fills the somata in their entirety, as well as the dendrites emanating from the soma (**Fig 1A-E**). Most cells have a multi-polar structure, with dendrites extending in different directions. Semi-quantitative scoring and computation of a Staining Density Index (see Methods) for each region allowed assessments of the prevalence of OXT+ cells.

The hypothalamic regions had the highest density of OXT+ cells (**Fig 1A & F**). The OXT+ cells are densest in the PVH and SON (Fig1B-C), followed by the tuberal nucleus (Tu) and periventricular hypothalamic preoptic part (PVpo). OXT+ cells are sparser in other regions, including the lateral hypothalamus (LH) and medial preoptic area (MPOA). An extrahypothalamic region, the BNST, consistently contains OXT+ cell bodies that closely line the ventricle and occasionally appear ectopic, and as such, do not belong to one particular brain region (**Fig 1D**). Dendrites of cells in PVH, SON, and BNST often are located close to and sometimes within the ventricular lining (**Fig 1B, C, & D**). As described before (Kelly et al. 2018; Kenkel et al. 2021), the distinction between magnocellular and parvocellular cells that are typically seen in other rodent models, such as mice and rats, is not as apparent in the prairie vole brain. Although the rostral part of the PVH primarily encompasses the magnocellular cell group and the caudal part encompasses the parvocellular group of the prairie vole, no differences were seen within the cell morphology of the PVH. For the full list of cell body locations see Appendix B, Table 1. Finally, light-sheet microscopy corroborated that the densest cell body localizations reside in the hypothalamus (**Fig1F**).

To reveal potential sexual dimorphisms, cell body SDI scores from 3 male and 3 female vole brains were compared using Welch's t-tests. No statistical differences were found (**Supplemental Figure 1a**), suggesting that sexual dimorphisms seen in behaviors modulated by OXT cannot be explained by the localization or the density of oxytocinergic cells.

To address potential species differences, we compared the localization of cells in each brain region of the prairie vole to previous studies in the mouse, hamster, and rat (Swaab et al. 1975; Laurent et al. 1989; Whitman and Albers 1998; Otero-García et al. 2016; Son et al. 2022). While most OXT+ cell localizations are similar, we noted two differences. First, similar to hamsters and unlike other rodents, the prairie vole has OXT+ cells within the median preoptic nucleus (MEPO) (Whitman and Albers 1998). Second, the prairie vole has a group of OXT+ cells located in the anteroventral periventricular nucleus (AVPV), which has not been noted in any other species (**Fig1E**). Interestingly, AVPV is among the regions in which processes project towards the ventricle and occasionally through the ependymal cell layer in the prairie vole (**Fig1E**).

Brain regions containing OXT-labeled axons

Next, we used DAB-labeling of OXT with brightfield microscopy to examine all major nuclei containing OXT axonal projections. On coronal sections, two distinct projection paths emerging from the PVH can be observed: one consists of a dense bundle of axons that courses dorso-laterally, and another that contains sparse and thin axonal fibers that project more ventro-medially (**Fig 1A**). The dorso-lateral axons extend horizontally above the anterior hypothalamic nucleus (AHN) and make a sharp ventral turn at the lateral hypothalamus (**Fig 1A, Fig 2A**). PVH axons seem to merge with another stream of axons emerging from the SON and these course along the ventral surface of the brain along the retrochiasmatic nucleus (RCH) and above the optic tract (opt) towards the median eminence (ME) (**Fig2B**). The axons of this dorso-lateral stream are thick and display swellings throughout their course (Fig **2A**).

The ventro-medial axons emerging from the PVH follow a less defined course, winding throughout the AHN (**Fig 2C**). These axons do not appear to be joining the OXT axon stream projecting towards the median eminence and are very fine displaying many varicosities (**Fig 2C**). Further, there are axons in other regions of the hypothalamus, anterior and posterior to the appearance of the PVH and SON, which show thick fibers with large swellings such as the MPOA (**Fig 2D**).

The OXT+ axons are dense in many non-hypothalamic subcortical brain regions, including the periaqueductal gray (PAG), ventral tegmental area (VTA), pons, nucleus reuniens of the thalamus (RE), BNST, and AcbSh and AcbC (**Fig 2E**. Note: classifications into "dense", "sparse", and "very sparse" were made based on tertiles that can be derived from the pooled data in Appendix B: Table 3. Dense regions: SDIs = 0.46-1; sparse regions: SDIs = 0.07-0.42; very sparse regions: SDIs = 0-0.05). Various sub-cortical regions appeared to have dense fiber staining, while labeled axons were extremely rare in cortical regions. Interestingly, OXT+ axons were observed touching all major ventricles and were prominent in many areas that border the ventricles, such as the lateral septum (LS), BNST, paraventricular nucleus of the thalamus (PVT), and PAG (**Fig 2E**; for the full list of axonal locations and the SDI's of individual subjects see

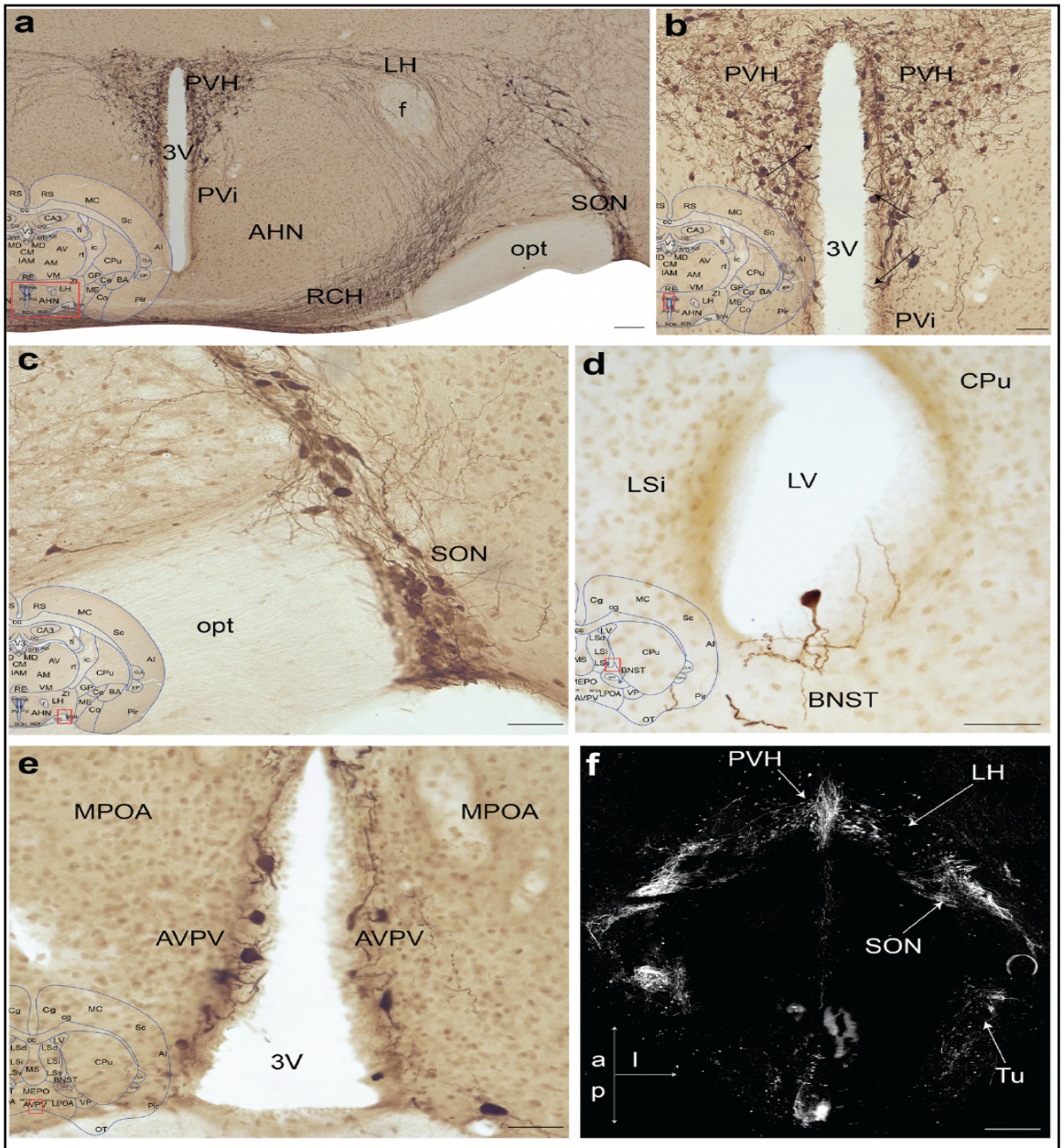

Figure 1: OXT+ cell bodies in prairie vole brain primarily reside in the hypothalamus. **A**) An OXT-stained coronal section through the hypothalamus reveals darkly stained cell bodies in the PVH, SON, and LH. The superimposed inset marks the region on a corresponding atlas section in red and applies to panels A to E. Scale bar = 100µm. **B**) Upon higher magnification, the OXT+ PVH cell bodies are multipolar. Those that are close to the ventricle extend dendrites into the ventricular lining (black arrows). Scale bar in B= 500µm and applies to panels B to E. **C**) In the SON, OXT+ somata are fusiform and multipolar, and project dendrites toward the ventral surface of the brain. **D**) Ventricular lining surrounding lateral ventricles occasionally displayed solitary OXT+ somata, which extend processes toward the ventricle. These are referred to as ectopic cells in the text as they cannot be identified as belonging to any brain nuclei. The example in panel D is close to BNST, the only extra-hypothalamic region that consistently contains OXT+ cells. **E**) The presence of OXT labeling in AVPV cells is unique to the prairie vole. **F**) Light-sheet microscope image of the hypothalamus at 5x objective in the horizontal plane, thick white arrows illustrate cell body groups within the PVH, LH, SON, and Tu, thin white arrows in the lower left corner indicate anterior (a), posterior (p), and lateral (l) directionality of the image, maximum intensity projection across 1100µm, scale bar = 500µm.

Appendix B, Table 2; for all axonal locations and the pooled SDI's see Appendix B, Table 3).

Sexual dimorphisms for OXT+ fibers were examined across 105 brain regions in 3 male and 3 female prairie vole brains. Regions that only had one score in either males or females were excluded because a mean value could not be calculated from one observation. While our sample size was not sufficient for statistical power in population comparisons, comparison of SDIs within each brain region revealed two regions that may be sexually dimorphic: the dorsal endopiriform cortex (EPd), and the prelimbic cortex (PrL) (**Supplemental Figure 1b**). Unlike in male brains, female brains did not display any fibers in Epd (0.17 ± 0.026 vs. 0 ± 0; mean ±SD; Welch's t-test, t(2) = -11.7, p = 0.007)) Males also had higher OXT fiber density in the PrL than females (0.25±0.07 vs. 0.04 ±0.06; Welch's t-test, t(3.95) = -3.88, p = 0.02; Supplemental Figure 1b). These results suggest that perhaps males utilize more OXT in the EPd and PrL than females, and this may play a role in downstream behavioral outcomes.

Comparison of brain regions with OXT+ fibers and Oxtr transcripts:

To confirm that the animals used in the current study displayed *Oxtr* expression patterns similar to that were recently described (Inoue et al. 2022), we examined sample brain regions that were reported to express high levels of *Oxtr*, yet show vast differences in their OXT+ fiber density in our study. In particular, we examined the *Oxtr* prevalence in the Nucleus Accumbens Shell (AcbSh), Core (AcbC), and Cingulate Cortex (Cg). Although both regions reportedly have high *Oxtr* levels (**Fig3A-B**), fiber density analysis yields different SDI values between the Acb (pooled SDI Sh: .67 and C: .53) and Cg (.05) (Appendix B, Table 3). The RNAScope visualization of *Oxtr* RNA transcripts (*Oxtr*) in 10 sections from 5 animals revealed that both the Acb (Sh and C) and Cg contain an abundance of *Oxtr*-producing cells (**Fig3A-B**). Specifically, 15.4% ± 6.9 of cells in AcbSh, 23.9% ± 13.1 of cells in AcbC, and the Cg 18.4% ± 5.3 of cells in Cg expressed *Oxtr*. The puncta density (i.e. counts of Oxtr puncta per cell) was 3.6 ± 1.6 in AcbSh, 3.4 ±1.8 in AcbC, and 8.4 ± 2.2 in Cg. These results confirm that the Acb and Cg cells both highly expressed *Oxtr* in our sample brains, comparable to the Inoue et al. 2022 *Oxtr* dataset, where the Cg received a score of 3, and the Acb (Sh and C) received scores of 4 (Fig3A-B; Appendix B, Table 3).

To analyze the relationship between OXT+ fiber density and *Oxtr* localization across the prairie vole brain, we compared our OXT+ fiber SDI data with a dataset of previously published quantitative distribution of *Oxtr* transcripts (Inoue et al. 2022) (Fig3C-I). We examined this relationship across 5 parent regions as established by the Allen Mouse Brian Atlas (mouse.brainmap.org): the cerebral cortex, hypothalamus, midbrain, striatum, pallidum, and the thalamus (for brain regions included in each category, Appendix B, Table 3). This analysis revealed a significant interaction effect between *Oxtr* and brain region, suggesting that the relationship between OXT+ fibers and *Oxtr* transcripts differs depending on region (linear regression, $F(1,63) = 2.47$, $p = 0.05$). Interestingly, the subregions within each parent category tend to cluster together in relation to their OXT fiber density, and they typically have a similar level of average *Oxtr* (**Fig 3I**). To further probe the differences amongst regions, we utilized linear trend analysis There was a general directionality of the trends yet, in most areas, the amount of

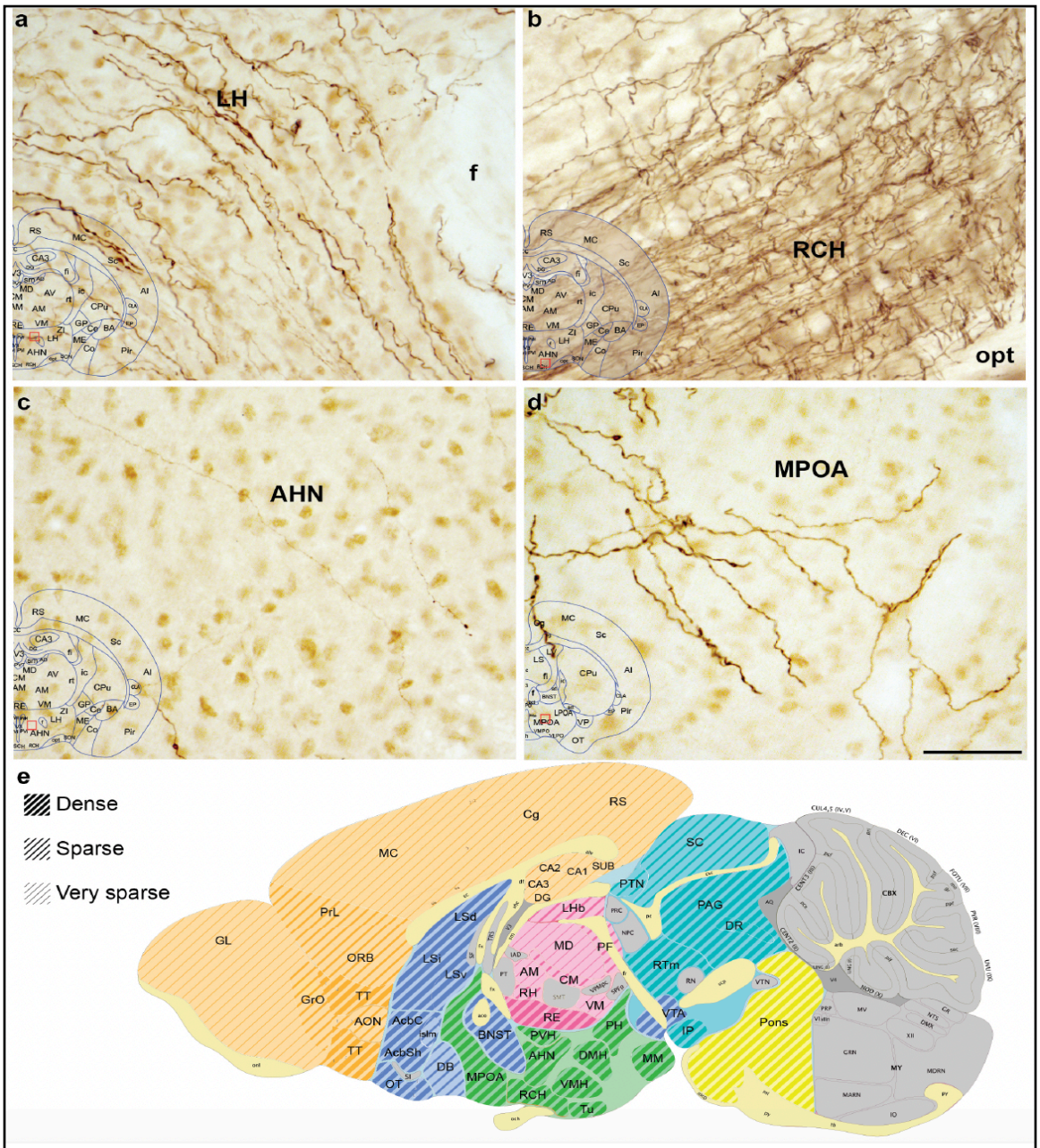

Figure 2: Locations of OXT+ fibers within the prairie vole LH (**A**), RCH (**B**), AHN (**C**), and MPOA (**D**). The superimposed inset marks the region on a corresponding atlas section in red. Scale bar = 50µm and applies to panels A to D. **E**) Illustration of fiber density data (Appendix B: Table 3) over a sagittal section adapted from Allen Mouse Brain Atlas (mouse.brainmap.org). The density of fibers (Appendix B: Table 3) is represented in tertiles (dense, sparse, and very sparse, which was determined within the cerebral cortex (orange), hindbrain (yellow), hypothalamus (green), striatum/pallidum (blue), midbrain (teal), and thalamus (pink). See Appendix B: Table 3 for full list of brain regions, their SDI's, and their classifications into the subregions (cerebral cortex, hindbrain, etc.)

OXT fibers was not correlated with the amount of *Oxtr*. There was a negative but non-significant relationship in the hypothalamus and midbrain; no relationship in striatum/pallidum, and a non-significant positive relationship in the cerebral cortex (**Fig 3H**). Only the thalamus category (which includes RE, PVT and CM) displays a

significant relationship between OXT+ fibers and *Oxtr* transcript (estimate linear trends analysis, Trend = 0.13, p = 0.001; Fig4C). This suggests that within the brain structures included in the thalamus category, the amount of *Oxtr* transcripts can be explained by the amount of OXT+ fibers. That is, the axonal release in the thalamus may constitute a primary source for OXTR protein binding.

In contrast, in the hypothalamus and midbrain categories, there is no significant relationship between OXT+ fibers and *Oxtr* (Trend = -0.04, p = 0.41; and Trend = -0.010, p = 0.54). While the fiber density in these areas is typically high, *Oxtr* density is low, suggesting that OXT+ fibers in these regions are likely axons of passage (**Fig 3D-E**). The striatum and pallidum display no significant relationship between OXT+ fibers and *Oxtr*. These areas typically have high amounts of *Oxtr* yet moderate to high (> 0.15SDI) levels of OXT+ fibers (Trend = -0.003, p = 0.95, **Fig 3F**). Similarly, the cerebral cortex category contains only a few regions with scant amounts of OXT+ fibers, but many regions display high levels of the *Oxtr* transcript (Trend = 0.03, p = 0.44, **Fig 3G**). This mismatch in the amount of OXT+ fibers and *Oxtr*, particularly in cortex and striatum/pallidum regions with high *Oxtr* but no or few OXT+ axons, indicates that the receptor localization cannot be explained by the presence of OXT+ fibers alone and that these regions may be getting the bulk of their oxytocin through non-axonal means.

Ultrastructural characteristics of OXT+ axons in regions with differing amounts of Oxtr transcripts

To characterize the fine morphological properties of OXT+ fibers in regions of high or low levels of *Oxtr*, we examined the LH, RCH, MPOA, and AHN regions immunostained for OXT using transmission electron microscopy. The OXT+ labeling was evident as the appearance of electron-dense DAB chromogen diffusely filling the profiles of neurons, dendrites, and axons (**Fig 4-5**). In regions where diffuse DAB label in profiles was too dense and obscured the organelles within, pre-embedding gold enhanced visualization approach was used, revealing OXT+ profiles with the appearance of irregularly shaped gold deposits (**Fig 5E**).

Within OXT+ profiles, darkly stained, large DCVs often appeared in clusters within labeled somata and neuropil (**Fig 4A-B**). Because DCVs of various sizes were also observed in unlabeled profiles (**Fig 4C**, yellow arrows), we quantified the size of labeled and unlabeled DCVs in the PVH to obtain a size criterion for OXT+ DCVs. The DCVs in labeled PVH cells were uniformly large (0.016μm2 ± 0.005, n=61; ~140nm in diameter) and these could be distinguished from other DCVs encountered in the OXT- neuropil (0.004μm^2 ± 0.002, n=60; ~70nm in diameter) (**Fig4B & C**, respectively). A cutoff value of 0.008μm^2 marks the intersection point of labeled and unlabeled DCV size distributions (**Fig 4D**). Only 5% of stained DCVs fall at or below this cutoff value. Thus, vesicles that are smaller than this cutoff are categorized as OXT- in our subsequent analysis.

In EM preparations of regions that contain many OXT+ fibers but few *Oxtr* transcripts, such as the LH and RCH (**Fig 5A-B**), OXT+ axons are uniformly non-myelinated and vary in diameter. To determine if oxytocin is likely released from these axons or if they are primarily axons of passage, we examined the LH and RCH using electron microscopy and quantified the incidences of OXT+ axons that contained OXT DCVs. Only 6% of axonal profiles in the LH (n=48) and 9% of the axonal profiles in the

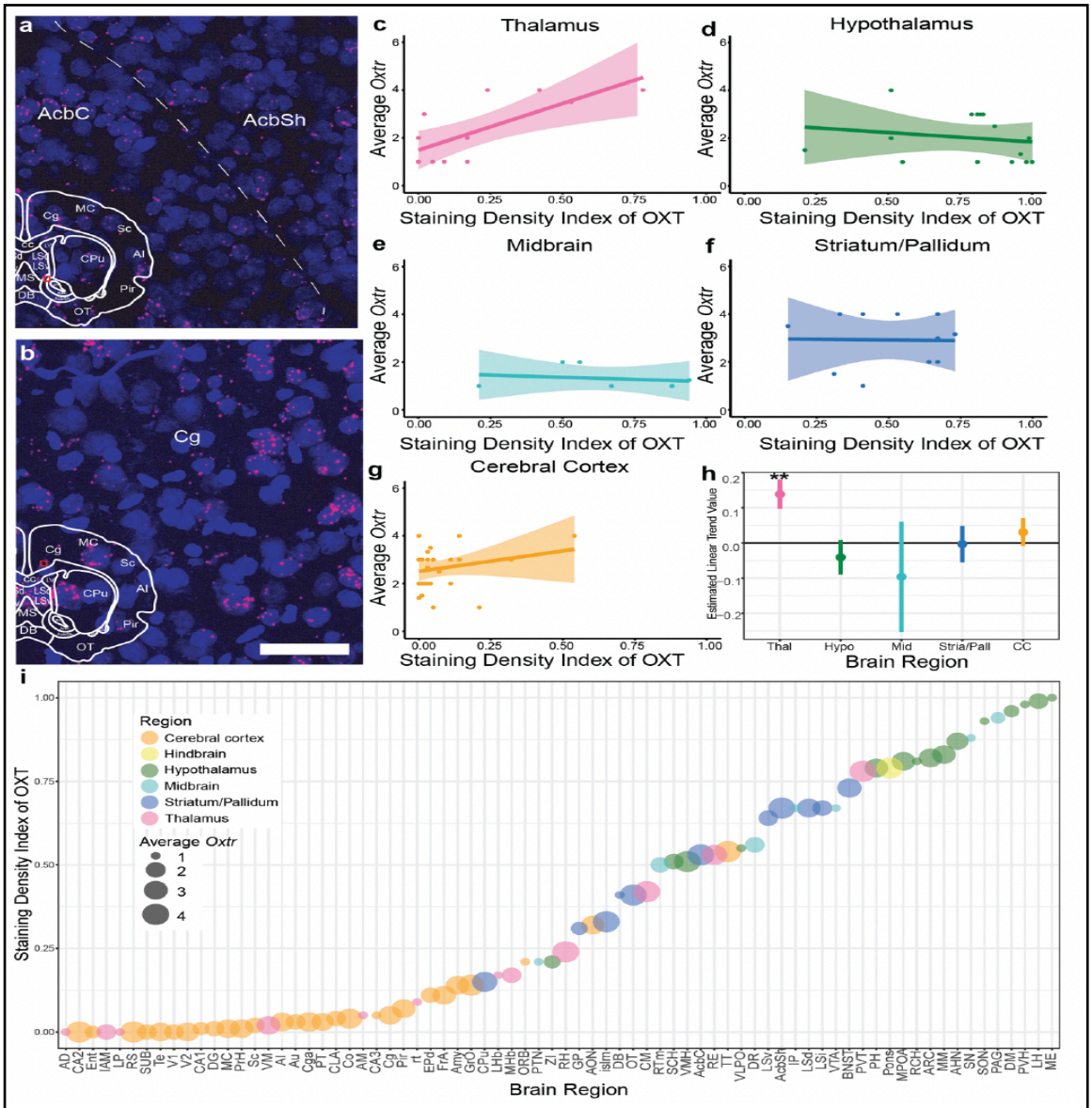

Figure 3: Correlation of OXT+ fibers and *Oxtr* across the whole brain. **A**) A confocal image of *Oxtr* transcript expression (pink) within the AcbSh and **B**) Cg, cell nuclei are stained with DAPI (blue). Scale bar = 50µm. **C-G**) Graphs shown are illustrations of the raw data (brain regions belonging to category are shown as points), regression lines (solid lines) and 95% confidence intervals (shaded areas around regression lines), these are shown for visualization purposes, see H for full statistical analyses. **C**) The density of OXT+ fibers within the thalamus is positively related to density of *Oxtr* transcript ($p = 0.001$), but not in hypothalamus (**D**, $p = 0.41$), midbrain (**E**, $p = 0.54$), striatum/pallidum (**F**, $p = 0.95$), or the cerebral cortex (**G**, $p = 0.44$). **H**) Graphical representation of estimated linear trend analysis illustrating that the thalamus (Thal, pink) is the only region where presence of OXT+ fibers predicts Oxtr. The hypothalamus (Hypo, green) and midbrain (Mid, teal) both have negative, non-significant trend values with a range of OXT+ fibers (often high) and little *Oxtr*. The striatum/pallidum (Stria/Pall, blue) has a trend value of near 0, thus no relationship between OXT+ fibers and *Oxtr*. The cerebral cortex (CC, orange) has a positive, nonsignificant trend value, indicating typically low OXT+ fibers and varying amounts *Oxtr* (often high). I) The staining density index (see Methods) at all regions in descending order from the highest density of OXT+ fibers (top) to the lowest density of OXT+ fibers (bottom) colored by region category. The relative amount of *Oxtr* is indicated by the size of the circle marker.

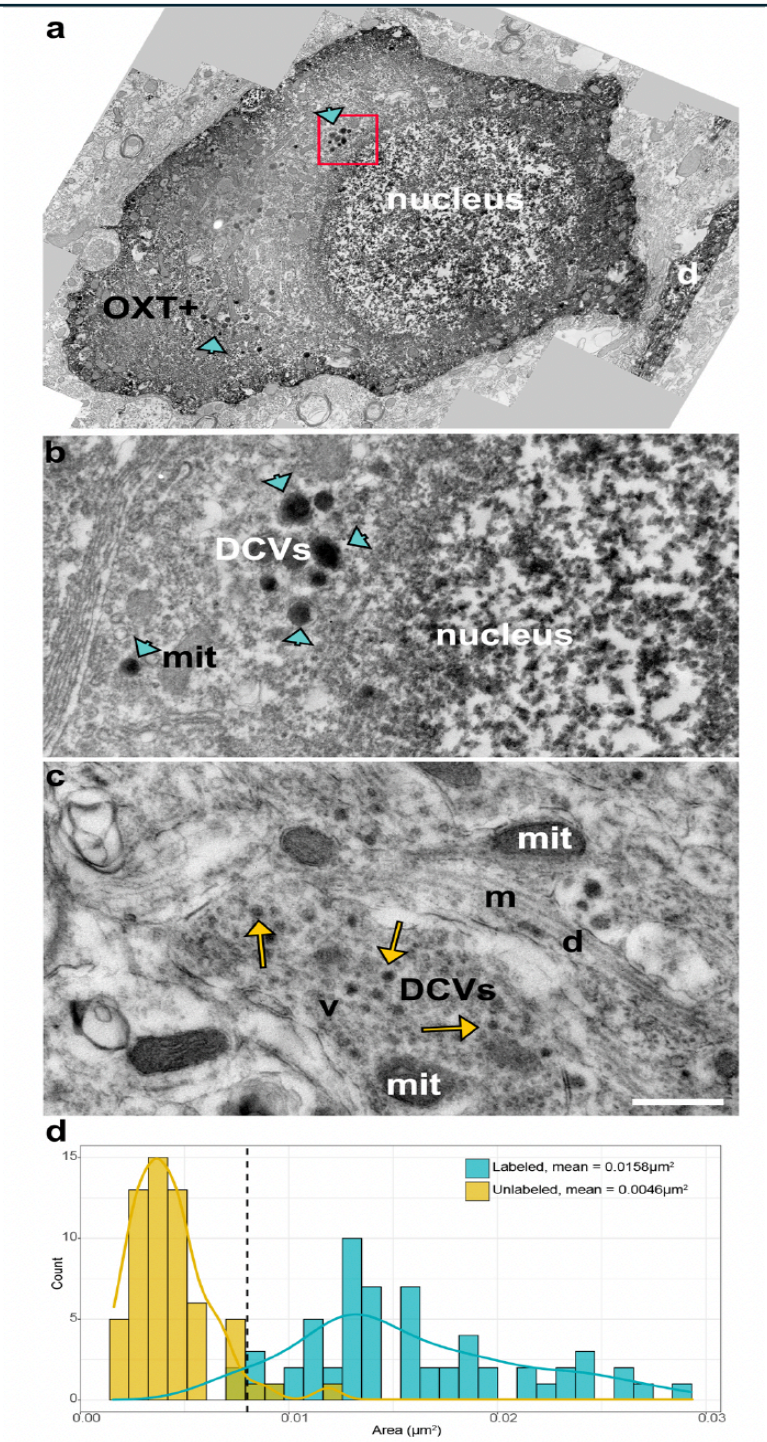

Figure 4: OXT+ somata in PVH (**A**) display clusters of dense cored vesicles (blue arrowheads, DCV's) in the cytoplasm (**A-B**). Unlabeled DCV's (yellow arrows) were also observed in PVH neuropil (**C**). Scale bar = 0.5 µm and applies to B and C. **D**) Frequency distribution histogram of OXT+ (blue bars, n = 61) and OXT- (yellow bars, n = 60) dense core vesicle areas, blue and yellow line overlays represent density curves for labeled and unlabeled distribution respectively. The dashed line marks the cutoff value for classifying DCVs as oxytocinergic. OXT+: oxytocin positive cell, DCVs: dense core vesicles, mit: mitochondria, m: microtubules, d: dendrite

RCH (n=44) displayed an OXT DCV. When present, DCVs were sparse, indicating that the labeled fibers are more likely axons of passage en route to median eminence (**Fig 5A & B**). In contrast, in the MPOA and AHN, many OXT+ profiles contain at least one large DCV (26% of profiles, n=54 and 23%, n=39, respectively) (**Fig 5C & D**), suggesting that oxytocin may be released from axons in MPOA and ANH, providing the neuropeptide ligand for the OXTR that is expressed in these regions.

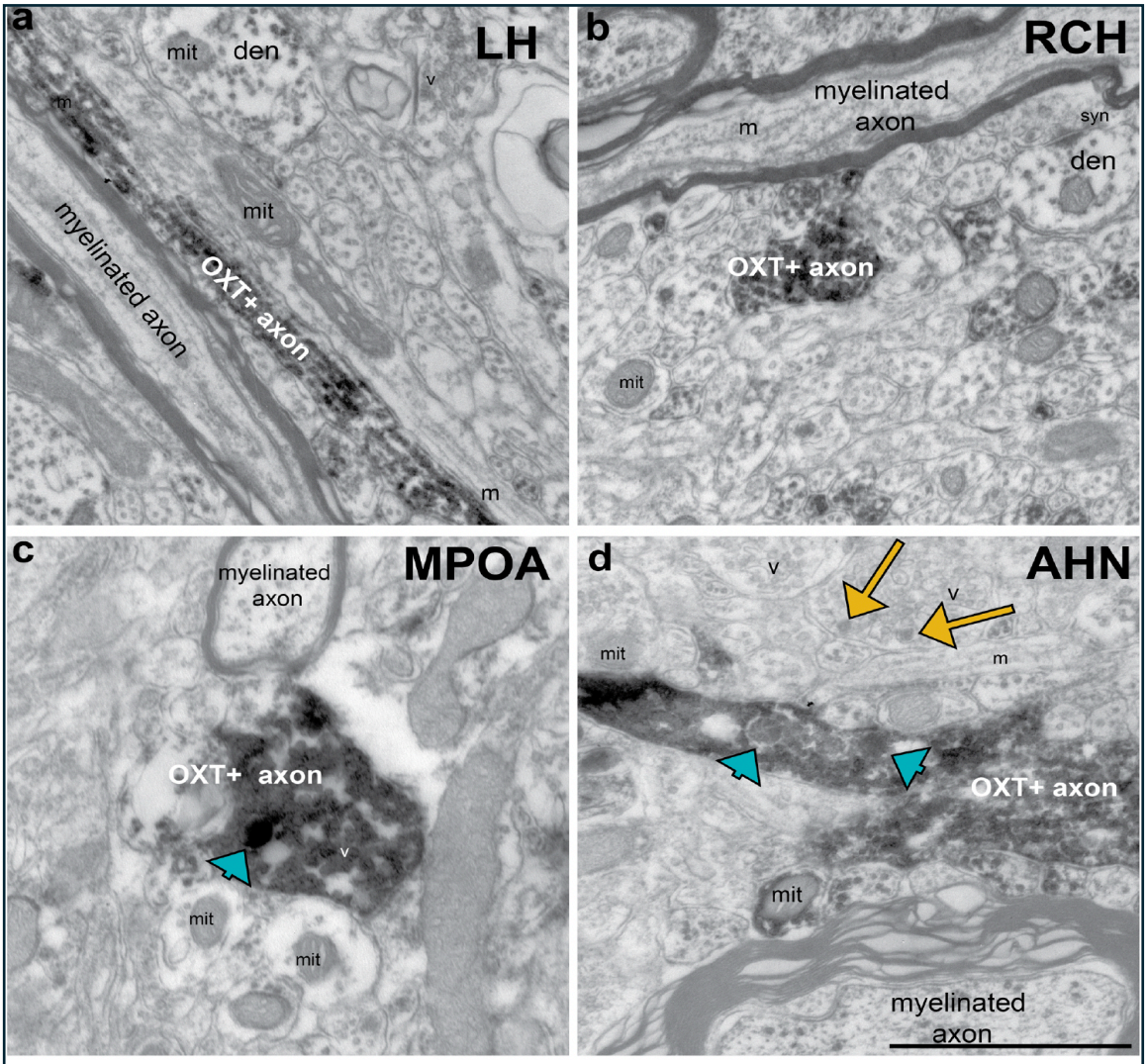

Figure 5: OXT+ axons of the LH and RCH typically do not contain DCV's, indicating they are likely axons of passage, while axons of the MPOA and AHN often contain DCV's. **A**) An Electron micrograph of OXT+ axons in the LH, and **B**) in the RCH, with no DCV's. **C**) EM image of an OXT+ axon in the MPOA with one DCVs (blue arrowhead), and D) an image of an axon in the AHN with two DCV's (blue arrowheads), and unstained neuropil with DCV's (yellow arrows), indicating in the MPOA and AHN oxytocin can be directly released to act on OXTR. Pixel resolution=1134.92 pixels/µm. Scale bar = 1µm. Mit: mitochondria, v: vesicles, den: dendrite, m: microtubules, syn: synapse.

Regions that contain *Oxtr* transcripts and no OXT+ fibers are especially puzzling, because the source of the oxytocin that could activate OXTR in these regions is not obvious. A possibility is the delivery of oxytocin to cortical extracellular space via CSF

circulation. Here, we provide evidence that the circulating CSF may contain OXT that is directly released from dendrites. Using light and electron microscopy, we observed many instances of PVH cell dendrites extending through the ependymal cell layer and directly contacting the third ventricle (**Fig 6A & B**). Of the PVH cell dendritic profiles that are in the ependymal zones, 13% (n=156) contained DCVs (**Fig 6C & D**). Thus, these dendrites are situated to exocytose oxytocin from dense-cored vesicles directly into the CSF. Oxytocin may then readily flow through the subarachnoid space along blood capillaries and reach OXTR in the cortical regions via volume transmission.

Finally, using DAB-labelled and gold-enhanced EM we revealed that 40% (N = 30) of dendrites in the SON contain DCV's (**Fig 6E**). These dendrites often appear densely packed with large DCV's (**Fig 6E**). Interestingly, we noticed using light microscopy, dendrites of the SON cells extend towards the ventral surface of the brain and appear to project through the ependymal cell layer, indicating the possibility that oxytocin can be released into the CSF from SON cells as well (**Fig 1C**).

Whole-Brain imaging of OXT+ staining reveals the extent of ventricular axonal staining

To confirm that ventricular OXT labeling is a prominent feature of the prairie vole brain, which was observed via the brightfield microscopy analysis in regions previously mentioned, such as the BNST, and PAG, we examined two brains that were prepared for whole brain clearing and light-sheet microscopy. Major ventricles have positive OXT staining and OXT+ axons appear to follow along ventricles to terminate in subcortical regions. The brains scanned at 5X magnification revealed a strong fluorescence signal lining 3rd ventricle flanked by the hypothalamus (**Fig 7A**), as well as the lateral ventricles throughout their anterio-posterior span (**Fig 7B**). However, whether these axons are filled with DCVs was not examined using electron microscopy.

Discussion

The current study provides the first comprehensive mapping of the oxytocinergic system of the prairie vole brain, revealing: 1) The localization of oxytocinergic cell bodies in the prairie vole brain fits the pattern demonstrated in other rodents with a few exceptions, including a prominent OXT+ cell group in the AVPV. 2) The prevalence of oxytocin-carrying axons are correlated with the amount of oxytocin receptor transcripts only in certain subcortical structures including anterior midline thalamic regions, suggesting that oxytocin action in these regions is primarily regulated by neuronal activity and axonal release. 3) While the dorso-lateral stream of oxytocinergic fibers courses through the hypothalamus, these contain only a few dense-cored vesicles, thus are likely axons of passage. The ventro-medial stream, however, contain many DCV's and likely release OXT to act on OXTR in these regions. 4) Similar to other rodent species, the prairie vole cerebral cortex areas are distinct in that they have an abundance of receptors yet no oxytocin axons, suggesting that these regions may utilize oxytocin from sources other than direct axonal release. 5) Finally, both the hypothalamic cell dendrites that protrude through the ependymal cell layer, and OXT+ axons that course along all ventricular surfaces are situated to release oxytocin into the CSF. We posit that CSF is oxytocin's primary route of access to the receptor-rich cerebral cortex, and

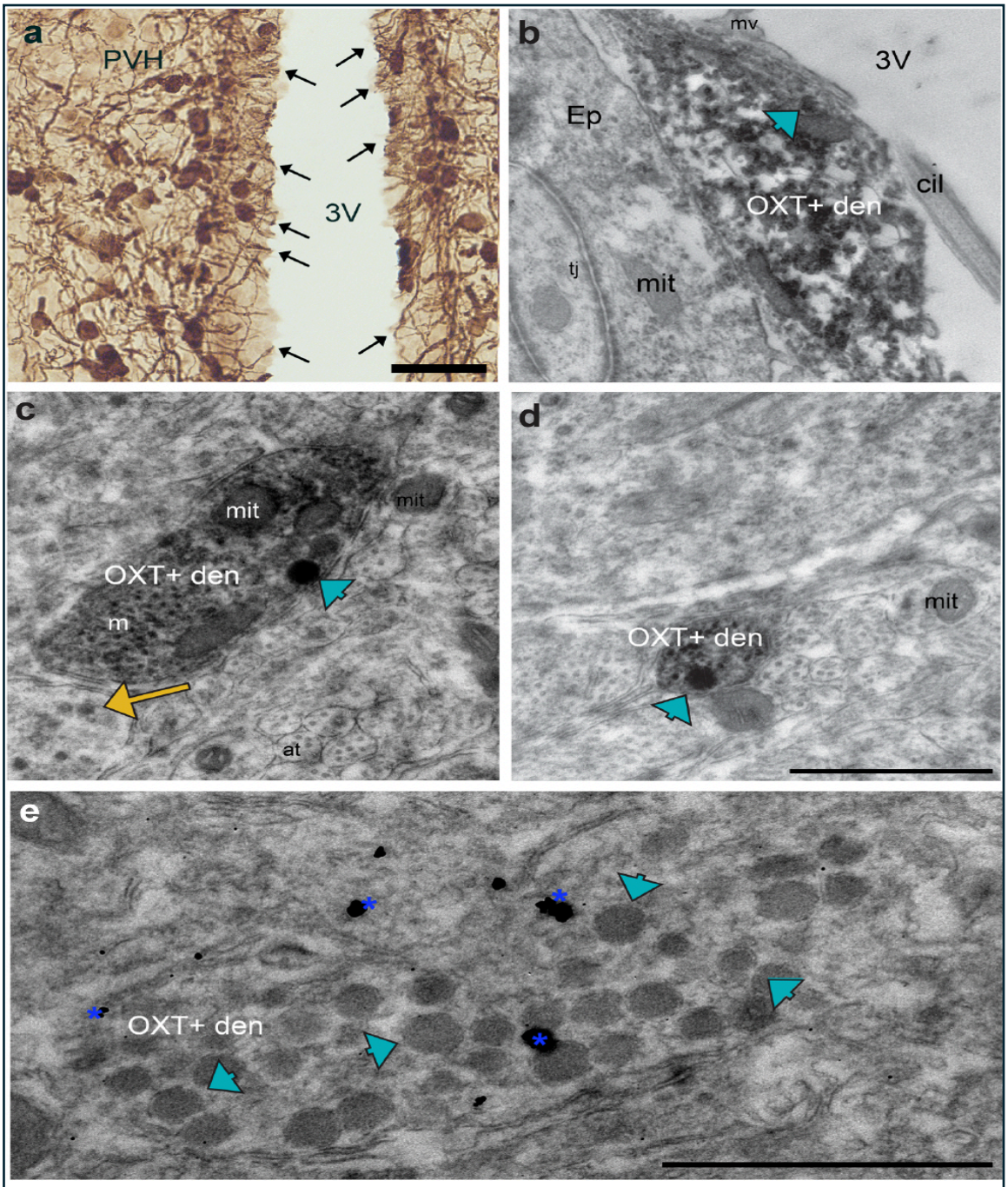

Figure 6: Dendrites of the PVH and SON contain DCVs and are positioned to release OXT into the CSF. **A**) OXT+ cells of the PVH extend their dendrites towards the third ventricle (3V), appearing to cross the ependymal cell layer. Scale bar = 500µm. **B**) Electron micrograph of an OXT+ dendrite (OXT+ den) with a DCV (blue arrowhead) located at ventricle-side of the ependymal cells (Ep). The dendrite directly contacts the third ventricle (3V). **C-D**) Dendrites (OXT+ den) within the PVH that contain DCVs (blue arrowhead). Other, smaller DCVs (yellow arrows) are often encountered in unlabeled neuropil in the same region as the OXT+ dendrites and axons. **E**) An immuno-gold labeled (blue asterisks) OXT+ dendrite within the SON, with a high density of large DCVs (blue arrowheads). Pixel resolution=1134.92 pixels/µm; scale bars on B-E = 1µm. Tj: tight junction of ependymal cell; mit: mitochondria; cil: cilia; mv: microvilli; at: axon terminal; v: vesicles.

potentially other regions of the striatum and pallidum, where the oxytocinergic axons are sparse.

Comparison of prairie vole to other rodents:

Oxytocin-producing cells in the prairie vole brain are in the hypothalamus and the BNST, and this is similar to what has been demonstrated in the mouse (Otero-García et al. 2016; Son et al. 2022). An exception to the general agreement in cell localization among prairie voles and other rodents is one area with OXT cells in the vole: the AVPV.

The AVPV is the brain region that is responsible for regulating the estrous cycle and initiating the onset of puberty (Hu et al. 2015; Marraudino et al. 2017). Unlike mice, prairie voles do not display an estrous cycle unless they are induced by exposure to male pheromones (Carter et al. 1987). Thus, the presence of OXT cells in this region may underlie the anatomical basis for the oxytocinergic modulation of this unique function. In addition, prolonged exposure to conspecific pheromones induces oxytocin-dependent pair-bonding behavior in both male and female prairie voles (Williams et al. 1992; Cho et al. 1999; Castro et al. 2022). Whether or not the presence of the oxytocinergic cells in AVPV implies a role for oxytocin in the induction of pair-bonding via induced estrous requires further research.

Humoral release of oxytocin:

Similar to other rodents (Brownstein et al. 1980; Brown et al. 2020; Zhang et al. 2021), the axons originating primarily from the prairie vole PVH and SON project to the posterior pituitary. In fact, the axons from the midline PVH take rather a circuitous route to form a girth around the lateral hypothalamus before they join axons from SON and extend ventrally to the median eminence in the midline again. Furthermore, PVH axons display varicosities, intimating that oxytocin may be released from PVH axons (Puder and Papka 2001; Veening et al. 2010a; Oti et al. 2021). However, our electron microscopy results are not consistent with the possibility that oxytocin is released from dense cored vesicles of PVH axons en route to the posterior pituitary. These varicosities may be a characteristic structural feature of OXT cells and axons, as has long been observed in immunostained OXT tissue (Theodosis 1985; Morris and Pow 1988; Veening et al. 2010a), but may not necessarily indicate release.

Axonal release of oxytocin on select brain regions:

Other regions of the hypothalamus with many fibers and an abundance of axonal swellings such as the AHN and MPOA contain dense cored vesicles, situated to release oxytocin, presumably via the neuronal activity that occurs at their cell bodies. Many other regions, including the AcbSh, RE of the thalamus, and olfactory cortex display oxytocin axons with similar morphological features and as such may also contain DCV's to release OXT directly. This is consistent with previous studies indicating that the release of oxytocin can be activity-dependent and will act quickly to modulate the activity of regions that contain oxytocin fibers and receptors (Ludwig et al. 2002; Rossoni et al. 2008; Knobloch et al. 2012; Chini et al. 2017; Carcea et al. 2021). The direct release of

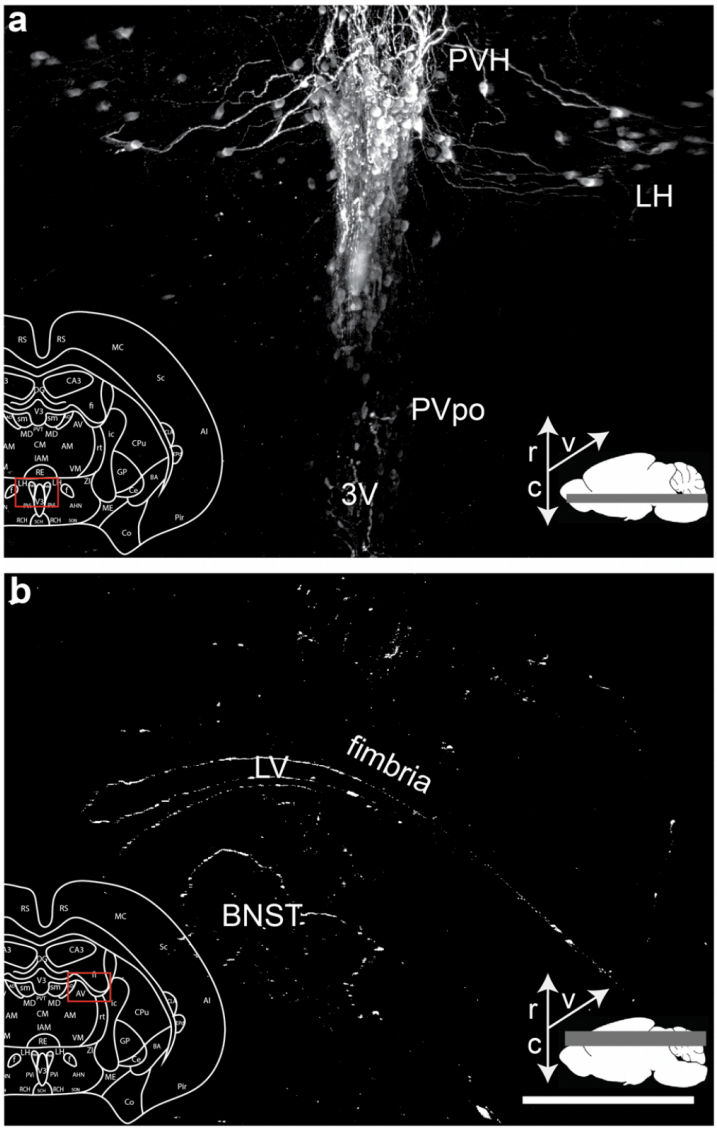

Figure 7: 3D whole-brain light-sheet microscopy verified that OXT+ axons border major ventricles. **A**) The PVH and PVpo both consistently contain cell bodies, and axons projecting from these regions to follow along the third ventricle (3V), with maximum intensity projection across 775µm. **B**) Representative image of the lateral ventricle (LV), fimbria, and BNST with axonal fibers again bordering a major ventricle, maximum intensity projection across 1554µm. Both images were derived from 3D whole-brain scan using a light sheet microscope at 5x objective, are shown in the horizontal plane, and further processed using Imaris software. The superimposed inset marks the region on a corresponding coronal atlas section in red, and thin white arrows in the lower right corner arrows indicate anterior (a), posterior (p), and ventral (v) orientations of the image. Scale bar = 300µm

OXT in these areas can bind to OXTR to impact unique prairie vole behaviors such as social monogamy and affiliative interactions (Ross et al. 2009; Ophir et al. 2012). The origins of oxytocinergic cells that provide these axons, and how those cells are activated to release their peptide warrant further investigation (Zhang et al. 2021; Li et al. 2024). For example, a recent study has demonstrated, in the mouse, that PVH cells that innervate subcortical limbic regions such as the amygdala and hindbrain regions are a

subpopulation distinct from those projecting to the pituitary (Li et al. 2024), suggesting that activity-dependent release of oxytocin in central regions may be independent of the conditions that lead to humoral release of oxytocin.

It was suggested that the low incidence of oxytocin fibers in the cerebral cortex may be a state-dependent observation, and that the oxytocin production surge in the hypothalamus during the birthing process may render cortical axons that otherwise contain low amounts of the neuropeptide detectable. In support of this idea, work in the mouse model has shown the presence of OXT+ fibers, albeit sparsely, in the auditory cortex of dams (Marlin et al. 2015), and suggested that axonally released oxytocin in this region may regulate maternal behavior that relies on sensory discrimination of pup calls, Future studies should examine in the prairie vole if, under certain circumstances, OXT fibers can be observed in other cortical regions as well.

Oxytocin in the CSF:

Oxytocin's presence in the CSF has been acknowledged in many studies (Mens et al. 1983; Veening et al. 2010a; Kagerbauer et al. 2013; Jurek and Neumann 2018). Furthermore, the CSF is confluent with the extracellular fluid of the neuropil through intercellular junctions between ependymal cells, it has been suggested that oxytocin might reach its receptor via volume transmission from the CSF (Ludwig et al. 2002; Veening et al. 2010a). However, how oxytocin gets to the CSF has been the subject of intense debate. One source of the CSF oxytocin could be the blood. Humorally released oxytocin may return to cerebral blood circulation and diffuse into the CSF (Lee et al. 2018; Yamamoto et al. 2019). However, one study found only about 0.002% of peripherally applied OXT reaches the CNS following IV injections (Mens et al. 1983), and later work has found similar results, (Freeman et al. 2016; Lee et al. 2018), suggesting that blood is not the primary source of the CSF oxytocin (although, see Yamamoto et al. 2019). Other evidence also supports the idea that CSF oxytocin may have a primary origin other than the blood (Ludwig et al. 2002; Leng and Ludwig 2008; Veening et al. 2010a; Kagerbauer et al. 2013; Lefevre et al. 2017). First, oxytocin concentration in the CSF of humans is consistently higher than in plasma and increases in plasma oxytocin is not a predictor of increases in the CSF oxytocin (Kagerbauer et al. 2013). In addition, the plasma oxytocin has a significantly shorter half-life (about 2-5 minutes) than the CSF oxytocin (about 20-30 minutes) (Mens et al. 1983; Leng and Ludwig 2008; Veening et al. 2010a), suggesting that plasma clearance rate may pose a bottleneck for sustaining the CSF oxytocin concentration.

Then, how does endogenous, central oxytocin reach the CSF? Our results provide further evidence that the dendrites of the oxytocinergic cells in the hypothalamus are ideally positioned to release oxytocin directly into the CSF. We have demonstrated that OXT+ dendrites frequently cross the ependymal cell layer and directly contact the ventricle. The medial hypothalamic cells that project to the posterior pituitary are situated in an opportune position because their dendrites readily line the ventricular surface and,

in many instances, protrude into the ventricles, potentially providing a basal amount of oxytocin in the CSF.

The conditions that are associated with large hormonal surges, such as birth, within the periphery also likely influence the oxytocin concentration in the CSF. For example, during labor, there is a pulsatile release of OXT into the periphery in amounts much higher than seen pre-pregnancy (Leake et al. 1981). Similarly, the peripheral release of oxytocin during gestation is high (Uvnäs-Moberg et al. 2019), and this may increase the central release of oxytocin into the CSF via dendritic exocytosis. This is particularly important because birth triggers many oxytocin-mediated central behaviors including the onset of maternal behavior in rodents (Numan 1988; Stolzenberg and Champagne 2016) and plasticity within cortical regions (Marlin et al. 2015; Mitre et al. 2016). Further, birth and exogenous oxytocin treatment trigger epigenetic changes to the oxytocin receptor that primes the system to prepare the animal for motherhood (Stolzenberg and Champagne 2016; Danoff et al. 2023). Thus, the birth-triggered robust plasticity within cortical regions must be mediated via oxytocin circulating within the CSF, and the release of oxytocin from PVH cell dendrites along the ependymal cell layer is the most likely source of the CSF oxytocin.

Ependymal cells not only contribute to CSF production and movement, but they also sift through the circulating fluid to clear accumulated waste and to maintain homeostasis between the extracellular space and CSF (Deng et al. 2023). Ependymal cells have also been found to contain transporters, such as the glucose transporter indicating they may play a critical role in the transport of essential substances between the extracellular space and the ventricles (Murakami et al. 2016; Deng et al. 2023). Therefore, the ependymal cells could play an active role in transporting oxytocin exocytosed from oxytocinergic dendrites from the extracellular space into the CSF. It should also be noted that oxytocin release into CSF can happen not only at the 3rd ventricle surrounded by the hypothalamus but also along the entire ventricular surface, due to an extensive stream of oxytocinergic axons as well as ectopic oxytocinergic cells that are located by the ventricles, something that has also been observed in the mouse model recently (Son et al. 2022). The presence of DCVs in the axons that border all major ventricles should be determined in future studies. Whether or not the dendritic and axonal oxytocin release into CSF is triggered by similar central activity also requires further examination.

Are there multiple oxytocinergic systems?

Our results highlight three different release modes of oxytocin: humoral release to the pituitary, axonal release, mostly in subcortical structures, and the dendritic, and potentially axonal release into ventricles. These three modes of release may differentially contribute to the diversity of oxytocin's action in the periphery and the central nervous system. For example, oxytocin's physiological effects on the body such as the initiation of contractions at birth and milk letdown during lactation (Soloff et al. 1979; Perkinson et al. 2021) is purely a function of oxytocin that is synthesized primarily in the

magnocellular cells of PVH and SON ((Vigneaud et al. 1953; Brownstein et al. 1980; Zhang et al. 2021; Li et al. 2024) and released in the pituitary, although there is also evidence for local synthesis of oxytocin in peripheral tissue as well (Einspanier and Ivell 1997; Jankowski et al. 1998; Carter et al. 2020). On the other hand, modifying the behaviors related to bonding and the stress response involves axonal oxytocin release in limbic regions, including the nucleus accumbens, the amygdala, and bed nucleus of the stria terminalis. The oxytocin-releasing axons in these regions originate from the PVH, (Zhang et al. 2021; Freda et al. 2022; Li et al. 2024) and, as we also demonstrated in the current study, they release oxytocin from axonal varicosities (Armstrong et al. 1982; Tweedle et al. 1989; Knobloch et al. 2012) to bind OXTR.

Finally, oxytocin's role in regulating aggressive behaviors, learning, and other more complex cognitive functions that require the involvement of sensory and association cortices (Bales and Carter 2003; Hurlemann et al. 2010; Marlin et al. 2015; Jurek and Neumann 2018). For example, maternal behavior in mice, which is typically displayed only after the oxytocin surge associated with giving birth, relies on plasticity within cortical regions and oxytocin to OXTR binding (Marlin et al. 2015; Froemke and Young 2021; Carcea et al. 2021). Similarly, the prairie vole displays consoling behavior after partner stress and separation which is also linked to OXTR binding in the prelimbic cortex (PrL) and anterior cingulate cortex (Cg), accentuating the importance of the availability of oxytocin to the cortex (Burkett et al. 2016). However, while many cortical regions contain an abundance of OXTR (Bosch et al. 2016; Newmaster et al. 2020; Inoue et al. 2022; Son et al. 2022) they lack a high density of oxytocin-containing fibers (Mitre et al. 2018; Liao et al. 2020; Manjila et al. 2022; Son et al. 2022), as demonstrated in the current study for the prairie voles, suggesting that oxytocin's effect in the cortex is independent of axonal or humoral oxytocin release (Veening et al. 2010b; Ferris et al. 2015; Mitre et al. 2016; Son et al. 2022). The results of the current study demonstrate structural evidence for substantial oxytocin release into the CSF and suggest that this third mode of oxytocin release may be the main source of oxytocin that mediates aggression, learning, and other higher cognitive functions in the cerebral cortex, where the axonal release of oxytocin is unpronounced.

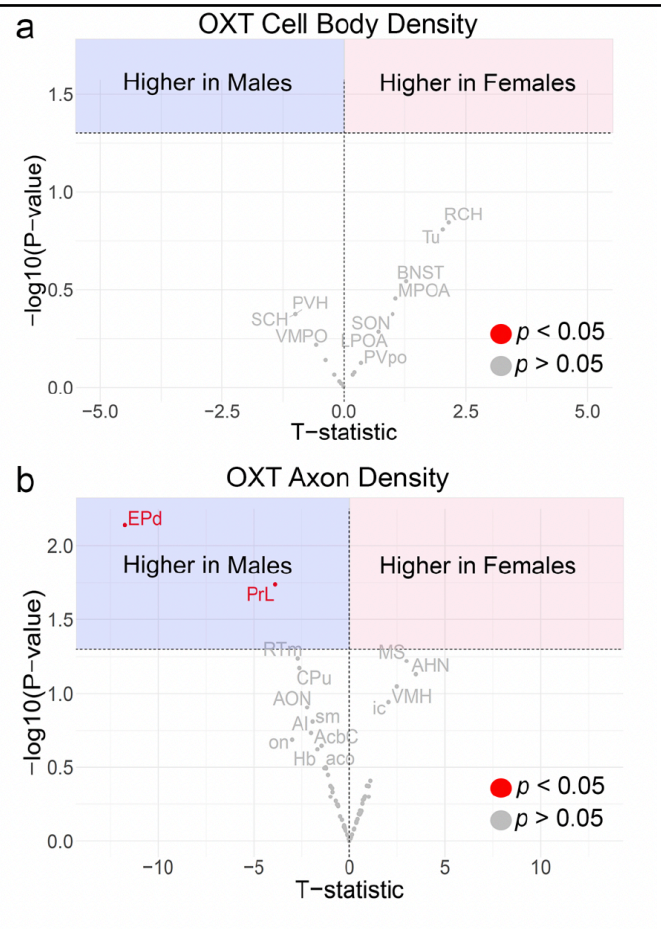

Supplemental Figure 1: Few sexual dimorphisms in OXT+ cell bodies and axons are seen between male and female prairie voles. In both plots, the x-axis illustrates the t-statistic where positive values indicate higher mean scores in females and negative values indicate higher mean scores in males. The y-axis represents the negative logarithm (base 10) of the p-values with higher values indicating greater statistical significance. Brain regions with p-values < 0.05 are indicated with a red circle and highlight significant differences. All non-significant regions are displayed with gray circles. **A**) There is not a significant difference in OXT+ cell body density in males vs. Females in any brain regions examined (examined using a Welch's t-test). **B**) Although there is not sufficient statistical power, two regions, the EPd (p = 0.007) and PrL (p = 0.02), may be sexually dimorphic, with males (EPd: Mean = 0.17 ± SD = 0.026, PrL: 0.25±0.07) showing higher SDI values than females (EPd: 0 ± 0, PrL: 0.04 ± 0.06)

References:

Allen Reference Atlas – Mouse Brain [Coronal Reference Atlas]. Available from atlas.brain-map.org.

Armstrong WE, Scho¨ler J, McNeill TH (1982) Immunocytochemical, Golgi and electron microscopic characterization of putative dendrites in the ventral glial lamina of the rat supraoptic nucleus. Neuroscience 7:679–694. https://doi.org/10.1016/0306-4522(82)90074-4

Bale TL, Davis AM, Auger AP, et al (2001) CNS Region-Specific Oxytocin Receptor Expression: Importance in Regulation of Anxiety and Sex Behavior. J Neurosci 21:2546–2552. https://doi.org/10.1523/JNEUROSCI.21-07-02546.2001

Bales KL, Carter CS (2003) Sex differences and developmental effects of oxytocin on aggression and social behavior in prairie voles (Microtus ochrogaster). Hormones and Behavior 44:178–184. https://doi.org/10.1016/S0018-506X(03)00154-5

Borland JM, Rilling JK, Frantz KJ, Albers HE (2019) Sex-dependent regulation of social reward by oxytocin: an inverted U hypothesis. Neuropsychopharmacol 44:97–110. https://doi.org/10.1038/s41386-018-0129-2

Bosch OJ, Dabrowska J, Modi ME, et al (2016) Oxytocin in the nucleus accumbens shell reverses CRFR2-evoked passive stress-coping after partner loss in monogamous male prairie voles. Psychoneuroendocrinology 64:66–78. https://doi.org/10.1016/j.psyneuen.2015.11.011

Brown CH, Ludwig M, Tasker JG, Stern JE (2020) Somato-dendritic vasopressin and oxytocin secretion in endocrine and autonomic regulation. J Neuroendocrinol 32:e12856. https://doi.org/10.1111/jne.12856

Brownstein MJ, Russell JT, Gainer H (1980) Synthesis, Transport, and Release of Posterior Pituitary Hormones. Science 207:373–378. https://doi.org/10.1126/science.6153132

Burkett JP, Andari E, Johnson ZV, et al (2016) Oxytocin-dependent consolation behavior in rodents. Science 351:375–378. https://doi.org/10.1126/science.aac4785

Carcea I, Caraballo NL, Marlin BJ, et al (2021) Oxytocin neurons enable social transmission of maternal behaviour. Nature 596:553–557. https://doi.org/10.1038/s41586-021-03814-7

Carter CS (1992) Oxytocin and sexual behavior. Neuroscience & Biobehavioral Reviews 16:131–144. https://doi.org/10.1016/S0149-7634(05)80176-9

Carter CS, Getz LL (1993) Monogamy and the Prairie Vole. Scientific American 268:100–106

Carter CS, Kenkel WM, MacLean EL, et al (2020) Is Oxytocin "Nature's Medicine"? Pharmacol Rev 72:829–861. https://doi.org/10.1124/pr.120.019398

Carter CS, Witt DM, Schneider J, et al (1987) Male stimuli are necessary for female sexual behavior and uterine growth in prairie voles (*Microtus ochrogaster*). Hormones and Behavior 21:74–82. https://doi.org/10.1016/0018-506X(87)90032-8

Castro AE, Domínguez-Ordoñez R, Young LJ, et al (2022) Pair-bonding and social experience modulate new neurons survival in adult male and female prairie voles (Microtus ochrogaster). Front Neuroanat 16:. https://doi.org/10.3389/fnana.2022.987229

Chini B, Verhage M, Grinevich V (2017) The Action Radius of Oxytocin Release in the Mammalian CNS: From Single Vesicles to Behavior. Trends in Pharmacological Sciences 38:982–991. https://doi.org/10.1016/j.tips.2017.08.005

Cho MM, DeVries AC, Williams JR, Carter CS (1999) The effects of oxytocin and vasopressin on partner preferences in male and female prairie voles (Microtus ochrogaster). Behavioral Neuroscience 113:1071–1079. https://doi.org/10.1037/0735-7044.113.5.1071

Crowley WR, Armstrong WE (1992) Neurochemical Regulation of Oxytocin Secretion in Lactation. 13:

Dabrowska J, Hazra R, Ahern TH, et al (2011) Neuroanatomical evidence for reciprocal regulation of the corticotrophin-releasing factor and oxytocin systems in the hypothalamus and the bed nucleus of the stria terminalis of the rat: Implications for balancing stress and affect. Psychoneuroendocrinology 36:1312–1326. https://doi.org/10.1016/j.psyneuen.2011.03.003

Dale HH (1906) On some physiological actions of ergot. The Journal of Physiology 34:163–206. https://doi.org/10.1113/jphysiol.1906.sp001148

Danoff JS, Page EA, Perkeybile AM, et al (2023) Transcriptional diversity of the oxytocin receptor in prairie voles: mechanistic implications for behavioral neuroscience and maternal physiology. Front Genet 14:. https://doi.org/10.3389/fgene.2023.1225197

Deng S, Gan L, Liu C, et al (2023) Roles of Ependymal Cells in the Physiology and Pathology of the Central Nervous System. Aging Dis 14:468–483. https://doi.org/10.14336/AD.2022.0826-1

Duchemin A, Seelke AMH, Simmons TC, et al (2017) Localization of oxytocin receptors in the prairie vole (Microtus ochrogaster) neocortex. Neuroscience 348:201–211. https://doi.org/10.1016/j.neuroscience.2017.02.017

Einspanier A, Ivell R (1997) Oxytocin and Oxytocin Receptor Expression in Reproductive Tissues of the Male Marmoset Monkey1. Biology of Reproduction 56:416–422. https://doi.org/10.1095/biolreprod56.2.416

Ferris CF, Yee JR, Kenkel WM, et al (2015) Distinct BOLD Activation Profiles Following Central and Peripheral Oxytocin Administration in Awake Rats. Frontiers in Behavioral Neuroscience 9:

Freda SN, Priest MF, Badong D, et al (2022) Brainwide input-output architecture of paraventricular oxytocin and vasopressin neurons. 2022.01.17.476652

Freeman SM, Samineni S, Allen PC, et al (2016) Plasma and CSF oxytocin levels after intranasal and intravenous oxytocin in awake macaques. Psychoneuroendocrinology 66:185–194. https://doi.org/10.1016/j.psyneuen.2016.01.014

Froemke RC, Young LJ (2021) Oxytocin, Neural Plasticity, and Social Behavior. Annual Review of Neuroscience 44:359–381. https://doi.org/10.1146/annurev-neuro-102320-102847

Giannotti G, Mottarlini F, Heinsbroek JA, et al (2022) Oxytocin and orexin systems bidirectionally regulate the ability of opioid cues to bias reward seeking. Transl Psychiatry 12:432. https://doi.org/10.1038/s41398-022-02161-z

Gimpl G, Fahrenholz F (2001) The Oxytocin Receptor System: Structure, Function, and Regulation. Physiological Reviews 81:629–683. https://doi.org/10.1152/physrev.2001.81.2.629

Hiura LC, Ophir AG (2018) Interactions of sex and early life social experiences at two developmental stages shape nonapeptide receptor profiles. Integrative Zoology 13:745–760. https://doi.org/10.1111/1749-4877.12338

Hu MH, Li XF, McCausland B, et al (2015) Relative Importance of the Arcuate and Anteroventral Periventricular Kisspeptin Neurons in Control of Puberty and Reproductive Function in Female Rats. Endocrinology 156:2619. https://doi.org/10.1210/en.2014-1655

Hurlemann R, Patin A, Onur OA, et al (2010) Oxytocin Enhances Amygdala-Dependent, Socially Reinforced Learning and Emotional Empathy in Humans. J Neurosci 30:4999–5007. https://doi.org/10.1523/JNEUROSCI.5538-09.2010

Inoue K, Ford CL, Horie K, Young LJ (2022) Oxytocin receptors are widely distributed in the prairie vole (Microtus ochrogaster) brain: Relation to social behavior, genetic polymorphisms, and the dopamine system. Journal of Comparative Neurology 530:2881–2900. https://doi.org/10.1002/cne.25382

Insel TR, Shapiro LE (1992) Oxytocin receptor distribution reflects social organization in monogamous and polygamous voles. Proc Natl Acad Sci USA 89:5981–5985. https://doi.org/10.1073/pnas.89.13.5981

Jankowski M, Hajjar F, Kawas SA, et al (1998) Rat heart: A site of oxytocin production and action. Proc Natl Acad Sci USA 95:14558–14563. https://doi.org/10.1073/pnas.95.24.14558

Jurek B, Neumann ID (2018) The Oxytocin Receptor: From Intracellular Signaling to Behavior. Physiological Reviews 98:1805–1908. https://doi.org/10.1152/physrev.00031.2017

Kagerbauer SM, Martin J, Schuster T, et al (2013) Plasma Oxytocin and Vasopressin do not Predict Neuropeptide Concentrations in Human Cerebrospinal Fluid. Journal of Neuroendocrinology 25:668–673. https://doi.org/10.1111/jne.12038

Kelly AM, Hiura LC, Ophir AG (2018) Rapid nonapeptide synthesis during a critical period of development in the prairie vole: plasticity of the paraventricular nucleus of the hypothalamus. Brain Struct Funct 223:2547–2560. https://doi.org/10.1007/s00429-018-1640-2

Kenkel WM, Gustison ML, Beery AK (2021) A Neuroscientist's Guide to the Vole. Current Protocols 1:e175. https://doi.org/10.1002/cpz1.175

Knobloch HS, Charlet A, Hoffmann LC, et al (2012) Evoked Axonal Oxytocin Release in the Central Amygdala Attenuates Fear Response. Neuron 73:553–566. https://doi.org/10.1016/j.neuron.2011.11.030

Laurent FM, Hindelang C, Klein MJ, et al (1989) Expression of the oxytocin and vasopressin genes in the rat hypothalamus during development: an in situ hybridization study. Developmental Brain Research 46:145–154. https://doi.org/10.1016/0165-3806(89)90152-1

LEAKE RD, WEITZMAN RE, GLATZ TH, FISHER DA (1981) Plasma Oxytocin Concentrations in Men, Nonpregnant Women, and Pregnant Women before and during Spontaneous Labor*. The Journal of Clinical Endocrinology & Metabolism 53:730–733. https://doi.org/10.1210/jcem-53-4-730

Lee MR, Scheidweiler KB, Diao XX, et al (2018) Oxytocin by intranasal and intravenous routes reaches the cerebrospinal fluid in rhesus macaques: determination using a novel oxytocin assay. Mol Psychiatry 23:115–122. https://doi.org/10.1038/mp.2017.27

Lefevre A, Mottolese R, Dirheimer M, et al (2017) A comparison of methods to measure central and peripheral oxytocin concentrations in human and non-human primates. Sci Rep 7:17222. https://doi.org/10.1038/s41598-017-17674-7

Lemos JR, Dayanithi G (eds) (2020) Neurosecretion: Secretory Mechanisms. Springer International Publishing, Cham

Leng G, Ludwig M (2008) Neurotransmitters and peptides: whispered secrets and public announcements. The Journal of Physiology 586:5625–5632. https://doi.org/10.1113/jphysiol.2008.159103

Li H, Jiang T, An S, et al (2024) Single-neuron projectomes of mouse paraventricular hypothalamic nucleus oxytocin neurons reveal mutually exclusive projection patterns. Neuron 112:1081-1099.e7. https://doi.org/10.1016/j.neuron.2023.12.022

Liao P-Y, Chiu Y-M, Yu J-H, Chen S-K (2020) Mapping Central Projection of Oxytocin Neurons in Unmated Mice Using Cre and Alkaline Phosphatase Reporter. Frontiers in Neuroanatomy 14:

Liu CM, Hsu TM, Suarez AN, et al (2020) Central oxytocin signaling inhibits food reward-motivated behaviors and VTA dopamine responses to food-predictive cues in male rats. Hormones and Behavior 126:104855. https://doi.org/10.1016/j.yhbeh.2020.104855

Loth MK, Donaldson ZR (2021) Oxytocin, Dopamine, and Opioid Interactions Underlying Pair Bonding: Highlighting a Potential Role for Microglia. Endocrinology 162:bqaa223. https://doi.org/10.1210/endocr/bqaa223

Ludwig M, Leng G (2006) Dendritic peptide release and peptide-dependent behaviours. Nat Rev Neurosci 7:126–136. https://doi.org/10.1038/nrn1845

Ludwig M, Sabatier N, Bull PM, et al (2002) Intracellular calcium stores regulate activity-dependent neuropeptide release from dendrites. Nature 418:85–89. https://doi.org/10.1038/nature00822

Makani V, Sultana R, Sie KS, et al (2013) Annexin A1 Complex Mediates Oxytocin Vesicle Transport. J Neuroendocrinology 25:1241–1254. https://doi.org/10.1111/jne.12112

Manjila SB, Betty R, Kim Y (2022) Missing pieces in decoding the brain oxytocin puzzle: Functional insights from mouse brain wiring diagrams. Frontiers in Neuroscience 16:

Marlin BJ, Mitre M, D'amour JA, et al (2015) Oxytocin enables maternal behaviour by balancing cortical inhibition. Nature 520:499–504. https://doi.org/10.1038/nature14402

Marraudino M, Miceli D, Farinetti A, et al (2017) Kisspeptin innervation of the hypothalamic paraventricular nucleus: sexual dimorphism and effect of estrous cycle in female mice. Journal of Anatomy 230:775–786. https://doi.org/10.1111/joa.12603

Mens WBJ, Witter A, Van Wimersma Greidanus TB (1983) Penetration of neurohypophyseal hormones from plasma into cerebrospinal fluid (CSF): Half-times of disappearance of these neuropeptides from CSF. Brain Research 262:143–149. https://doi.org/10.1016/0006-8993(83)90478-X

Mitre M, Marlin BJ, Schiavo JK, et al (2016) A Distributed Network for Social Cognition Enriched for Oxytocin Receptors. J Neurosci 36:2517–2535. https://doi.org/10.1523/JNEUROSCI.2409-15.2016

Mitre M, Minder J, Morina EX, et al (2018) Oxytocin Modulation of Neural Circuits. In: Hurlemann R, Grinevich V (eds) Behavioral Pharmacology of Neuropeptides: Oxytocin. Springer International Publishing, Cham, pp 31–53

Morris JF, Pow DV (1988) Capturing and Quantifying the Exocytotic Event. Journal of Experimental Biology 139:81–103. https://doi.org/10.1242/jeb.139.1.81

Murakami R, Chiba Y, Tsuboi K, et al (2016) Immunoreactivity of glucose transporter 8 is localized in the epithelial cells of the choroid plexus and in ependymal cells. Histochem Cell Biol 146:231–236. https://doi.org/10.1007/s00418-016-1444-5

Newmaster KT, Nolan ZT, Chon U, et al (2020) Quantitative cellular-resolution map of the oxytocin receptor in postnatally developing mouse brains. Nat Commun 11:1885. https://doi.org/10.1038/s41467-020-15659-1

Numan M (1988) Neural basis of maternal behavior in the rat. Psychoneuroendocrinology 13:47–62. https://doi.org/10.1016/0306-4530(88)90006-6

Olazábal DE, Young LJ (2006) Species and individual differences in juvenile female alloparental care are associated with oxytocin receptor density in the striatum and the lateral septum. Hormones and Behavior 49:681–687. https://doi.org/10.1016/j.yhbeh.2005.12.010

Olff M, Frijling JL, Kubzansky LD, et al (2013) The role of oxytocin in social bonding, stress regulation and mental health: An update on the moderating effects of context and interindividual differences. Psychoneuroendocrinology 38:1883–1894. https://doi.org/10.1016/j.psyneuen.2013.06.019

Ophir AG, Gessel A, Zheng D-J, Phelps SM (2012) Oxytocin receptor density is associated with male mating tactics and social monogamy. Hormones and Behavior 61:445–453. https://doi.org/10.1016/j.yhbeh.2012.01.007

Otero-García M, Agustín-Pavón C, Lanuza E, Martínez-García F (2016) Distribution of oxytocin and co-localization with arginine vasopressin in the brain of mice. Brain Struct Funct 221:3445–3473. https://doi.org/10.1007/s00429-015-1111-y

Oti T, Satoh K, Uta D, et al (2021) Oxytocin Influences Male Sexual Activity via Non-synaptic Axonal Release in the Spinal Cord. Current Biology 31:103-114.e5. https://doi.org/10.1016/j.cub.2020.09.089

Perkeybile AM, Delaney-Busch N, Hartman S, et al (2015) Intergenerational transmission of alloparental behavior and oxytocin and vasopressin receptor distribution in the prairie vole. Front Behav Neurosci 9:. https://doi.org/10.3389/fnbeh.2015.00191

Perkinson MR, Kim JS, Iremonger KJ, Brown CH (2021) Visualising oxytocin neurone activity in vivo: The key to unlocking central regulation of parturition and lactation. J Neuroendocrinology 33:e13012. https://doi.org/10.1111/jne.13012

Puder BA, Papka RE (2001) Hypothalamic paraventricular axons projecting to the female rat lumbosacral spinal cord contain oxytocin immunoreactivity. J of Neuroscience Research 64:53–60. https://doi.org/10.1002/jnr.1053

Ramos, Erin; Erisir, Alev, 2024, "The Histochemical Brain Atlas of the Prairie Vole (Microtus ochrogaster)", https://doi.org/10.18130/V3/LSAONY, University of Virginia Dataverse, V1

Ross HE, Freeman SM, Spiegel LL, et al (2009) Variation in Oxytocin Receptor Density in the Nucleus Accumbens Has Differential Effects on Affiliative Behaviors in Monogamous and Polygamous Voles. J Neurosci 29:1312–1318. https://doi.org/10.1523/JNEUROSCI.5039-08.2009

Rossoni E, Feng J, Tirozzi B, et al (2008) Emergent Synchronous Bursting of Oxytocin Neuronal Network. PLoS Comput Biol 4:e1000123. https://doi.org/10.1371/journal.pcbi.1000123

Smith CJW, DiBenedictis BT, Veenema AH (2019) Comparing vasopressin and oxytocin fiber and receptor density patterns in the social behavior neural network: Implications for cross-system signaling. Frontiers in Neuroendocrinology 53:100737. https://doi.org/10.1016/j.yfrne.2019.02.001

Soloff MS, Alexandrova M, Fernstrom MJ (1979) Oxytocin Receptors: Triggers for Parturition and Lactation? Science 204:1313–1315. https://doi.org/10.1126/science.221972

Son S, Manjila SB, Newmaster KT, et al (2022) Whole-Brain Wiring Diagram of Oxytocin System in Adult Mice. J Neurosci 42:5021–5033. https://doi.org/10.1523/JNEUROSCI.0307-22.2022

Stolzenberg DS, Champagne FA (2016) Hormonal and non-hormonal bases of maternal behavior: The role of experience and epigenetic mechanisms. Hormones and Behavior 77:204–210. https://doi.org/10.1016/j.yhbeh.2015.07.005

Swaab DF, Pool CW, Nijveldt F (1975) Immunofluorescence of vasopressin and oxytocin in the rat hypothalamo-neurohypophyseal system. J Neural Transmission 36:195–215. https://doi.org/10.1007/BF01253126

Theodosis DT (1985) Oxytocin-immunoreactive terminals synapse on oxytocin neurones in the supraoptic nucleus. Nature 313:682–684. https://doi.org/10.1038/313682a0

Tweedle CD, Smithson KG, Hatton GI (1989) Neurosecretory endings in the rat neurohypophysis are *en passant*. Experimental Neurology 106:20–26. https://doi.org/10.1016/0014-4886(89)90140-4

Uvnäs-Moberg K, Ekström-Bergström A, Berg M, et al (2019) Maternal plasma levels of oxytocin during physiological childbirth – a systematic review with implications for uterine contractions and central actions of oxytocin. BMC Pregnancy Childbirth 19:285. https://doi.org/10.1186/s12884-019-2365-9

Vanderwall DK, Rasmussen DM, Carnahan KG, Davis TL (2012) Effect of Administration of Oxytocin During Diestrus on Corpus Luteum Function and Endometrial Oxytocin Receptor Concentration in Cycling Mares. Journal of Equine Veterinary Science 32:536–541. https://doi.org/10.1016/j.jevs.2011.12.011

Veening JG, de Jong T, Barendregt HP (2010a) Oxytocin-messages via the cerebrospinal fluid: Behavioral effects; a review. Physiology & Behavior 101:193–210. https://doi.org/10.1016/j.physbeh.2010.05.004

Veening JG, de Jong T, Barendregt HP (2010b) Oxytocin-messages via the cerebrospinal fluid: Behavioral effects; a review. Physiology & Behavior 101:193–210. https://doi.org/10.1016/j.physbeh.2010.05.004

Vigneaud VD, Ressler C, Swan CJM, et al (1953) THE SYNTHESIS OF AN OCTAPEPTIDE AMIDE WITH THE HORMONAL ACTIVITY OF OXYTOCIN. J Am Chem Soc 75:4879–4880. https://doi.org/10.1021/ja01115a553

Whitman DC, Albers HE (1998) Oxytocin immunoreactivity in the hypothalamus of female hamsters. Cell and Tissue Research 291:231–237. https://doi.org/10.1007/s004410050993

Williams JR, Catania KC, Carter CS (1992) Development of partner preferences in female prairie voles (*Microtus ochrogaster*): The role of social and sexual experience. Hormones and Behavior 26:339–349. https://doi.org/10.1016/0018-506X(92)90004-F

Yamamoto Y, Liang M, Munesue S, et al (2019) Vascular RAGE transports oxytocin into the brain to elicit its maternal bonding behaviour in mice. Commun Biol 2:76. https://doi.org/10.1038/s42003-019-0325-6

Zhang B, Qiu L, Xiao W, et al (2021) Reconstruction of the Hypothalamo-Neurohypophysial System and Functional Dissection of Magnocellular Oxytocin Neurons in the Brain. Neuron 109:331-346.e7. https://doi.org/10.1016/j.neuron.2020.10.032

CHAPTER 4

Overall Conclusions and Future Directions

Overall Conclusions:

The aim of this dissertation is to elucidate the neuroanatomical circuitry of the oxytocinergic system in the prairie vole brain, which regulates its social behaviors (Leng et al. 2005; Kenkel et al. 2021). These behaviors, analogous to those in humans, are crucial for quality of life, and dysfunction in this system can lead to significant impairments (Abramova et al. 2020). While previous studies have extensively examined oxytocin receptors in prairie voles (Perkeybile et al. 2015, 2019; Inoue et al. 2022; Danoff et al. 2023), the oxytocin projectome remains poorly understood. In this dissertation, I mapped the brain-wide projections of oxytocin, their relationship to oxytocin receptor expression, and their pathways to cortical regions. This study's findings reveal that the oxytocinergic cells and axonal projections in the prairie vole closely resemble those of other rodents (Swaab et al. 1975; Laurent et al. 1989; Whitman and Albers 1998; Otero-García et al. 2016; Son et al. 2022), except for the unique presence of oxytocinergic cells in the anteroventral periventricular nucleus (AVPV), indicating a primarily evolutionarily conserved system. Additionally, the correlation of OXT axonal projections and *Oxtr* transcripts are mostly absent, suggesting that some regions contain axons of passage, while others with many receptors but no fibers bind OXT released by different mechanisms. Furthermore, regions such as the cerebral cortex, striatum, and pallidum, which do not show significant correlation between OXT fibers and *Oxtr* transcript expression, likely bind OXT released into the cerebrospinal fluid (CSF) from OXT+ dendrites with dense core vesicles. These findings pave the way for further research questions and suggest that OXT's actions in subcortical and cortical regions may be independent, highlighting the need for additional studies to explore how OXT can be utilized as a therapeutic tool. Additionally, I developed a histochemical brain atlas of the prairie vole, an essential tool for further exploring the vole brain's circuitry. This brain atlas is vital for researchers employing specific techniques, such as electron microscopy (EM), which examines tissues at 5,000-20,000x magnification. At such high magnifications, tissue landmarks are lost, making it essential to have a reference atlas to confidently navigate the tissue and accurately determine brain region locations during all steps of EM processing. Furthermore, to analyze whole-brain images using automated processing, a reference atlas is typically required. Having a brain atlas enables researchers to employ more automated methods of tissue analysis, thereby saving time and resources.

My dissertation focused on a specific animal model because prairie voles are crucial for studying the neural circuitry underlying social behaviors like pair bonding and alloparental care, behaviors that are absent in typical rodent models (Rogers and Bales 2019; Kenkel et al. 2021) . Prior research has highlighted how oxytocin may modulate such behaviors in various models, including monogamous rodents (Carter and Getz 1993; Aragona and Wang 2004; Kenkel et al. 2021) and non-human primates (Chang et al. 2012; Chang and Platt 2014; Freeman et al. 2016; Putnam et al. 2018; Arias Del Razo et

al. 2020), yet significant gaps remain in prairie vole studies, particularly regarding the origins and projections of central oxytocinergic pathways. This dissertation fills that gap by describing the oxytocinergic pathway and each of the three systems it acts on: the viscera, central regions binding OXT released from axons, and central regions binding to OXT released from dendrites. Additionally, comparing the findings to the relatively well-documented oxytocinergic system in mice and rats (Swaab et al. 1975; Zhang et al. 2021; Li et al. 2024). In Chapter 3 of this dissertation, I have mapped the oxytocinergic cells and projections of the prairie vole and revealed that the oxytocinergic pathways are largely conserved in voles, except for a region, AVPV, which uniquely contains oxytocin cell bodies.

This is noteworthy because the anteroventral periventricular nucleus (AVPV) is crucial for regulating the estrous cycle and initiating puberty (Hu et al. 2015; Marraudino et al. 2017). Unlike many mammals, prairie voles do not cycle naturally and require male pheromones to enter estrus (Carter et al. 1987). Upon exposure to male pheromones (Carter et al. 1987), female voles form pair bonds within 18-24 hours, showing a preference to spend more time with their partners (Wang and Aragona 2004). This pair bonding is dependent on central oxytocinergic signaling(Aragona and Wang 2004; Wang and Aragona 2004), but the specific cells that release oxytocin (OXT) in this process are unknown. I hypothesize that the unique OXT cells in the AVPV may play a significant role in pair bond formation. As detailed in Chapter 1, estrogen binding to estrogen receptor β (ERβ) stimulates OXT production (Patisaul and Scordalakes 2003; Nishimura et al. 2022). The proposed mechanism involves male pheromones activating the vomeronasal organ (Carter et al. 1987), which triggers a cascade in the olfactory bulbs, may lead to estrogen production. Estrogen, synthesized primarily in the ovaries (Hillier et al. 1981), circulates through the body, crosses the blood-brain barrier (Pardridge et al. 1980; Banks 2012), and binds to ERβ in the AVPV, stimulating OXT production (Richard and Zingg 1990; Fuentes and Silveyra 2019). I speculate that the axons of OXT cells in the AVPV project to the nucleus accumbens (Acb) to release OXT, facilitating partner preference formation. Notably, the AVPV of male voles, which also form partner preferences contains OXT+ cells as well. Given the sexual dimorphisms in this behavior, studying the significance of the cells in both sexes is essential to understanding their role fully.

Additionally, in experiments outlined in Chapter 3 of this dissertation, I mapped all regions of the vole brain containing oxytocin axons and examined their relationship to oxytocin receptor (*Oxtr*) expression. Notably, similar to findings in mice (Son et al. 2022), there is no significant correlation between oxytocin fibers and *Oxtr* expression across the brain, particularly in cortical regions rich in *Oxtr* but lacking oxytocin fibers. This discrepancy remains a major question in the field, as discussed in the chapter 1 introduction.

In the introduction chapter, I outlined three primary modes of oxytocin (OXT) release and utilization: 1) release into the posterior pituitary from axon terminals of magnocellular hypothalamic cells, affecting visceral regions with oxytocin receptors (OXTR); 2) release from axons in subcortical regions with OXT-positive fibers acting on local OXTR; and 3) somato-dendritic release, acting locally and through the third ventricle, circulating OXT in the subarachnoid space to reach cortical regions with OXTR but no OXT axons. In Chapter 3, I provide evidence for all three roles of OXT in

the prairie vole brain. I found that thick axons originating from the PVH and SON, likely release OXT directly to the blood via the posterior pituitary, which carries the hormone to the visceral organs. Using EM, I demonstrated that the axons display only a few dense core vesicles (DCVs) in axons en route, indicating minimal release, consistent with low *Oxtr* expression in those regions. Certain subcortical regions, particularly in the hypothalamus, showed many OXT+ axons with DCVs and *Oxtr* transcript expression, suggesting OXT release matches the local OXTR presence. A noteworthy outcome of my dissertation is the unequivocal demonstration that OXT+ dendrites in the PVH and SON contain abundant DCVs, suggesting local action and volume transmission to nearby OXTR. Importantly, I observed DCVs within OXT+ dendrites extending into the third ventricle, supporting the hypothesis that CSF, not the plasma, is the main carrier of oxytocin to the sites that are low in oxytocinergic fibers yet express high levels of *Oxtr*. This is significant because, as discussed in Chapter 1, OXT has a prominent role in complex cognitive functions and aggression mediated via cortical structures. In Chapter 3, I proposed that OXT+ dendrites projecting through the ependymal cell layer release OXT directly into the CSF, and thereby become the primary source of the neuropeptide for OXT-OXTR binding in the cortex. This study is the first to use electron microscopy to show OXT+ dendrites extending past the ependymal cell layer barrier. Additionally, similar to observations in mice (Son et al. 2022), I noted extensive branching of OXT+ axons along major ventricles in prairie voles, suggesting that oxytocin release into CSF is not confined to the hypothalamic dendritic release. My findings also reinforce the three modes of OXT release model discussed in Chapter 1 and indicate that the primary route for oxytocin to reach the cerebral cortex may be its direct release into ventricles from hypothalamic OXT+ cell dendrites.

The Histochemical Atlas of the Prairie Vole, developed for Chapter 3, addresses a long-standing need in the field. Previous studies often relied on rat or mouse brain atlases, which, while useful, lacked the specificity required for prairie vole research. Recently, an MRI-based vole brain atlas was created (Yee et al. 2016), but it does not provide histochemical borders. Our atlas delineates major histochemical boundaries of nuclei, subnuclei, and myelinated tracts, enabling more detailed investigations into the neuroanatomy of prairie voles and their unique social behaviors. I have designed the atlas as an editable PDF, allowing researchers to overlay it onto their own histochemically-stained sections. In the future, this atlas will facilitate advanced methods for whole-brain examinations and automated tissue processing, a benefit that has long been available to mouse and rat researchers. An accurate brain atlas is essential for these studies, and we anticipate that this tool will significantly advance prairie vole research.

Future studies and directions:

My work outlined in this dissertation and its findings in the prairie vole brain pave the way for several intriguing future studies. First, while I observed that OXT+ dendrites extend into the ventricle, it is crucial to demonstrate that oxytocin is exocytosed from the dendrites and circulates through the ventricular system to access the cerebral cortex extracellular space to bind to OXTR.

First, it is essential to understand that oxytocin is increased in the CSF during a time when coordination of cortical and subcortical regions is necessary to change and modulate behavior, such as at birth to stimulate maternal behavior. One way to do this would be using microdialysis during the birth process, which has previously been done in rats in the PVH and SON (Neumann et al. 1993). This experiment would entail surgically implanting a microdialysis probe into the lateral ventricle or another CSF-accessible brain region of pregnant prairie voles shortly before they give birth. By continuously perfusing the probe with artificial CSF and collecting samples at regular intervals throughout the birthing process, researchers could monitor real-time fluctuations in oxytocin levels. This approach would provide valuable insights into the dynamics of oxytocin release, likely from OXT+ dendrites, during parturition, enhancing our understanding of CSF OXT's role in maternal behaviors of prairie voles.

Another beneficial study would examine potential OXT release through humoral, axonal, and dendritic modes at birth, as OXT release peaks during this time, providing the best opportunity to observe significant changes. To investigate humoral release, blood samples should be taken at specific intervals, considering the pulsatile nature of OXT and its rapid breakdown in the bloodstream (Mens et al. 1983; Leng and Ludwig 2008). Examining axonal release is more challenging but can be approached in two ways. High-Performance Liquid Chromatography (HPLC) (Buck et al. 2009) can be utilized during the birthing process to measure axonal release of oxytocin (OXT) in specific brain regions, such as the medial preoptic area (MPOA) and nucleus accumbens (Acb), two regions with many OXT+ axons and intimately involved in the modulation of maternal behavior (Stolzenberg et al. 2007; Numan 2007; Numan and Stolzenberg 2009). Microdialysis probes can be surgically implanted in these target regions shortly before labor. During the birthing process, the probes continuously collect extracellular fluid samples. The samples are then analyzed using HPLC to quantify the concentration of oxytocin, allowing researchers to monitor real-time changes in oxytocin release from axons in these specific brain regions. This approach provides valuable insights into the dynamics of oxytocin release associated with parturition and its role in maternal behaviors. Further, genetically encoded fluorescent sensors could be used. $GRAB_{OT1.0}$ (Qian et al. 2023)is a G-protein-coupled receptor activation-based oxytocin sensor that enables researchers to image OXT release. Upon binding to OXT, the sensor changes fluorescence and allows for precise spatial and temporal resolution of OXT release events (Qian et al. 2023). To determine if OXT is released from dendrites into the CSF at birth, thereby bathing the brain in OXT and triggering a widespread effect across the brain, researchers could again use this sensor, $GRAB_{OT1.0}$ within the PVN to observe dendritic release (Qian et al., 2023). Further, researchers could fluorescently tag OXT and inject it into a ventricle, and then track its distribution into the cerebral cortex. A potential drawback of tagging OXT is that it might interfere with its ability to bind to oxytocin receptors (OXTR), possibly hindering its detection in the cortex. However, if it successfully reaches the cortex, researchers could then investigate its co-localization with OXTR-expressing cells using confocal microscopy. Currently, there is a lack of suitable antibodies for OXTR, necessitating the use of RNAScope to assess this co-localization. If

an OXTR antibody becomes available, a proximity ligation assay (PLA) would be the most advantageous method to confirm that OXT from the CSF binds to OXTR in the cerebral cortex. However, using the GRAB $_{OT1.0}$ and fluorescently tagging OXT should be sufficient evidence that OXT is released into the CSF and reaches the cerebral cortex.

OXT is not the sole hormone or peptide found in the CSF; in fact, numerous peptides reside there and can quickly spread throughout the brain. Peptides and small-molecule neurotransmitters such as thyrotropin-releasing hormone, somatostatin, dopamine, and substance P are all present in the CSF and, if they reach the cerebral cortex, could potentially modulate various downstream pathways and circuitries (Wood 1983; Goldstein et al. 2012). There are many implications for the peptide distribution through the CSF. One suggestion is that CSF hormone and peptide levels could serve as a baseline for patients (Wood 1983), offering potentially a more accurate reflection of central hormone levels compared to plasma. Thus, how a patient responds to treatment involving the regulation of hormone levels may be better assessed. However, obtaining CSF typically involves a spinal tap, which is considerably more invasive than blood collection. Finding an alternative method for CSF collection would be advantageous.

In attempts to treat autism spectrum disorders, many researchers have explored the use of intranasal OXT(Sikich et al. 2021), but results have been mixed (Huang et al. 2021). This variability could stem from the widespread distribution of OXT in the CSF, reaching numerous regions throughout the cerebral cortex and along major ventricles. This distribution of OXT may initiate multiple intracellular cascades and systemic changes that do not necessarily improve social behaviors, as OXT binds broadly across various brain regions rather than targeting specific areas. This underscores the need to understand how CSF OXT is functionally utilized and suggests that intranasal OXT may not be the optimal treatment for conditions like autism spectrum disorders. Another avenue of research that should be examined is to determine whether OXT is released at *en passant* terminals, terminal boutons, or both. This gap in the literature is surprising, given the assumption that varicosities on OXT+ axons indicate release (Chini et al. 2017; Grinevich and Ludwig 2021). Our findings suggest otherwise; for instance, OXT+ axons of PVH and SON cells projecting to the posterior pituitary have few OXT+ DCVs despite exhibiting the typical varicosities. Future research should focus on understanding the exact locations and mechanisms of OXT release, whether it occurs along the axon length or at the terminal bouton.

The creation of the prairie vole brain atlas opens up endless possibilities for future research. This atlas aims to help researchers investigate various questions about the neuroanatomical circuitry of the prairie vole brain, particularly the mechanisms driving their unique and complex behaviors. By exploring these circuits, we can gain valuable insights into social behaviors that may inform human research and lead to new treatments for disorders affecting social behavior, such as autism. We hope this atlas significantly contributes to the current literature on oxytocin and its functions, inspiring further studies in prairie voles and advancing knowledge in this field.

Additionally, this work can enhance our understanding of complex social behaviors related to anxiety and aggression, which are often linked to dysfunctions in cortical regions and top-down control (Bale et al. 2001; Bosch et al. 2005; Calcagnoli et al. 2014; Sabihi et al. 2014). This dysfunction could indicate a deficiency or defect in

OXT release into the CSF, OXTR expression in the cerebral cortex, or both. OXT released into the CSF through dendrites is stimulated by activity-dependent mechanisms (Ludwig and Leng 2006; Qian et al. 2023) but acts more slowly due to circulation of the CSF. In contrast, subcortical regions binding axonally released OXT would do so more rapidly. Different disorders may be associated with specific dysfunctions within this system. For instance, autism spectrum disorders could be linked to subcortical OXT release dysfunction, affecting social bonding abilities. Meanwhile, anxiety and aggression-related disorders may involve dysfunction in CSF OXT binding within cortical regions. Alternatively, these disorders may not solely involve dysfunction in one mode of OXT release, but rather a broader dysfunction across the entire oxytocin-utilizing circuitry. This underscores the need to comprehensively understand each release mode and its utilization to better grasp system dysfunction.

In summary, my research has significantly advanced the understanding of the neuroanatomical circuitry and oxytocinergic system in the prairie vole brain, particularly in relation to social behaviors such as pair bonding and alloparental care. I designed a Histochemical Atlas of the Prairie Vole, addressing the need for a detailed and specific tool that delineates histochemical borders of nuclei, subnuclei, and myelinated tracts, facilitating advanced neuroanatomical research. Our findings revealed three primary modes of oxytocin release: humoral release into the viscera, axonal release in subcortical regions, and somato-dendritic release into the cerebral cortex via the CSF. We also identified unique regions, such as the AVPV, and mapped oxytocin projections and receptor expression across the brain. I found that OXT fibers generally do not align with receptor expression. Future research should verify the functional pathways of oxytocin circulation and release mechanisms and investigate whether OXT in the CSF is the primary means of delivery to the cerebral cortex.

This work not only enhances the understanding of prairie vole neuroanatomy but also offers valuable insights into human social behavior and potential treatments for related disorders, such as autism, anxiety, and aggression. We hope this atlas and our findings inspire further research and contribute to the broader field of oxytocin and social behavior.

References:

Abramova O, Zorkina Y, Ushakova V, et al (2020) The role of oxytocin and vasopressin dysfunction in cognitive impairment and mental disorders. Neuropeptides 83:102079. https://doi.org/10.1016/j.npep.2020.102079

Aragona BJ, Wang Z (2004) The Prairie Vole (Microtus ochrogaster): An Animal Model for Behavioral Neuroendocrine Research on Pair Bonding. ILAR Journal 45:35–45. https://doi.org/10.1093/ilar.45.1.35

Arias Del Razo R, Berger T, Conley AJ, et al (2020) Effects of chronic intranasal oxytocin on behavior and cerebral glucose uptake in juvenile titi monkeys. Psychoneuroendocrinology 113:104494. https://doi.org/10.1016/j.psyneuen.2019.104494

Bale TL, Davis AM, Auger AP, et al (2001) CNS Region-Specific Oxytocin Receptor Expression: Importance in Regulation of Anxiety and Sex Behavior. J Neurosci 21:2546–2552. https://doi.org/10.1523/JNEUROSCI.21-07-02546.2001

Banks WA (2012) Brain Meets Body: The Blood-Brain Barrier as an Endocrine Interface. Endocrinology 153:4111–4119. https://doi.org/10.1210/en.2012-1435

Bosch OJ, Meddle SL, Beiderbeck DI, et al (2005) Brain Oxytocin Correlates with Maternal Aggression: Link to Anxiety. J Neurosci 25:6807–6815. https://doi.org/10.1523/JNEUROSCI.1342-05.2005

Buck K, Voehringer P, Ferger B (2009) Rapid analysis of GABA and glutamate in microdialysis samples using high performance liquid chromatography and tandem mass spectrometry. Journal of Neuroscience Methods 182:78–84. https://doi.org/10.1016/j.jneumeth.2009.05.018

Calcagnoli F, De Boer SF, Beiderbeck DI, et al (2014) Local oxytocin expression and oxytocin receptor binding in the male rat brain is associated with aggressiveness. Behavioural Brain Research 261:315–322. https://doi.org/10.1016/j.bbr.2013.12.050

Carter CS, Getz LL (1993) Monogamy and the Prairie Vole. Scientific American 268:100–106

Carter CS, Witt DM, Schneider J, et al (1987) Male stimuli are necessary for female sexual behavior and uterine growth in prairie voles (*Microtus ochrogaster*). Hormones and Behavior 21:74–82. https://doi.org/10.1016/0018-506X(87)90032-8

Chang SWC, Barter JW, Ebitz RB, et al (2012) Inhaled oxytocin amplifies both vicarious reinforcement and self reinforcement in rhesus macaques (*Macaca mulatta*). Proc Natl Acad Sci USA 109:959–964. https://doi.org/10.1073/pnas.1114621109

Chang SWC, Platt ML (2014) Oxytocin and social cognition in rhesus macaques: Implications for understanding and treating human psychopathology. Brain Research 1580:57–68. https://doi.org/10.1016/j.brainres.2013.11.006

Chini B, Verhage M, Grinevich V (2017) The Action Radius of Oxytocin Release in the Mammalian CNS: From Single Vesicles to Behavior. Trends in Pharmacological Sciences 38:982–991. https://doi.org/10.1016/j.tips.2017.08.005

Danoff JS, Page EA, Perkeybile AM, et al (2023) Transcriptional diversity of the oxytocin receptor in prairie voles: mechanistic implications for behavioral neuroscience and maternal physiology. Front Genet 14:. https://doi.org/10.3389/fgene.2023.1225197

Freeman SM, Samineni S, Allen PC, et al (2016) Plasma and CSF oxytocin levels after intranasal and intravenous oxytocin in awake macaques. Psychoneuroendocrinology 66:185–194. https://doi.org/10.1016/j.psyneuen.2016.01.014

Fuentes N, Silveyra P (2019) Estrogen receptor signaling mechanisms. In: Advances in Protein Chemistry and Structural Biology. Elsevier, pp 135–170

Goldstein DS, Holmes C, Sharabi Y (2012) Cerebrospinal fluid biomarkers of central catecholamine deficiency in Parkinson's disease and other synucleinopathies. Brain 135:1900–1913. https://doi.org/10.1093/brain/aws055

Grinevich V, Ludwig M (2021) The multiple faces of the oxytocin and vasopressin systems in the brain. J Neuroendocrinology 33:e13004. https://doi.org/10.1111/jne.13004

Hillier SG, Reichert LE, Van Hall EV (1981) Control of Preovulatory Follicular Estrogen Biosynthesis in the Human Ovary. The Journal of Clinical Endocrinology & Metabolism 52:847–856. https://doi.org/10.1210/jcem-52-5-847

Hu MH, Li XF, McCausland B, et al (2015) Relative Importance of the Arcuate and Anteroventral Periventricular Kisspeptin Neurons in Control of Puberty and Reproductive Function in Female Rats. Endocrinology 156:2619. https://doi.org/10.1210/en.2014-1655

Huang Y, Huang X, Ebstein RP, Yu R (2021) Intranasal oxytocin in the treatment of autism spectrum disorders: A multilevel meta-analysis. Neuroscience & Biobehavioral Reviews 122:18–27. https://doi.org/10.1016/j.neubiorev.2020.12.028

Inoue K, Ford CL, Horie K, Young LJ (2022) Oxytocin receptors are widely distributed in the prairie vole (Microtus ochrogaster) brain: Relation to social behavior, genetic polymorphisms, and the dopamine system. Journal of Comparative Neurology 530:2881–2900. https://doi.org/10.1002/cne.25382

Kenkel WM, Gustison ML, Beery AK (2021) A Neuroscientist's Guide to the Vole. Current Protocols 1:e175. https://doi.org/10.1002/cpz1.175

Laurent FM, Hindelang C, Klein MJ, et al (1989) Expression of the oxytocin and vasopressin genes in the rat hypothalamus during development: an in situ hybridization study. Developmental Brain Research 46:145–154. https://doi.org/10.1016/0165-3806(89)90152-1

Leng G, Caquineau C, Sabatier N (2005) Regulation of Oxytocin Secretion. In: Vitamins & Hormones. Elsevier, pp 27–58

Leng G, Ludwig M (2008) Neurotransmitters and peptides: whispered secrets and public announcements. The Journal of Physiology 586:5625–5632. https://doi.org/10.1113/jphysiol.2008.159103

Li H, Jiang T, An S, et al (2024) Single-neuron projectomes of mouse paraventricular hypothalamic nucleus oxytocin neurons reveal mutually exclusive projection patterns. Neuron 112:1081-1099.e7. https://doi.org/10.1016/j.neuron.2023.12.022

Ludwig M, Leng G (2006) Dendritic peptide release and peptide-dependent behaviours. Nat Rev Neurosci 7:126–136. https://doi.org/10.1038/nrn1845

Marraudino M, Miceli D, Farinetti A, et al (2017) Kisspeptin innervation of the hypothalamic paraventricular nucleus: sexual dimorphism and effect of estrous cycle in female mice. Journal of Anatomy 230:775–786. https://doi.org/10.1111/joa.12603

Mens WBJ, Witter A, Van Wimersma Greidanus TB (1983) Penetration of neurohypophyseal hormones from plasma into cerebrospinal fluid (CSF): Half-times of disappearance of these neuropeptides from CSF. Brain Research 262:143–149. https://doi.org/10.1016/0006-8993(83)90478-X

Neumann I, Russell JA, Landgraf R (1993) Oxytocin and vasopressin release within the supraoptic and paraventricular nuclei of pregnant, parturient and lactating rats: A microdialysis study. Neuroscience 53:65–75. https://doi.org/10.1016/0306-4522(93)90285-N

Nishimura K, Yoshino K, Ikeda N, et al (2022) Oestrogen-dependent hypothalamic oxytocin expression with changes in feeding and body weight in female rats. Commun Biol 5:912. https://doi.org/10.1038/s42003-022-03889-6

Numan M (2007) Motivational systems and the neural circuitry of maternal behavior in the rat. Developmental Psychobiology 49:12–21. https://doi.org/10.1002/dev.20198

Numan M, Stolzenberg DS (2009) Medial preoptic area interactions with dopamine neural systems in the control of the onset and maintenance of maternal behavior

in rats. Frontiers in Neuroendocrinology 30:46–64. https://doi.org/10.1016/j.yfrne.2008.10.002

Otero-García M, Agustín-Pavón C, Lanuza E, Martínez-García F (2016) Distribution of oxytocin and co-localization with arginine vasopressin in the brain of mice. Brain Struct Funct 221:3445–3473. https://doi.org/10.1007/s00429-015-1111-y

Pardridge WM, Mietus LJ, Frumar AM, et al (1980) Effects of human serum on transport of testosterone and estradiol into rat brain. American Journal of Physiology-Endocrinology and Metabolism 239:E103–E108. https://doi.org/10.1152/ajpendo.1980.239.1.E103

Patisaul HB, Scordalakes EM (2003) Oxytocin, But Not Oxytocin Receptor, is Regulated by Oestrogen Receptor b in the Female Mouse Hypothalamus. Journal of Neuroendocrinology

Perkeybile AM, Carter CS, Wroblewski KL, et al (2019) Early nurture epigenetically tunes the oxytocin receptor. Psychoneuroendocrinology 99:128–136. https://doi.org/10.1016/j.psyneuen.2018.08.037

Perkeybile AM, Delaney-Busch N, Hartman S, et al (2015) Intergenerational transmission of alloparental behavior and oxytocin and vasopressin receptor distribution in the prairie vole. Front Behav Neurosci 9:. https://doi.org/10.3389/fnbeh.2015.00191

Putnam PT, Young LJ, Gothard KM (2018) Bridging the gap between rodents and humans: The role of non-human primates in oxytocin research. American J Primatol 80:e22756. https://doi.org/10.1002/ajp.22756

Qian T, Wang H, Wang P, et al (2023) A genetically encoded sensor measures temporal oxytocin release from different neuronal compartments. Nat Biotechnol 41:944–957. https://doi.org/10.1038/s41587-022-01561-2

Richard S, Zingg HH (1990) The human oxytocin gene promoter is regulated by estrogens. Journal of Biological Chemistry 265:6098–6103. https://doi.org/10.1016/S0021-9258(19)39297-X

Rogers FD, Bales KL (2019) Mothers, Fathers, and Others: Neural Substrates of Parental Care. Trends in Neurosciences 42:552–562. https://doi.org/10.1016/j.tins.2019.05.008

Sabihi S, Durosko NE, Dong SM, Leuner B (2014) Oxytocin in the prelimbic medial prefrontal cortex reduces anxiety-like behavior in female and male rats. Psychoneuroendocrinology 45:31–42. https://doi.org/10.1016/j.psyneuen.2014.03.009

Sikich L, Kolevzon A, King BH, et al (2021) Intranasal Oxytocin in Children and Adolescents with Autism Spectrum Disorder. N Engl J Med 385:1462–1473. https://doi.org/10.1056/NEJMoa2103583

Son S, Manjila SB, Newmaster KT, et al (2022) Whole-Brain Wiring Diagram of Oxytocin System in Adult Mice. J Neurosci 42:5021–5033. https://doi.org/10.1523/JNEUROSCI.0307-22.2022

Stolzenberg DS, McKenna JB, Keough S, et al (2007) Dopamine D_1 receptor stimulation of the nucleus accumbens or the medial preoptic area promotes the onset of maternal behavior in pregnancy-terminated rats. Behavioral Neuroscience 121:907–919. https://doi.org/10.1037/0735-7044.121.5.907

Swaab DF, Pool CW, Nijveldt F (1975) Immunofluorescence of vasopressin and oxytocin in the rat hypothalamo-neurohypophyseal system. J Neural Transmission 36:195–215. https://doi.org/10.1007/BF01253126

Wang Z, Aragona BJ (2004) Neurochemical regulation of pair bonding in male prairie voles. Physiology & Behavior 83:319–328. https://doi.org/10.1016/j.physbeh.2004.08.024

Whitman DC, Albers HE (1998) Oxytocin immunoreactivity in the hypothalamus of female hamsters. Cell and Tissue Research 291:231–237. https://doi.org/10.1007/s004410050993

Wood JH (1983) Physiology and Pharmacology of Peptide, Steroid, and Other Hormones in Cerebrospinal Fluid. In: Wood JH (ed) Neurobiology of Cerebrospinal Fluid 2. Springer US, Boston, MA, pp 43–65

Yee JR, Kenkel WM, Kulkarni P, et al (2016) BOLD fMRI in awake prairie voles: A platform for translational social and affective neuroscience. NeuroImage 138:221–232. https://doi.org/10.1016/j.neuroimage.2016.05.046

Zhang B, Qiu L, Xiao W, et al (2021) Reconstruction of the Hypothalamo-Neurohypophysial System and Functional Dissection of Magnocellular Oxytocin Neurons in the Brain. Neuron 109:331-346.e7. https://doi.org/10.1016/j.neuron.2020.10.032

APPENDIX A

The Histochemical Brain Atlas of the Prairie Vole (*Microtus ochrogaster*)

The Histochemical Brain Atlas

of

The Prairie Vole
(*Microtus ochrogaster*)

By:
Erin Ramos
Griffin Jiron
Zoe Anderson
Anna Graczyk, Ph.D.
Alev Erisir, Ph.D.

University of Virginia, Department of Psychology

Table of Contents

Introduction

The prairie vole (*Microtus ochrogaster*) is an emerging animal model for the study of its unique social behaviors, such as biparental care and alloparenting, many of which have been linked to oxytocinergic signaling within the brain. However, there has not been a histochemically annotated brain atlas until now. We have created a brain atlas that delineates major nuclei, subnuclei, and myelinated tracks across one entire male vole brain spanning 6,400 μm anterior to posterior. This atlas is produced between 2021-2024.

Methods

One male vole was deeply anesthetized with an overdose of sodium pentobarbital, and transcardially perfused with Tyrode's followed by 10-15 ml of 4% paraformaldehyde. After 24 hours post-fixation in the same aldehyde solution, the brain was sectioned coronally on a vibratome at 50μm and collected in four series. The second and fourth series were mounted on glass slides and stained for Myelin and Nissl, respectively. The first and third series were rinsed in 1% sodium borohydride and stored in 0.05% sodium azide in 0.01 M PBS at 4^{o}C until immunostaining experiments for oxytocin. all Nissl and Myelin-stained series were imaged using a Leica MC170 HD microscope at 1.6x magnification. Composites of each image were made with Adobe Photoshop. Adobe Illustrator was used to outline cytoarchitectural borders for Nissl sections, yielding all major brain nuclei, major myelinated axon bundles were outlined by using the myelin-stained sections. The Allen Mouse brain atlas (Allen Institute for Brain Science, 2004), the Paxinos and Watson rat brain atlas (Paxinos & Watson, 2007), and the prairie vole MRI vole brain atlas (Yee et al. 2016), were all consulted for naming the analogous prairie vole brain structures. After regions were determined using the Nissl and Myelin-stained sections, the outlines were overlayed onto all OXT-stained sections.

The atlas extends from the olfactory bulb anteriorly to the pons posteriorly, using the anterior-most coronal section that contains the optic chiasm (oc) as the anterior-posterior zero coordinates. Regions anterior to the oc are labeled "oc-" and those posterior are "oc+". Each series of four is included in one set. For example, set one is oc-3100 to oc-3250, indicating that these sections are between 3100μm to 3250μm anterior to the first appearance of the optic chiasm. In set 2, the proper OXT stained sections could not be aligned and are excluded. Scale bars on all images = 1 mm.

Purpose

Our hope is that the prairie vole brain atlas will be a useful reference tool for prairie vole researchers to utilize. We hope that it enables more scientists to probe questions regarding the neuroanatomical make-up of the prairie vole brain.

Abbreviations

Abbreviation	Region	Atlas Sections (Set)
ac	anterior commissure	17
AcbC	nucleus accumbens core	10, 11, 12, 13, 14,
AcbSh	nucleus accumbens shell	11, 12, 13, 14
aco	anterior commissure, olfactory limb	1, 2, 3, 4, 5, 6, 7, 8, 9, 10, 11, 12, 13, 14, 15, 16
act	anterior commissure, temporal limb	17, 18
AD	anterodorsal nucleus of the thalamus	20, 21, 22, 23
AHN	anterior hypothalamic nucleus	21, 22, 23, 24, 25
AI	agranular insular area	5, 6, 7, 8, 9, 10, 11, 12, 13, 14, 15, 16, 17, 18, 19, 20, 21, 22, 23, 24
AM	anteromedial nucleus of the thalamus	21, 22, 23
AOB	accessory olfactory bulb	1
AON	anterior olfactory nucleus	1, 2, 3, 4, 5, 6, 7, 8, 9
aq	cerebral aqueduct	31, 32, 33
ARC	arcuate nucleus	25, 26, 27, 28
Au	auditory cortex	25, 26, 27, 28, 29, 30, 31
AV	anteroventral nucleus of the thalamus	20, 21, 22, 23
AVPV	anteroventral periventricular nucleus	15, 16, 17
BA	basomedial/basolateral amygdalar nucleus	20, 21, 22, 23, 24, 25, 26, 27, 28, 29, 30, 31
BNST	bed nucleus of the stria terminalis	15, 16, 17, 18, 19, 20
bsc	brachium of superior colliculus	30, 31
CA1	hippocampal area 1	23, 24, 25, 26, 27, 28, 29, 30, 31, 32
CA2	hippocampal area 2	24, 25, 26, 27, 28, 29, 30, 31
CA3	hippocampal area 3	20, 21, 22, 23, 24, 25, 26, 27, 28, 29, 30, 31
cc	corpus callosum	10, 11, 12, 13, 14, 15, 16, 17, 18, 19, 20, 21, 22, 23, 24, 25, 26, 27, 28, 29, 30, 31
Ce	central amygdalar nucleus	20, 21, 22, 23, 24, 25, 26, 27, 28, 29
cg	cingulum bundle	12, 13, 14, 15, 16, 17, 18, 19, 20
Cg	cingulate cortex	11, 12, 13, 14, 15, 16, 17, 18, 19, 20
Cga	cingulate area-anterior	7, 8, 9, 10
CLA	claustrum	8, 9, 10, 11, 12, 13, 14, 15, 16, 17, 18, 19, 20, 21, 22, 23
CM	central medial thalamic nucleus	21, 22, 23, 24, 25, 26, 27, 28, 29
Co	cortical amygdaloid nucleus	19, 20, 21, 22, 23, 24, 25, 26, 27, 28, 29, 30, 31
cpd	cerebral peduncle	27, 28, 29, 30, 31, 32
CPu	caudate putamen	10, 11, 12, 13, 14, 15, 16, 17, 18, 19, 20, 21, 22, 23, 24, 25, 26, 27, 28, 29
csc	superior colliculus commissure	32, 33
DB	diagonal band of Broca	10, 11, 12, 13, 14
DG	dentate gyrus	21, 22, 23, 24, 25, 26, 27, 28, 29, 30, 31, 32, 33
dhc	dorsal hippocampal commissure	32, 33
DLG	dorsal lateral geniculate nucleus	28, 29, 30, 31

DM	dorsal medial nucleus of the hypothalamus	24, 25, 26, 27, 28
DR	dorsal raphe	33
emt	external medullary lamina of the thalamus	31
Ent	entorhinal cortex	30, 31, 32, 33
EP	endopiriform	7, 8, 9, 10, 11, 12, 13, 14, 15, 16, 17, 18, 19, 20, 21, 22, 23
f	fornix	16, 17, 18, 19, 20, 21, 22, 23, 24, 25, 26, 27, 28, 29, 30, 31
fa	corpus callosum- anterior forceps	8, 9, 10
fi	fimbria	18, 19, 20, 21, 22, 23, 24, 25, 26, 27, 28, 29, 30, 31
fr	fasciculus retroflex	29, 30. 31. 32
FrA	frontal association cortex	1, 2, 3, 4
GL	glomerular layer of the olfactory bulb	1, 2
GP	globus pallidus	19, 20, 21, 22, 23, 24, 25, 26, 27
GrO	granular cell layer olfactory limb	1, 2, 3, 4, 5
Hb	habenula	24
IAM	interanteromedial nucleus of the thalamus	22, 23
ic	internal capsule	17, 18, 19, 20, 21, 22, 23, 24, 25, 26, 27, 28
IL	infralimbic cortex	7, 8, 9, 10, 11
IMD	intermediodorsal nucleus of the thalamus	24, 25, 26, 27, 28, 29
IP	interpeduncular nucleus	33
islm	major island of Calleja	12
LA	lateral amgydalar nucleus	27, 28, 29, 30
LD	lateral dorsal thalamic nucleus	23, 24, 25, 26
LGN	lateral geniculate nucleus	26, 27
LH	lateral hypothalamic nucleus	21, 22, 23, 24, 25, 26, 27, 28, 29, 30
LHb	lateral habenular nucleus	25, 26, 27, 28, 29
lot	lateral olfactory tract	5, 6
LP	lateral posterior thalamic nucleus	27, 28, 29, 30, 31
LPOA	lateral preoptic area	15, 16, 17, 18, 19, 20
LS	lateral septum	8, 9, 10, 11, 12, 16, 17
LSd	lateral septum - dorsal	13, 14, 15
LSi	lateral septum - intermediate	15
LSv	lateral septum - ventral	13, 14, 15
LV	lateral ventricle	9, 10, 11, 12, 13, 14, 15, 16, 17, 18, 19, 20, 21
MC	motor cortex	5, 6, 7, 8, 9, 10, 11, 12, 13, 14, 15, 16, 17, 18, 19, 20, 21, 22, 23, 24, 25, 26, 27, 28
MD	mediodorsal nucleus of the thalamus	22, 23, 24, 25, 26, 27
ME	median eminence	26
Me	medial amygdalar nucleus	21, 22, 23, 24, 25, 26, 27, 28, 29
MEPO	median preoptic nucleus	15, 16, 17, 18
MGN	medial geniculate nucleus	32, 33
MHb	medial habenular nucleus	25, 26, 27, 28, 29
ml	medial lemniscus	29, 30, 31

MM	mammillary nucleus	31, 32
MOBopl	Main olfactory bulb – outer plexiform layer	1
MPOA	medial preoptic area	15, 16, 17, 18, 19, 20
MS	medial septal nucleus	12, 13, 14, 15, 16
mtt	mammillothalamic tract	25, 26, 27, 28, 29, 30, 31, 32
och	optic chiasm	17, 18, 19, 20
opt	optic tract	21, 22, 23, 24, 25, 26, 27, 28, 29, 30
ORB	orbital area	1, 2, 3, 4, 5, 6, 7, 8, 9, 10, 11, 12
OT	olfactory tubercle	9, 10, 11, 12, 13, 14, 15, 16, 17, 18
PAG	periaqueductal gray	30, 31, 32, 33
PF	parafascicular thalamic nucelus	29, 30, 31
PH	posterior hypothalamic nucleus	27, 28, 29, 30, 31
Pir	piriform cortex	6, 7, 8, 9, 10, 11, 12, 13, 14, 15, 16, 17, 18, 19, 20, 21, 22, 23, 24, 25, 26
Po	posterior complex of the thalamus	24, 25, 26, 27, 28, 29, 30, 31
Pons	Pons	33
PRh	perirhinal cortex	24, 25, 26, 27, 28, 29, 30
PrL	prelimbic cortex	3, 4, 5, 6, 7, 8, 9, 10
Pt	parietal cortex	29, 30, 31
PTN	pretectal nucleus	30, 31
PVH	paraventricular hypothalamic nucleus	20, 21, 22, 23, 24, 25, 26
PVi	periventricular hypothalamic nucleus - intermediate	22, 23, 24, 25, 26
PVpo	periventricular hypothalamic preoptic part	18, 19, 20
PVT	paraventricular nucleus of the thalamus	20, 21, 22, 23, 24, 25, 26, 27, 28, 29
RCH	retrochiasmatic area	22, 23, 24
RE	nucleus of reuniens	21, 22, 23, 24, 25, 26, 27, 28
RH	rhomboid nucleus	23, 24, 25, 26, 27, 28
RS	retrosplineal area	21, 22, 23, 24, 25, 26, 27, 28, 29, 30, 31, 32, 33
rt	reticular nucleus of the thalamus	20, 21, 22, 23, 24, 25, 26, 27, 28, 29
RTm	reticular nucleus -midbrain	31, 32, 33
Sc	somatosensory cortex	8, 9, 10, 11, 12, 13, 14, 15, 16, 17, 18, 19, 20, 21, 22, 23, 24, 25, 26, 27, 28, 29, 30, 31
SC	superior colliculus	32, 33
SCH	suprachiasmatic nucleus	21, 22, 23
scp	superior cerebelar peduncles	33
sm	stria medularis	19, 20, 21, 22, 23, 24
SN	substantia nigra	31
SNR	substantia nigra reticular part	32, 33
SON	supraoptic nucleus	19, 20, 21, 22, 23, 24, 25
st	stria terminalis	18, 19, 20, 21
SUB	subiculum	31, 32, 33
Te	temporal cortex	32, 33
TT	taenia tecta	6, 7, 8, 9, 10, 11, 12

Tu	tuberal nucleus	25, 26, 27, 28, 29
V1	visual 1 cortex	32, 33
V3	third ventricle	18, 19, 20, 21, 22, 23, 24, 25, 26, 27, 28, 29, 30, 31
vhc	ventral hippocampal commissure	18, 19, 20
VLPO	ventrolateral preoptic area	16, 17, 18
VM	ventral medial thalamic nucleus	22, 23, 24, 25, 26, 27, 28, 29, 30
VMH	ventromeidal hypothalamus	25, 26, 27
VMPO	ventromedial preoptic area	16, 17, 18
VP	ventral pallidum	15, 16
VTA	ventral tegmental area	31, 32, 33
vtd	ventral tegmental decussation	32, 33
ZI	zona incerta	22, 23, 24, 25, 26, 27, 28, 29, 30, 31

Set 1: OXT oc -3250µm

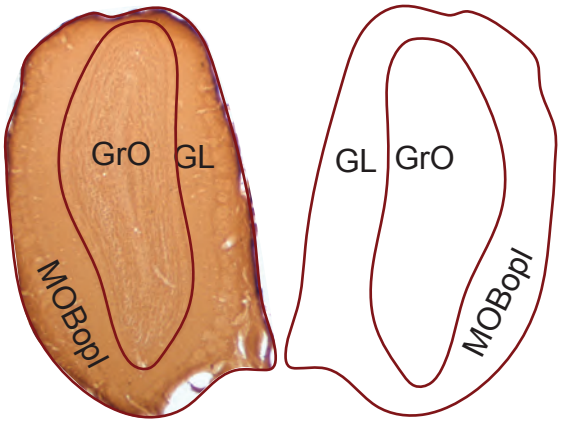

Set 1: Nissl oc -3200µm

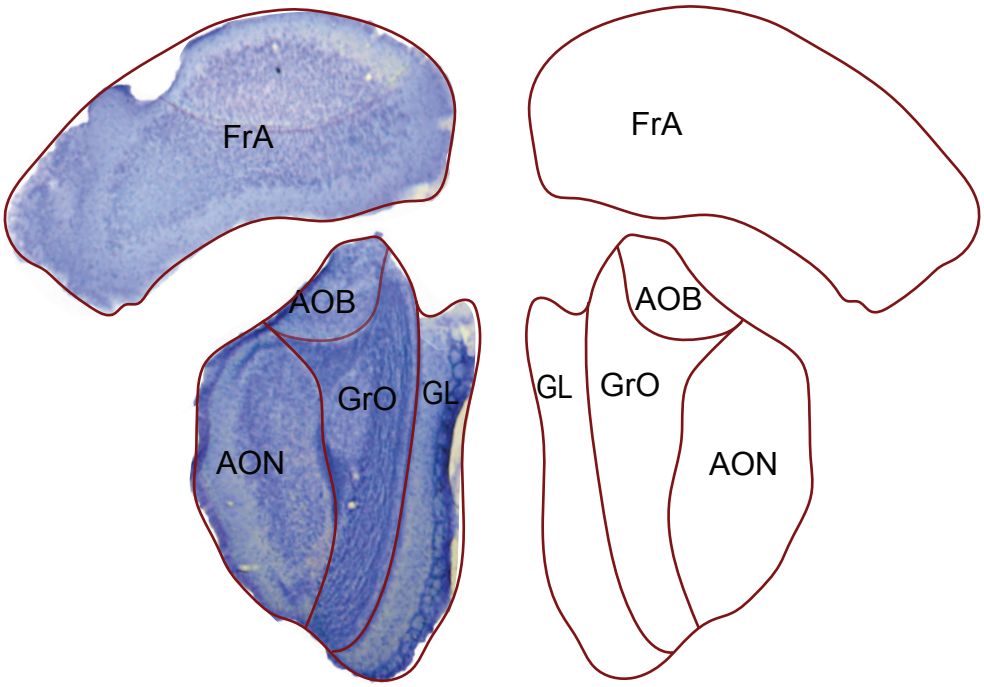

Set 1: OXT oc -3150µm

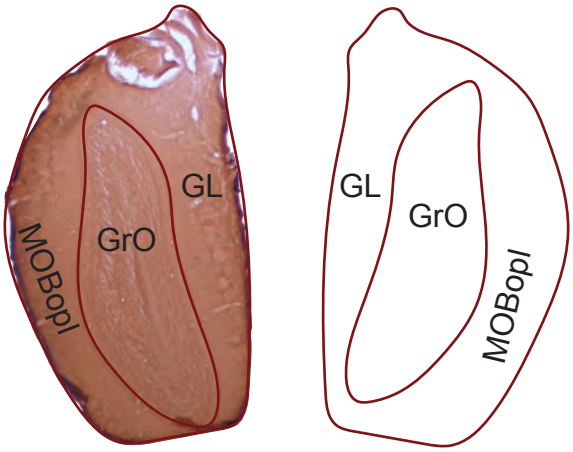

Set 1: Myelin oc -3100µm

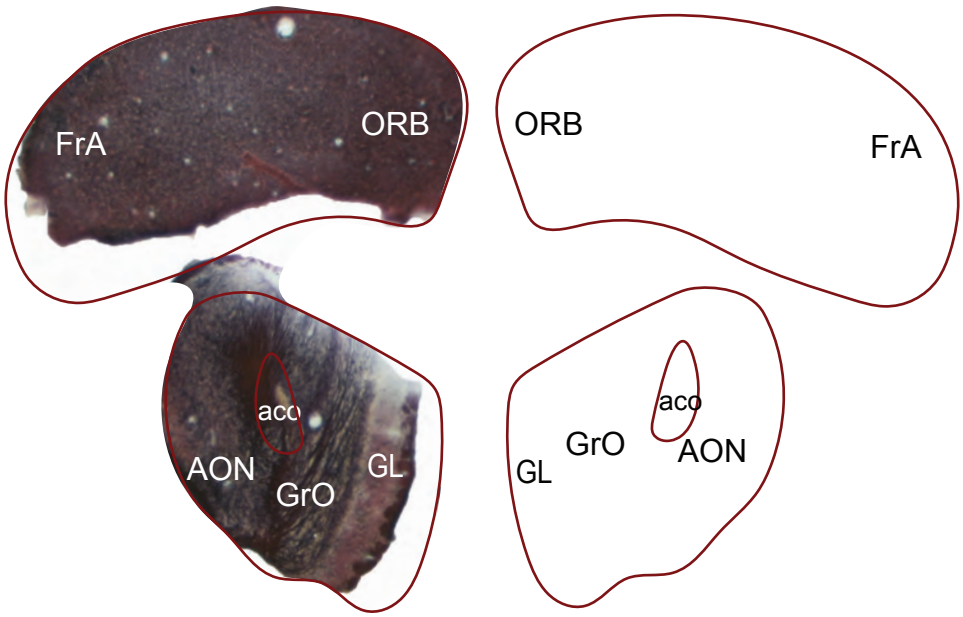

Set 2: Nissl oc -3000µm

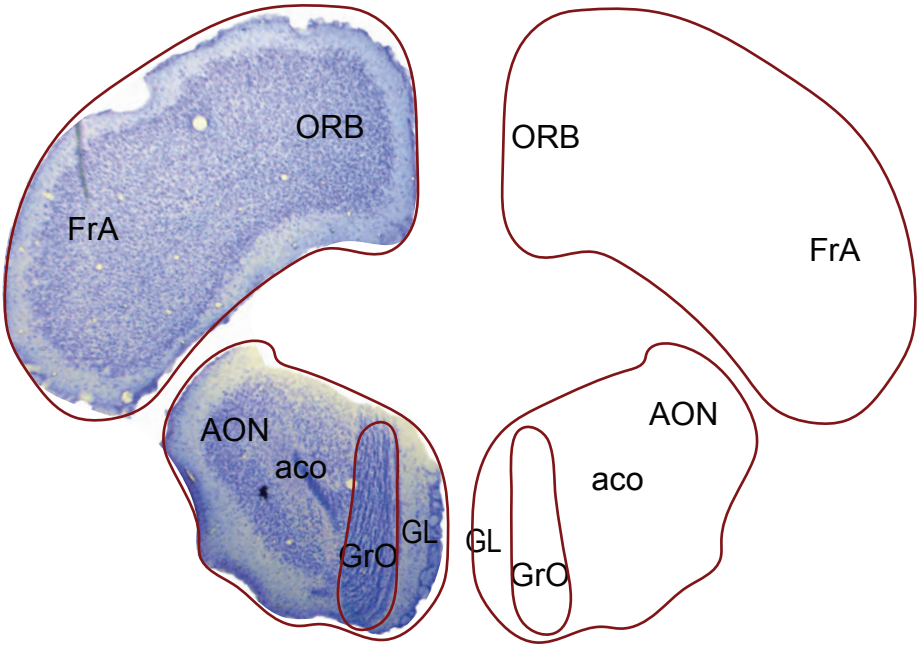

Set 2: Myelin oc -2900µm

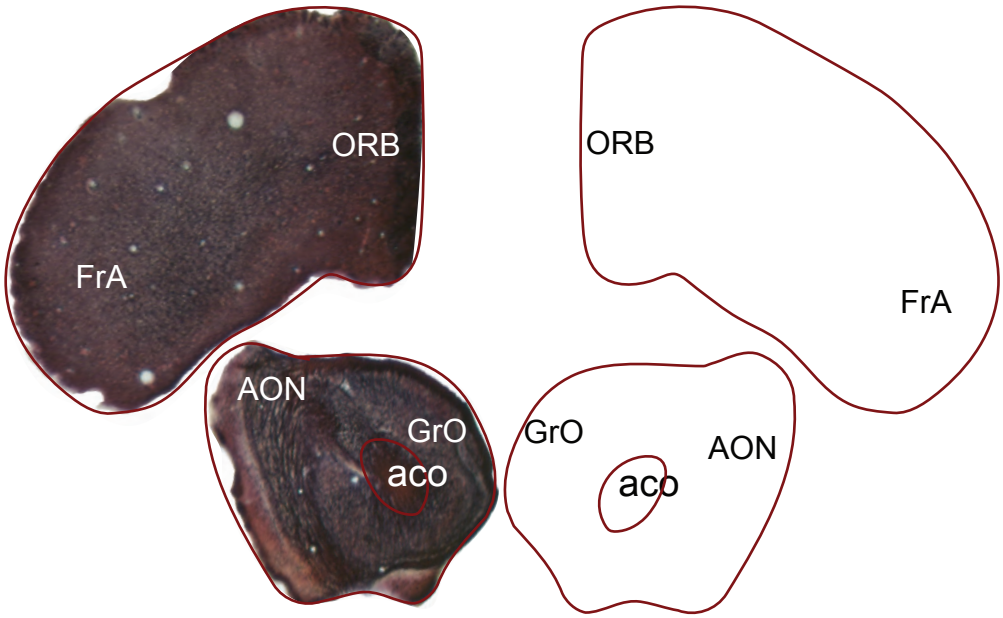

Set 3: OXT oc -2850µm

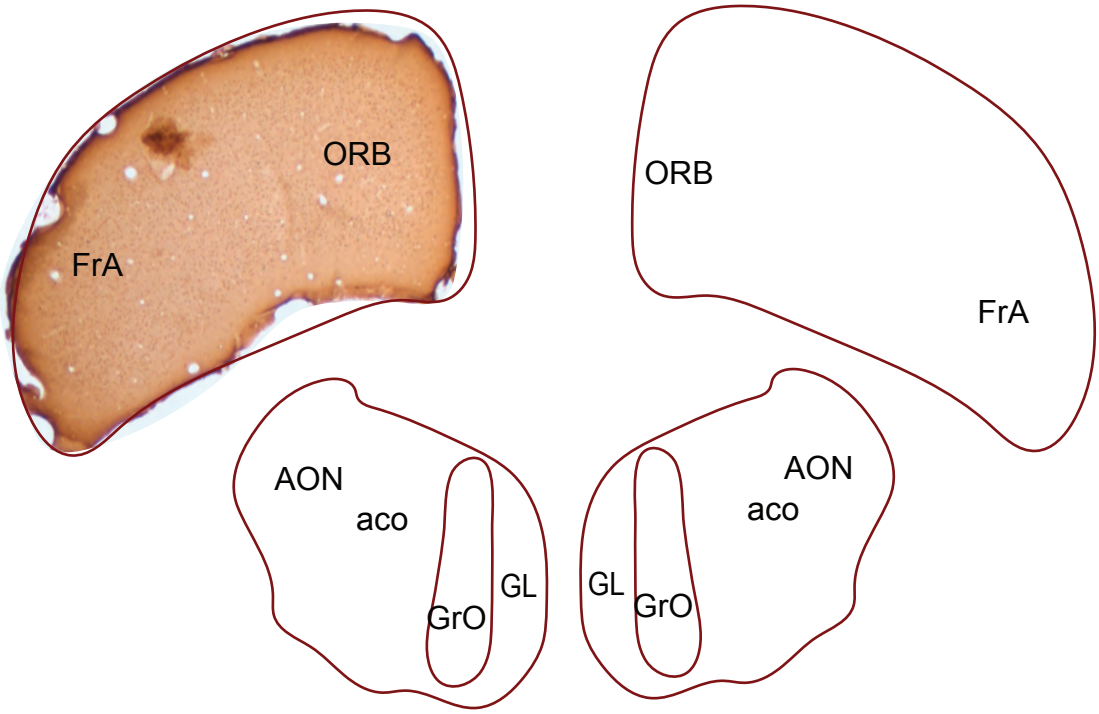

Set 3: Nissl oc -2800µm

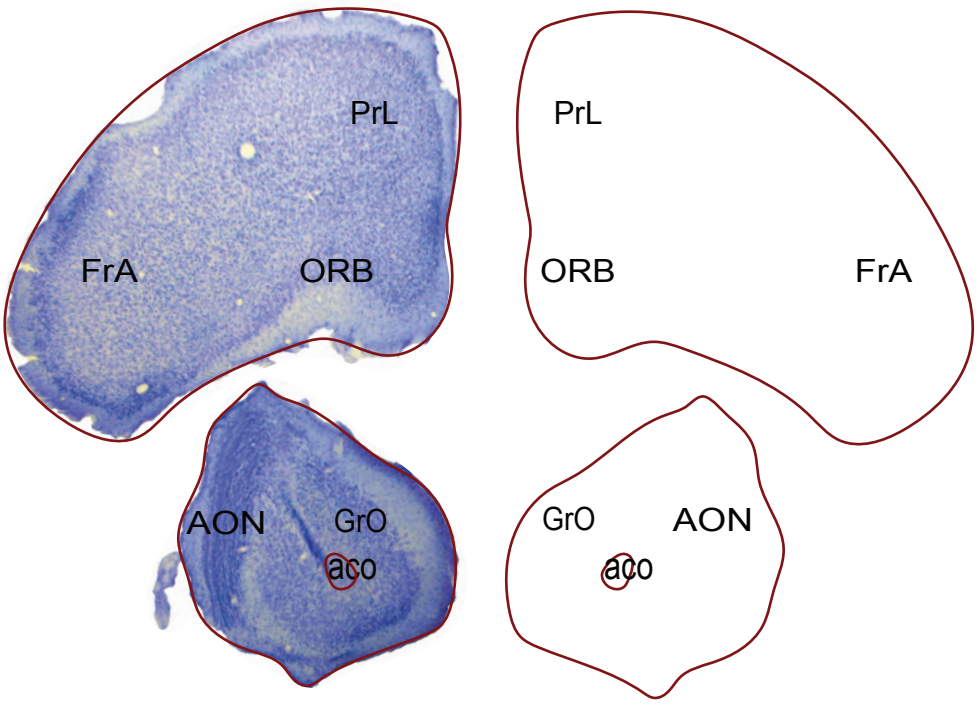

Set 3: OXT oc -2750µm

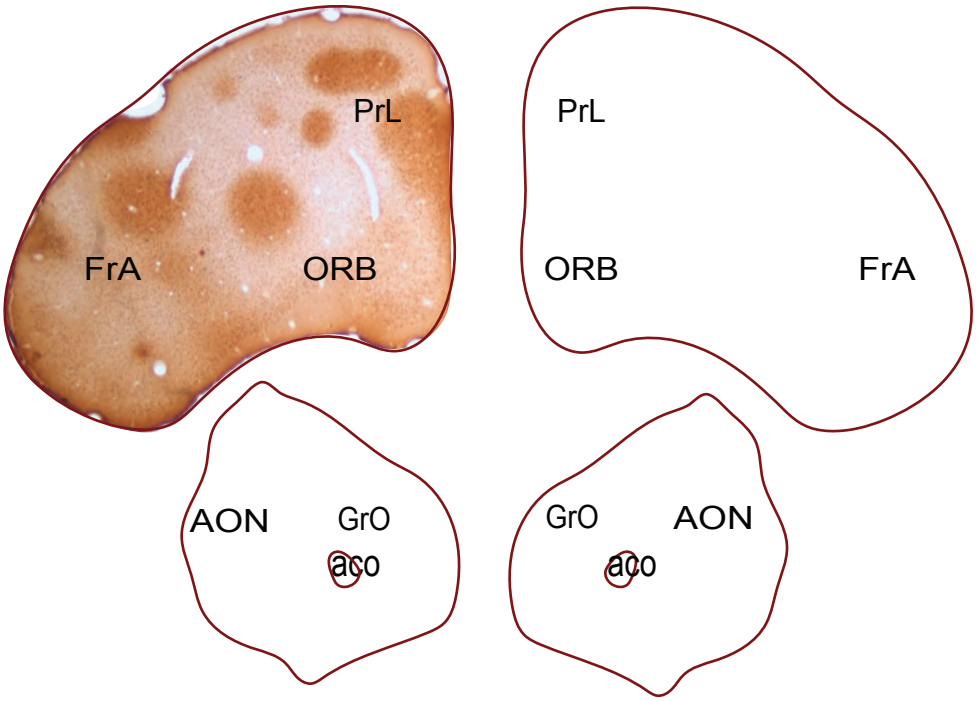

Set 3: Myelin oc -2700µm

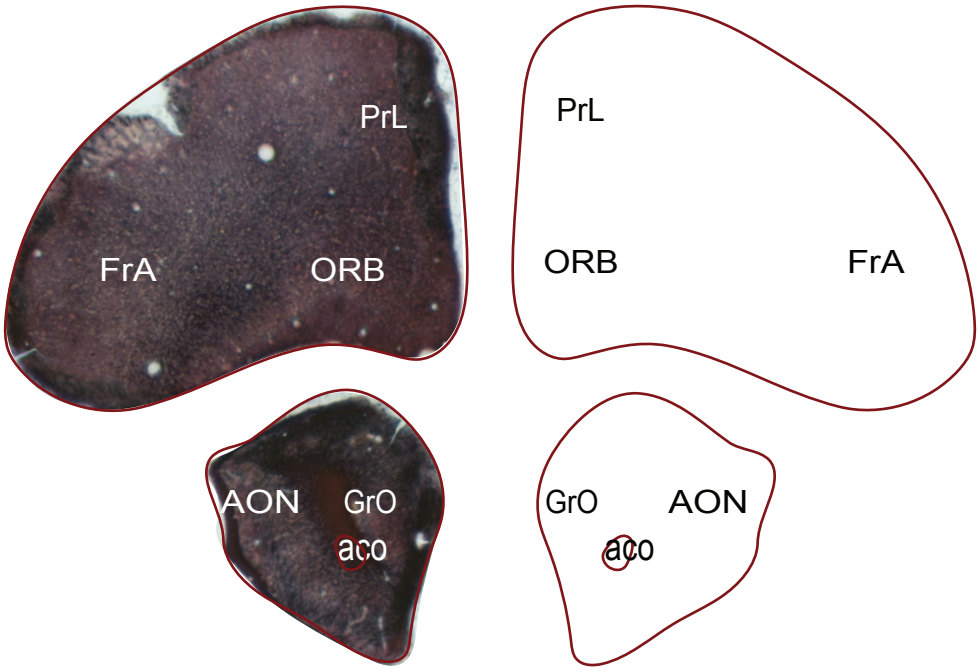

Set 4: OXT oc -2650µm

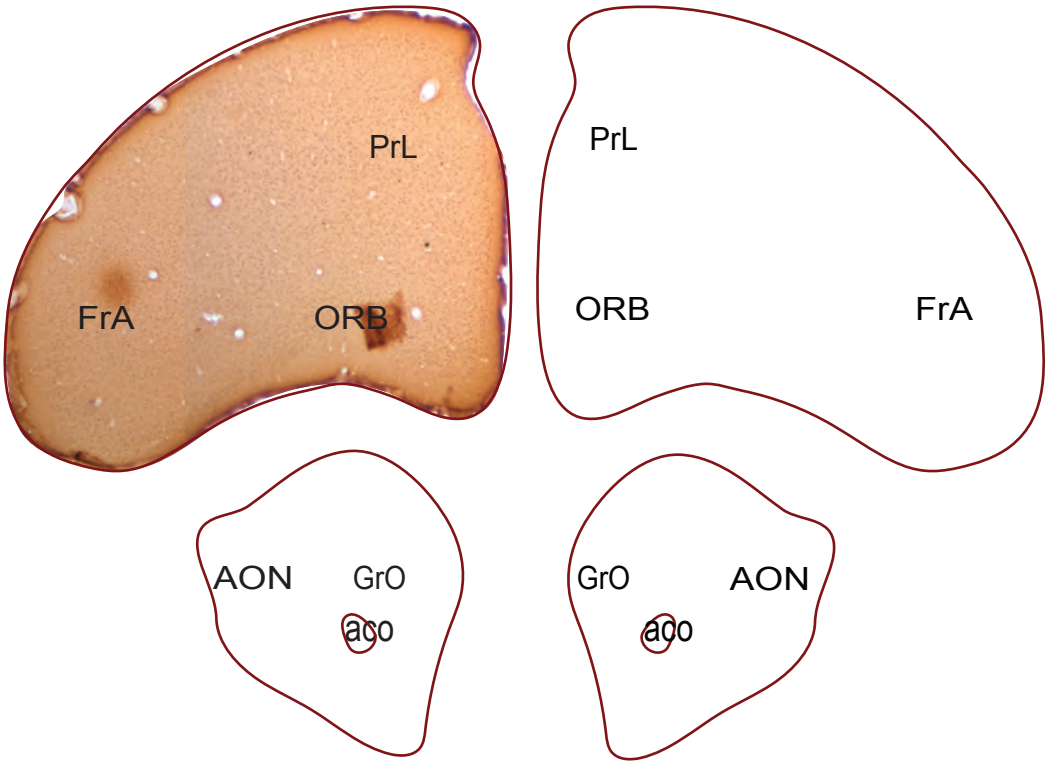

Set 4: Nissl oc -2600µm

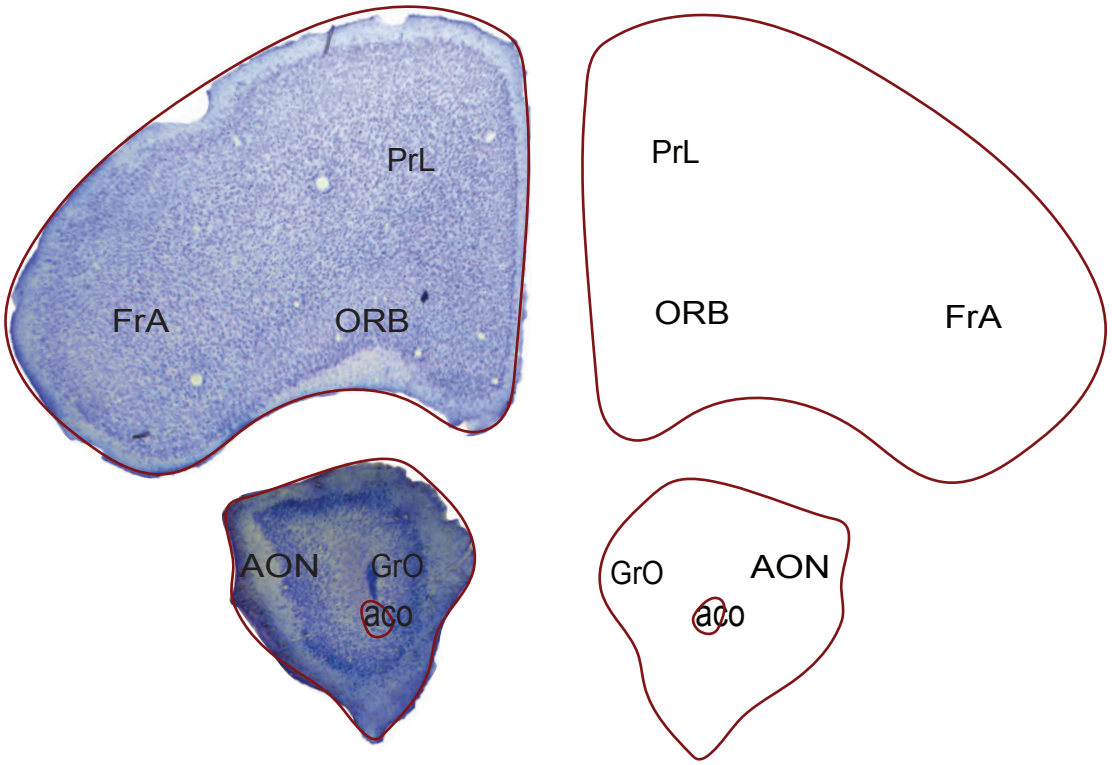

Set 4: OXT oc -2550µm

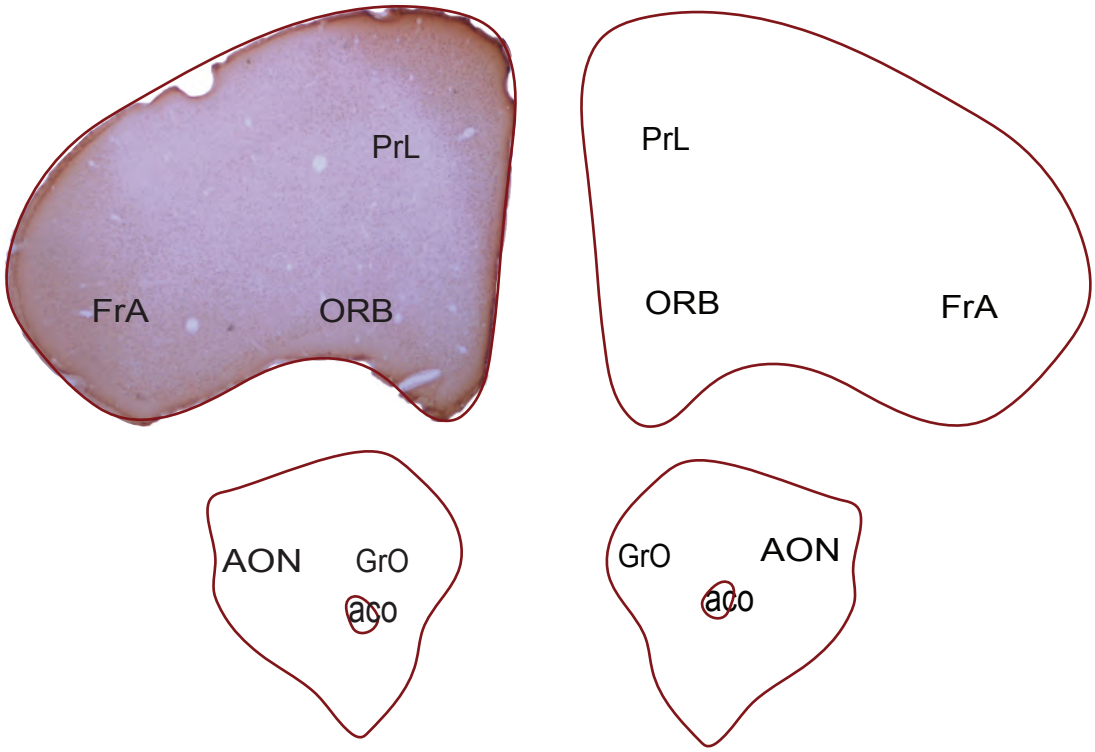

Set 4: Myelin oc -2500µm

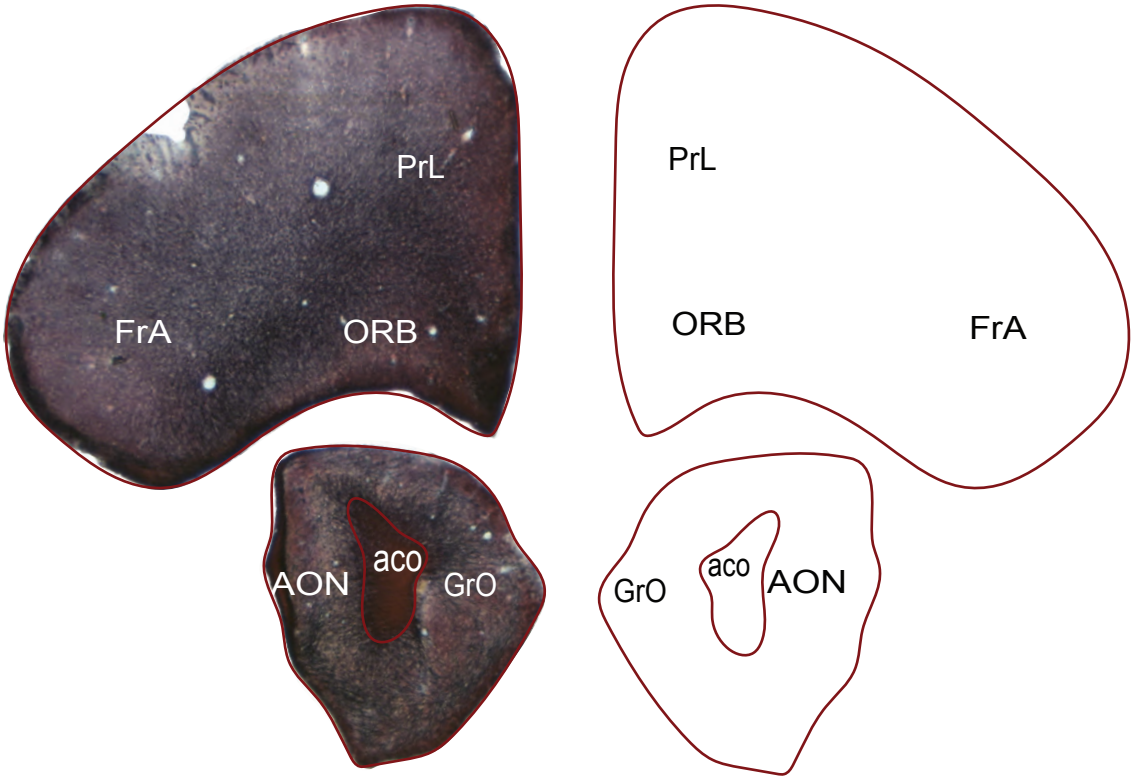

Set 5: OXT oc -2450µm

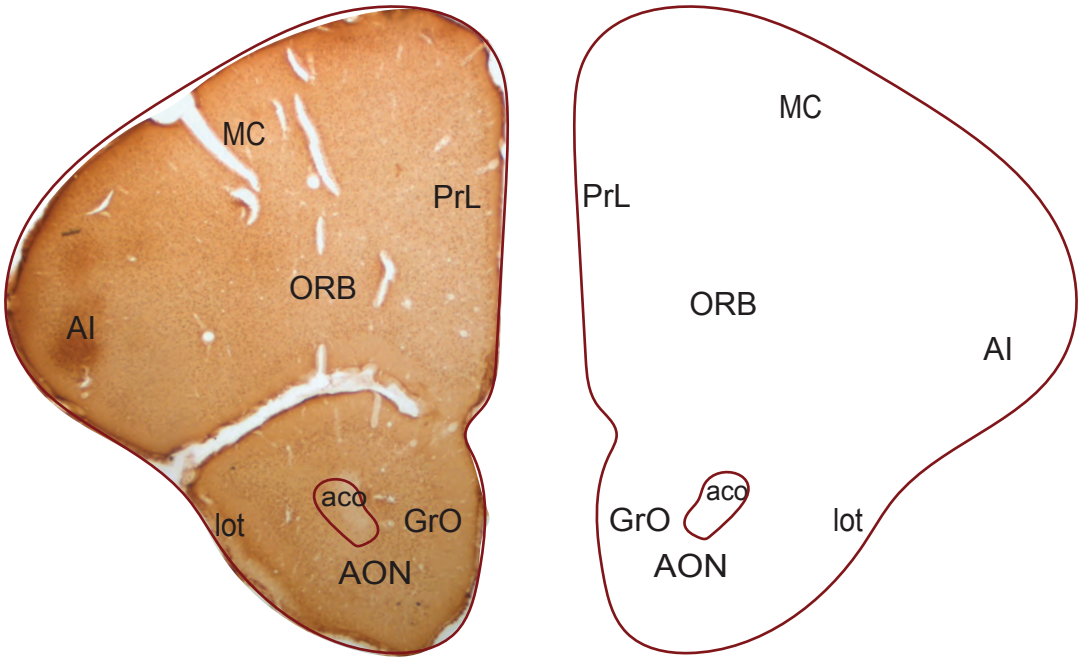

Set 5: Nissl oc -2400µm

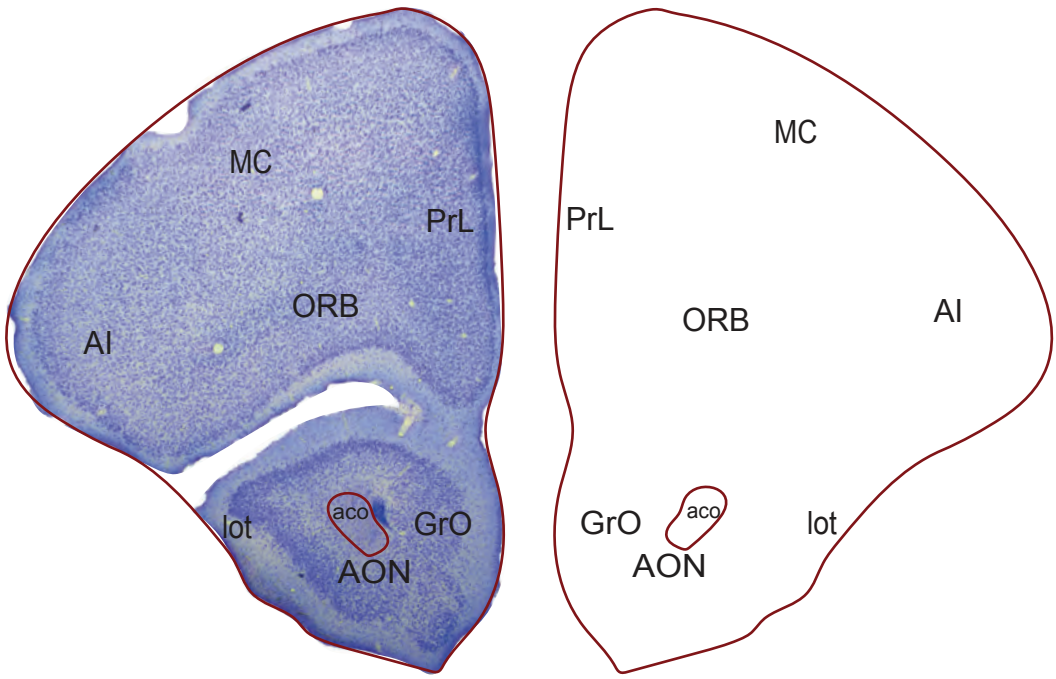

Set 5: OXT oc -2350µm

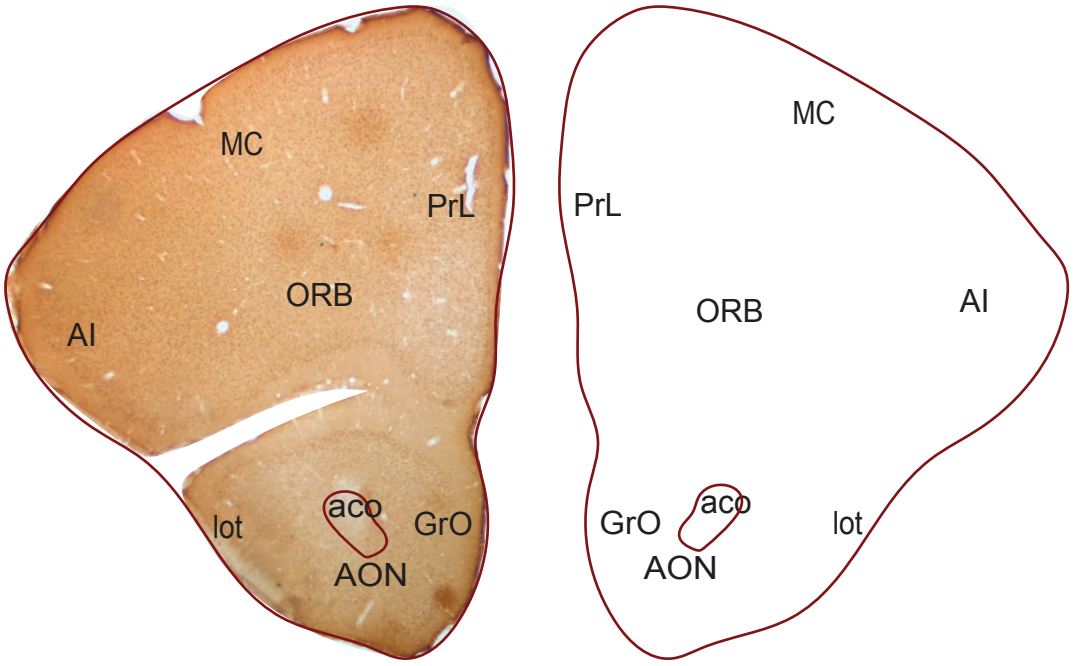

Set 5: Myelin oc -2300µm

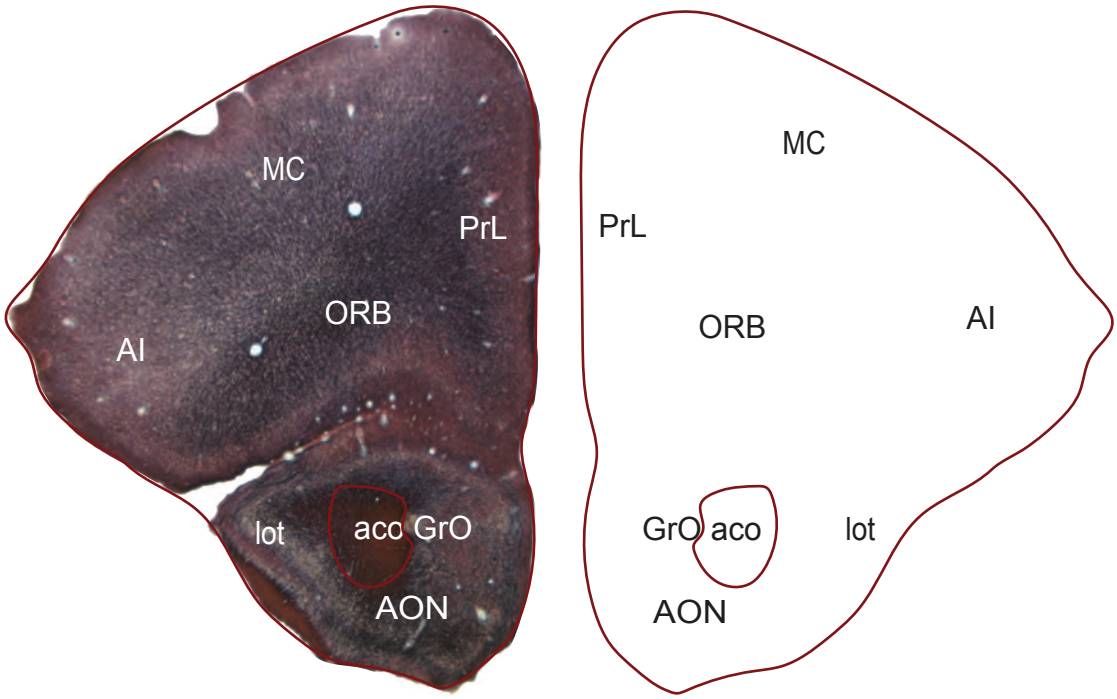

Set 6: OXT oc -2150µm

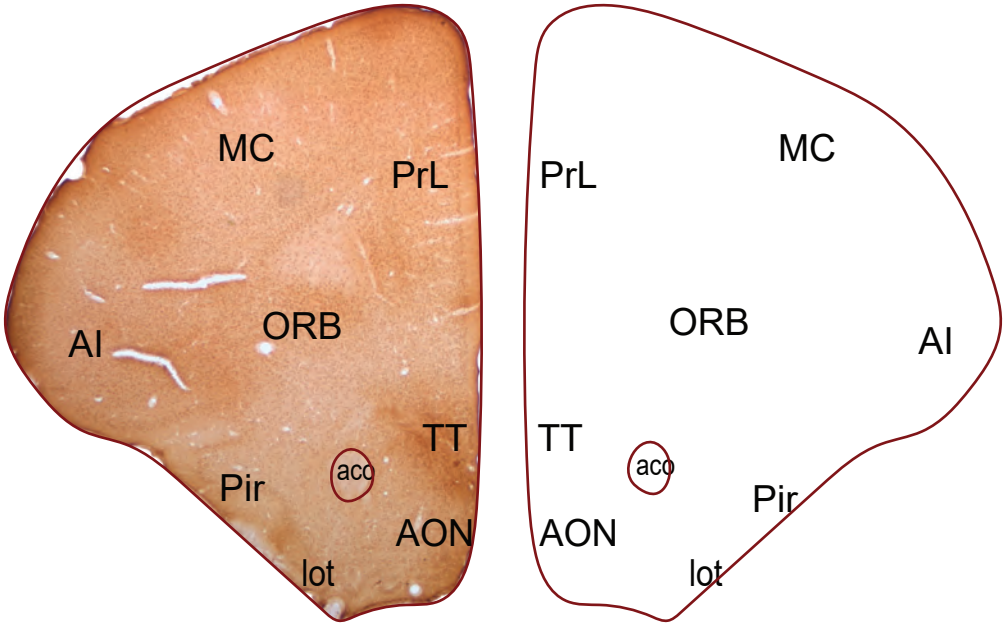

Set 6: Nissl oc -2200µm

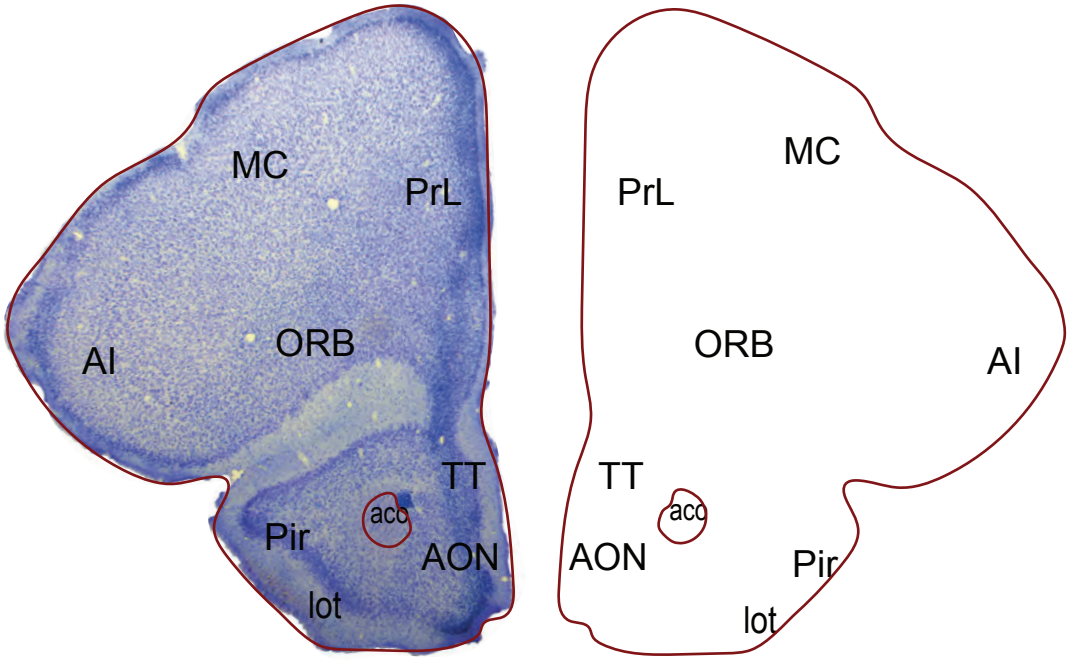

Set 6: OXT oc -2150µm

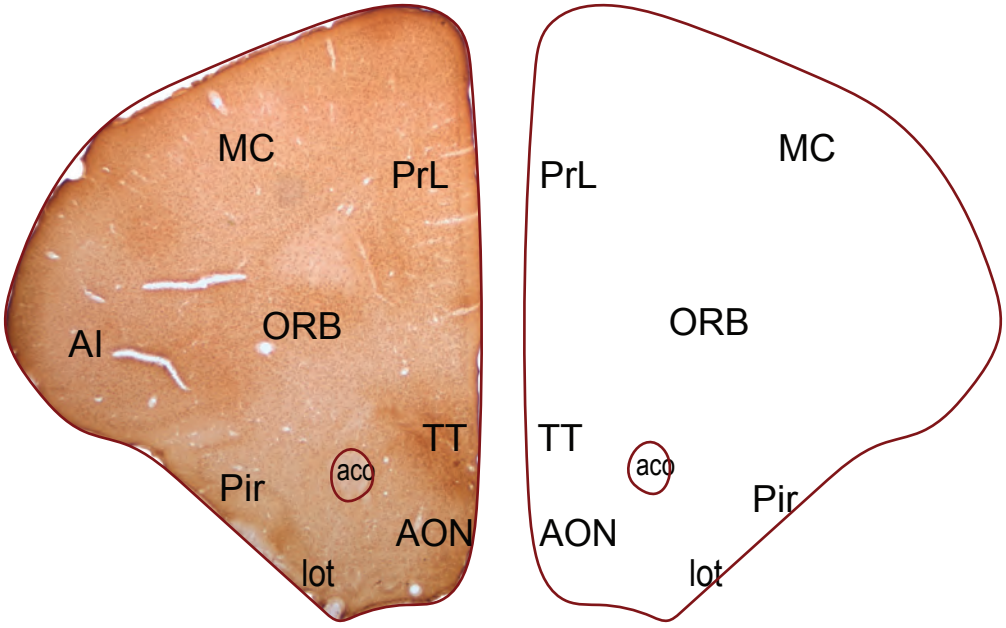

Set 6: Myelin oc -2100µm

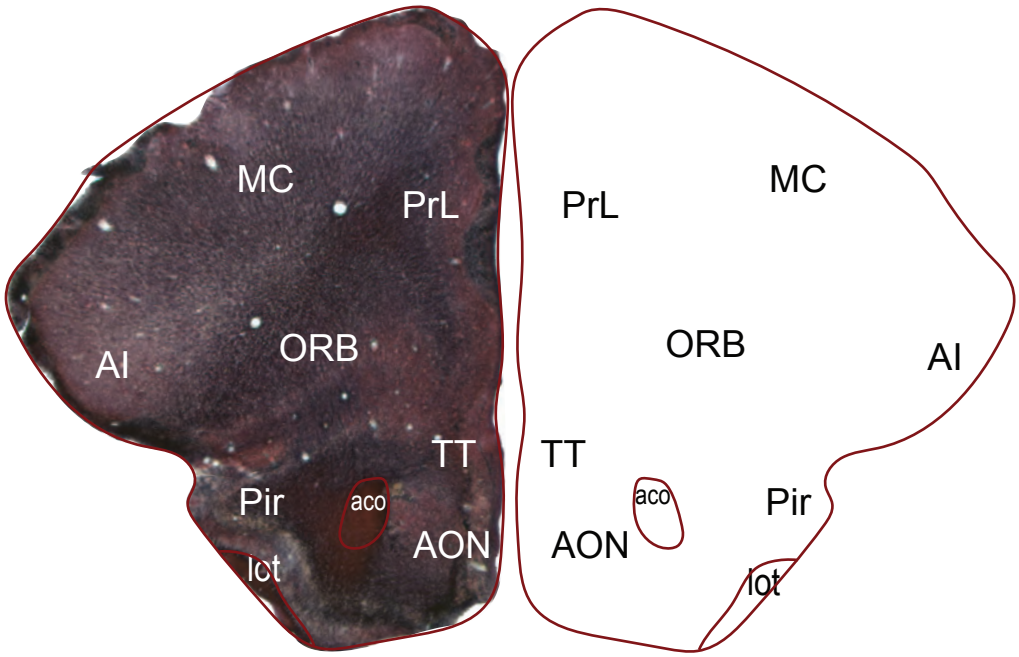

Set 7: OXT oc -2050µm

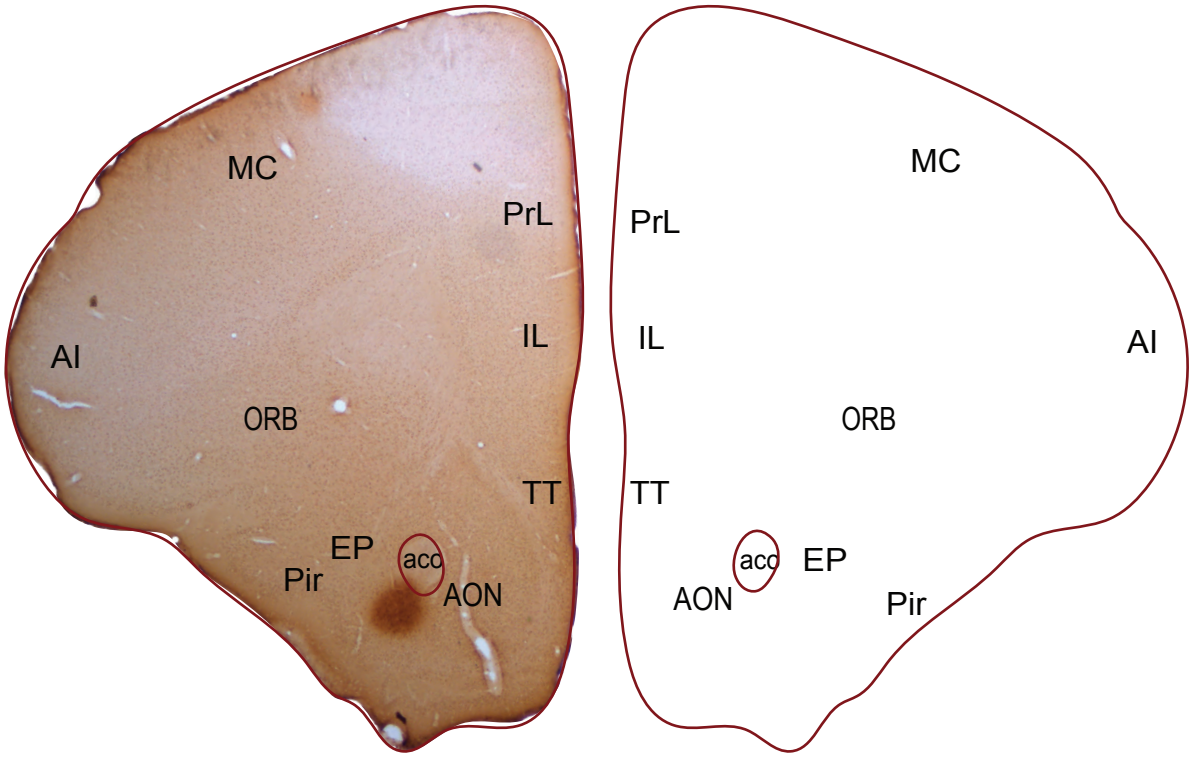

Set 7: Nissl oc -2000µm

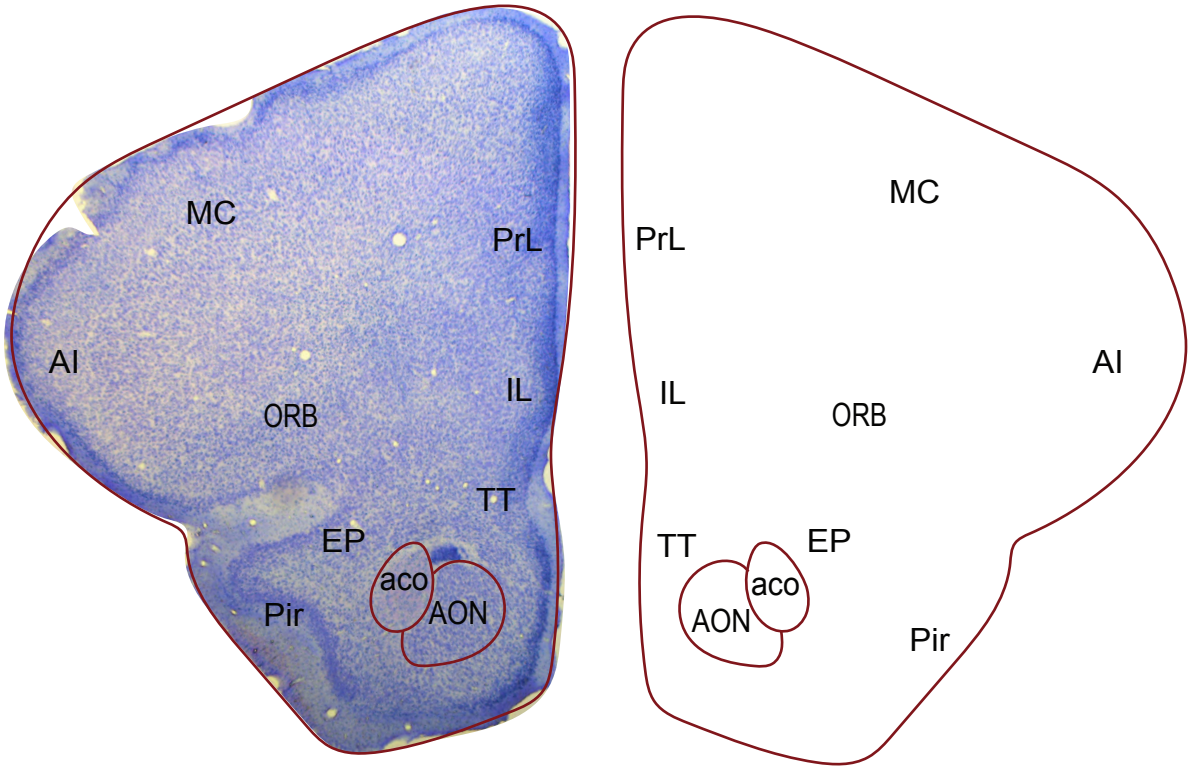

Set 7: OXT oc -1950µm

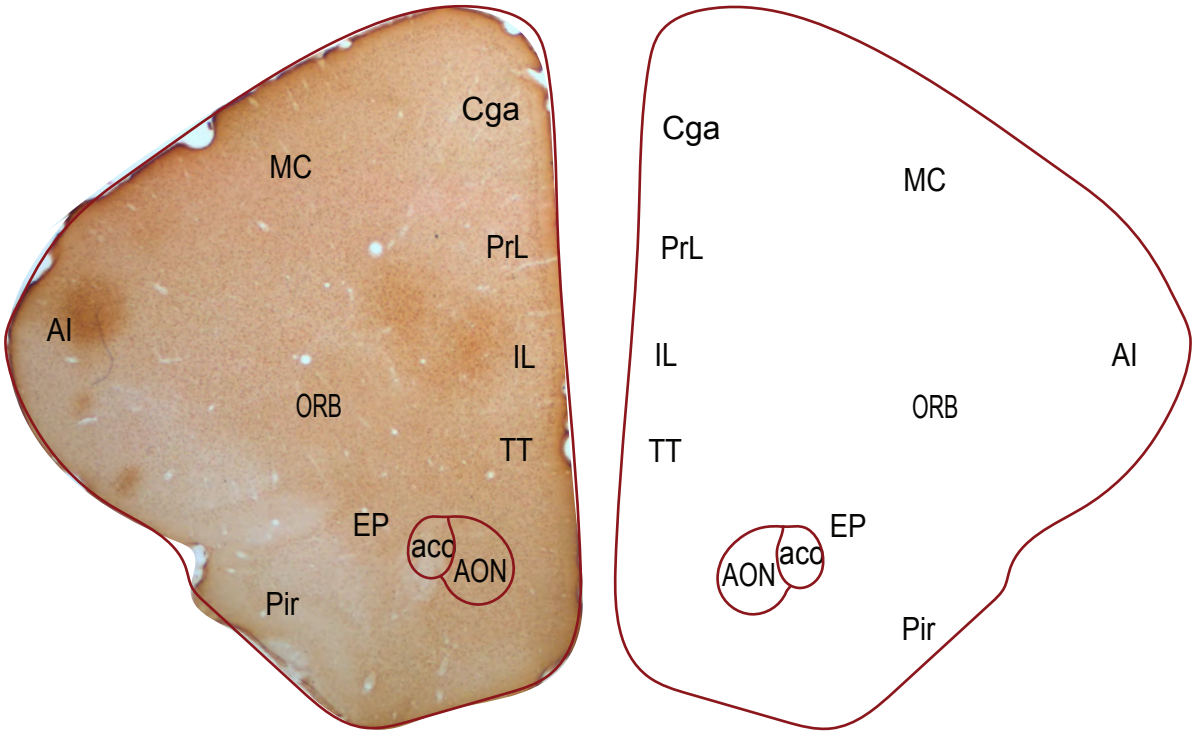

Set 7: OXT oc -1900µm

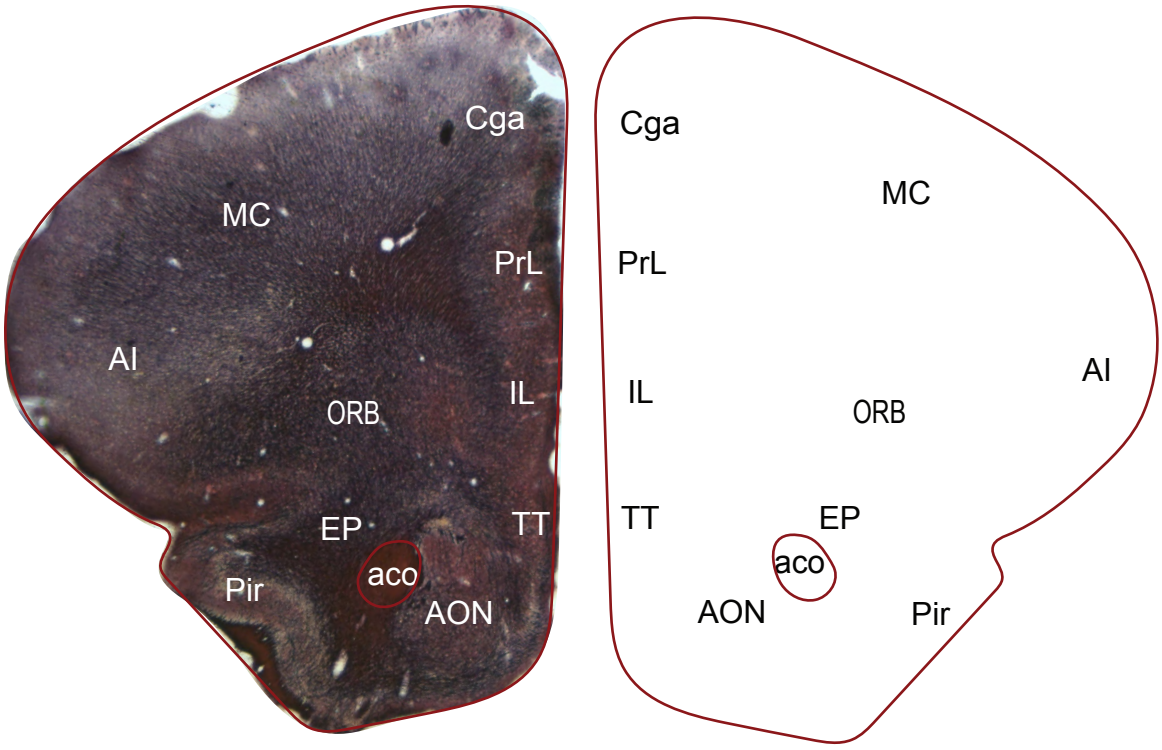

Set 8: OXT oc -1850µm

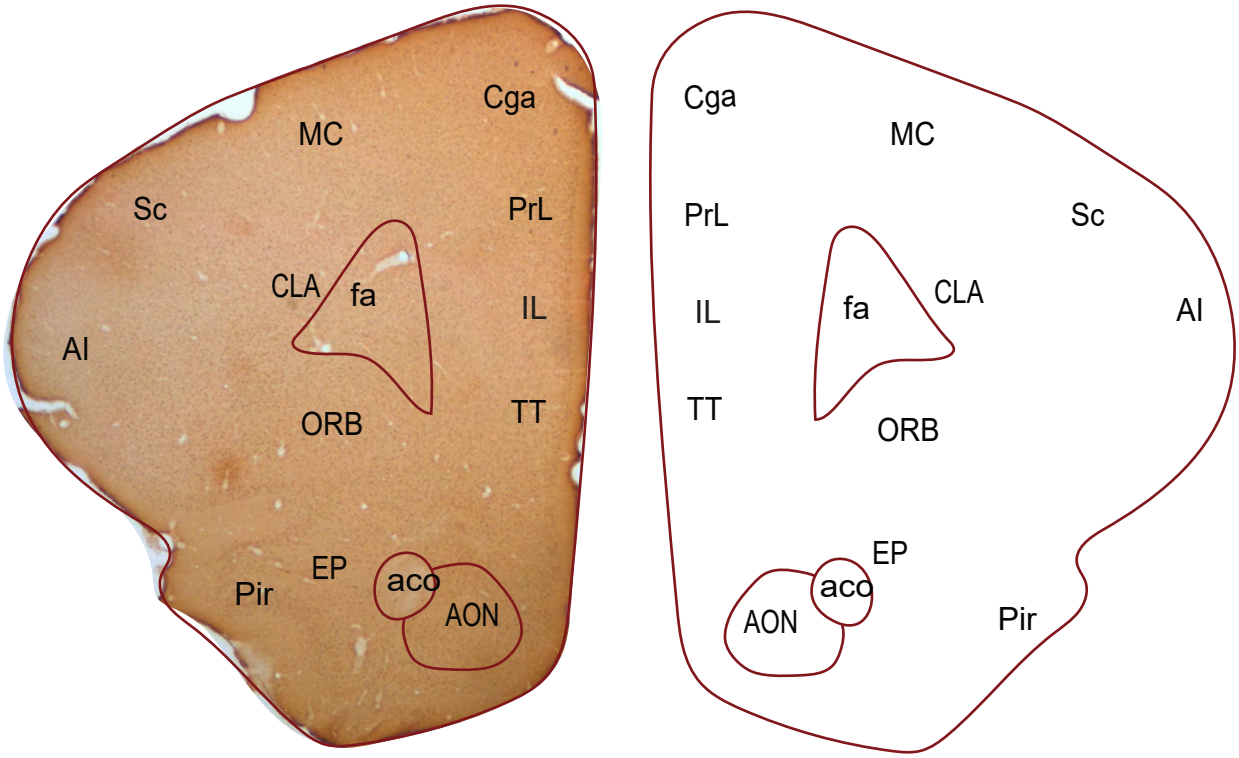

Set 8: Nissl oc -1800µm

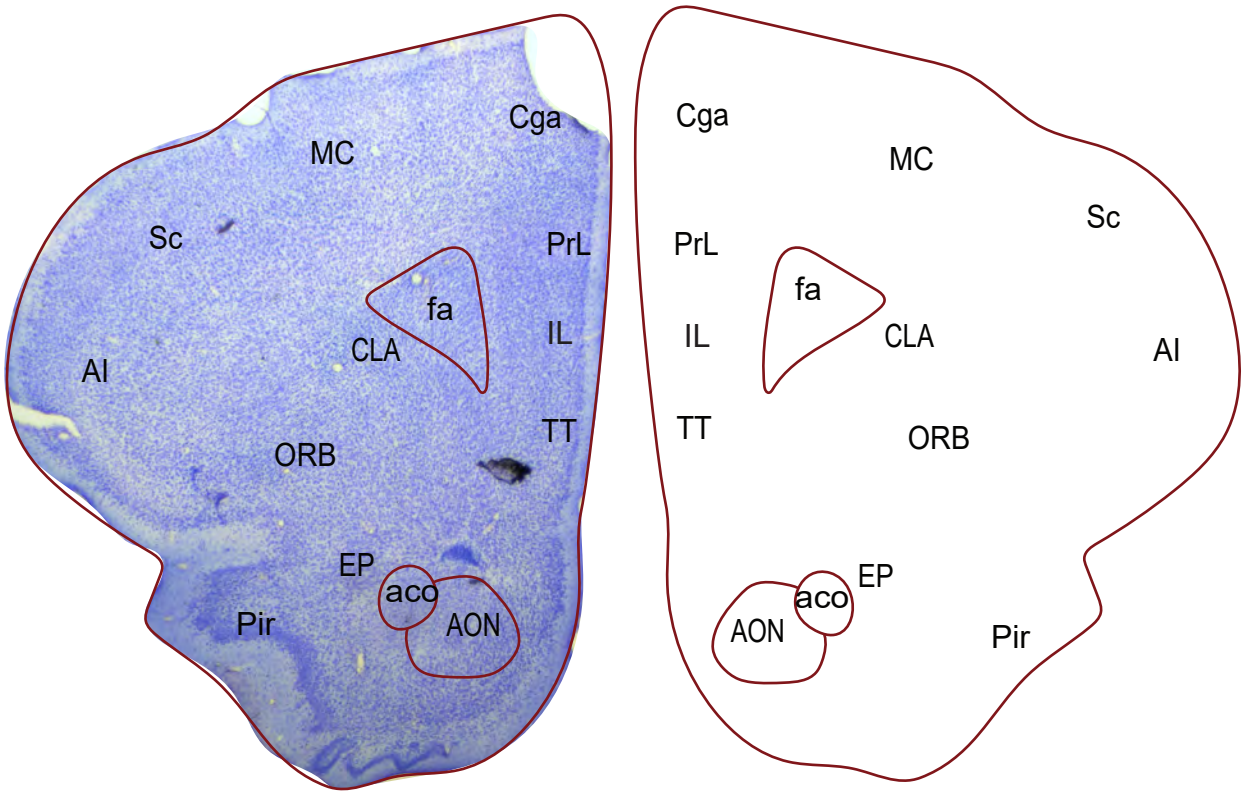

Set 8: OXT oc -1750µm

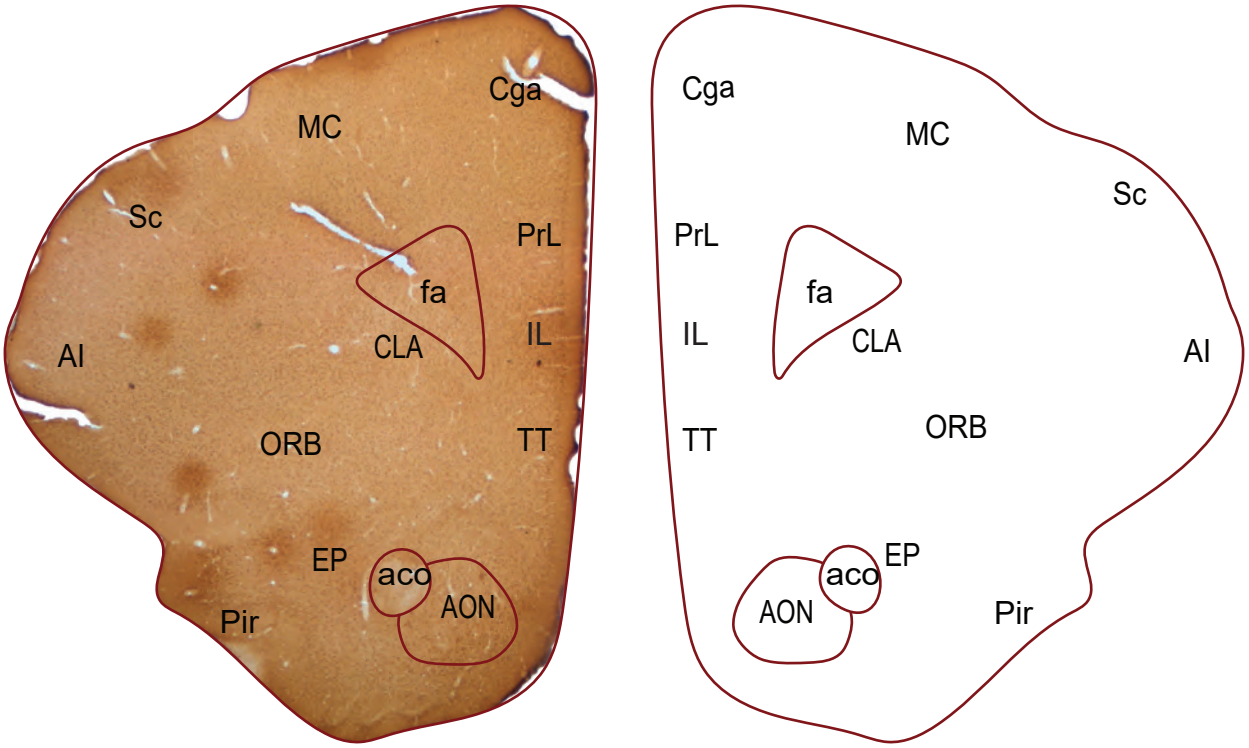

Set 8: Myelin oc -1700µm

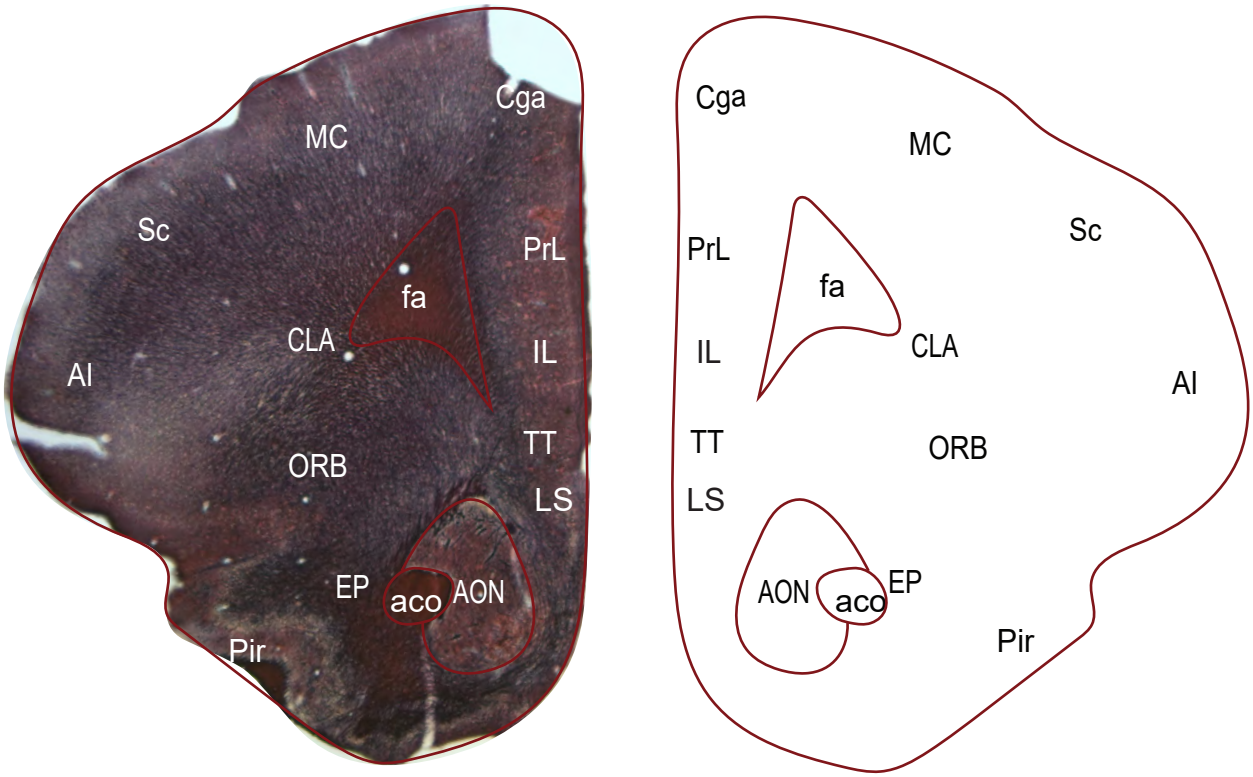

Set 9: OXT oc -1650µm

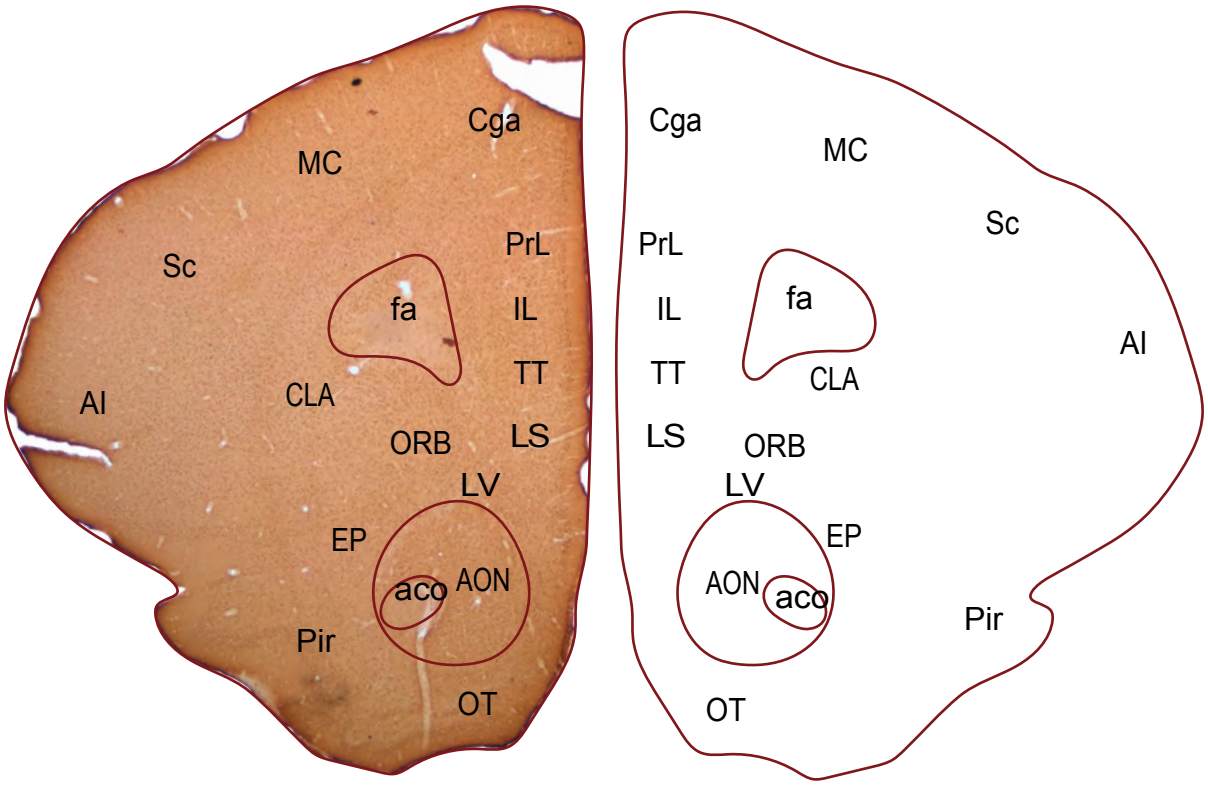

Set 9: Nissl oc -1600µm

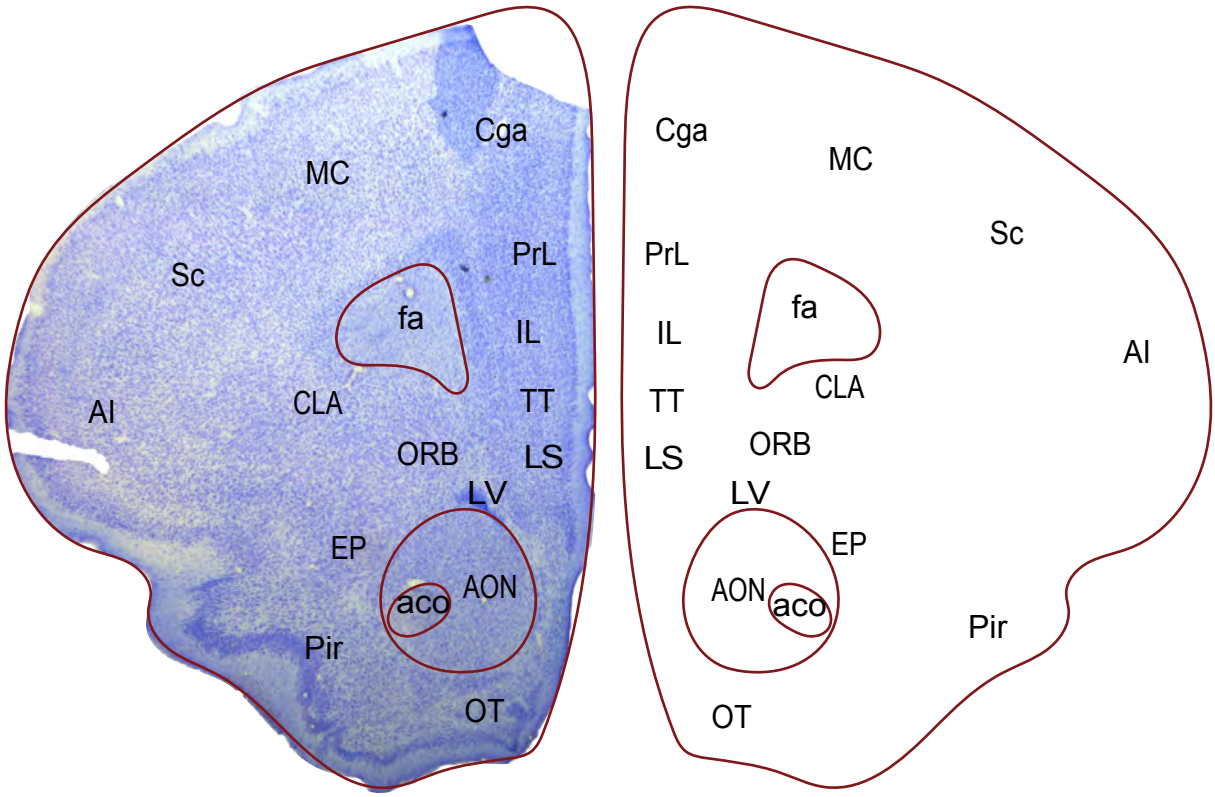

Set 9: OXT oc -1550µm

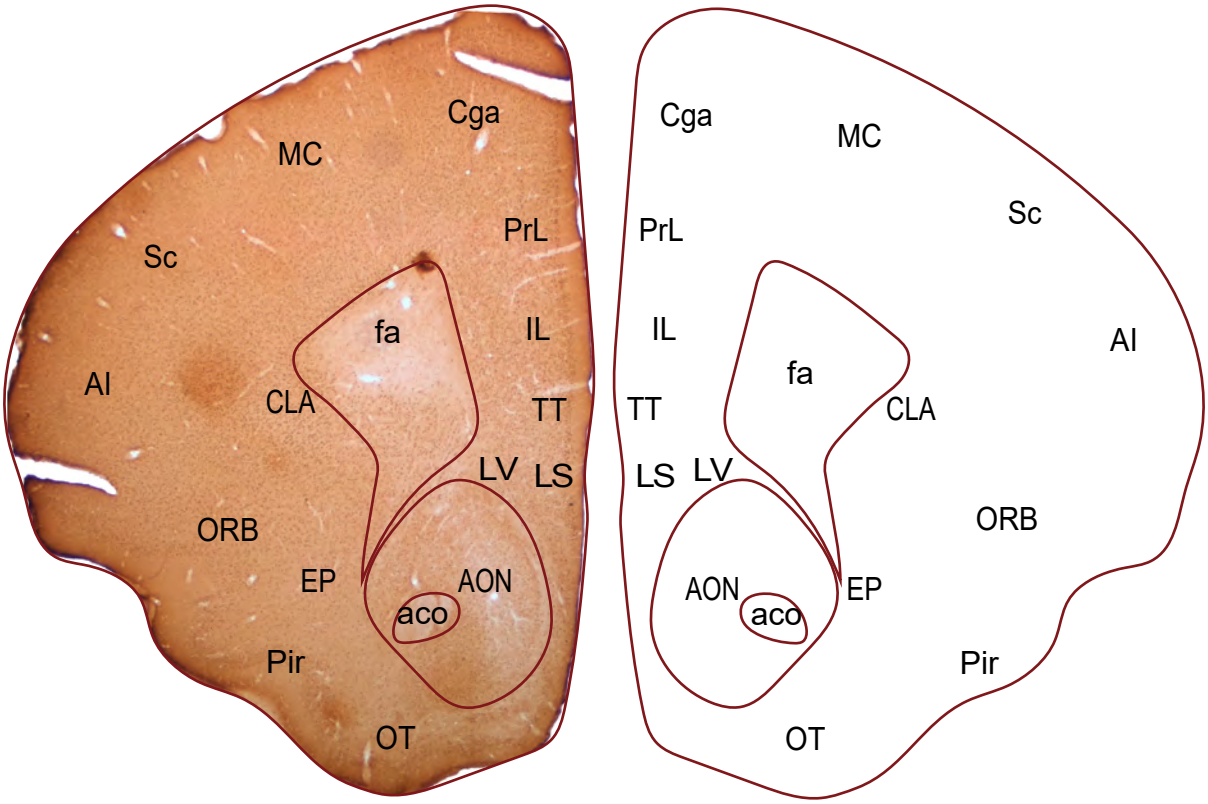

Set 9: Myelin oc -1500µm

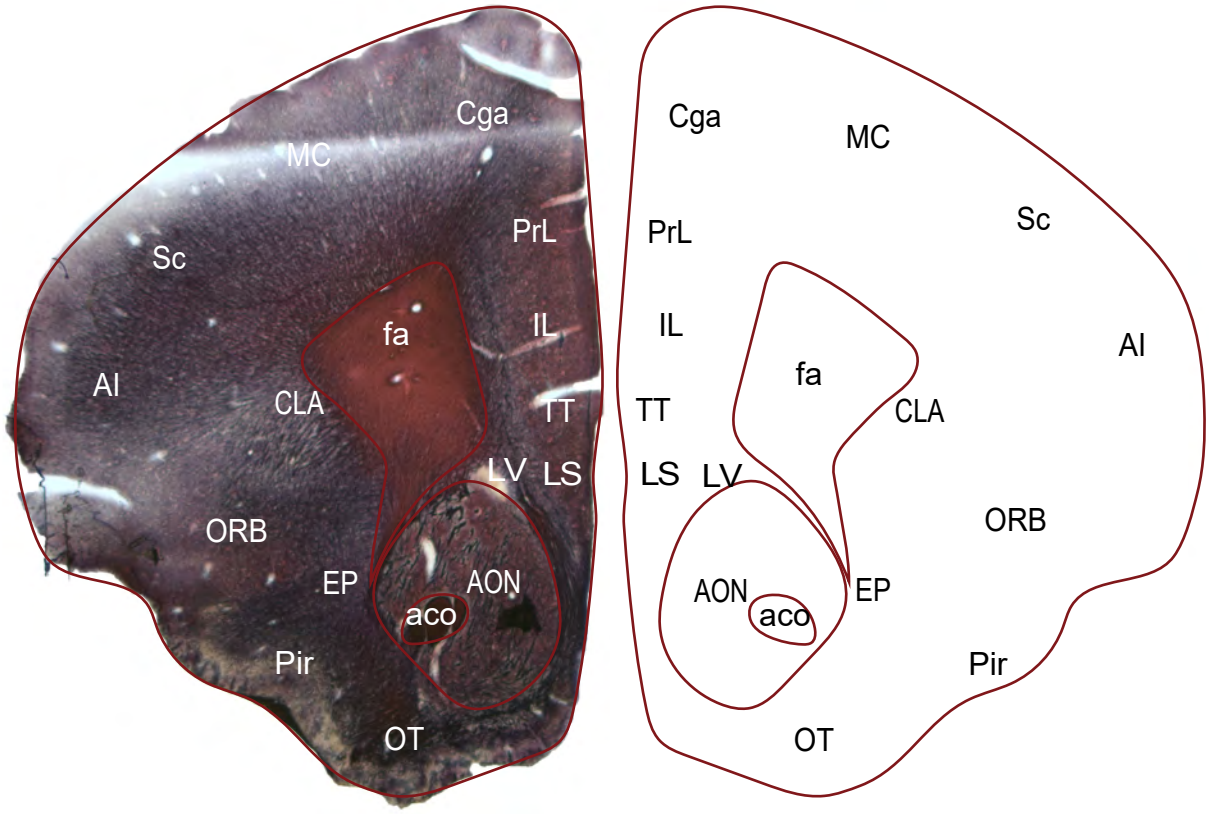

Set 10: OXT oc -1450µm

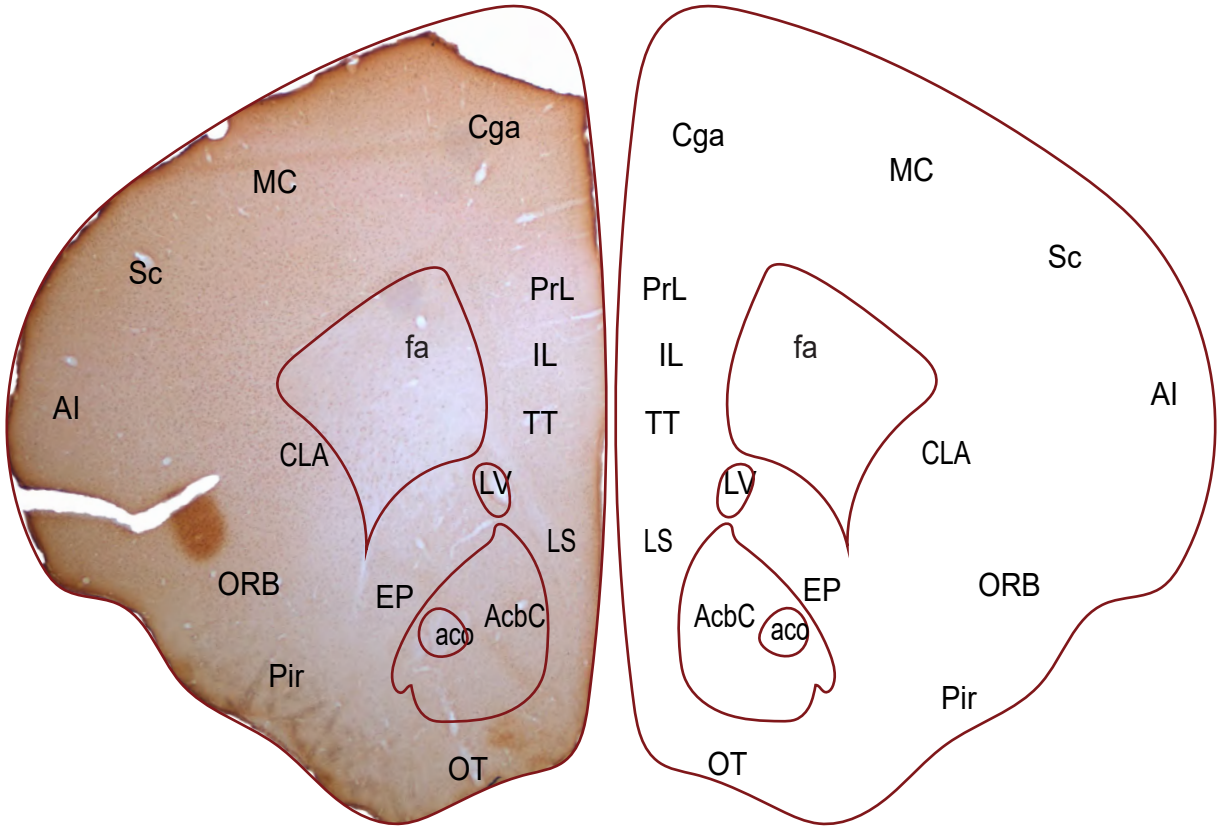

Set 10: Nissl oc -1400µm

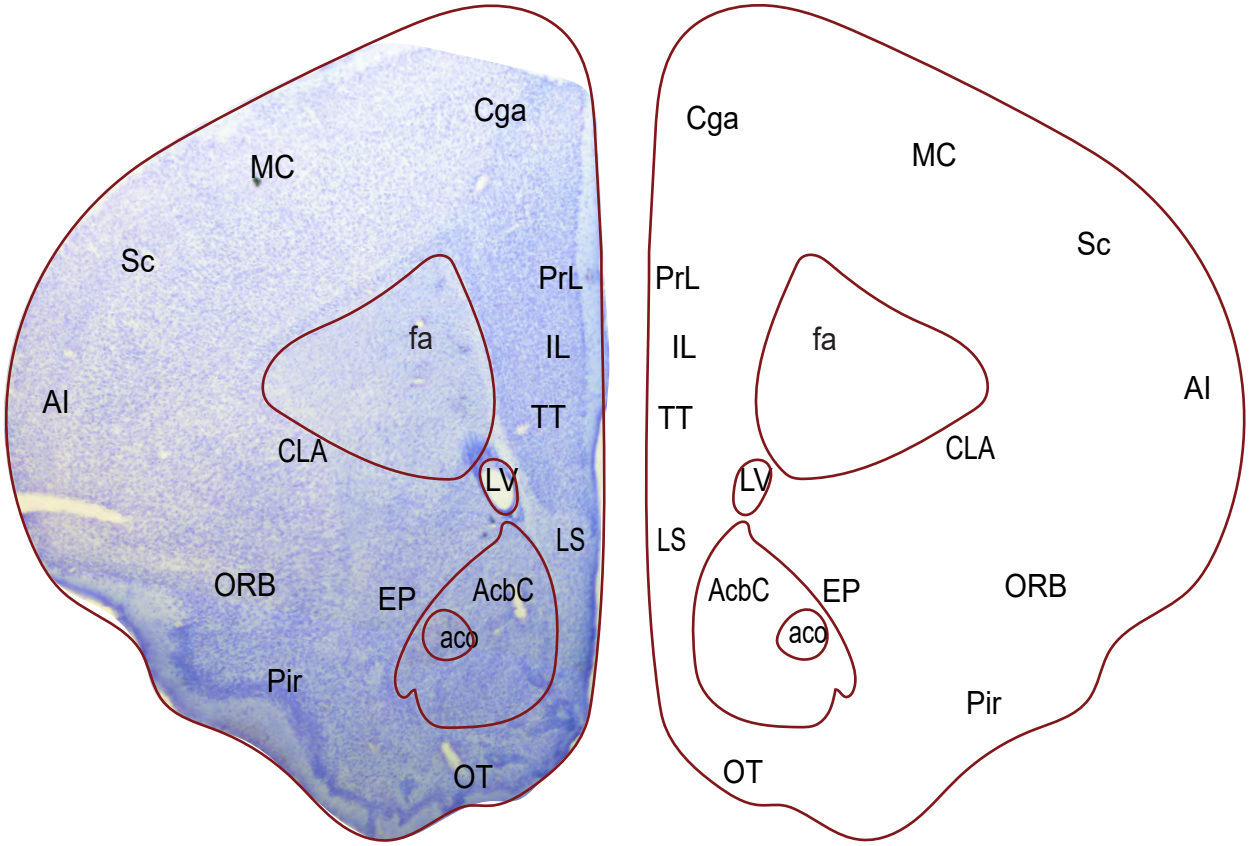

Set 10: OXT oc -1350µm

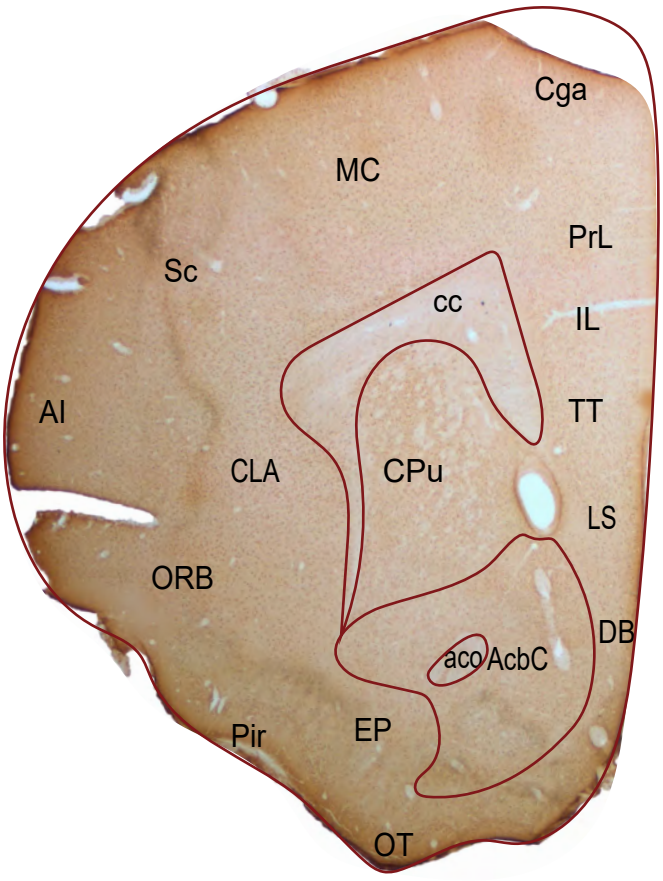

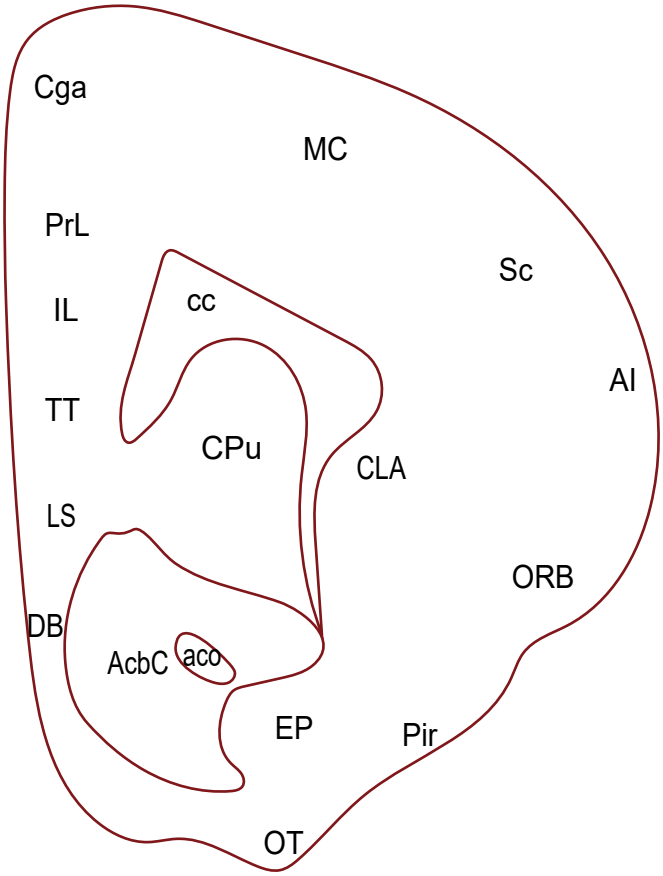

Set 10: Myelin oc -1300µm

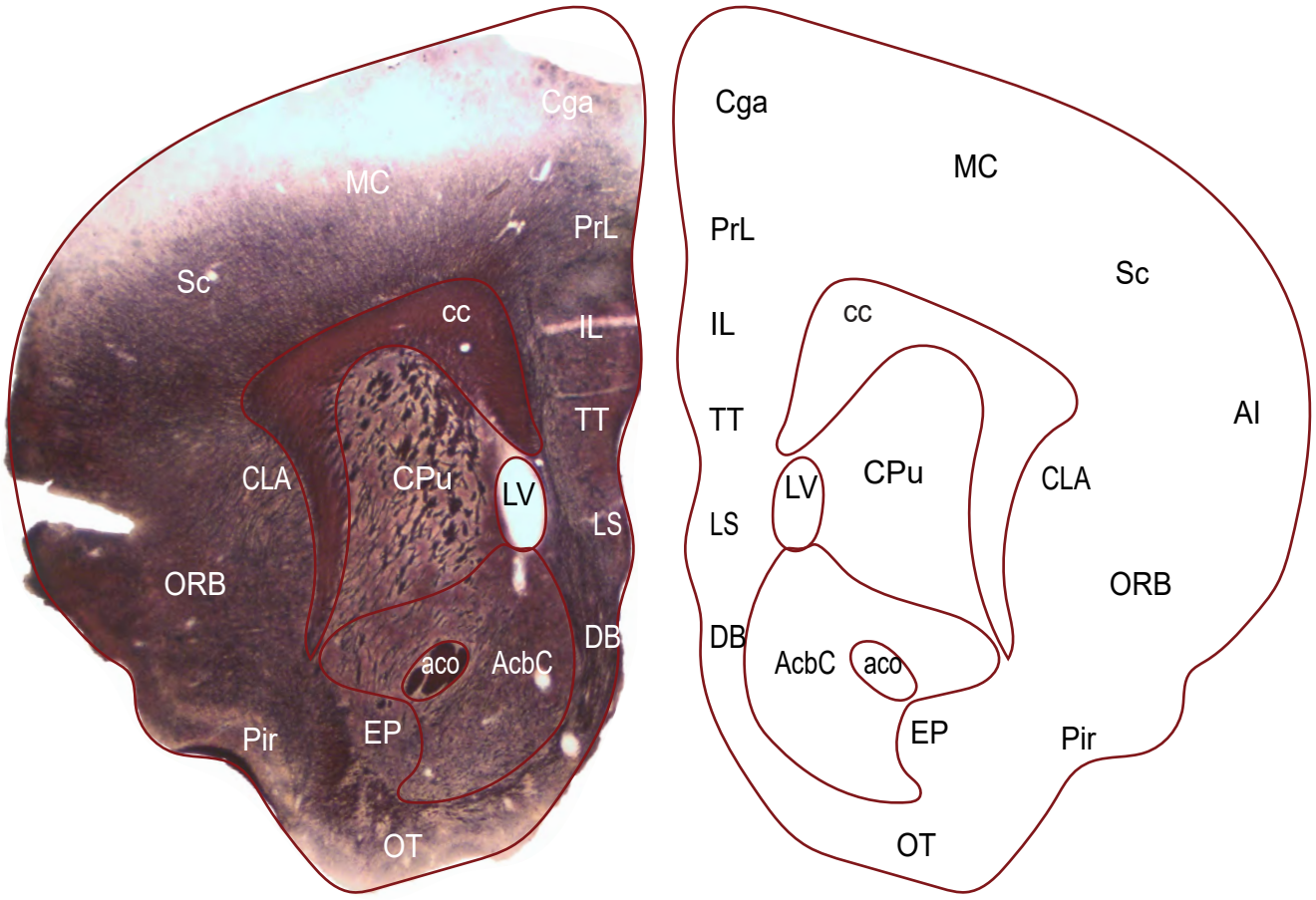

Set 11:OXT oc -1250µm

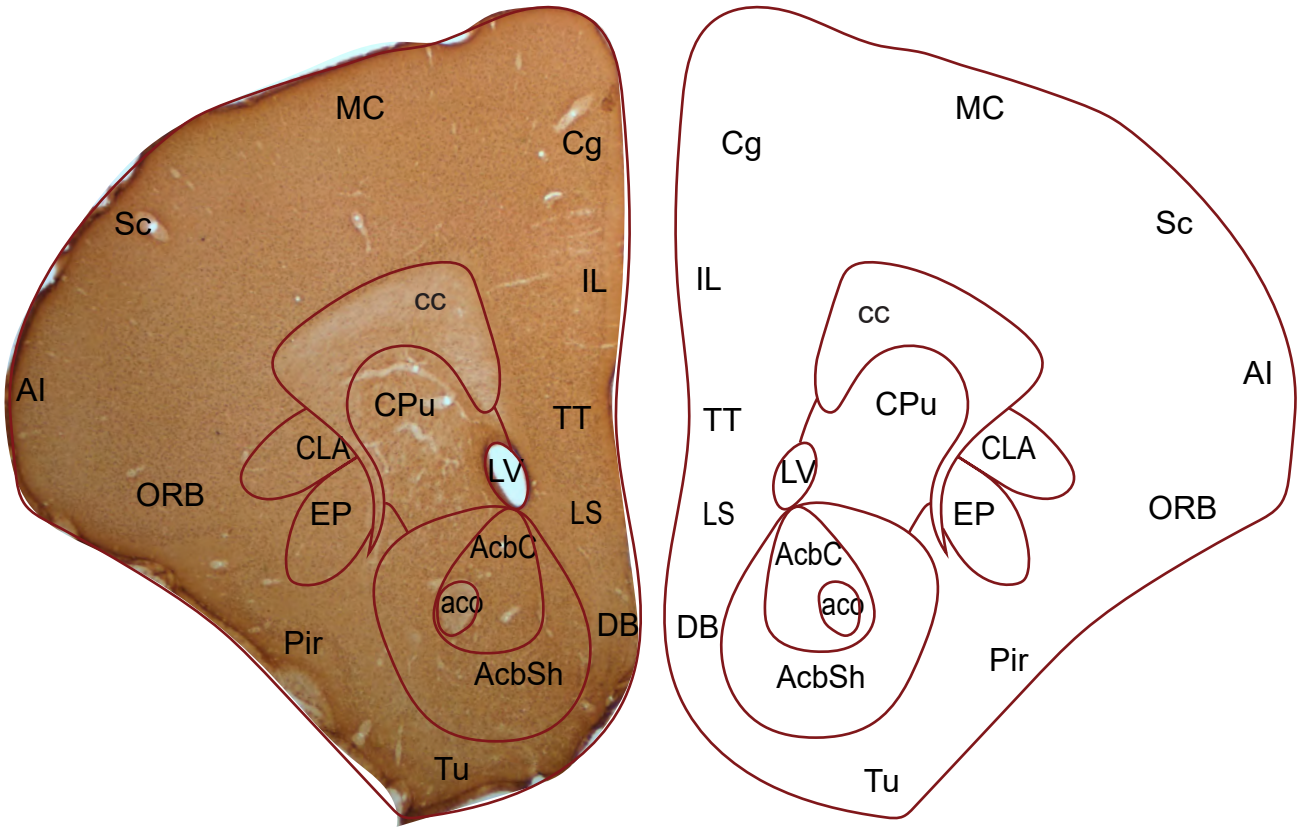

Set 11: Nissl oc -1200µm

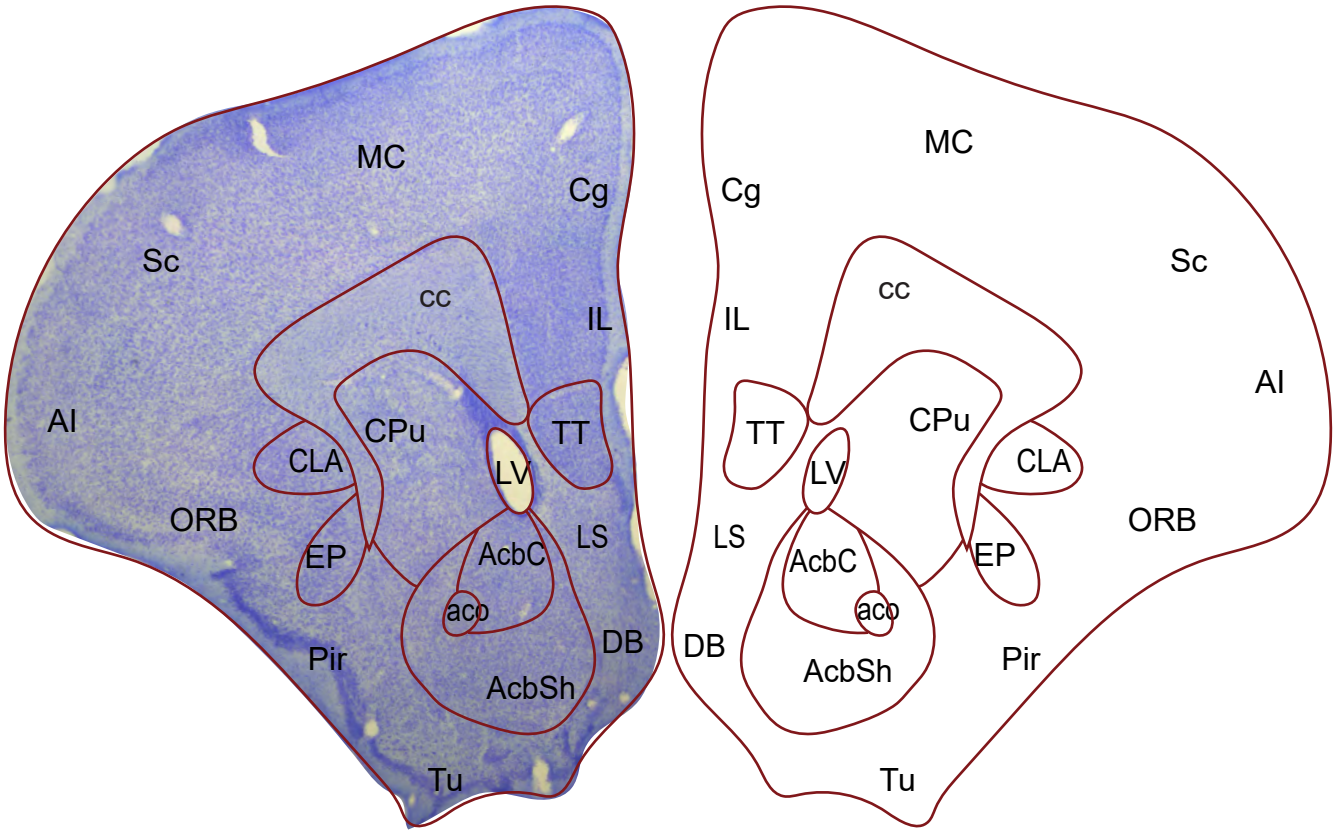

Set 11: OXT oc -1150µm

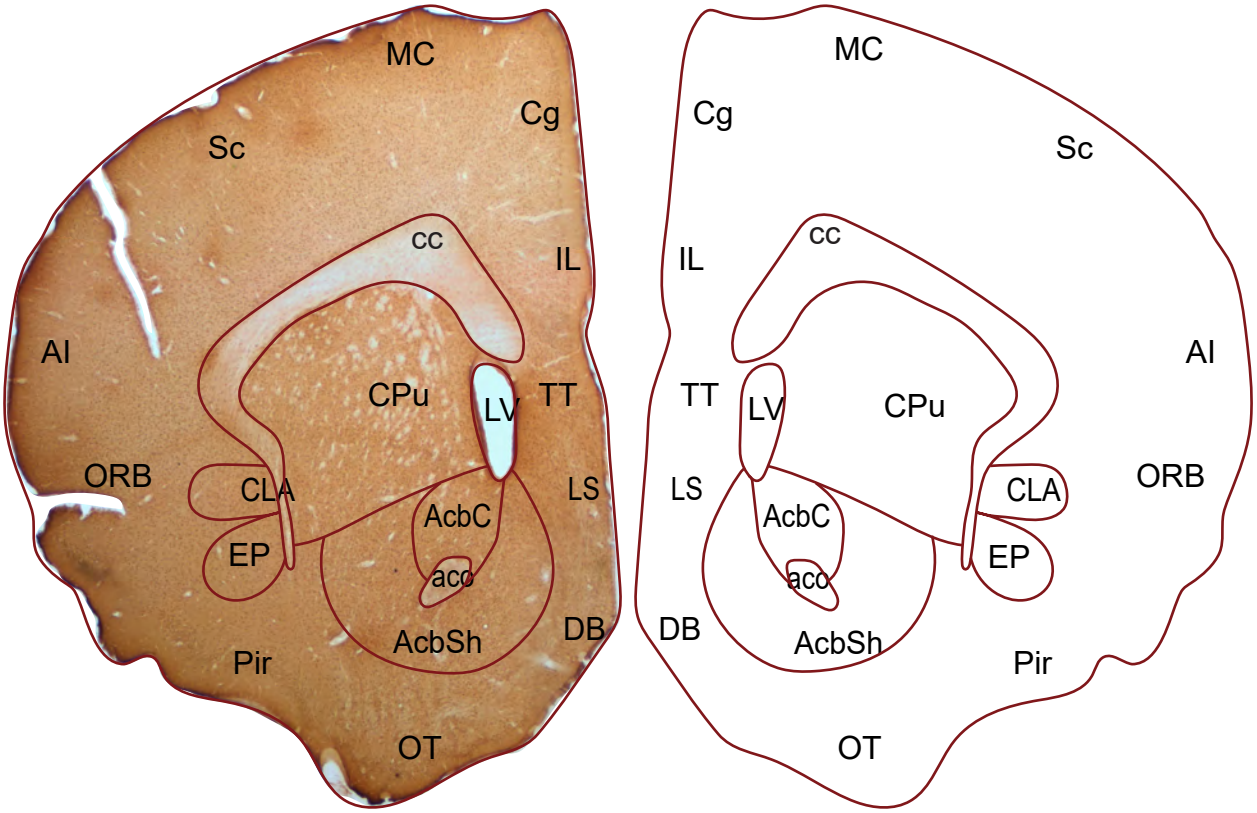

Set 11: Myelin oc -1100µm

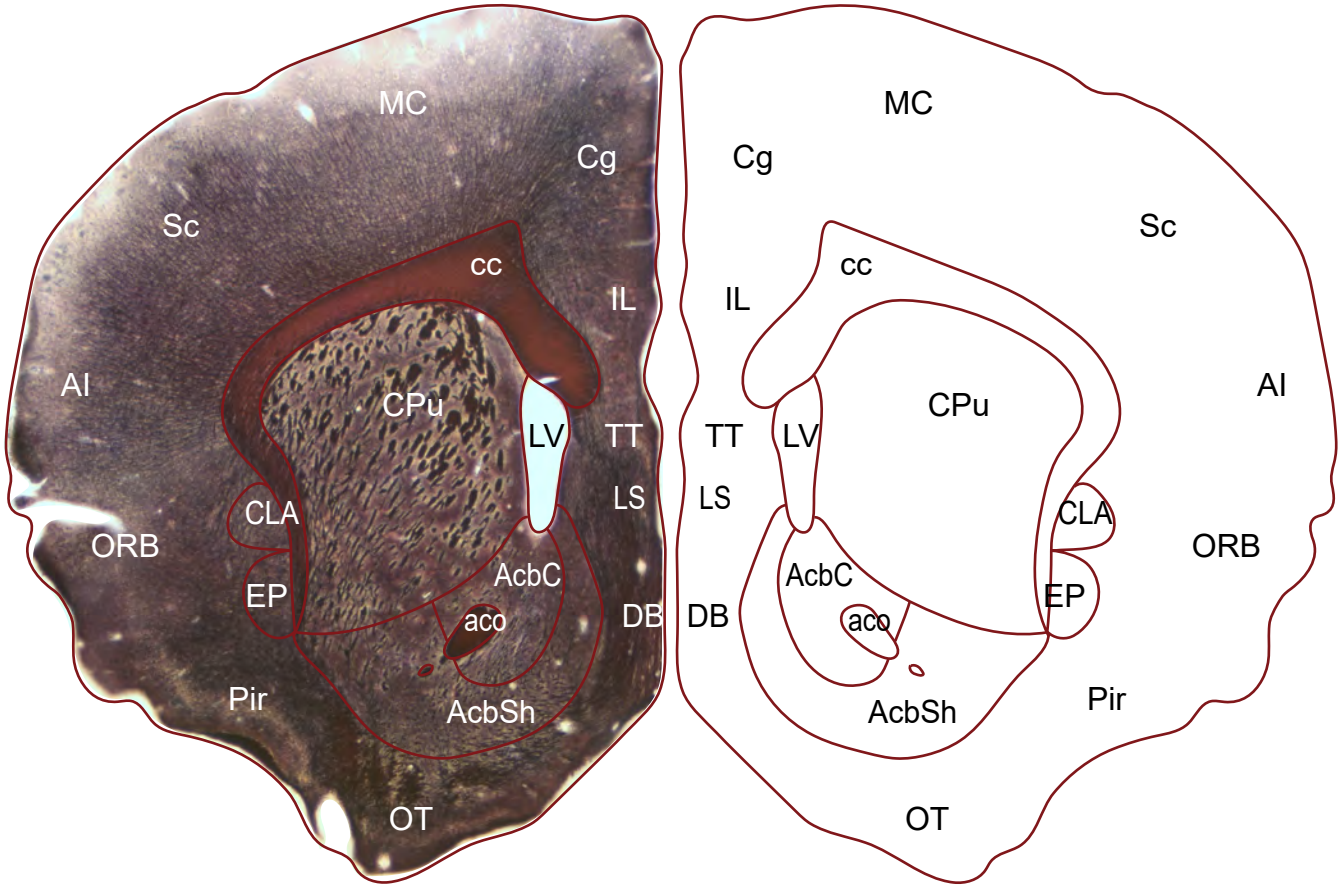

Set 12: OXT oc -1050µm

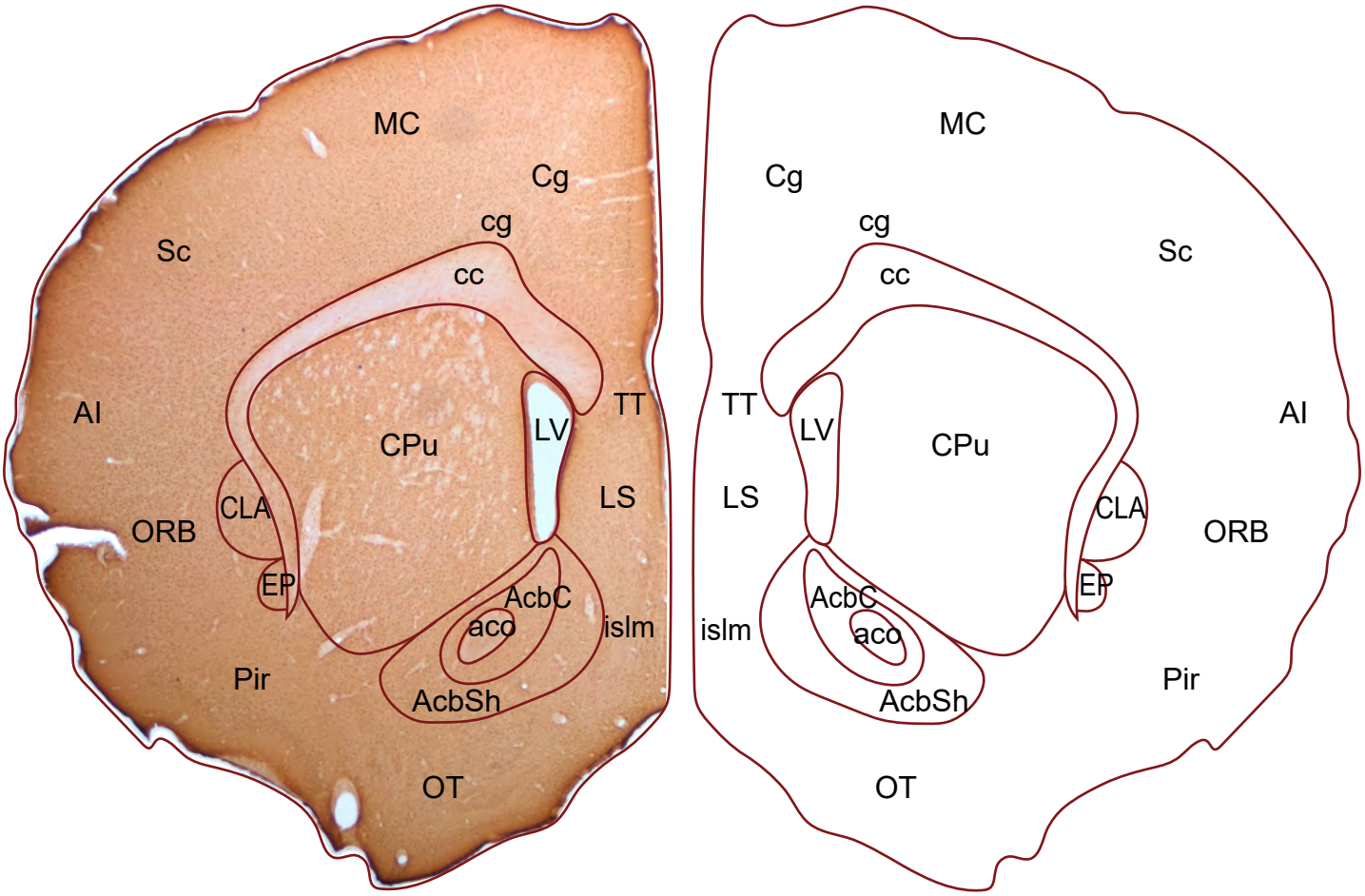

Set 12: Nissl oc -1000µm

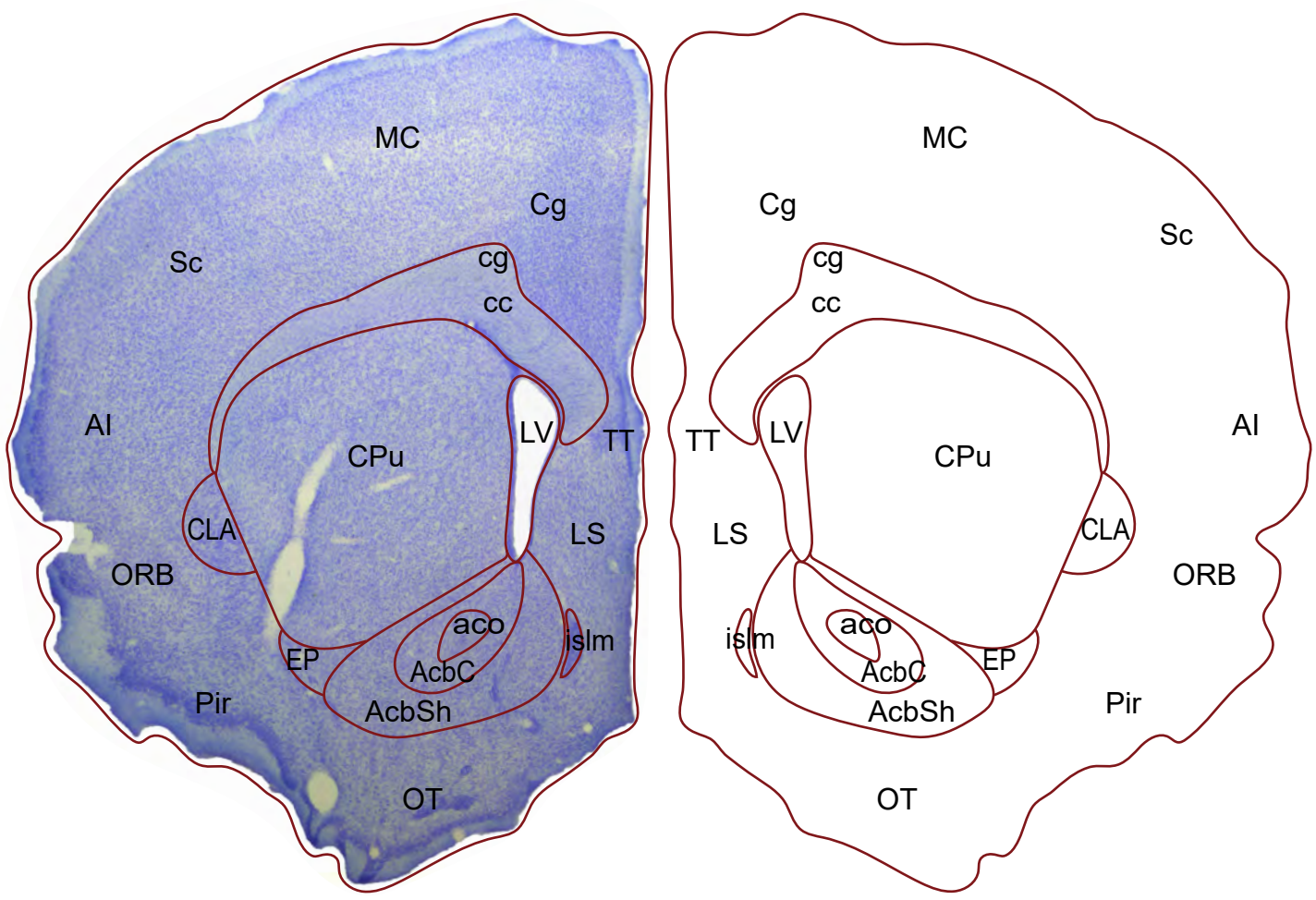

Set 12: OXT oc -950µm

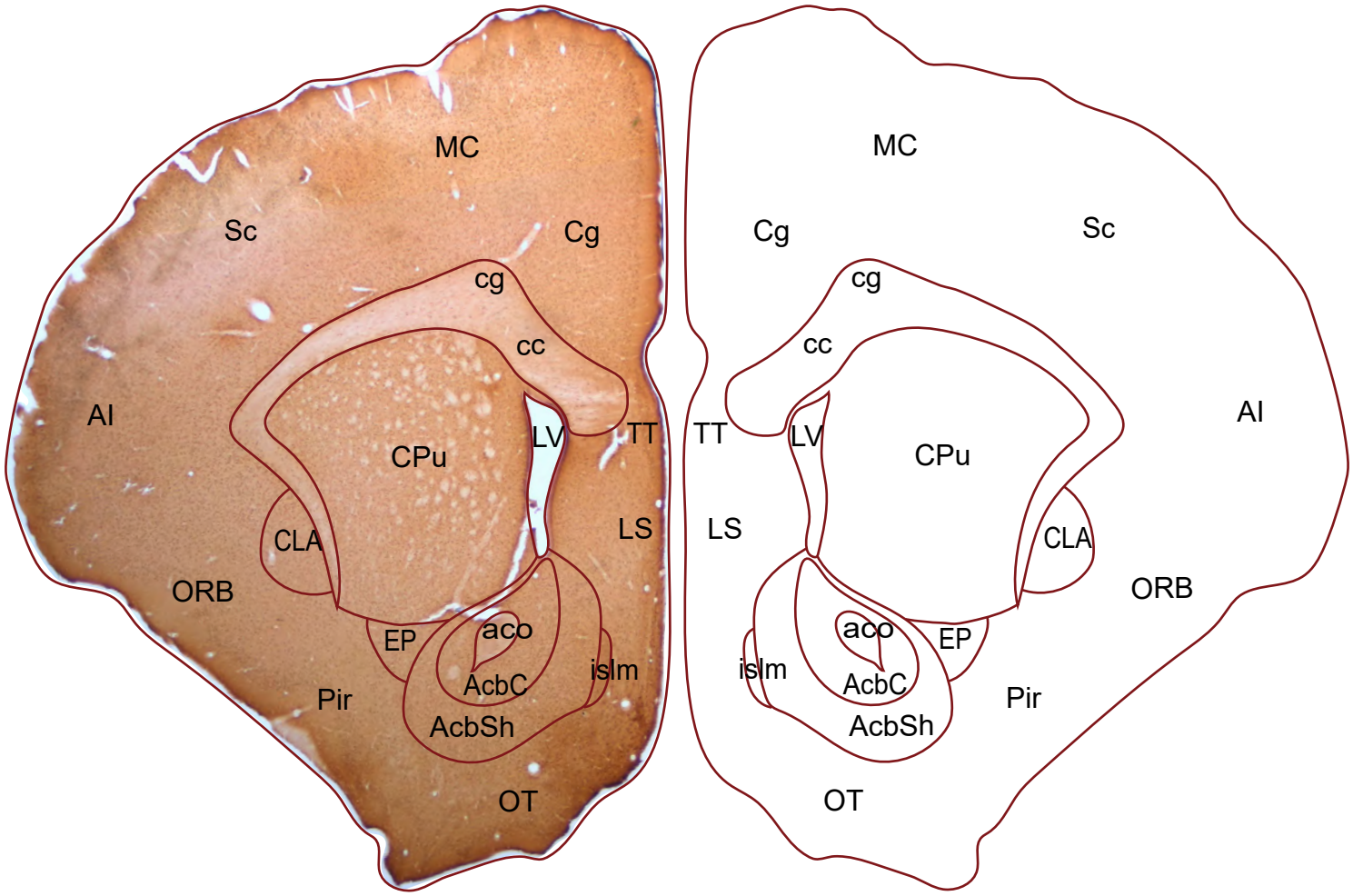

Set 12: Myelin oc -900µm

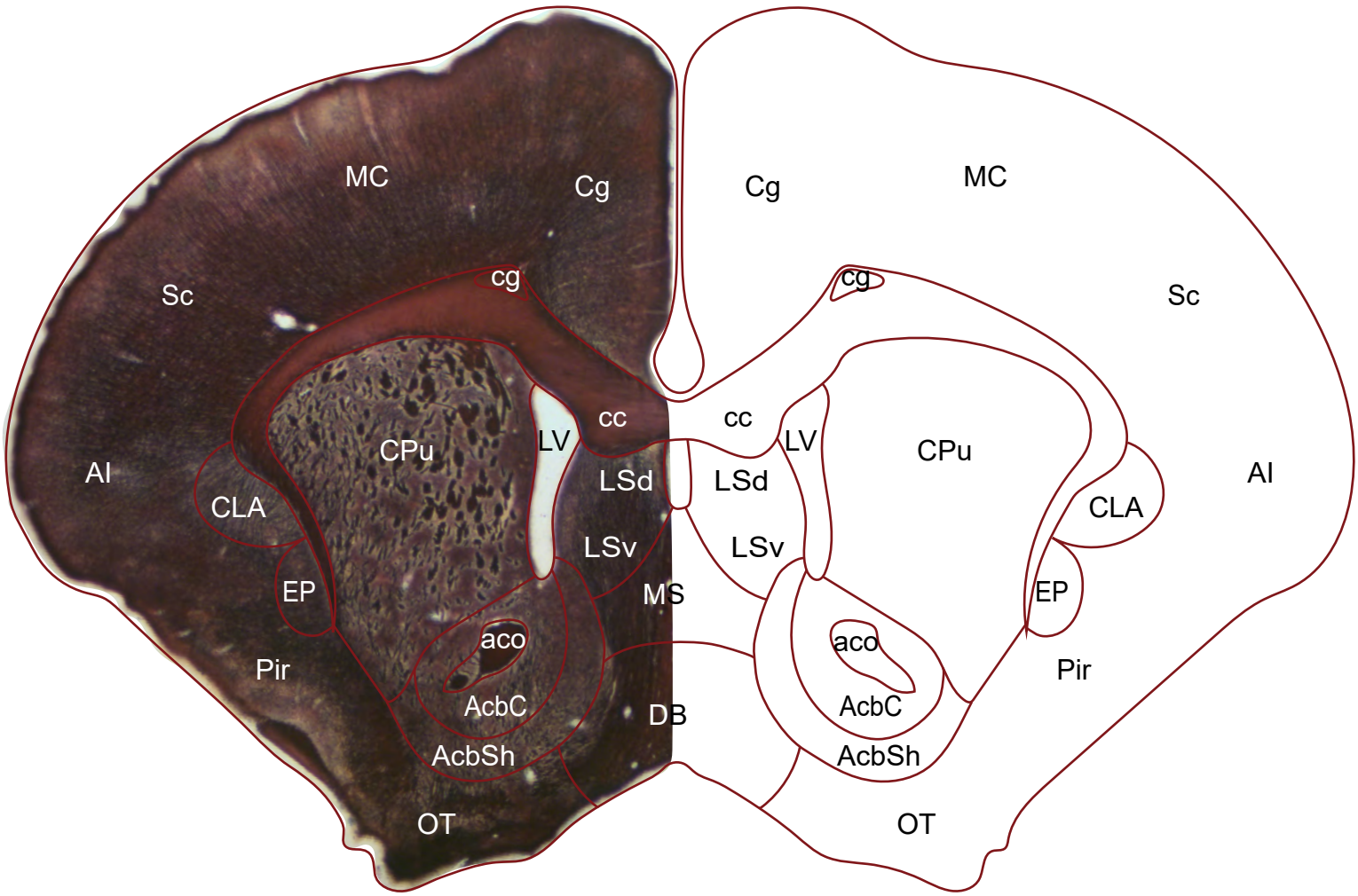

Set 13: OXT oc -850µm

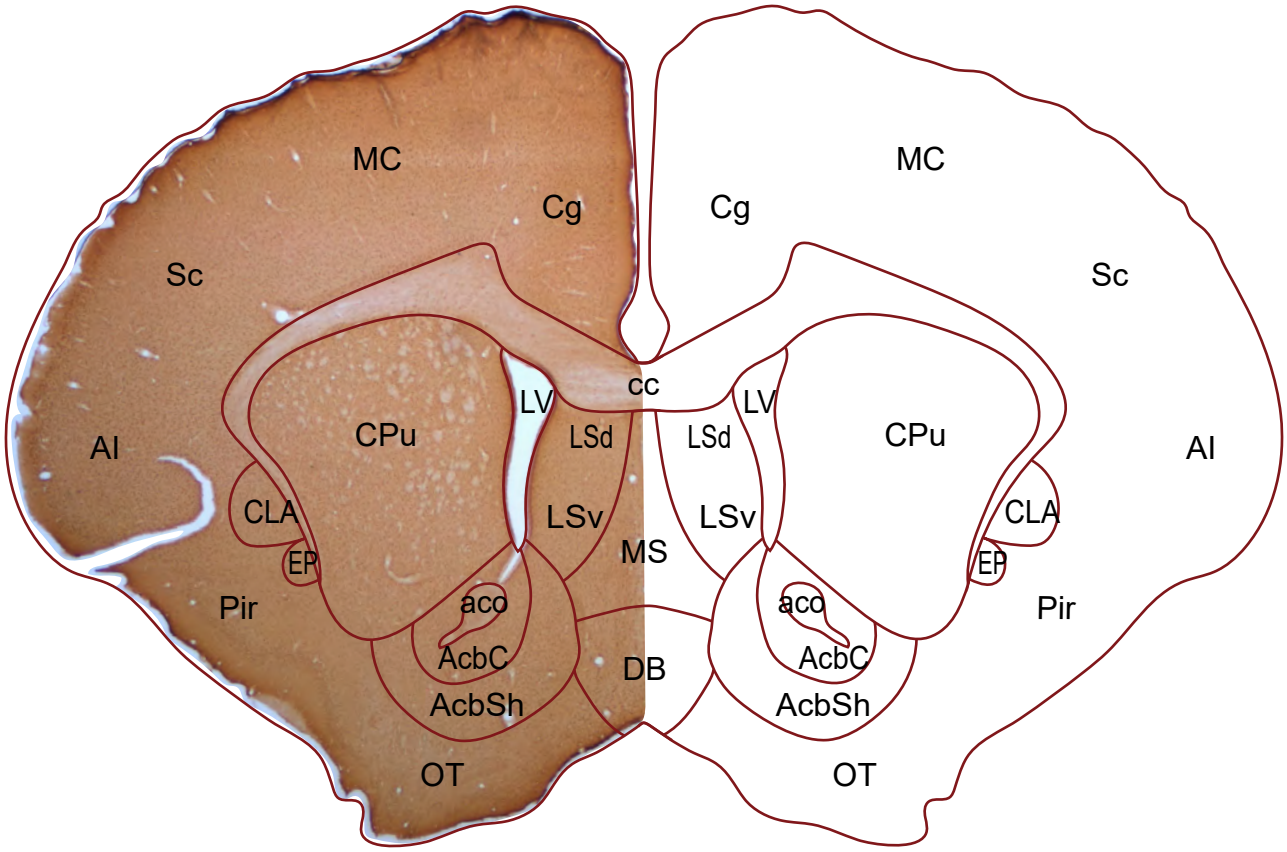

Set 13: Nissl oc -800µm

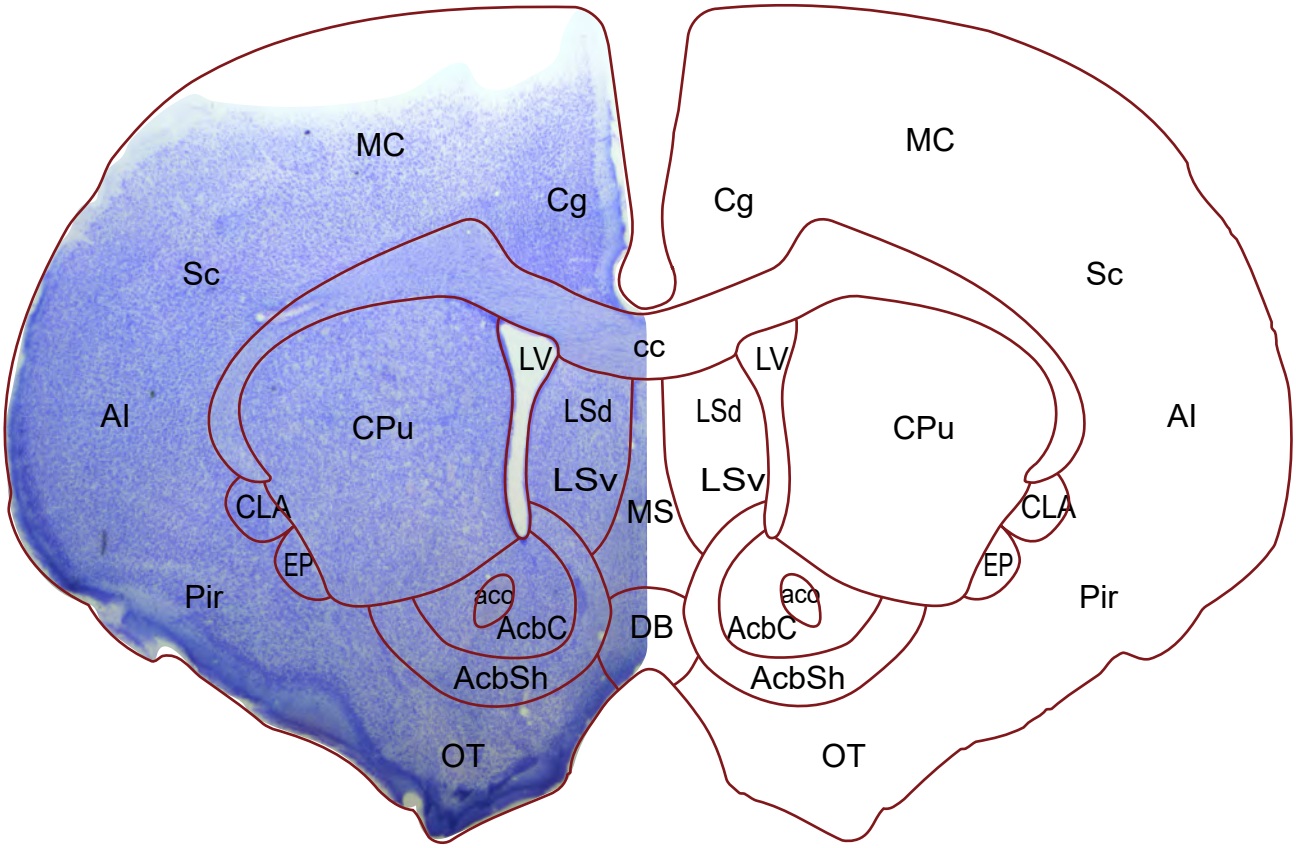

Set 13: OXT oc -750µm

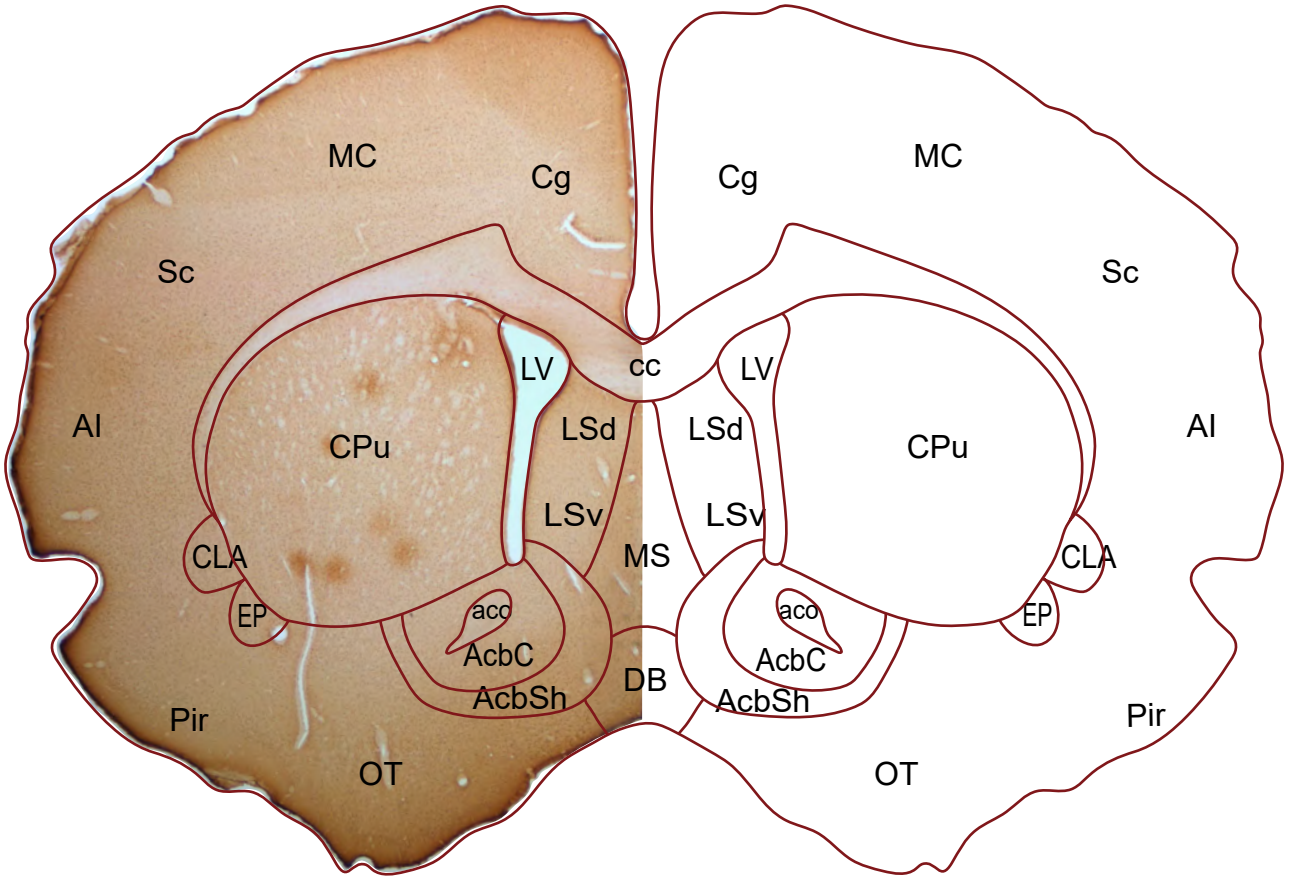

Set 13: Myelin oc -700µm

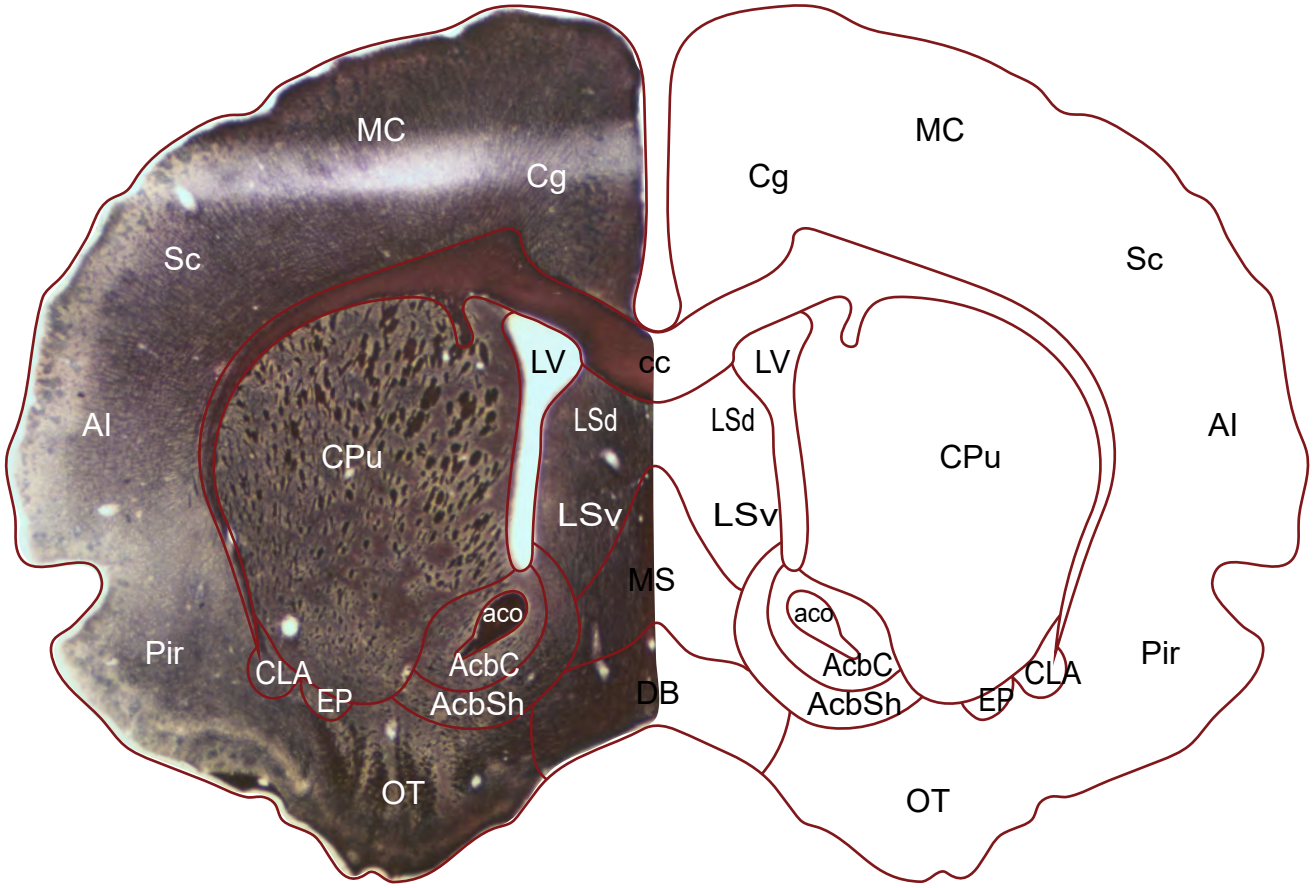

Set 14: OXT oc -650µm

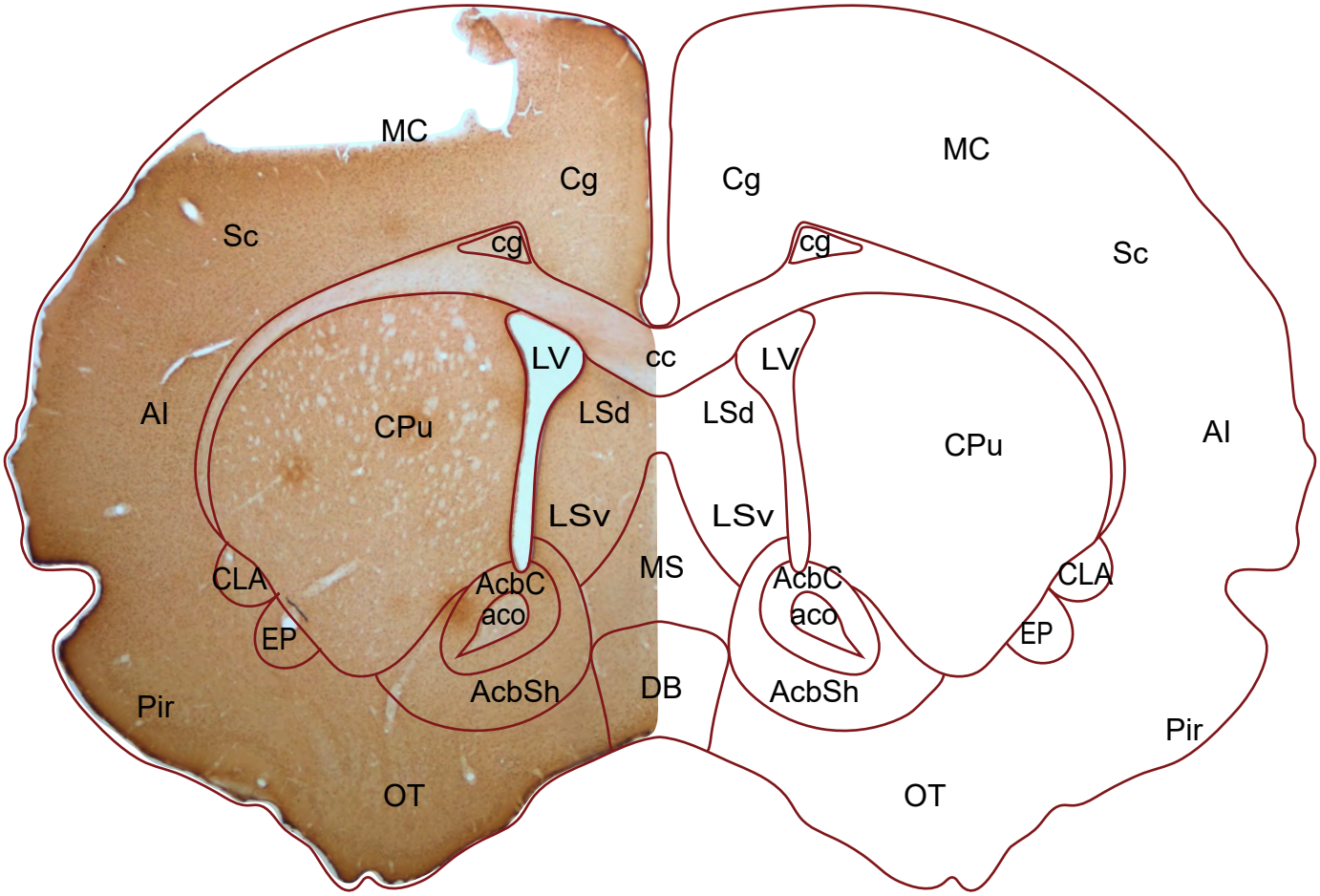

Set 14: Nissl oc -600µm

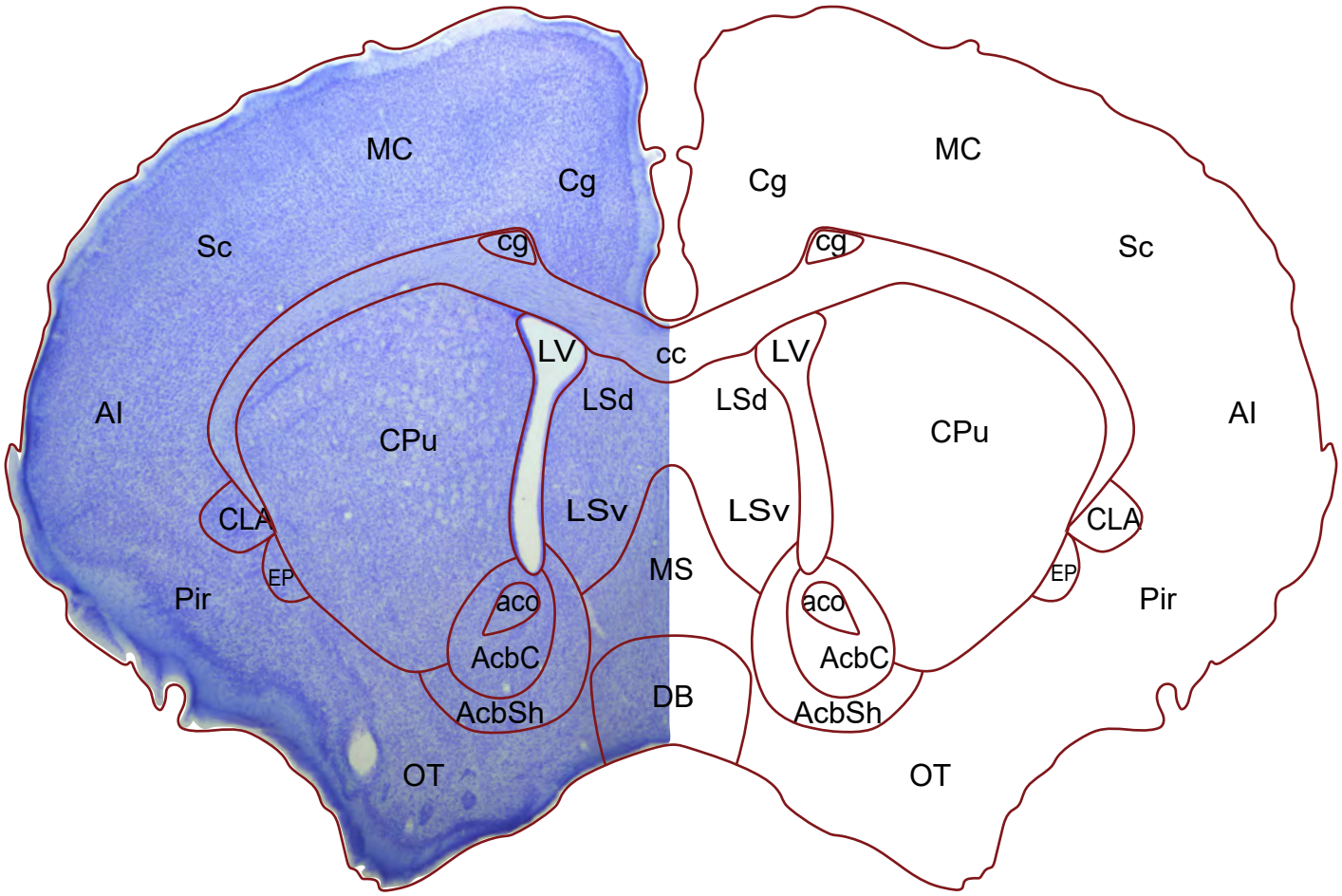

Set 14: OXT oc -550µm

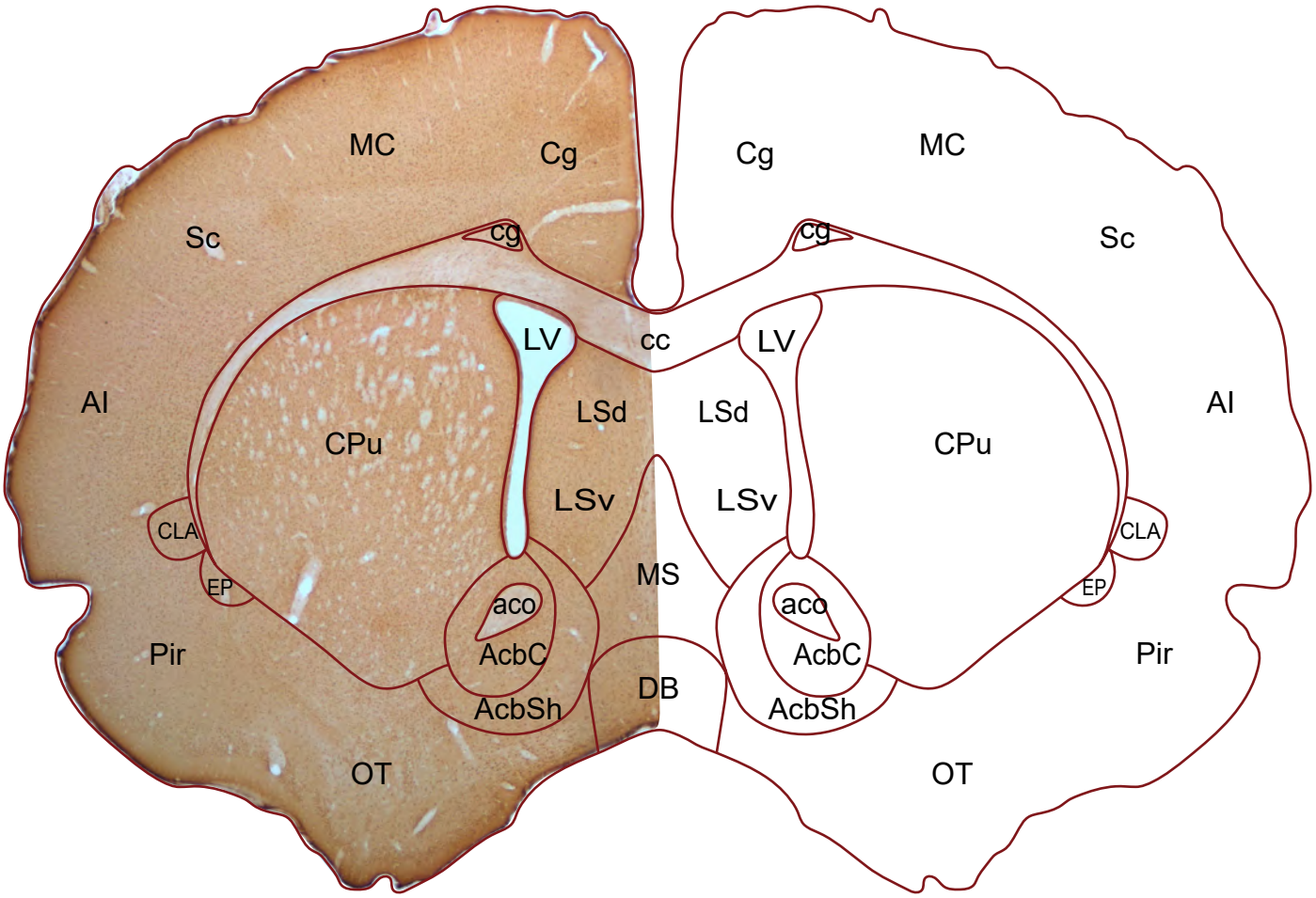

Set 14: Myelin oc -500µm

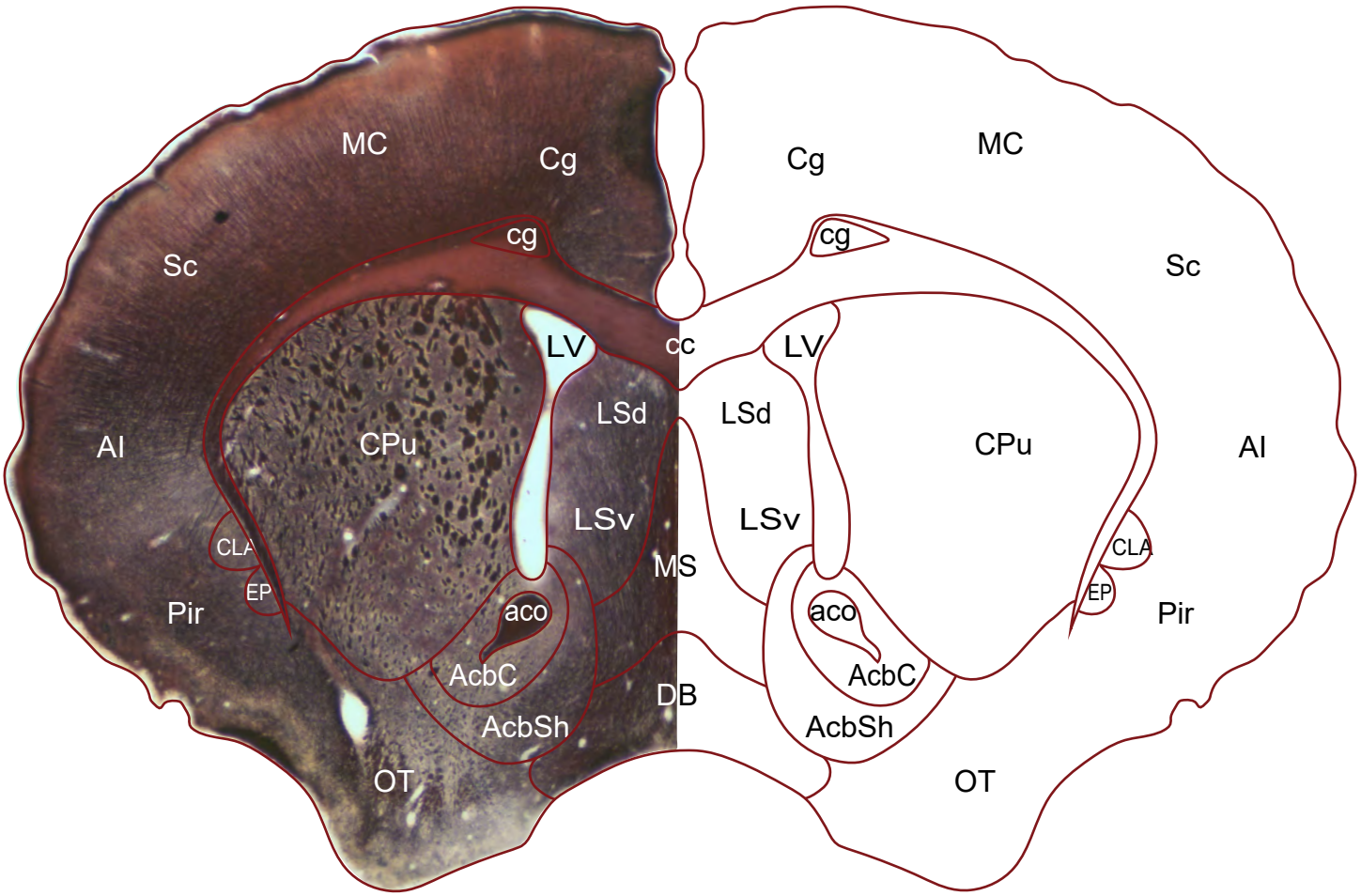

Set 15: OXT oc -450µm

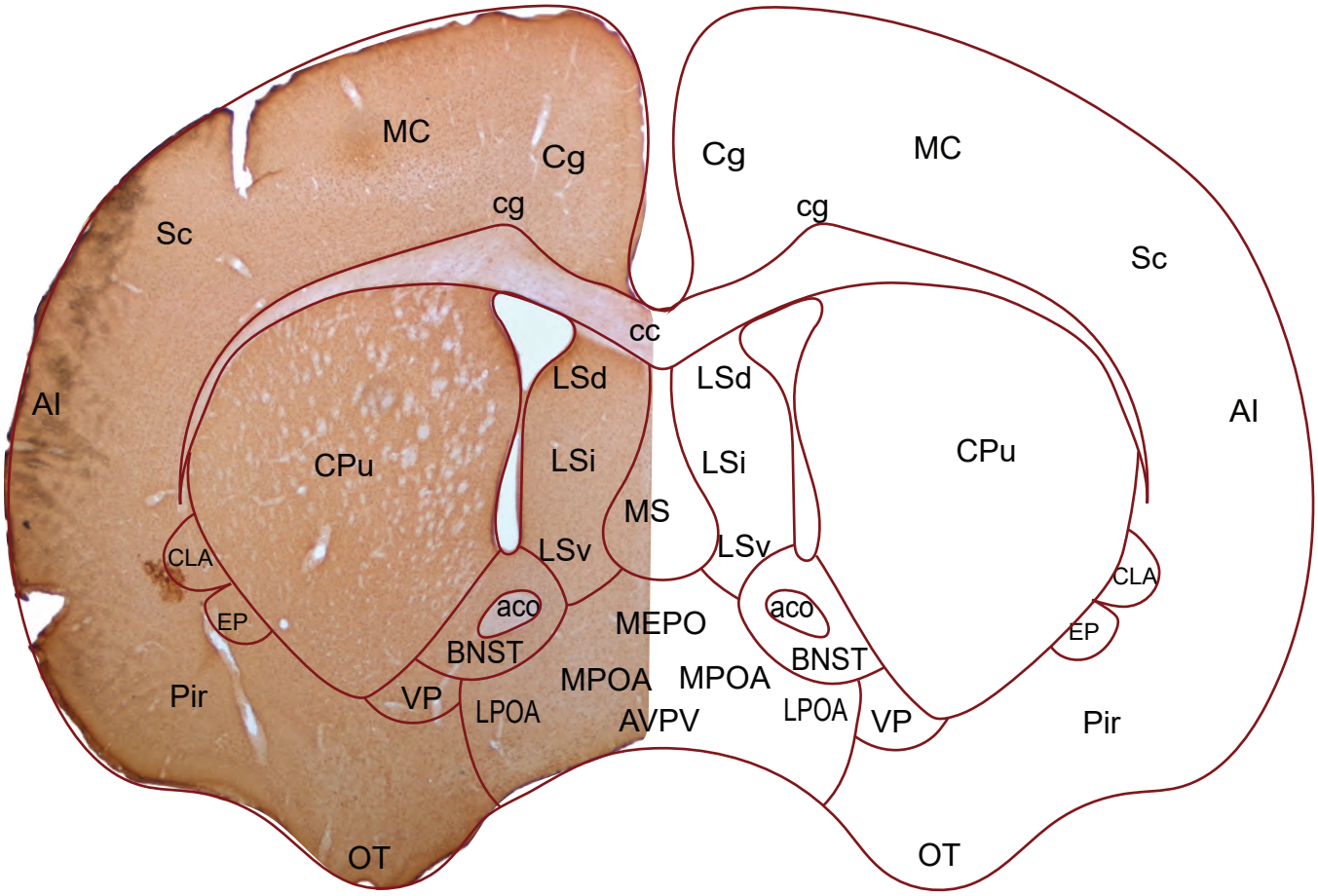

Set 15: Nissl oc -400µm

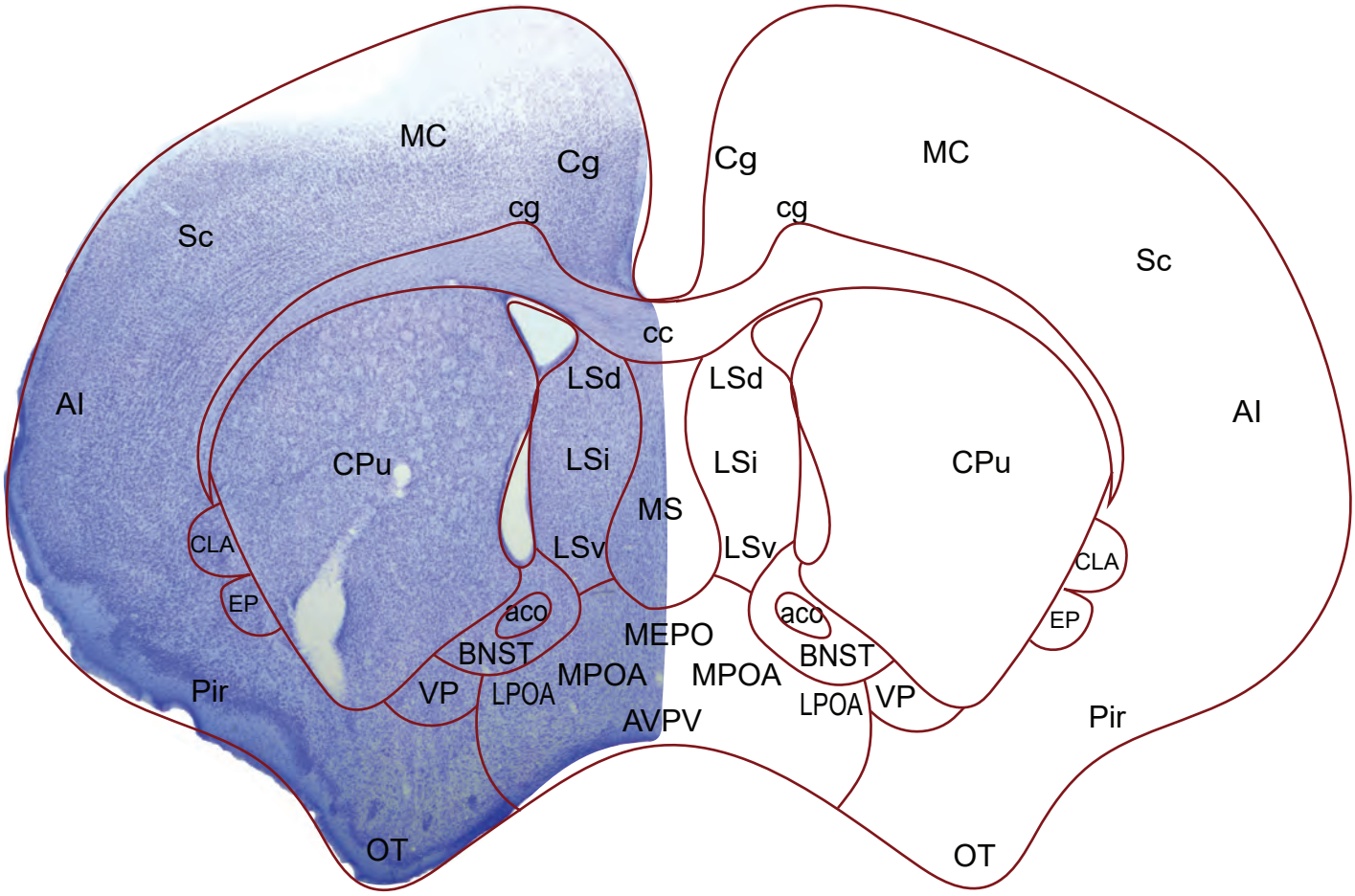

Set 15: OXT oc -350µm

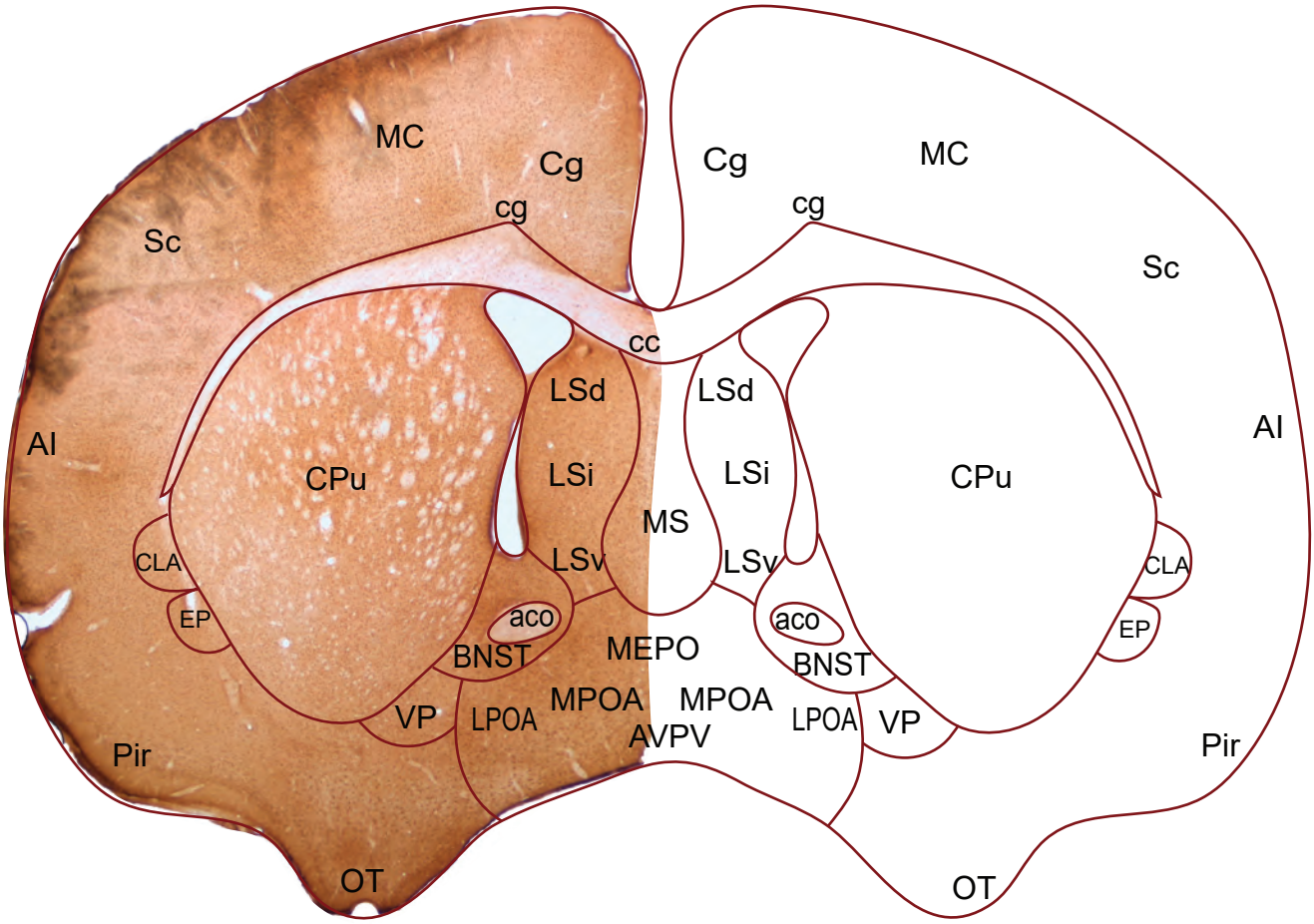

Set 15: Myelin oc -300µm

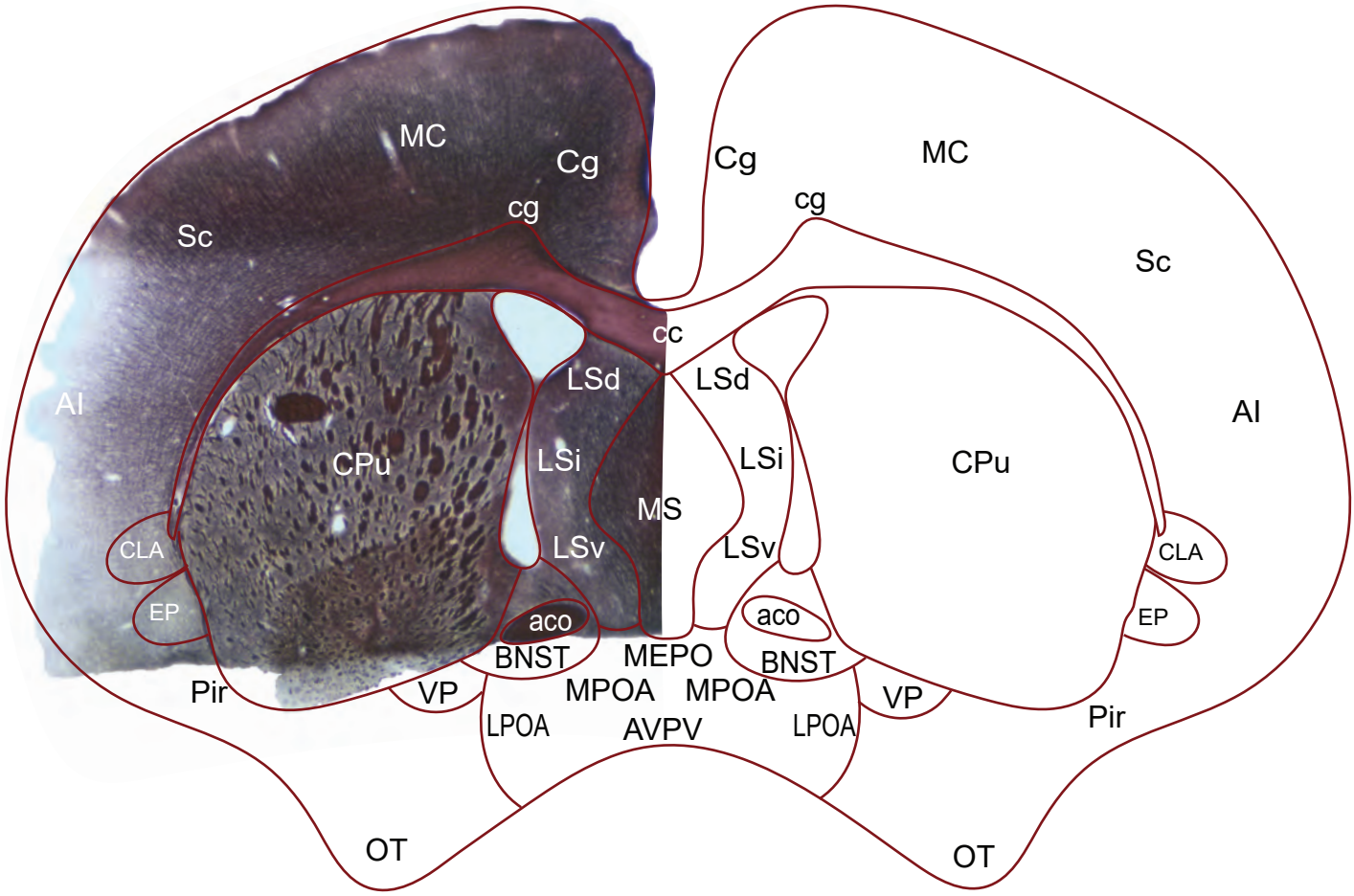

Set 16: OXT oc -250µm

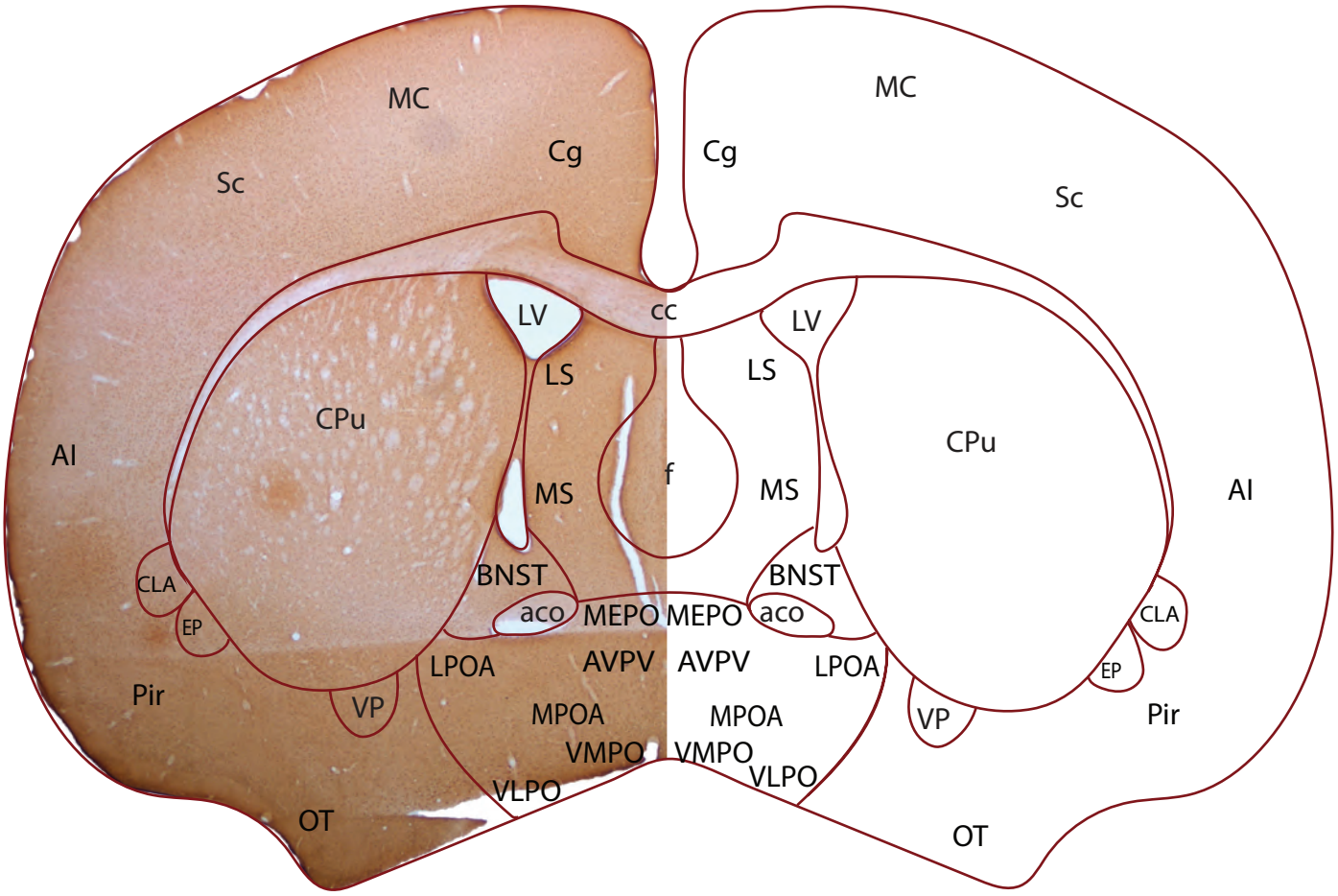

Set 16: Nissl oc -200µm

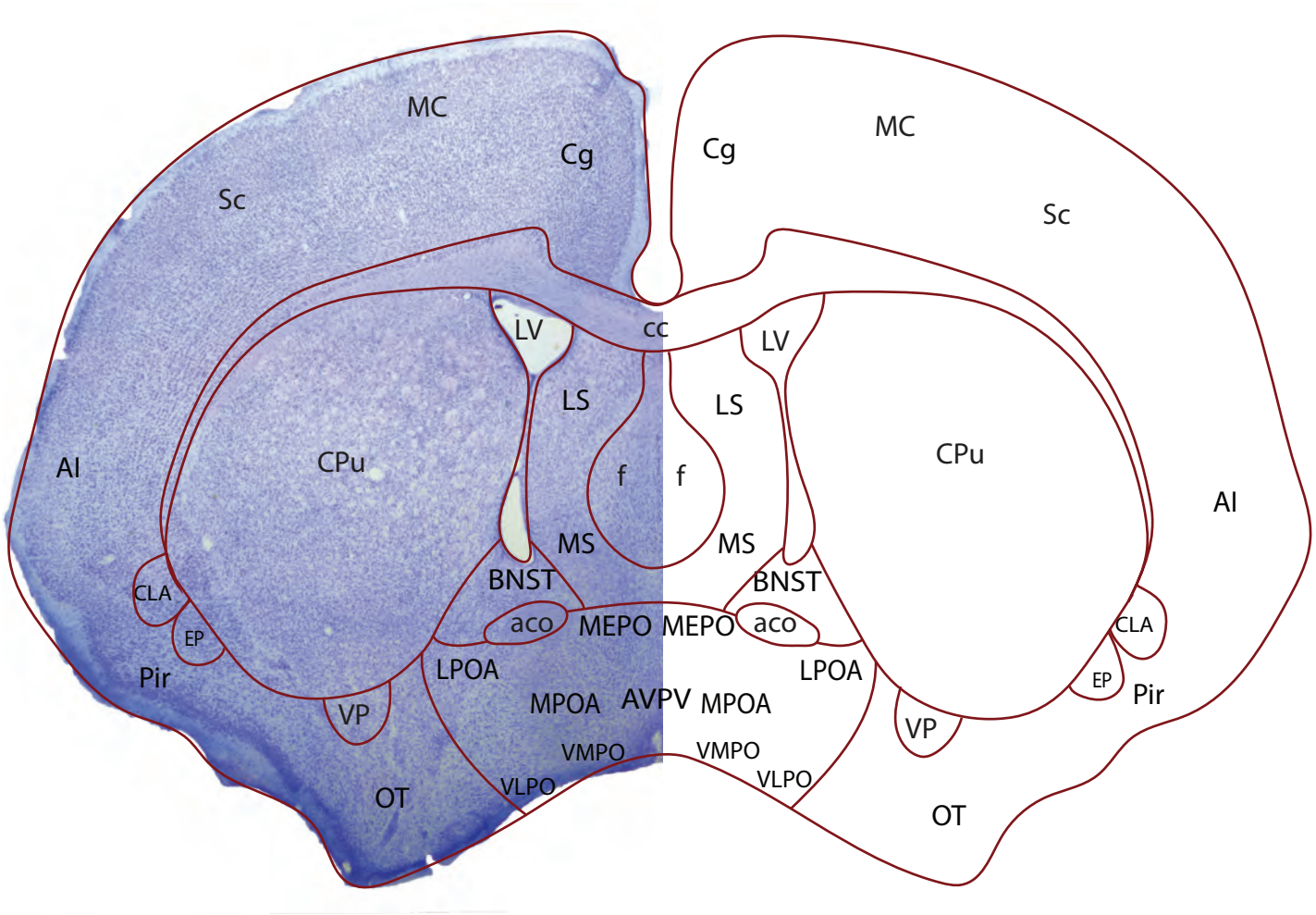

Set 16: OXT oc -150µm

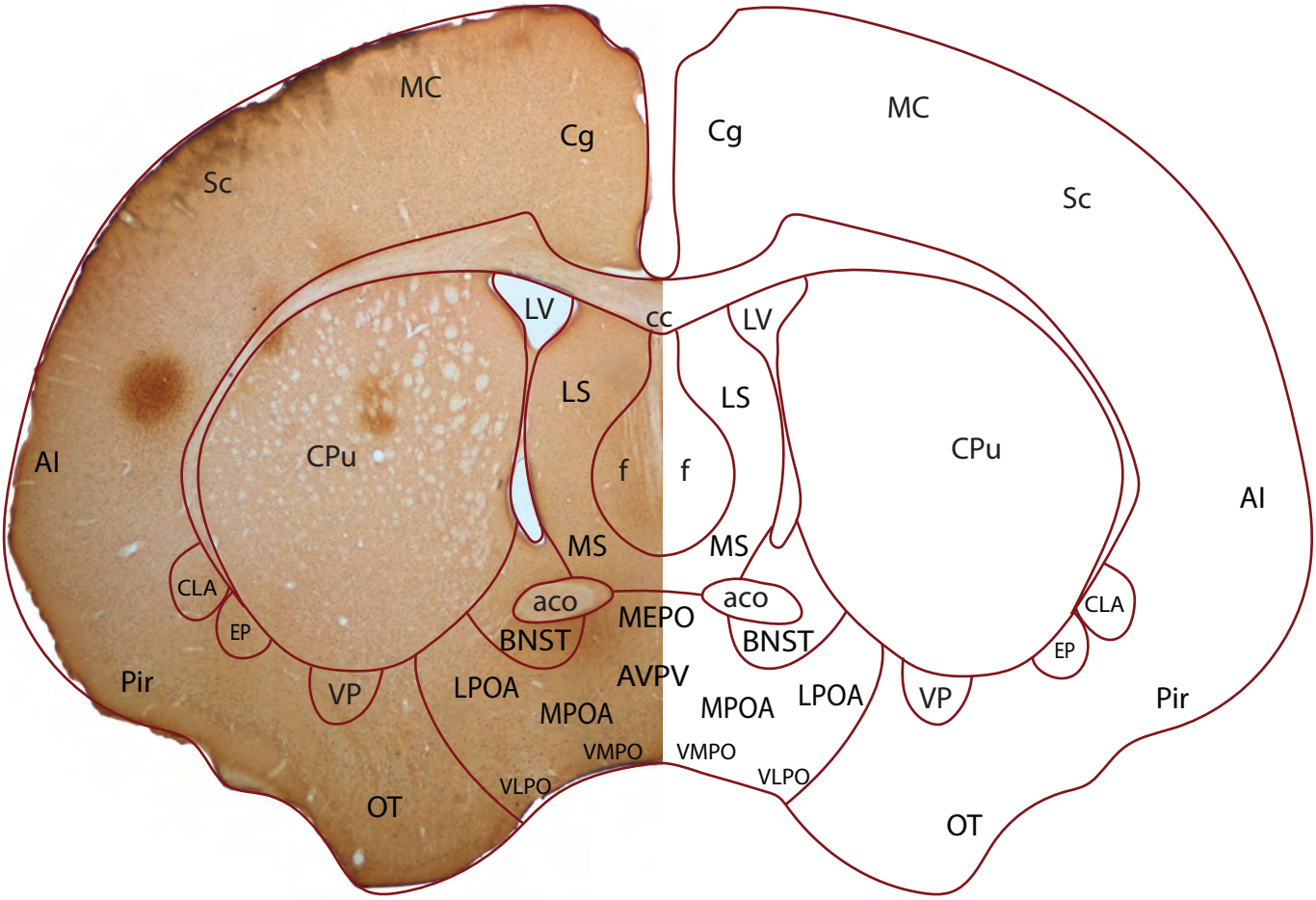

Figure 16: Myelin oc -100µm

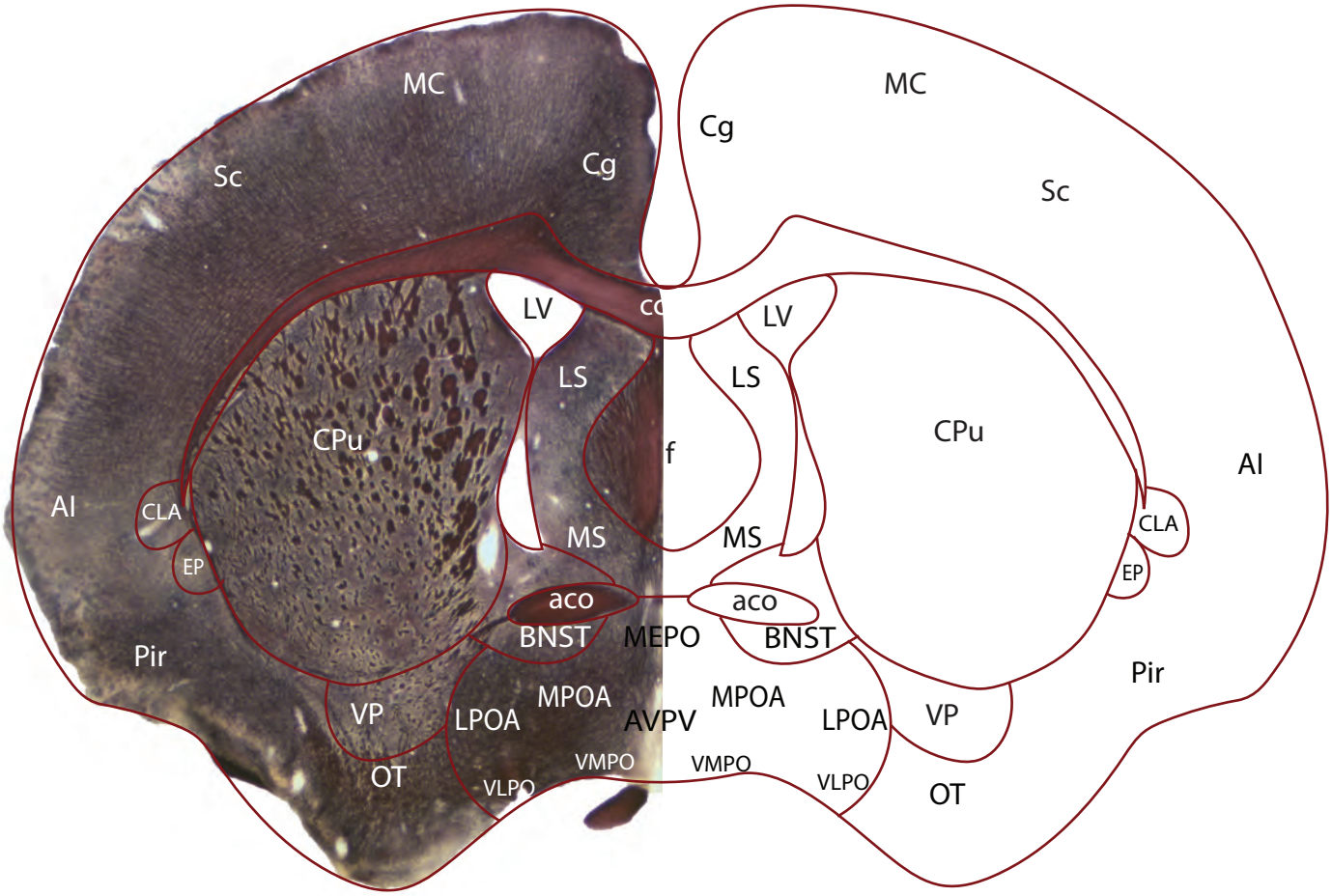

Set 17: OXT oc -50µm

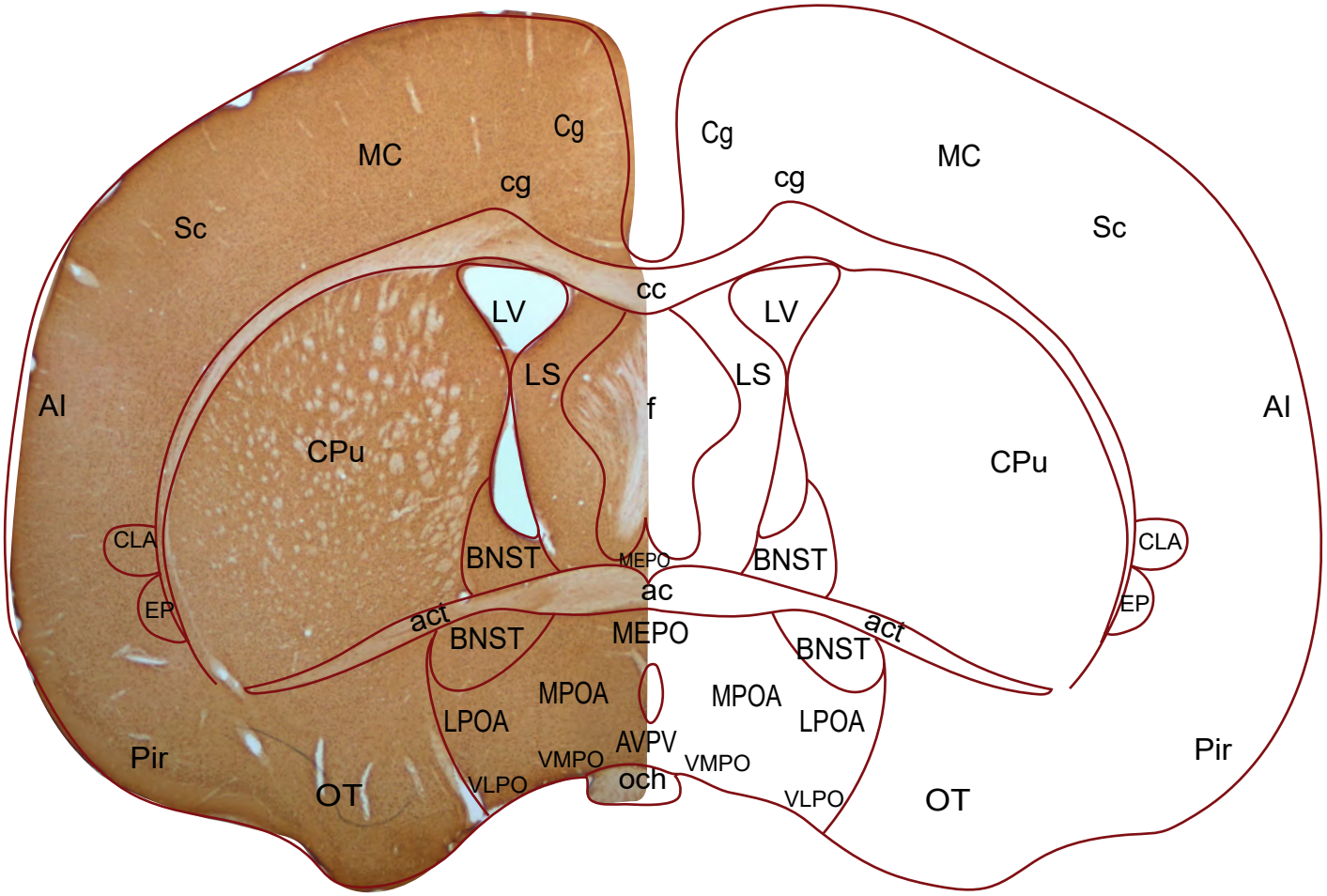

Set 17: Nissl oc 0µm

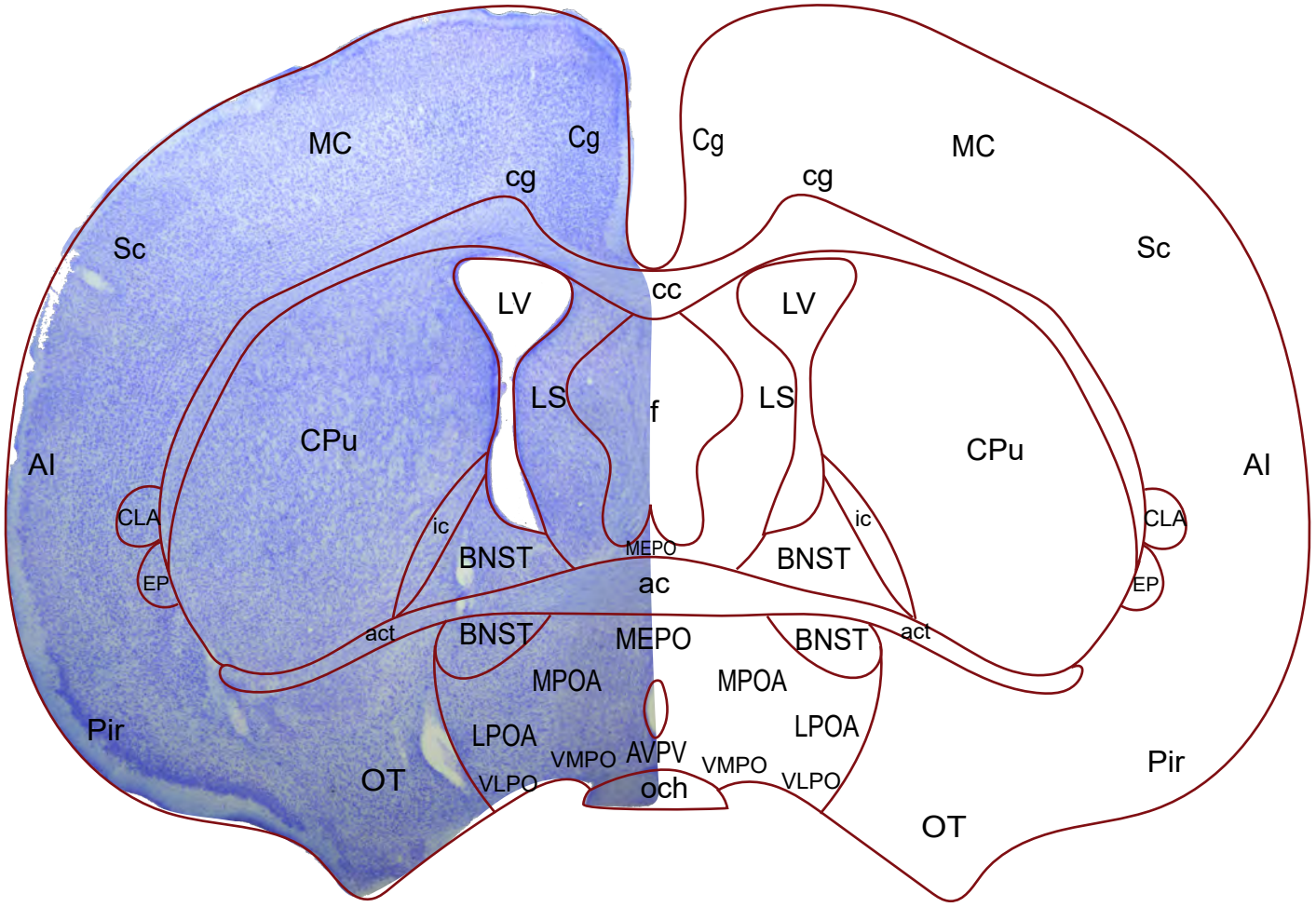

Set 17: OXT oc +50µm

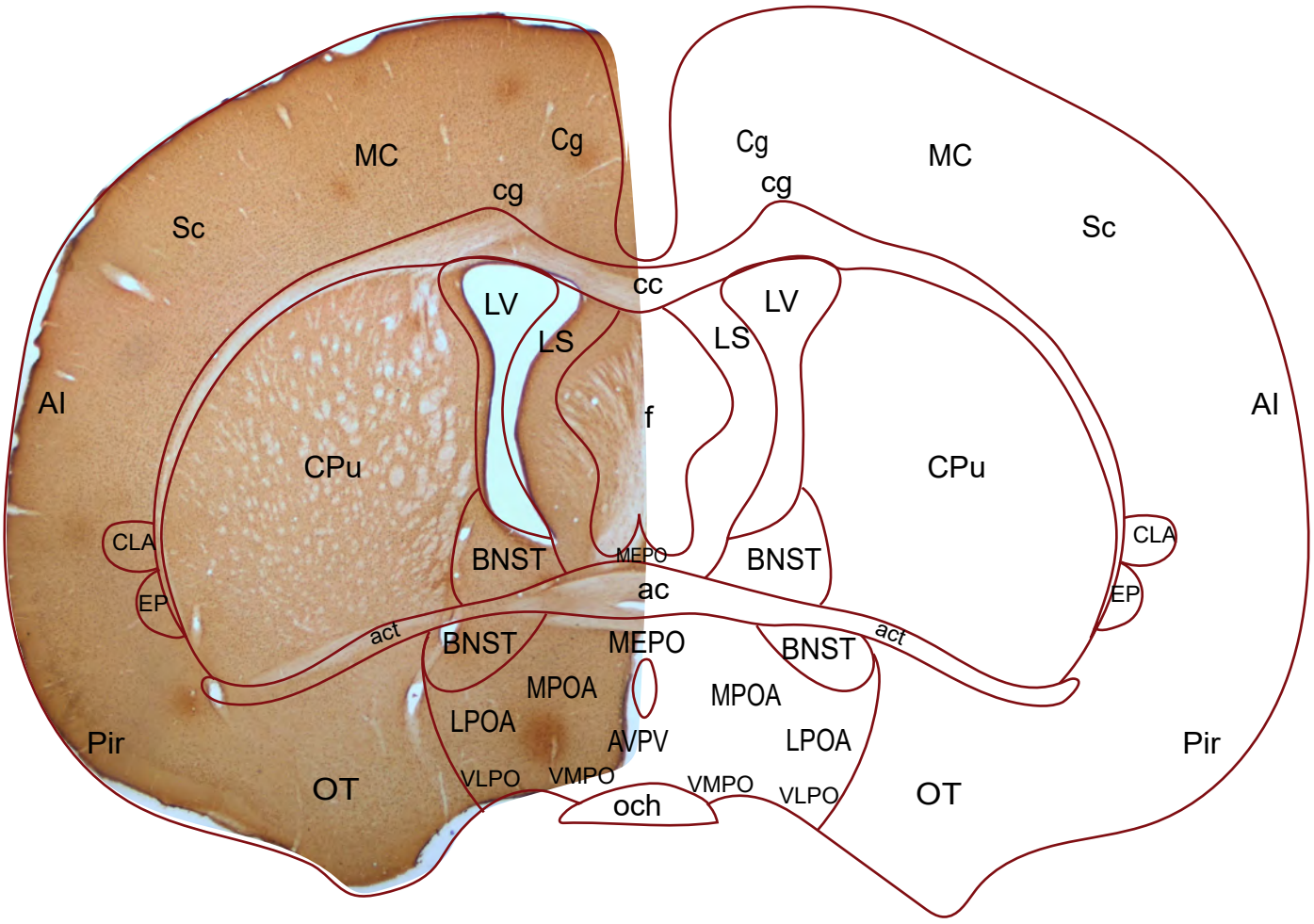

Set 17: Myelin oc +100µm

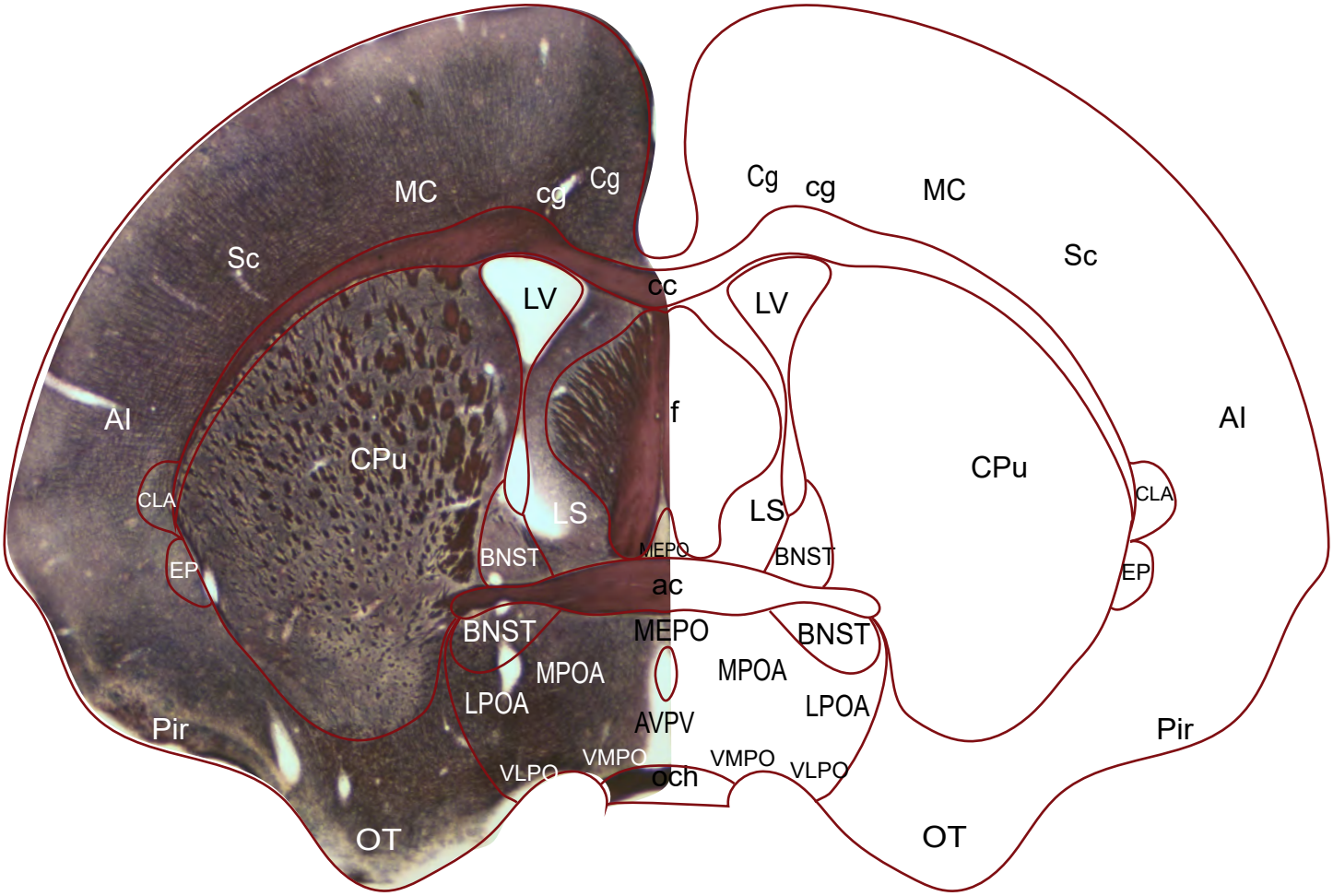

Set 18: OXT oc +150µm

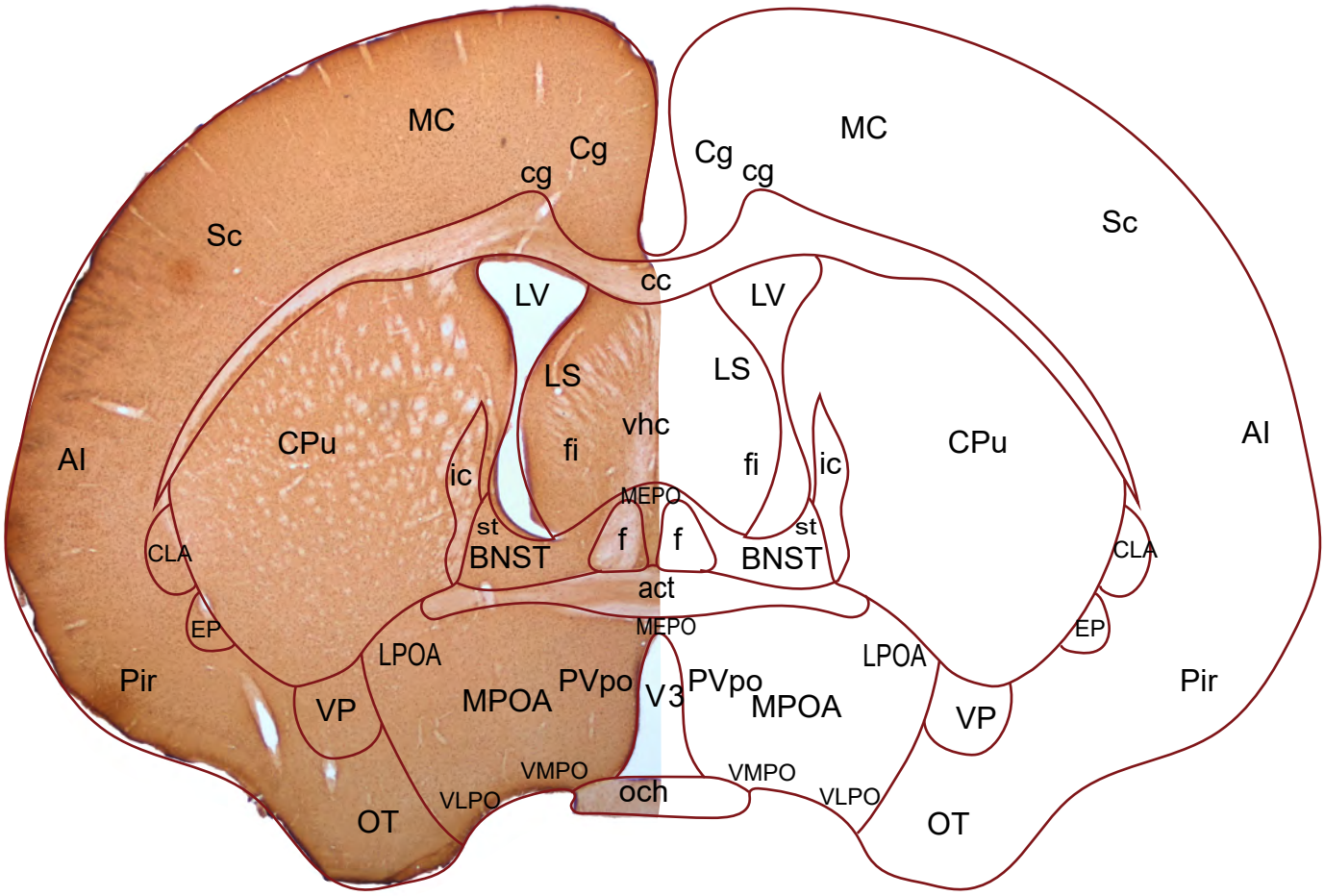

Set 18: Nissl oc +200µm

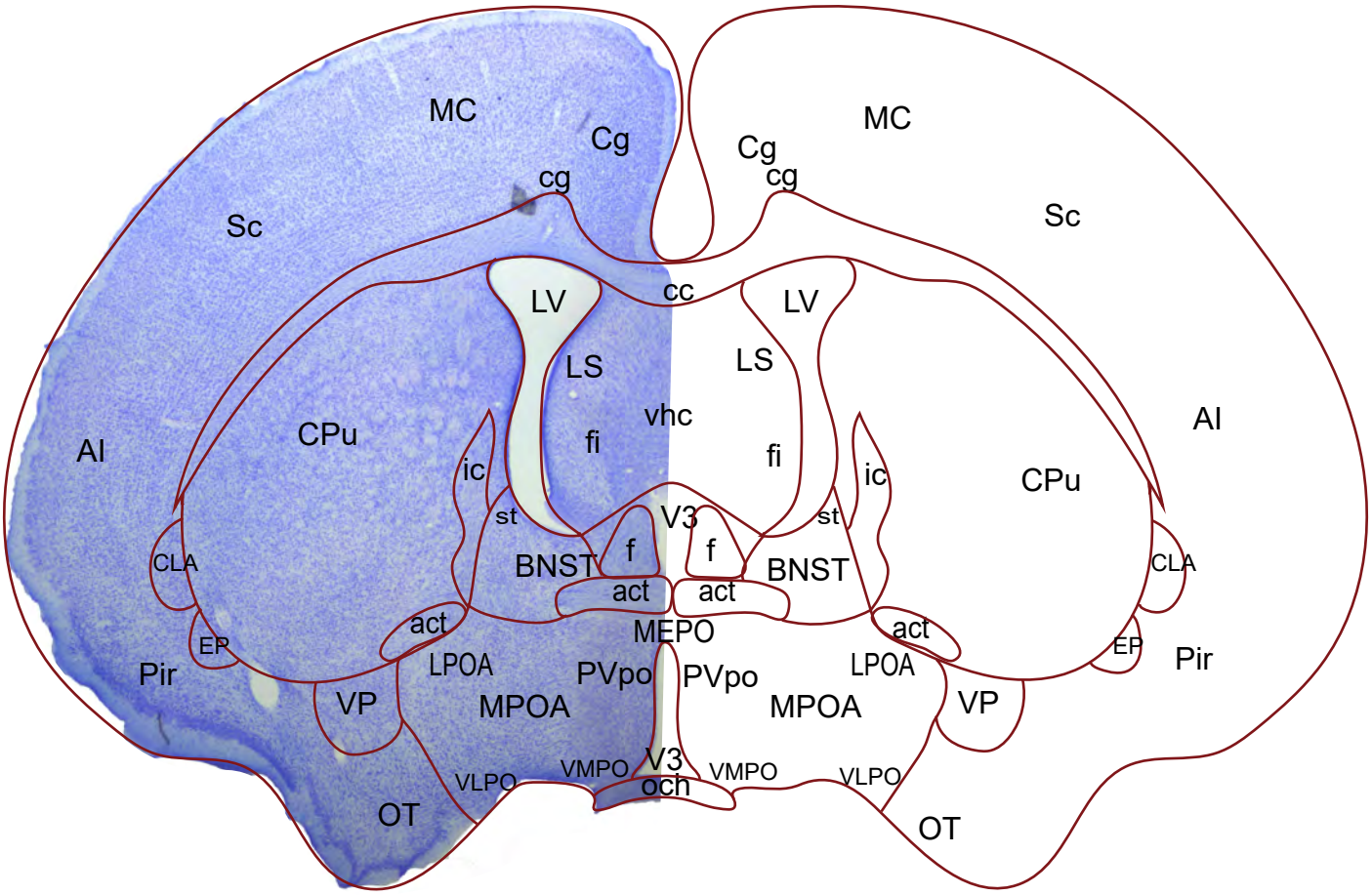

Set 18: OXT oc +250µm

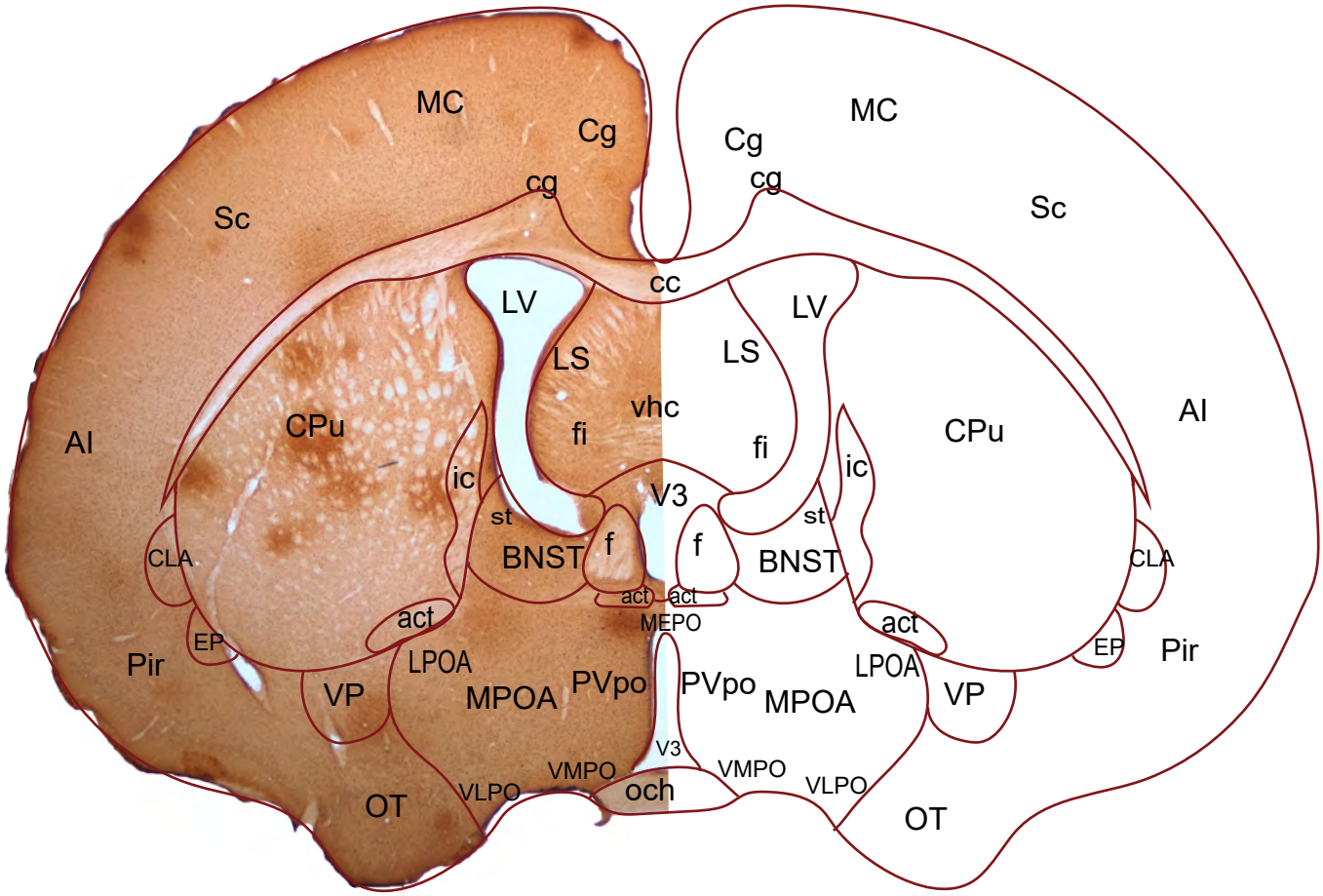

Set 18: Myelin oc +300µm

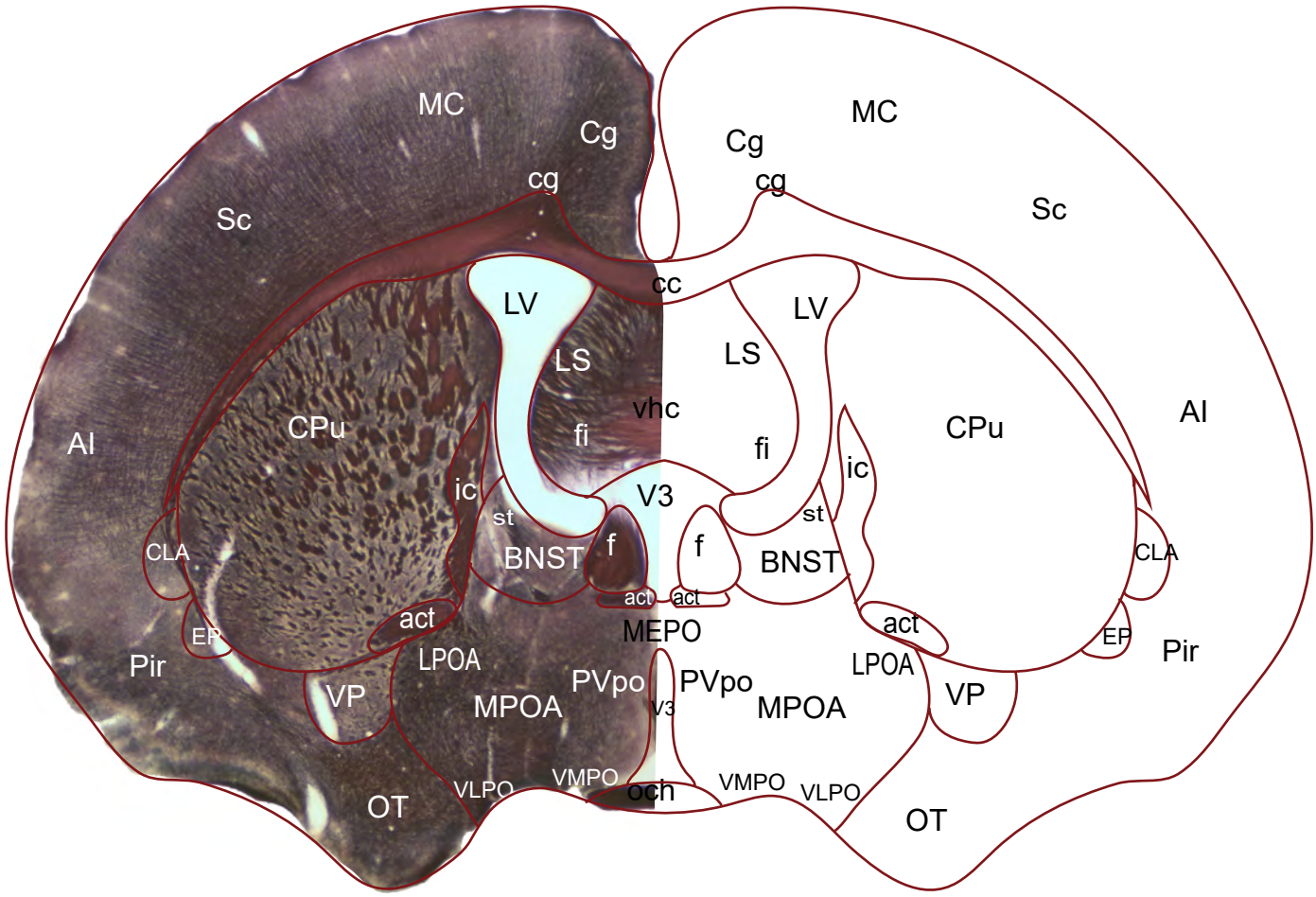

Set 19: OXT oc +350µm

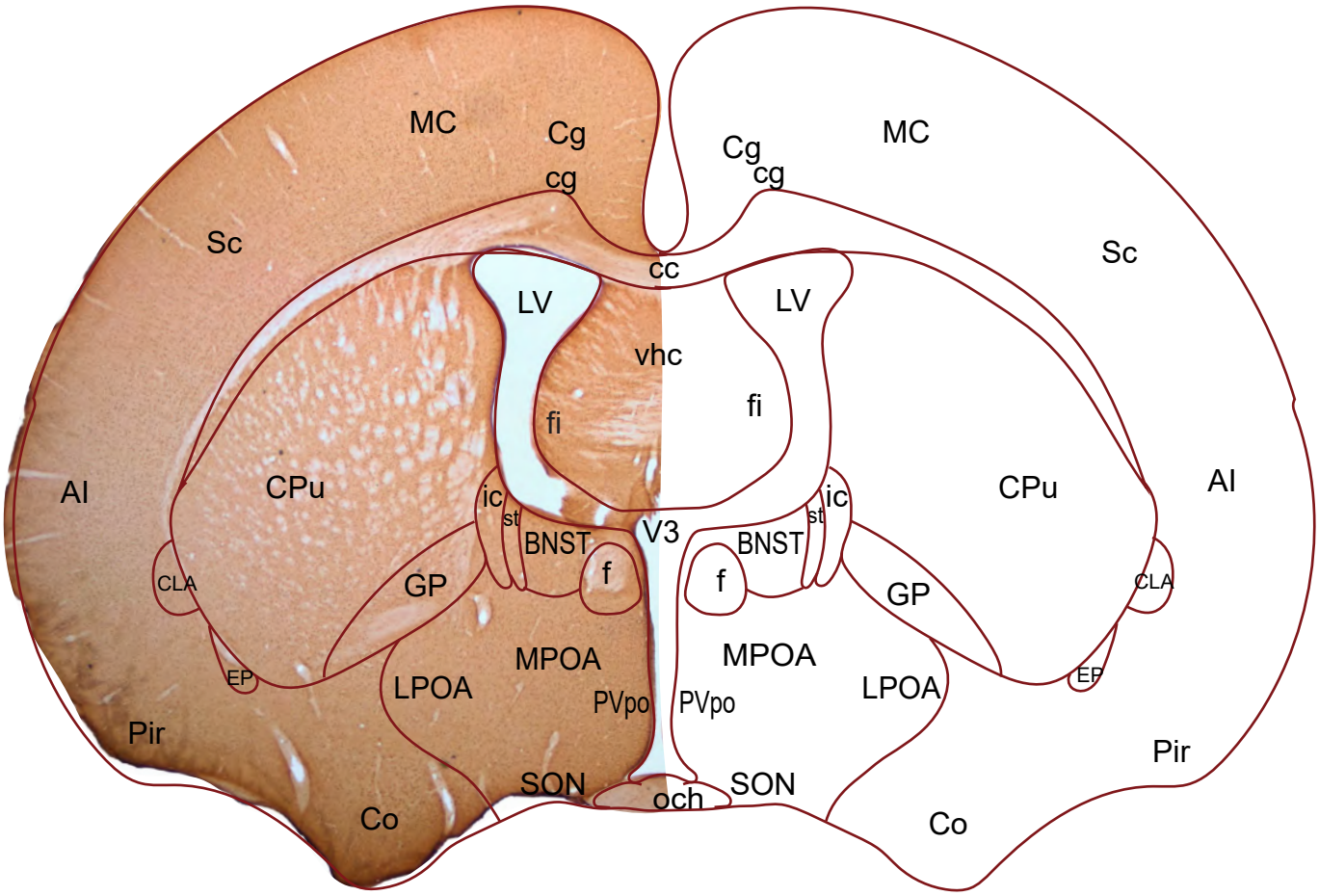

Set 19: Nissl oc +400µm

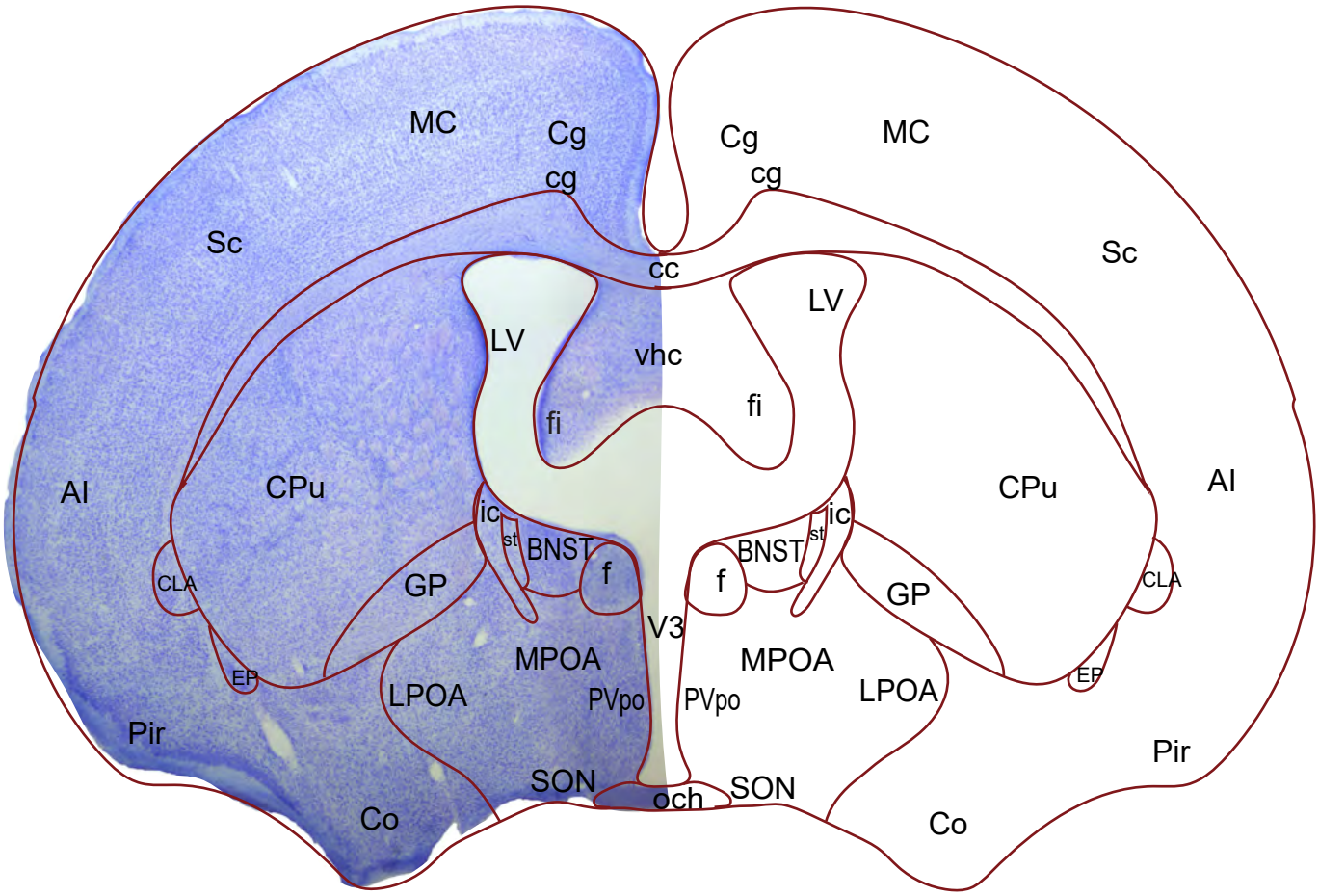

Set 19: OXT oc +450µm

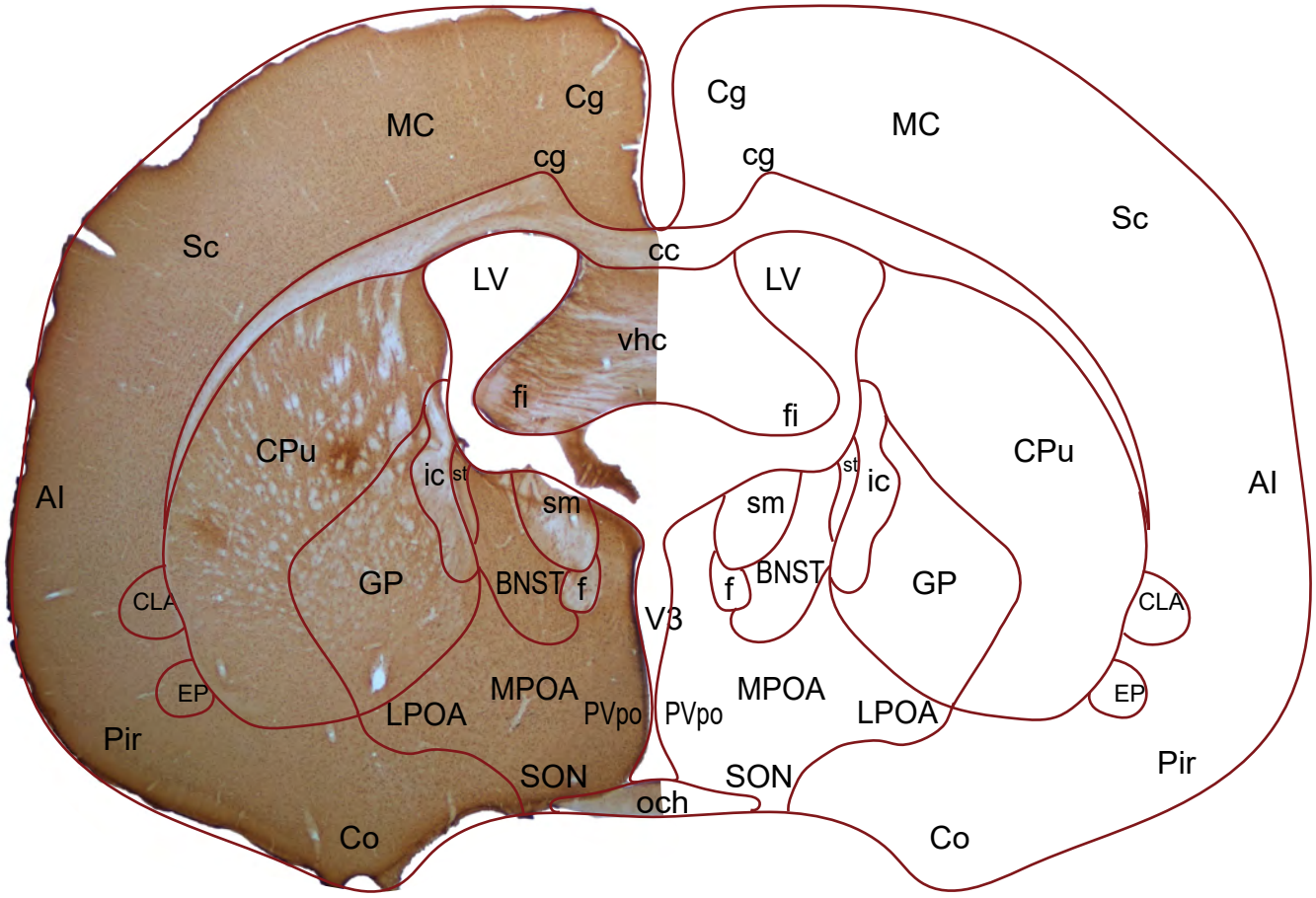

Set 19: Myelin oc +500µm

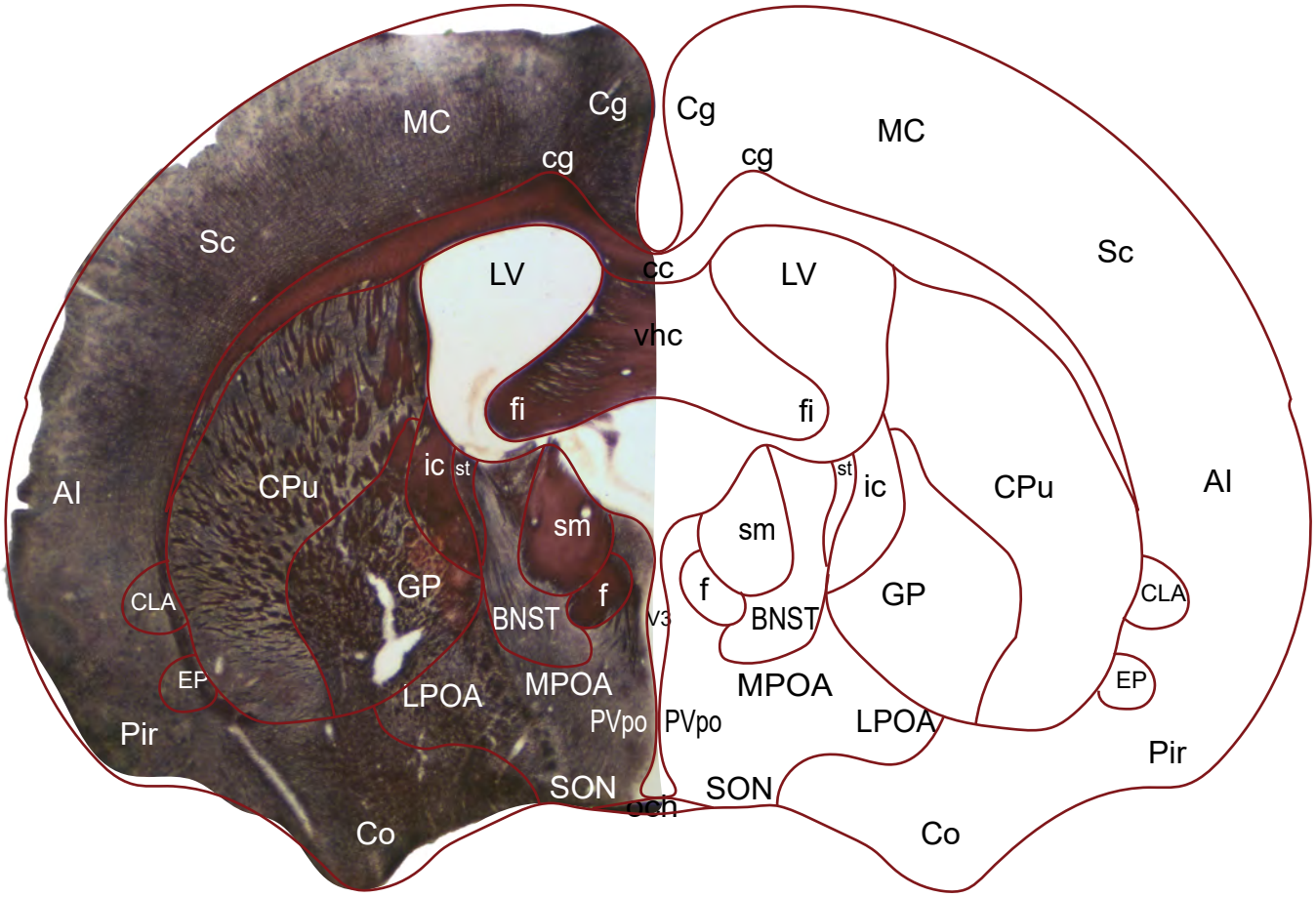

Set 20: OXT oc +550µm

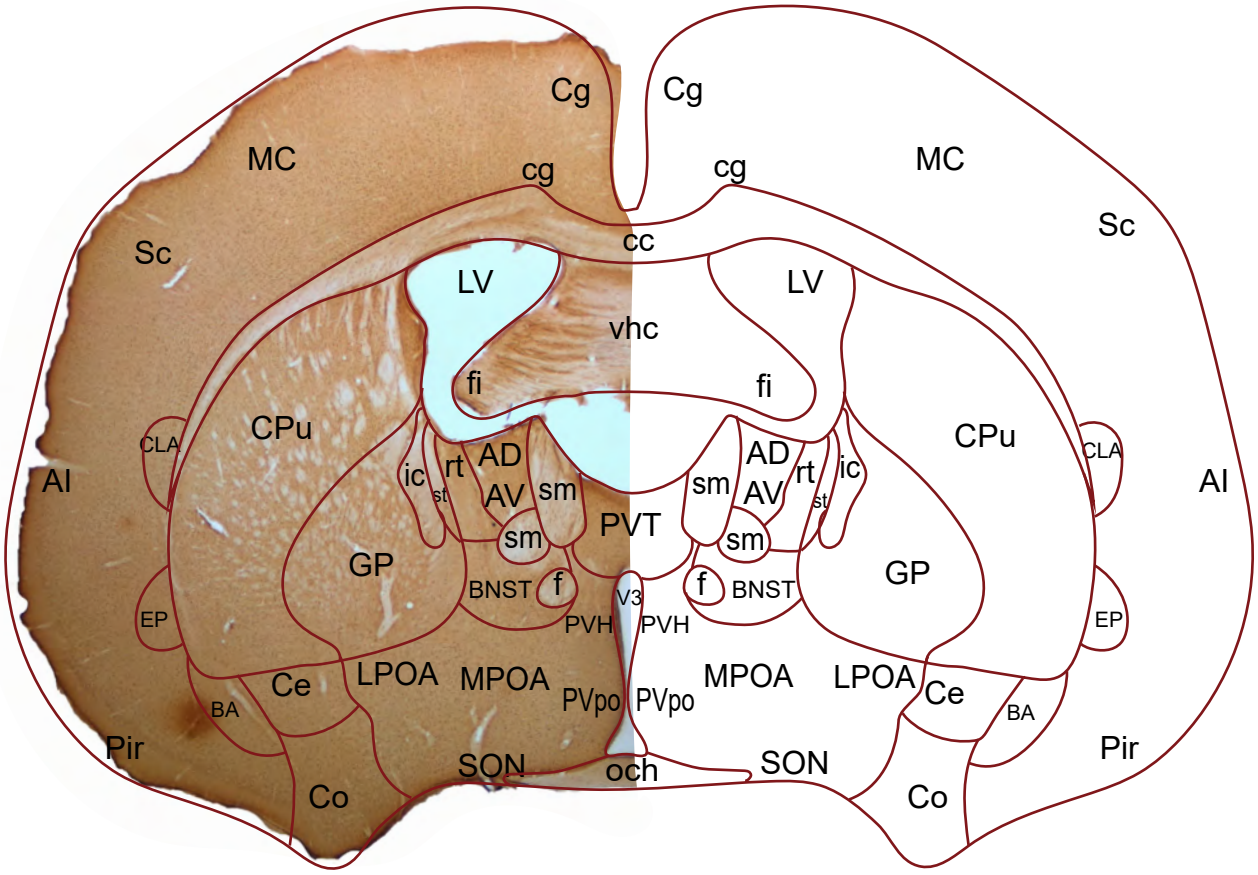

Set 20: Nissl oc +600µm

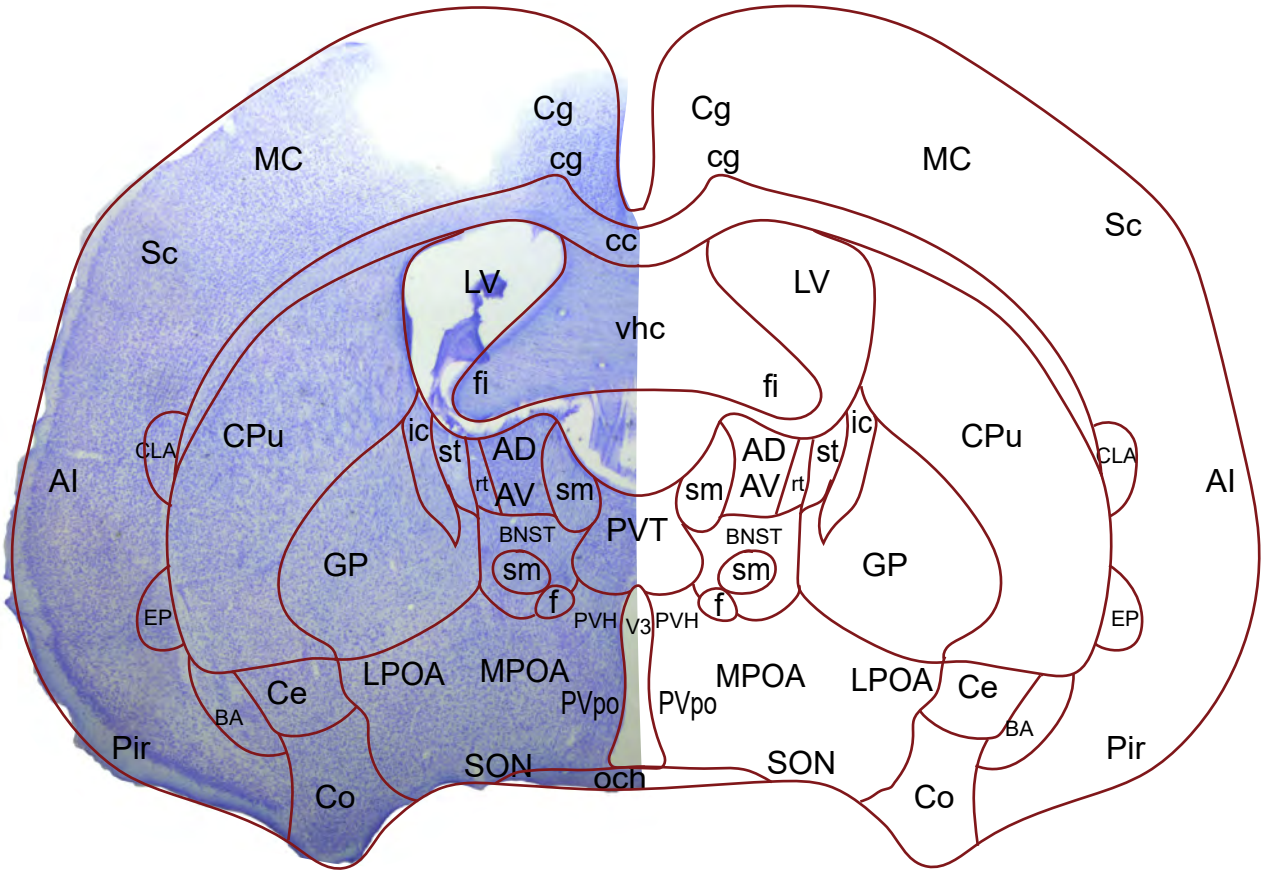

Set 20: OXT oc +650µm

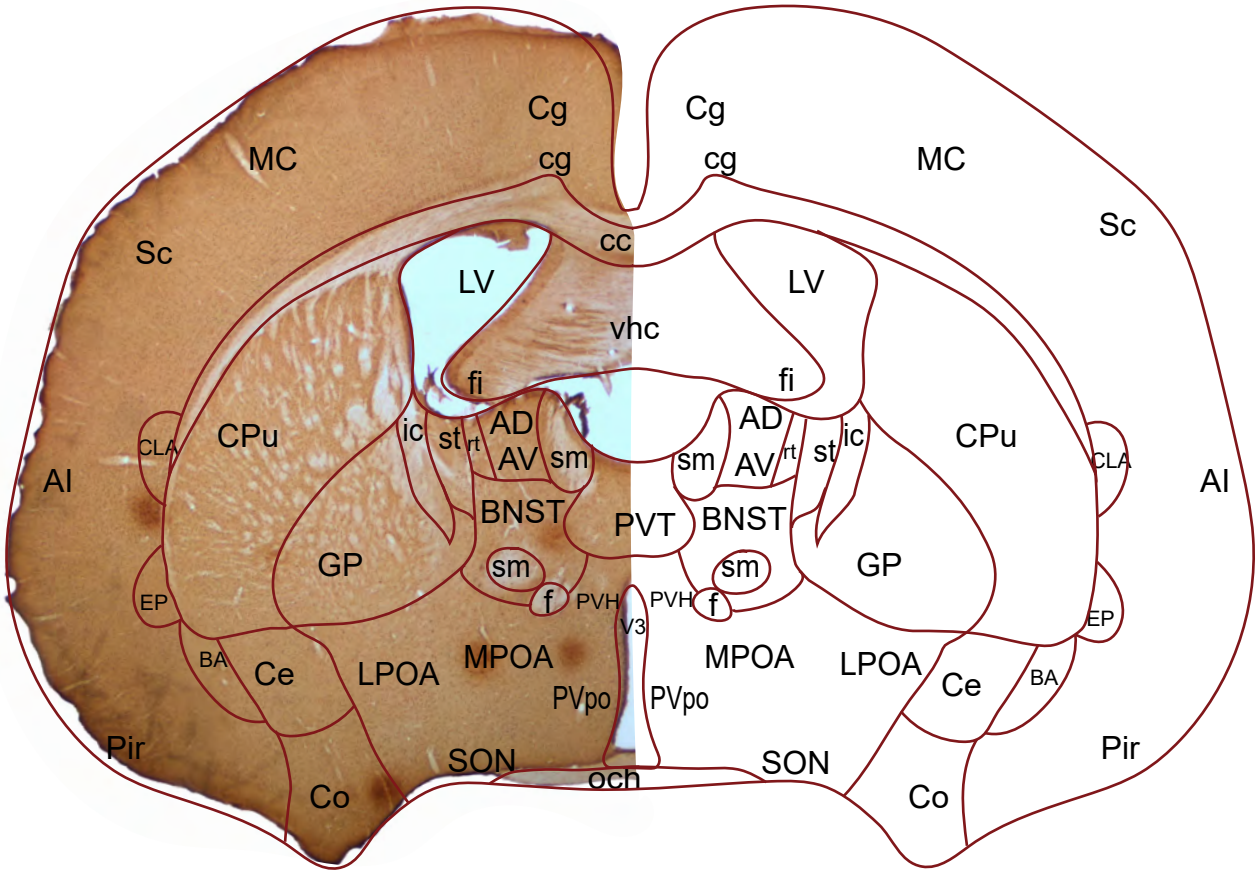

Set 20: Myelin oc +700µm

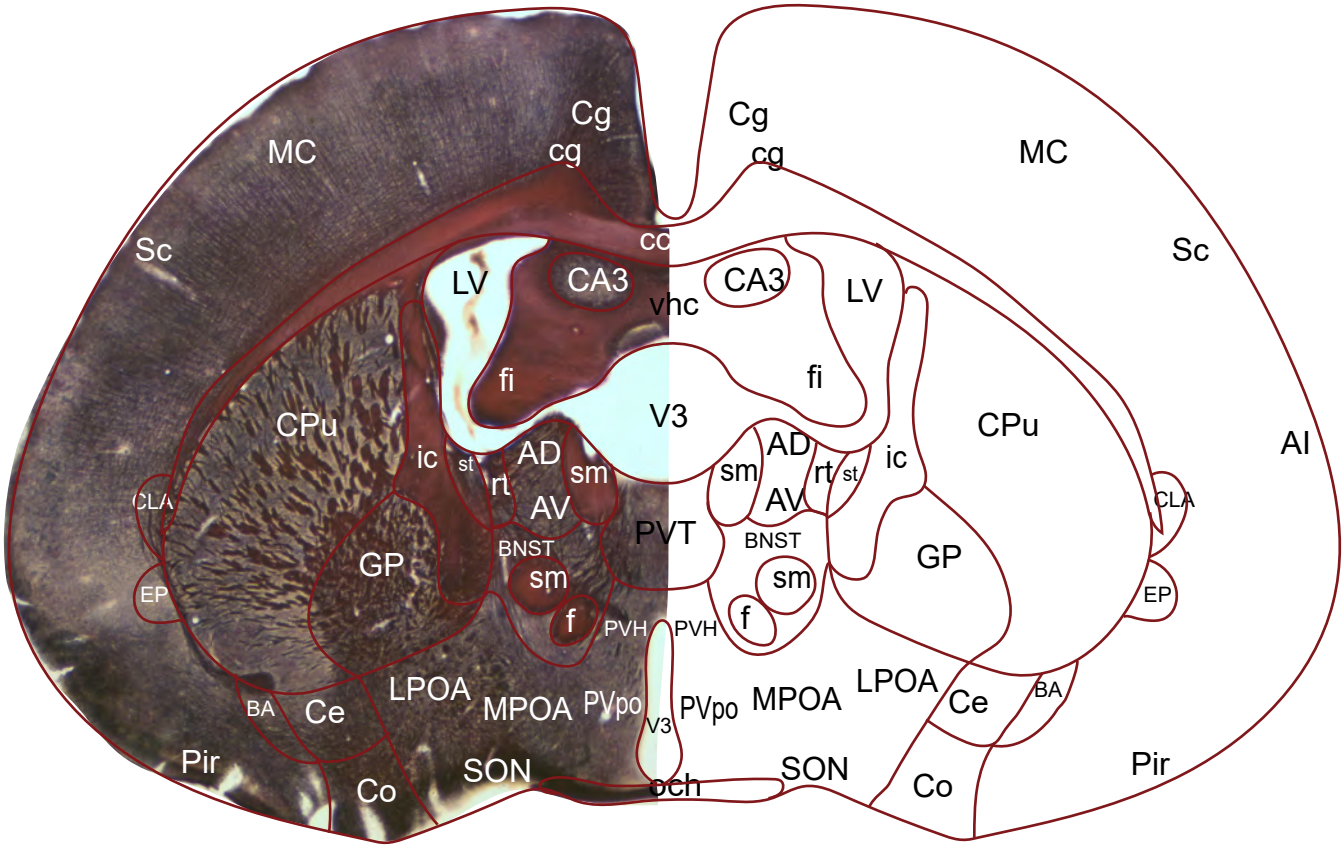

Set 21: OXT oc +750µm

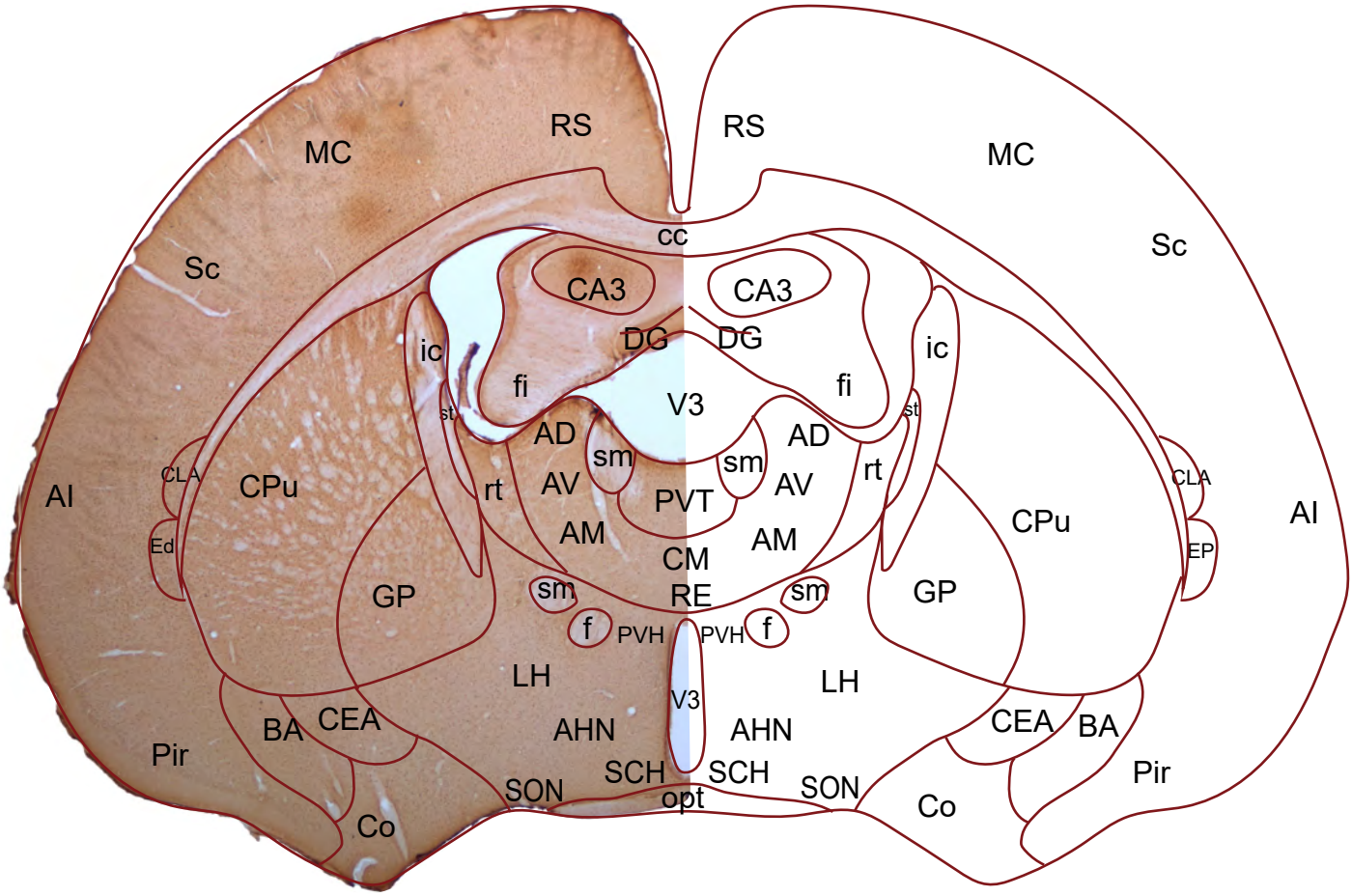

Set 21: Nissl oc +800µm

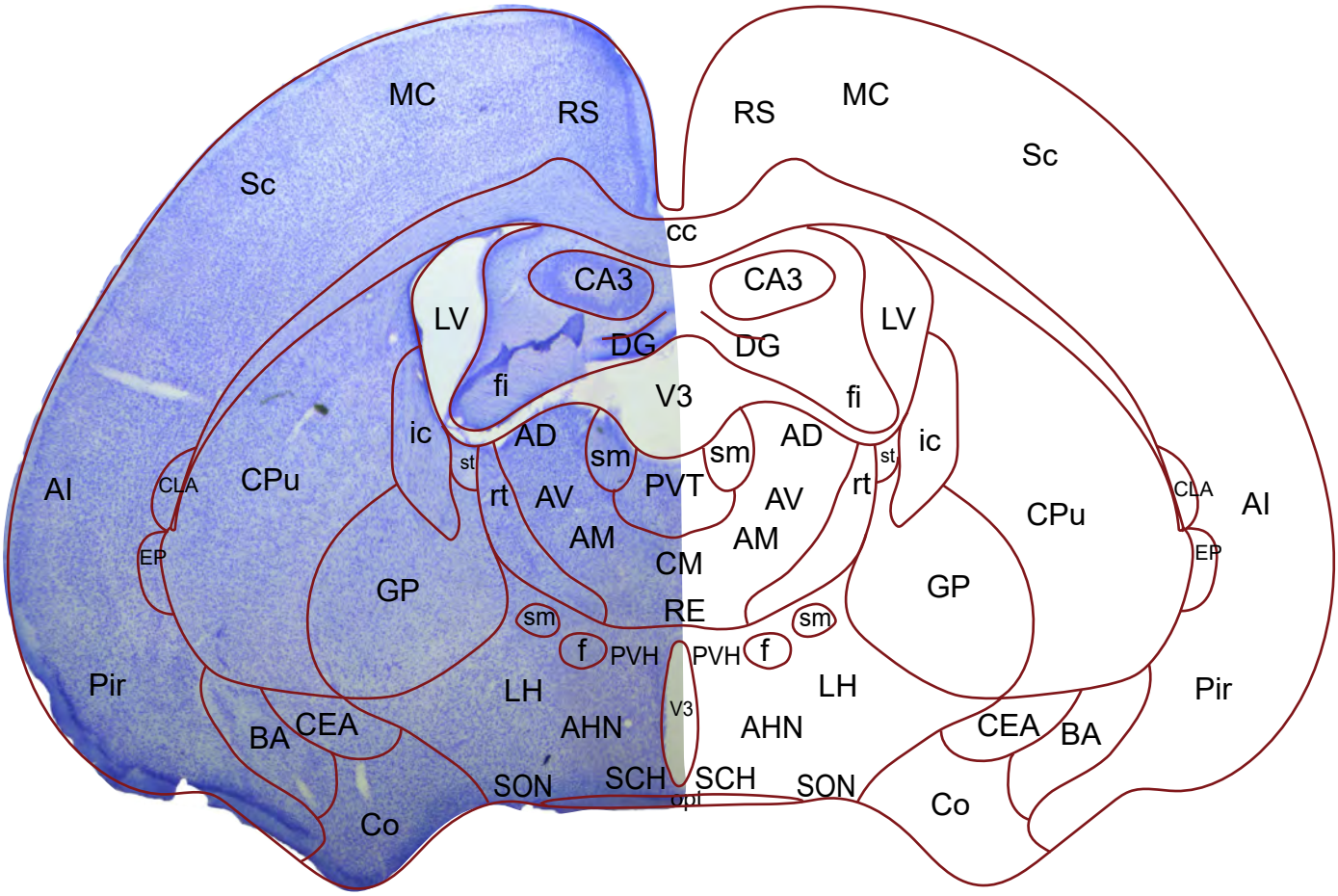

Set 21: OXT oc +850µm

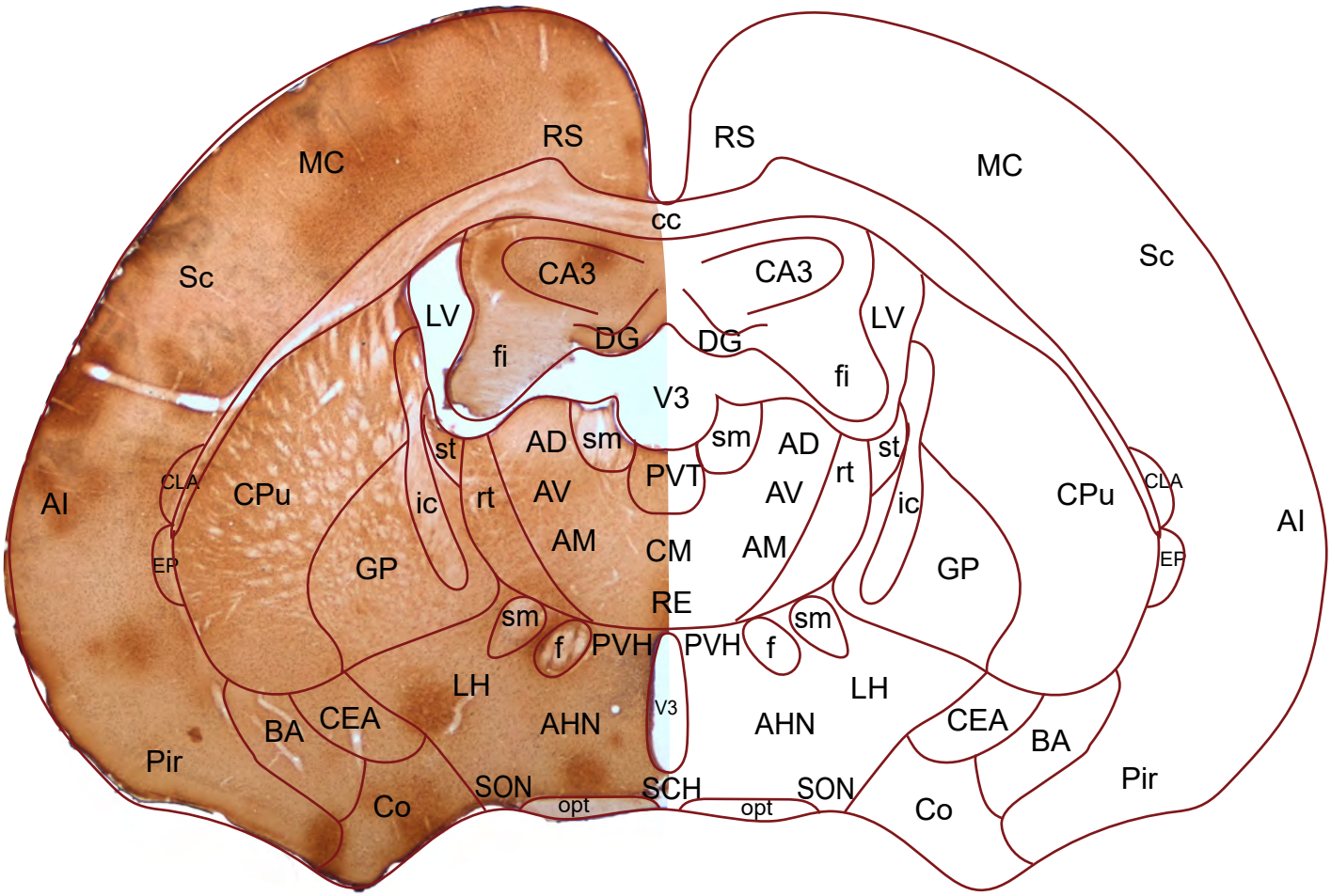

Set 21: Myelin oc +900µm

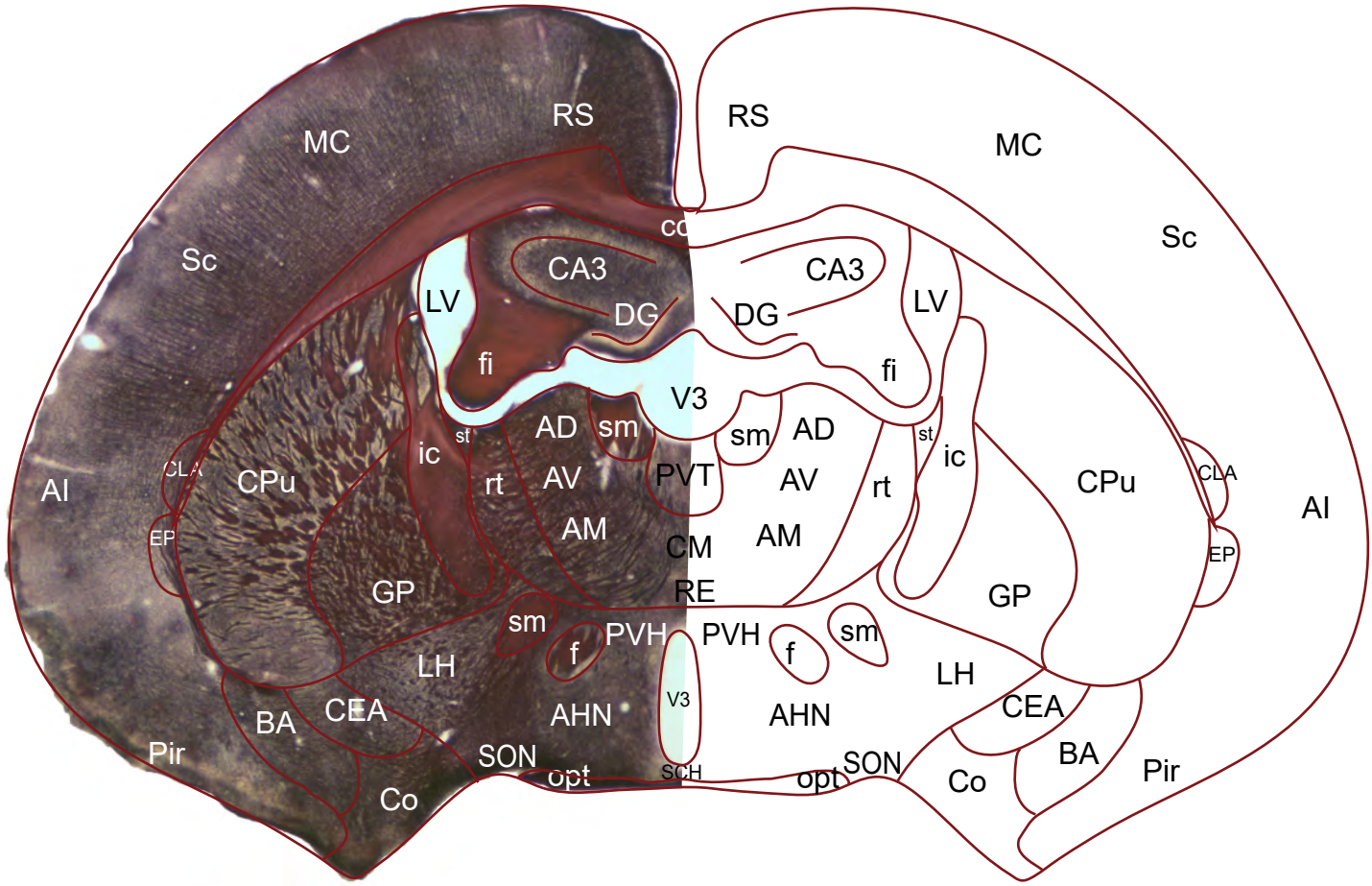

Set 22: OXT oc +950µm

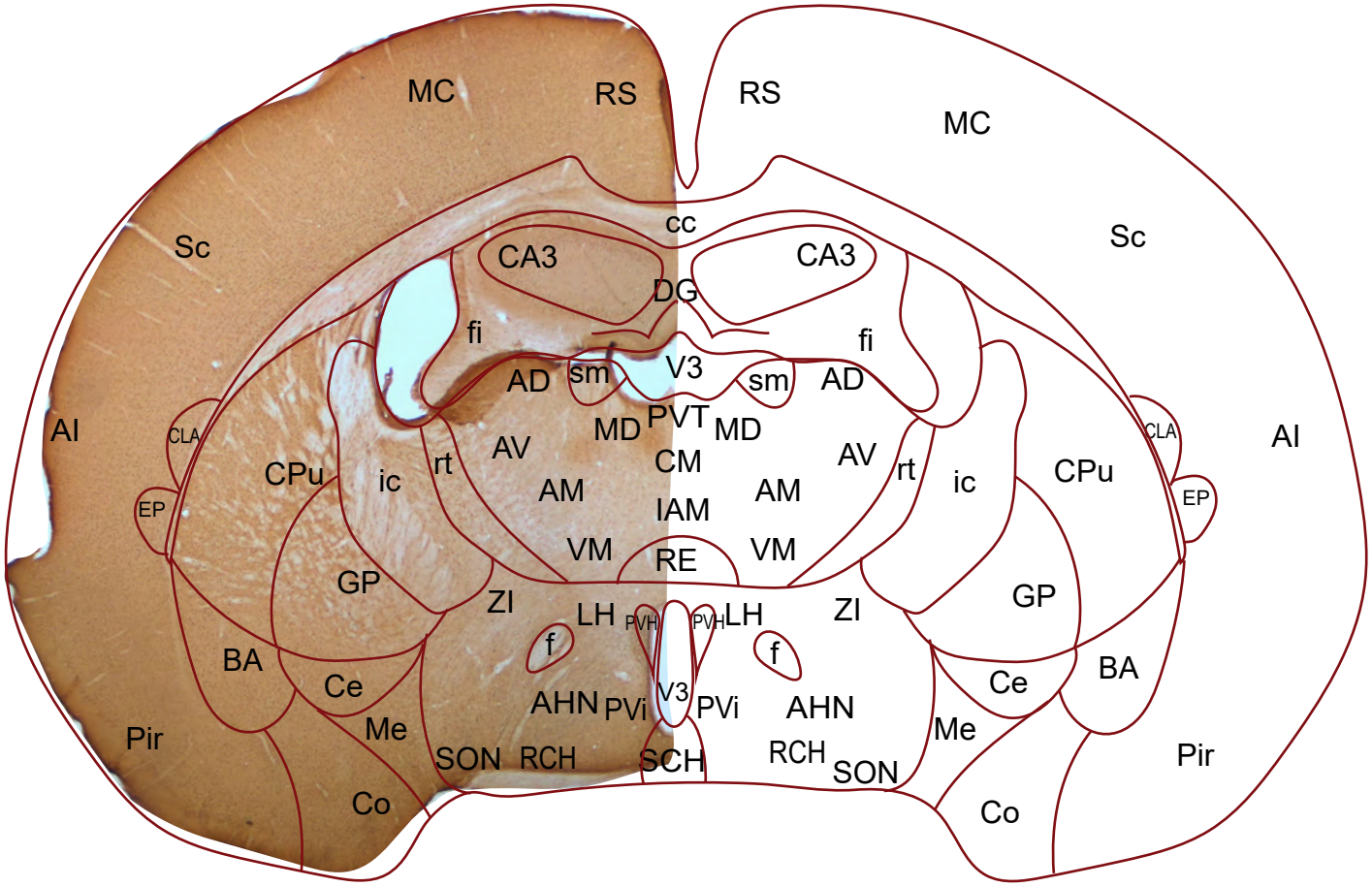

Set 22: Nissl oc +1000µm

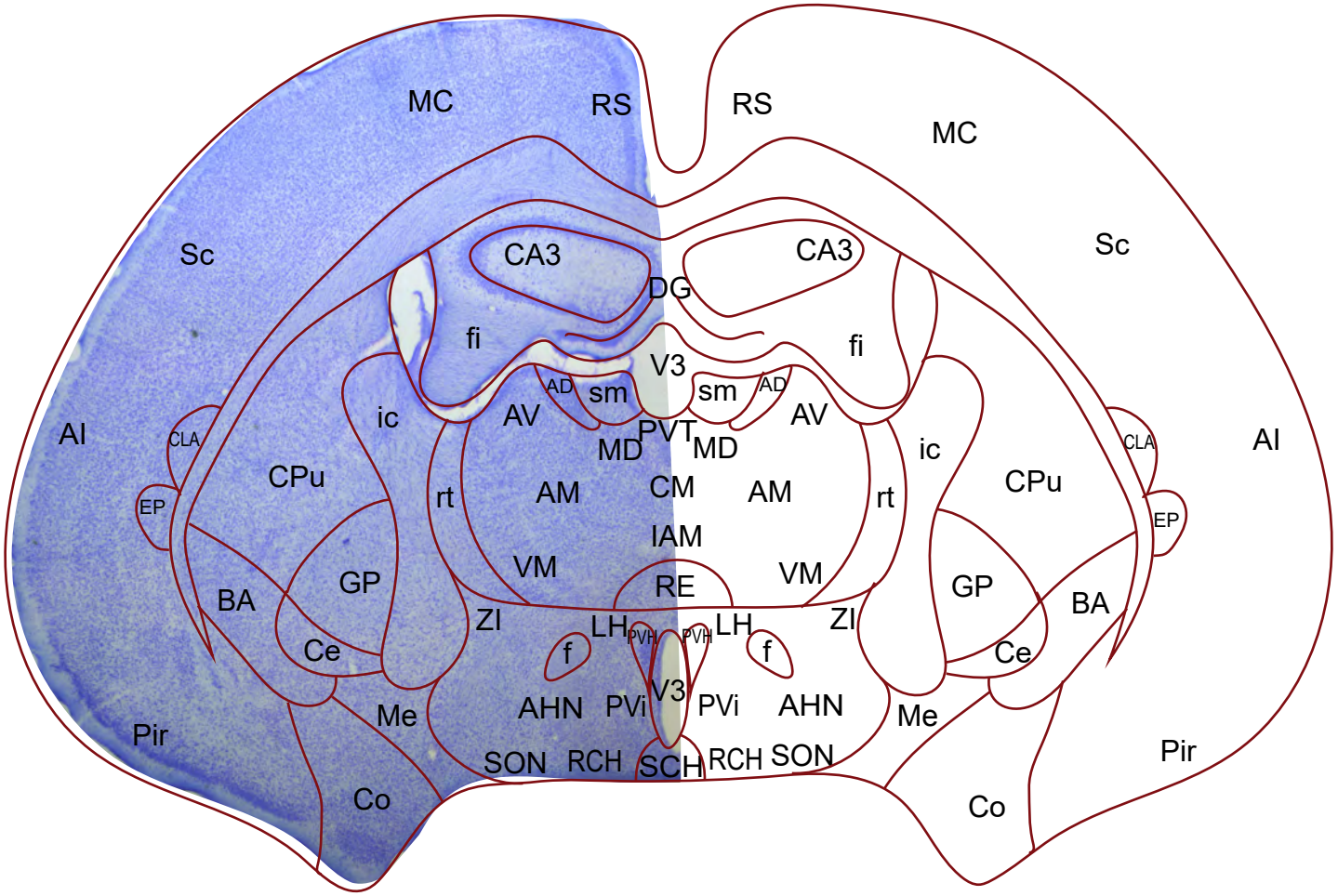

Set 22: OXT oc +1050µm

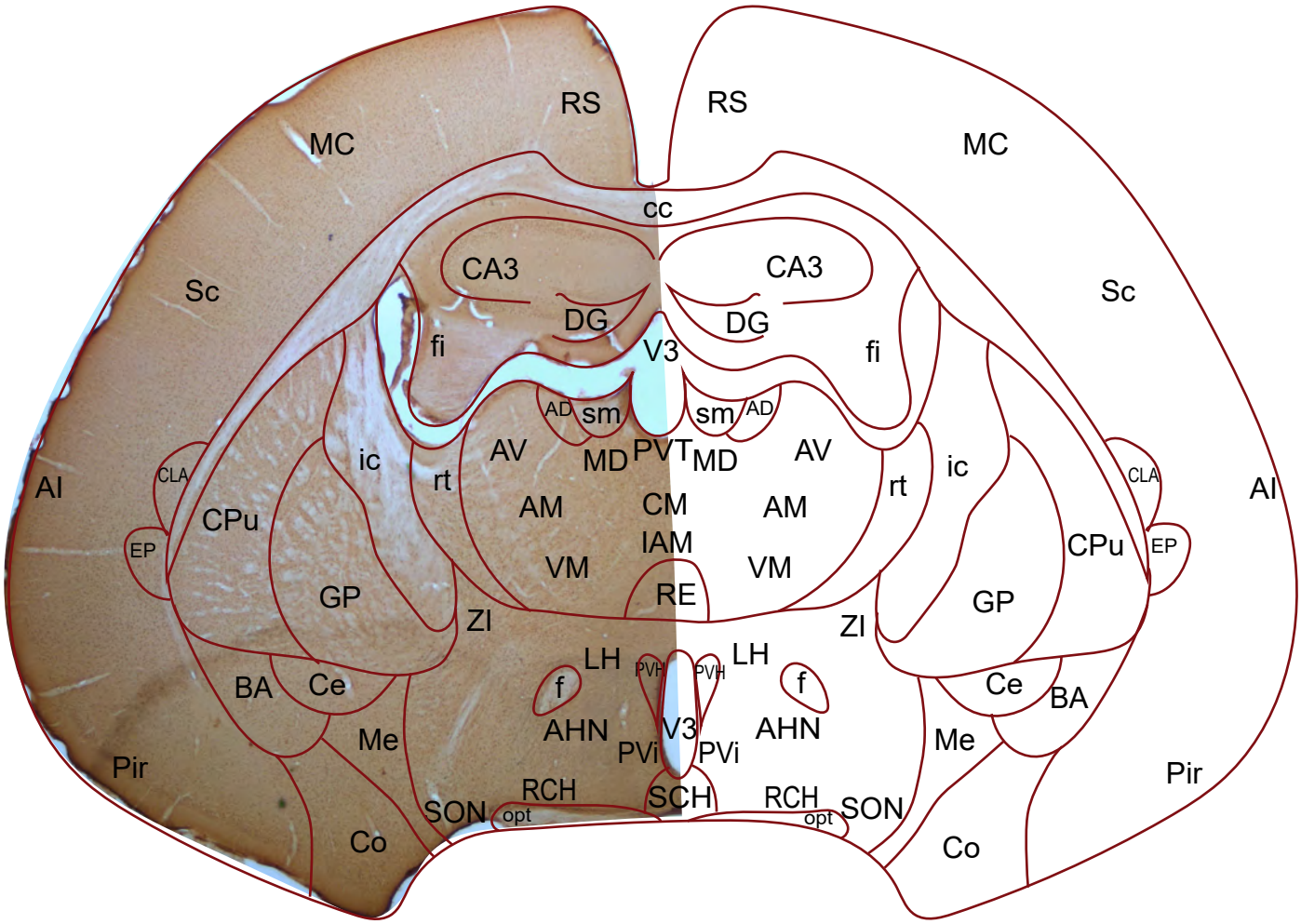

Set 22: Myelin oc +1100µm

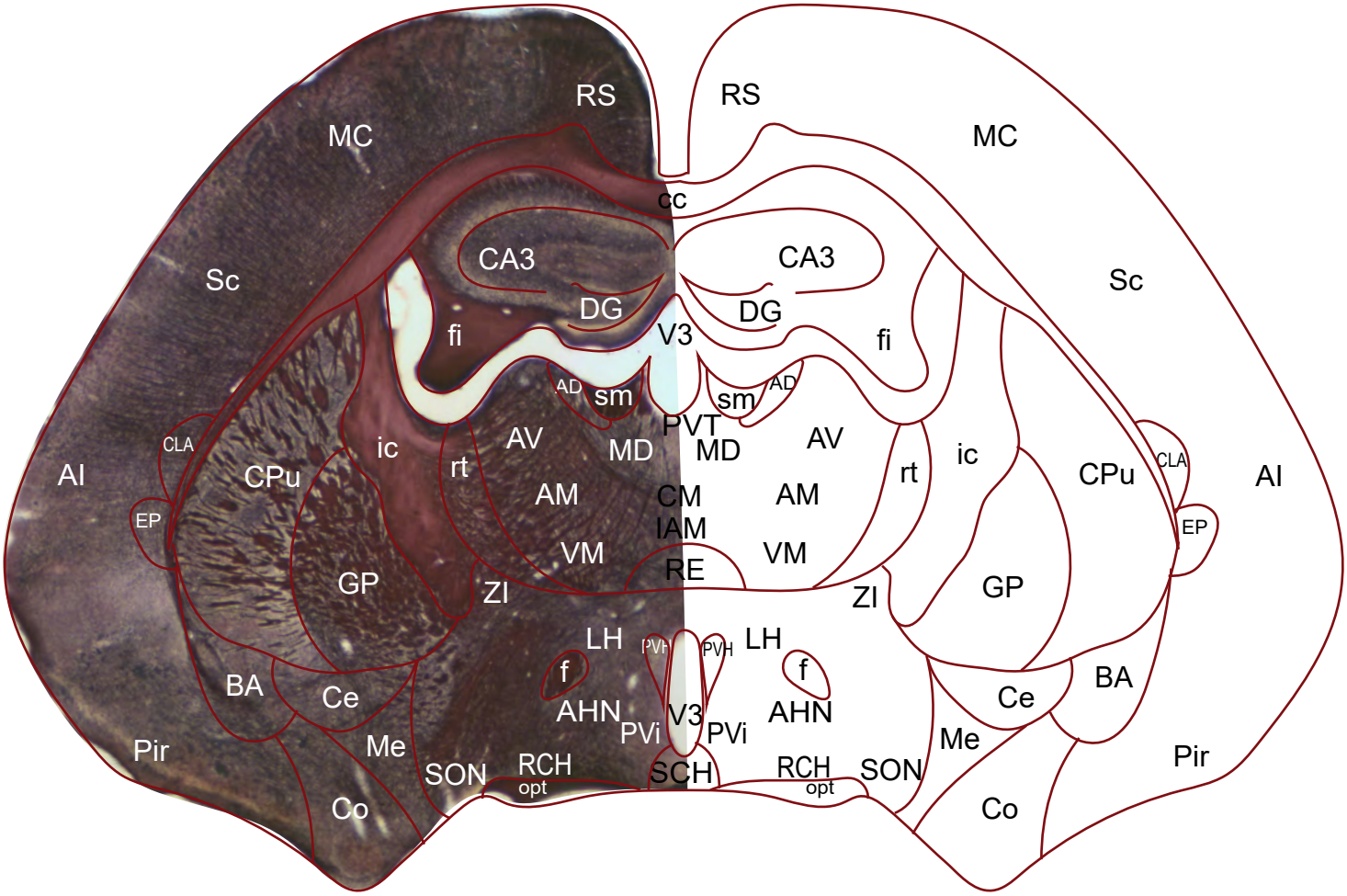

Set 23: OXT oc +1150µm

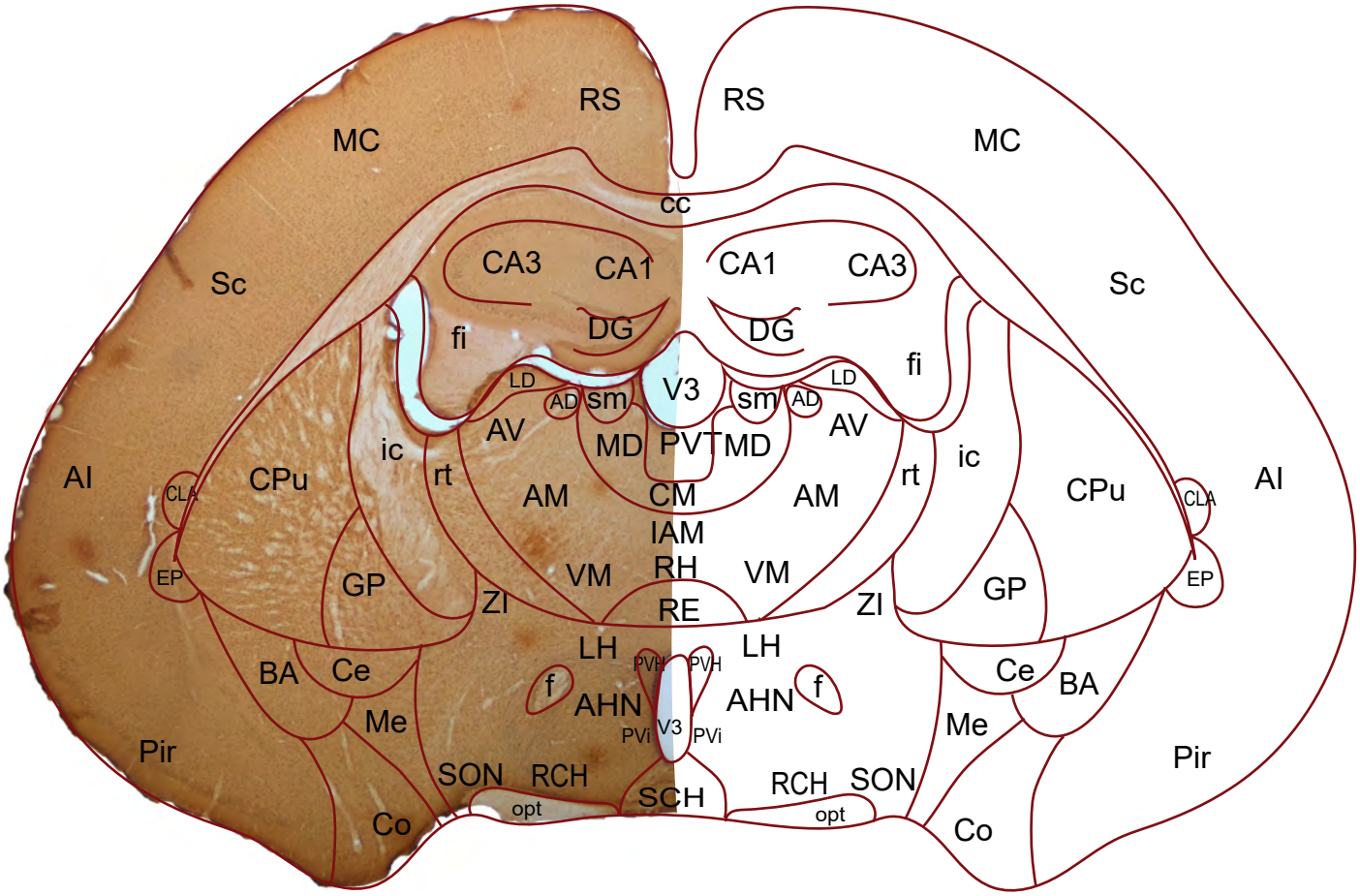

Set 23: Nissl oc +1200µm

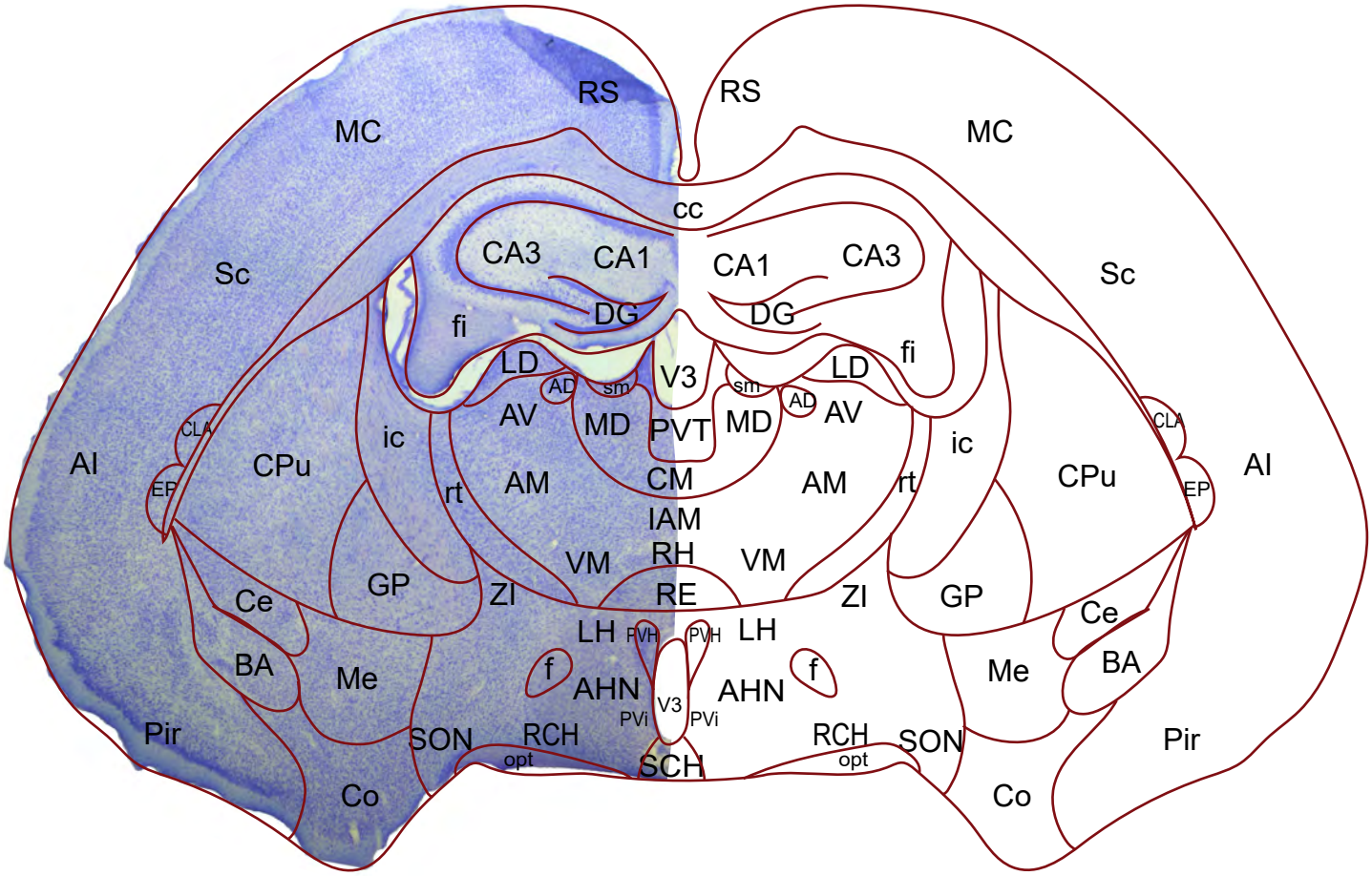

Set 23: OXT oc +1250µm

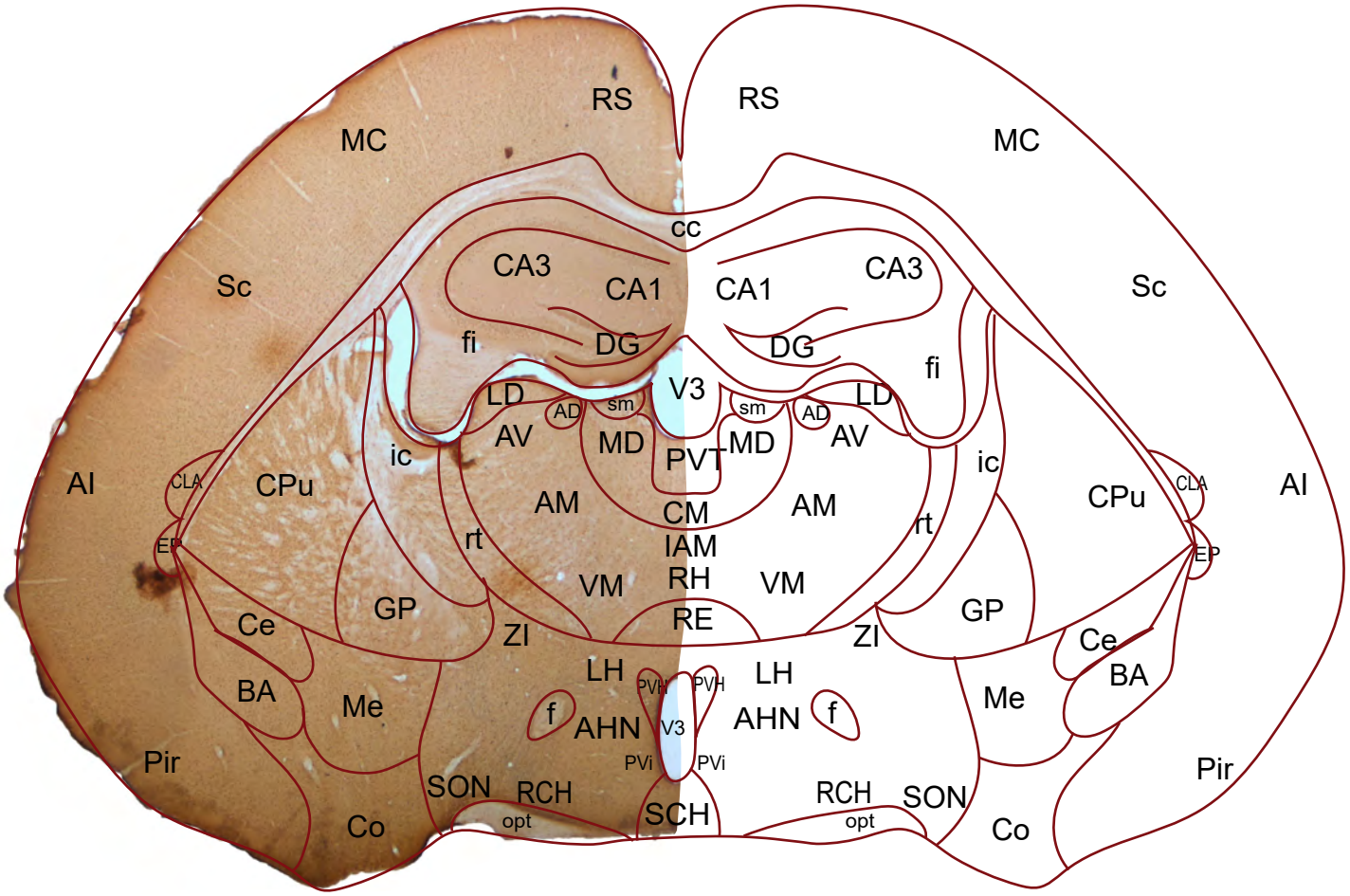

Set 23: Myelin oc +1300µm

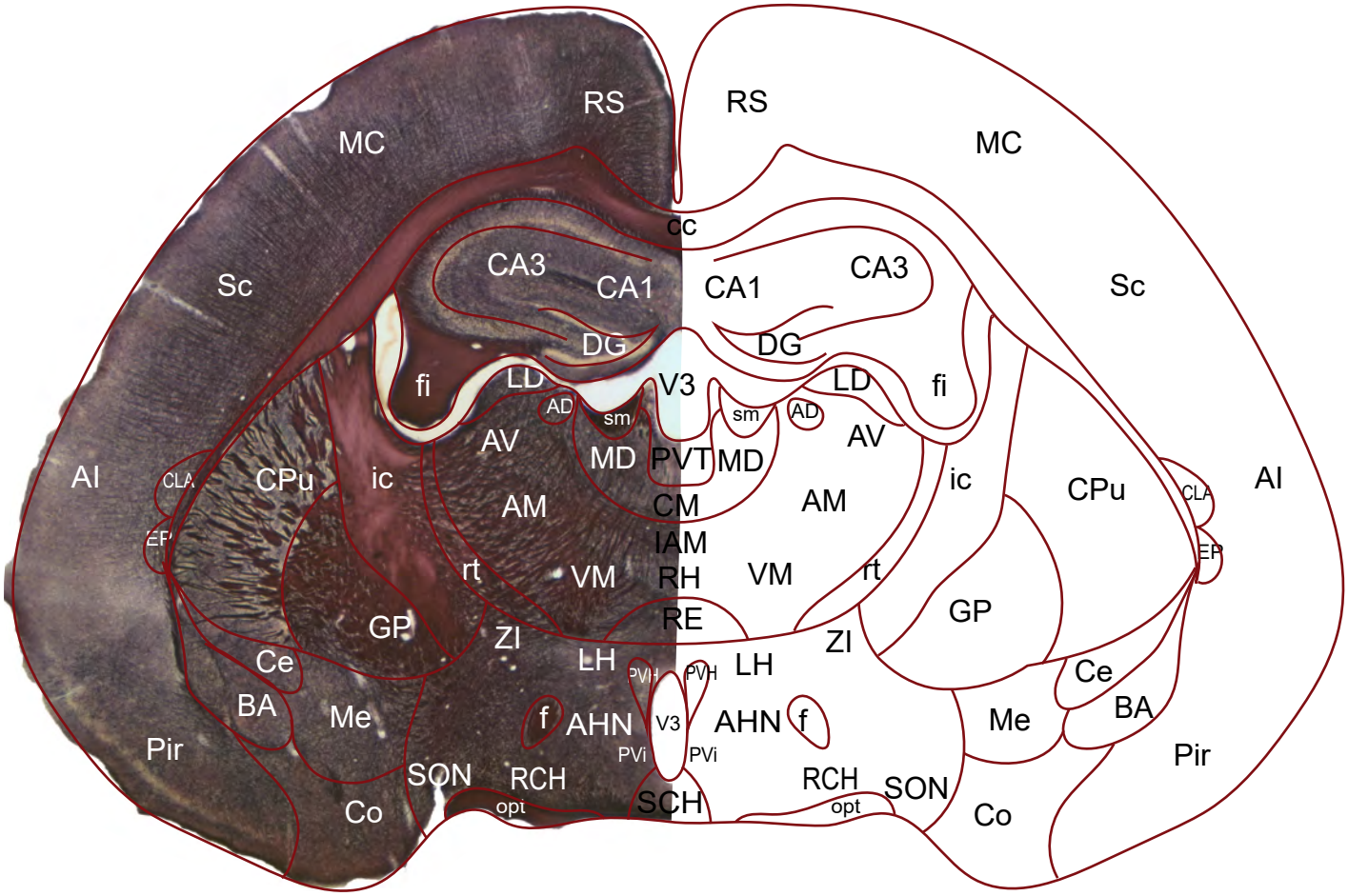

Set 24: OXT oc +1350µm

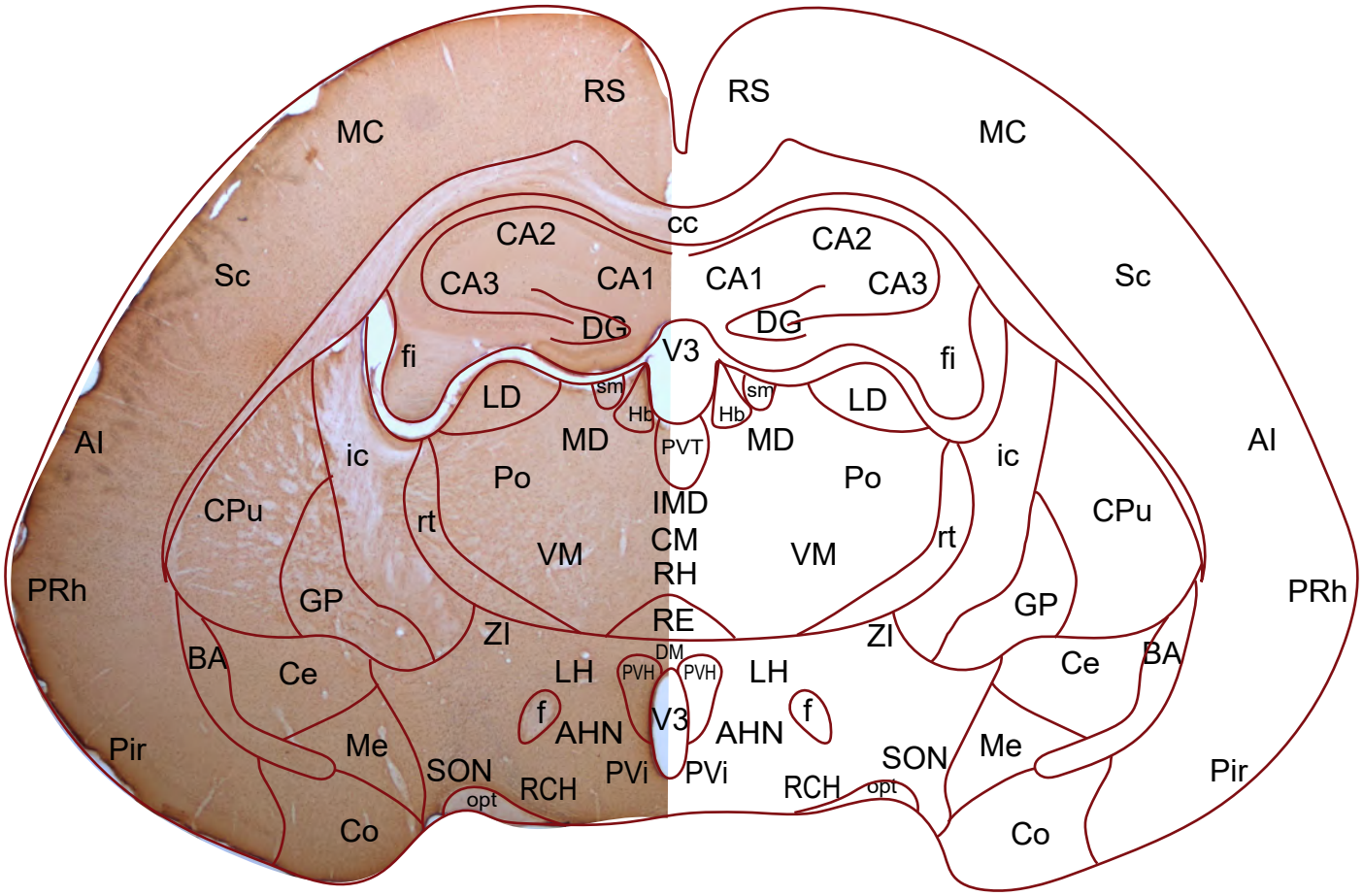

Set 24: Nissl oc +1400µm

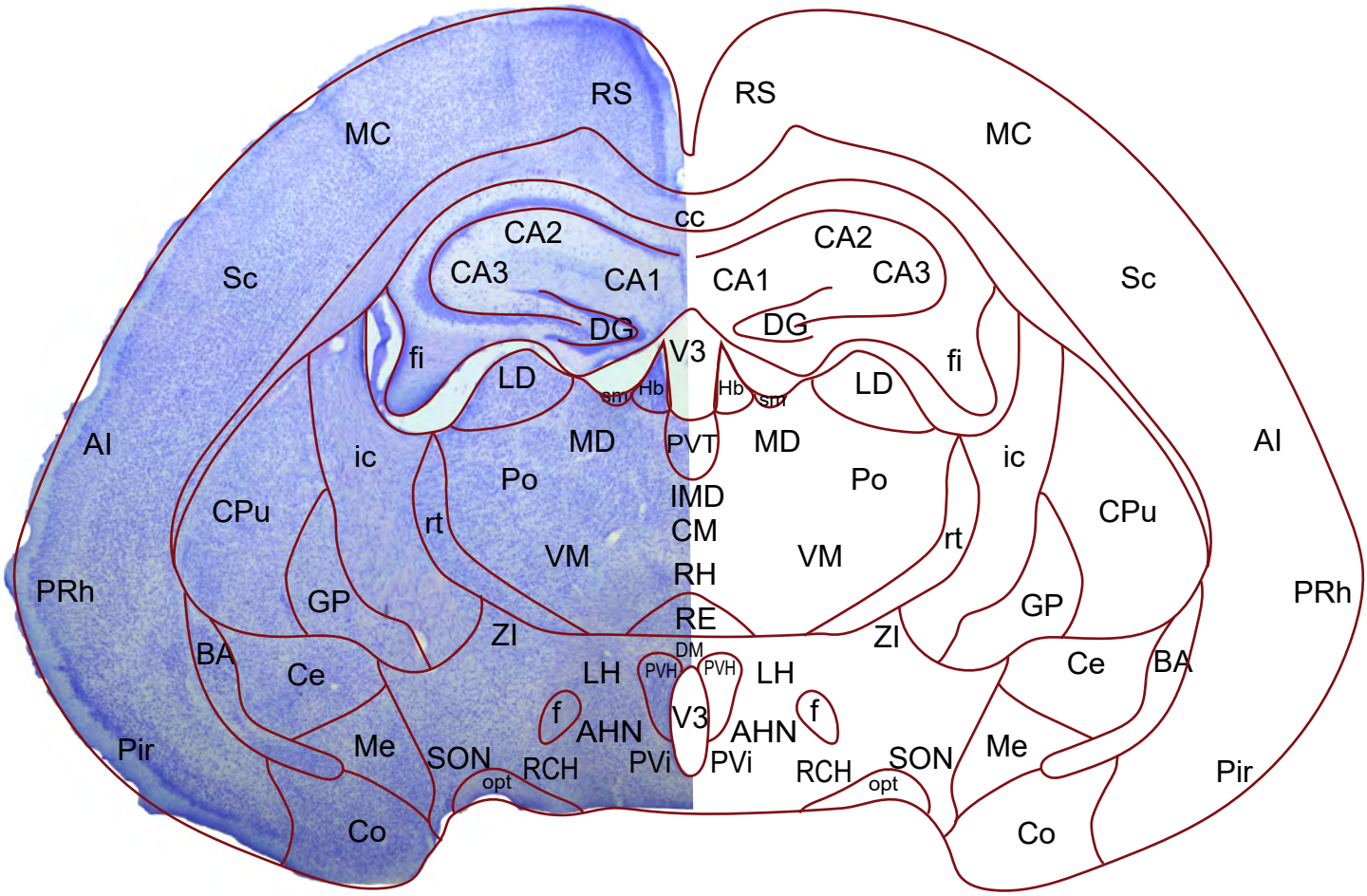

Set 24: OXT oc +1450µm

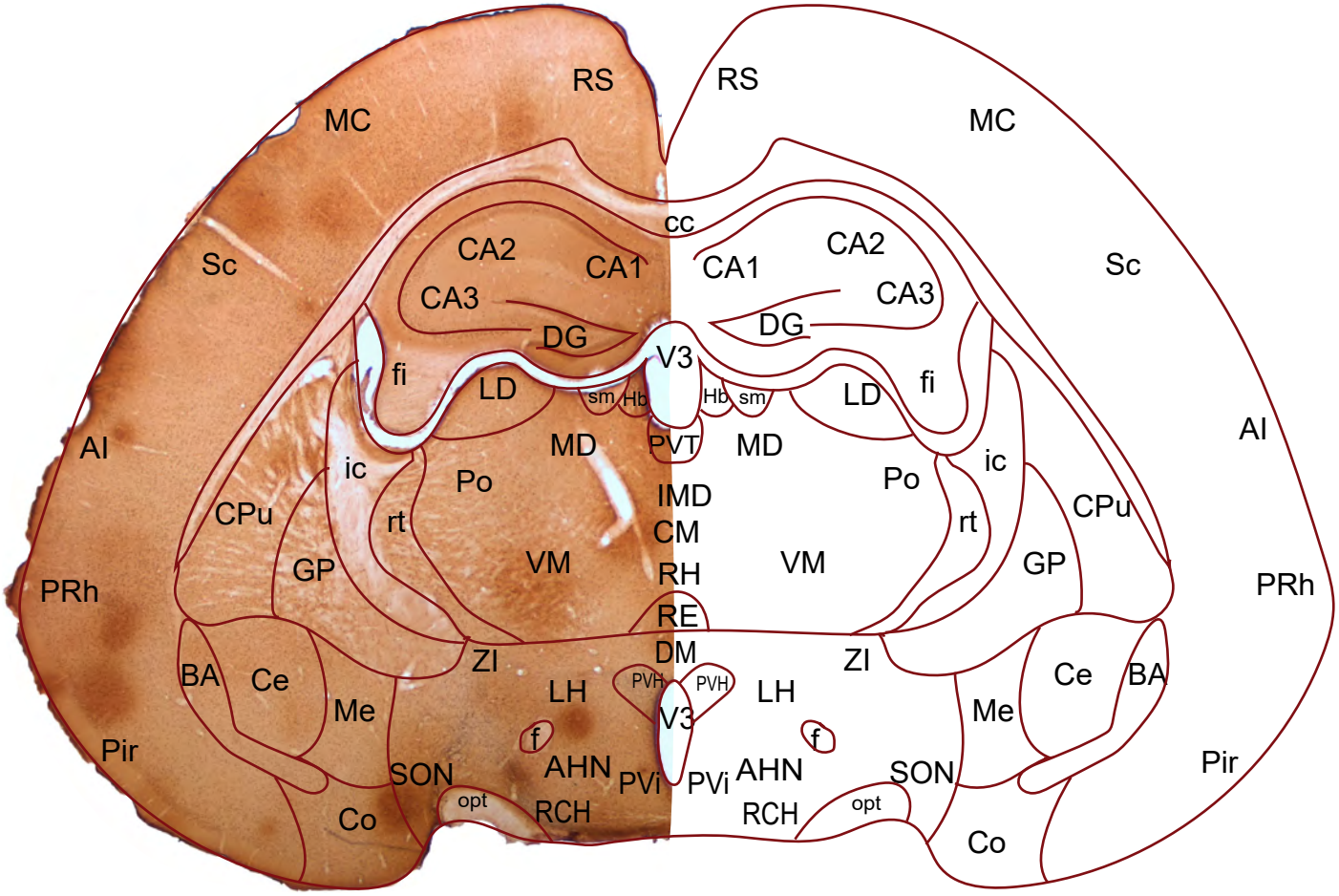

Set 24: Myelin oc +1500µm

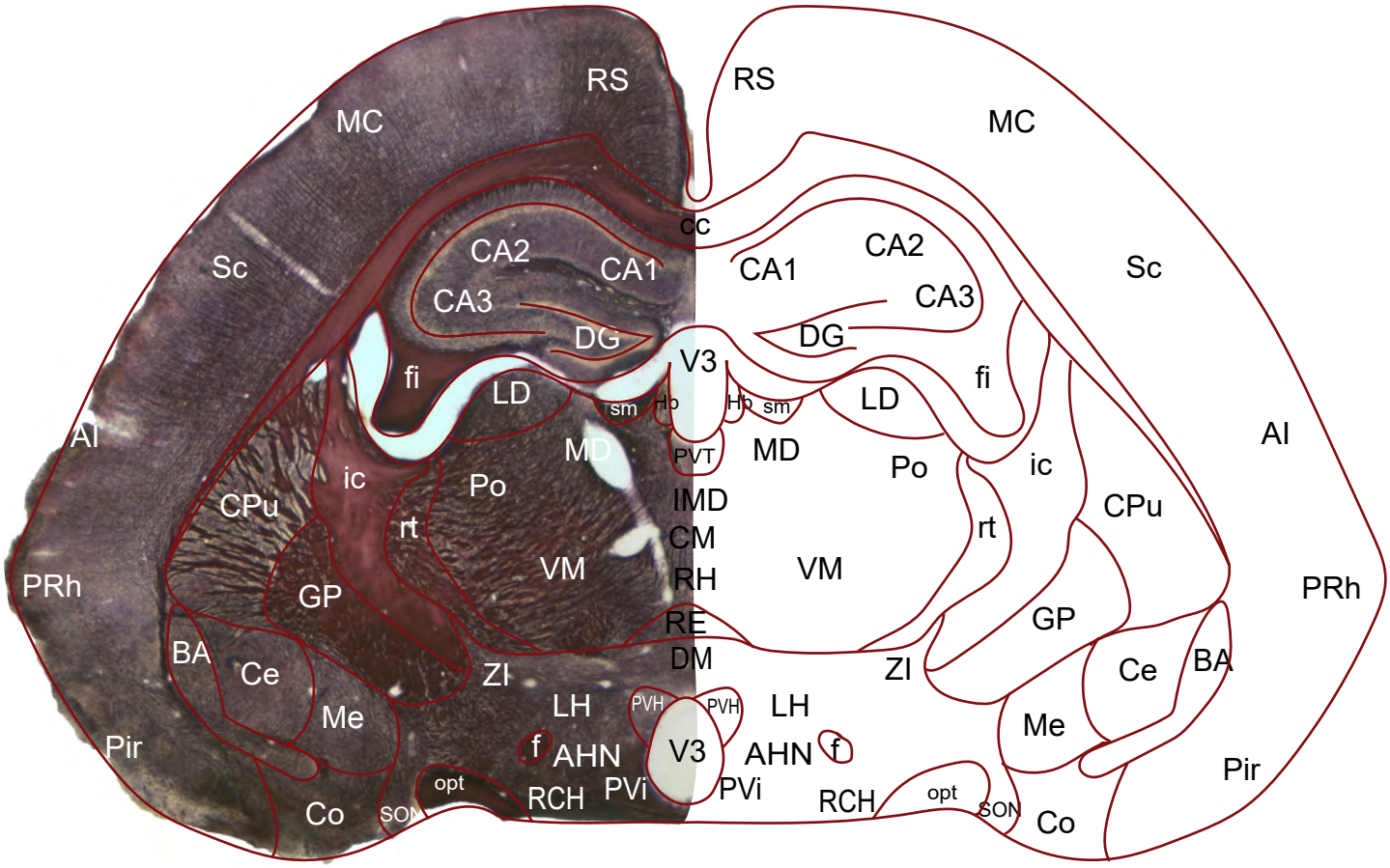

Set 25: OXT oc +1550µm

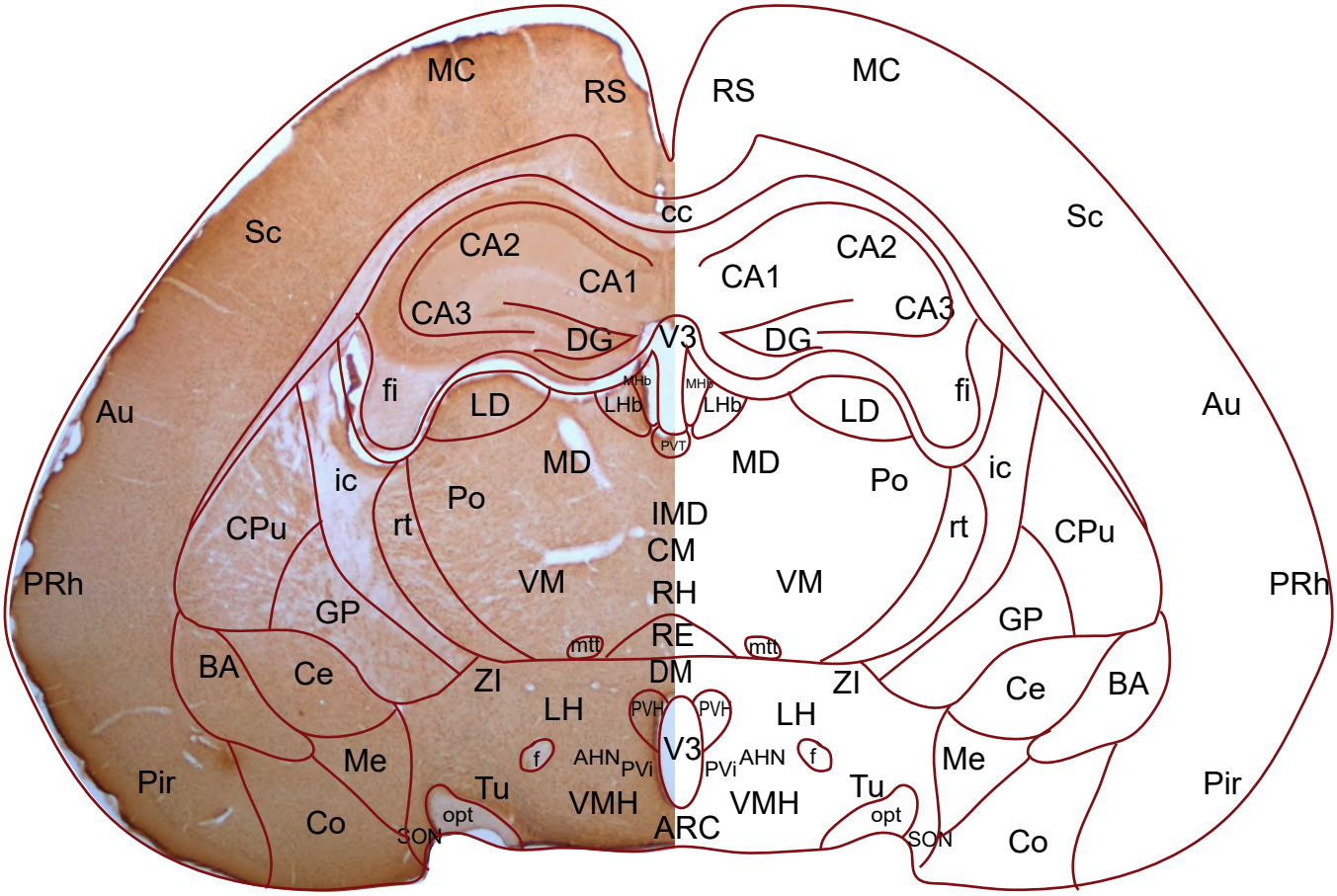

Set 25: Nissl oc +1600µm

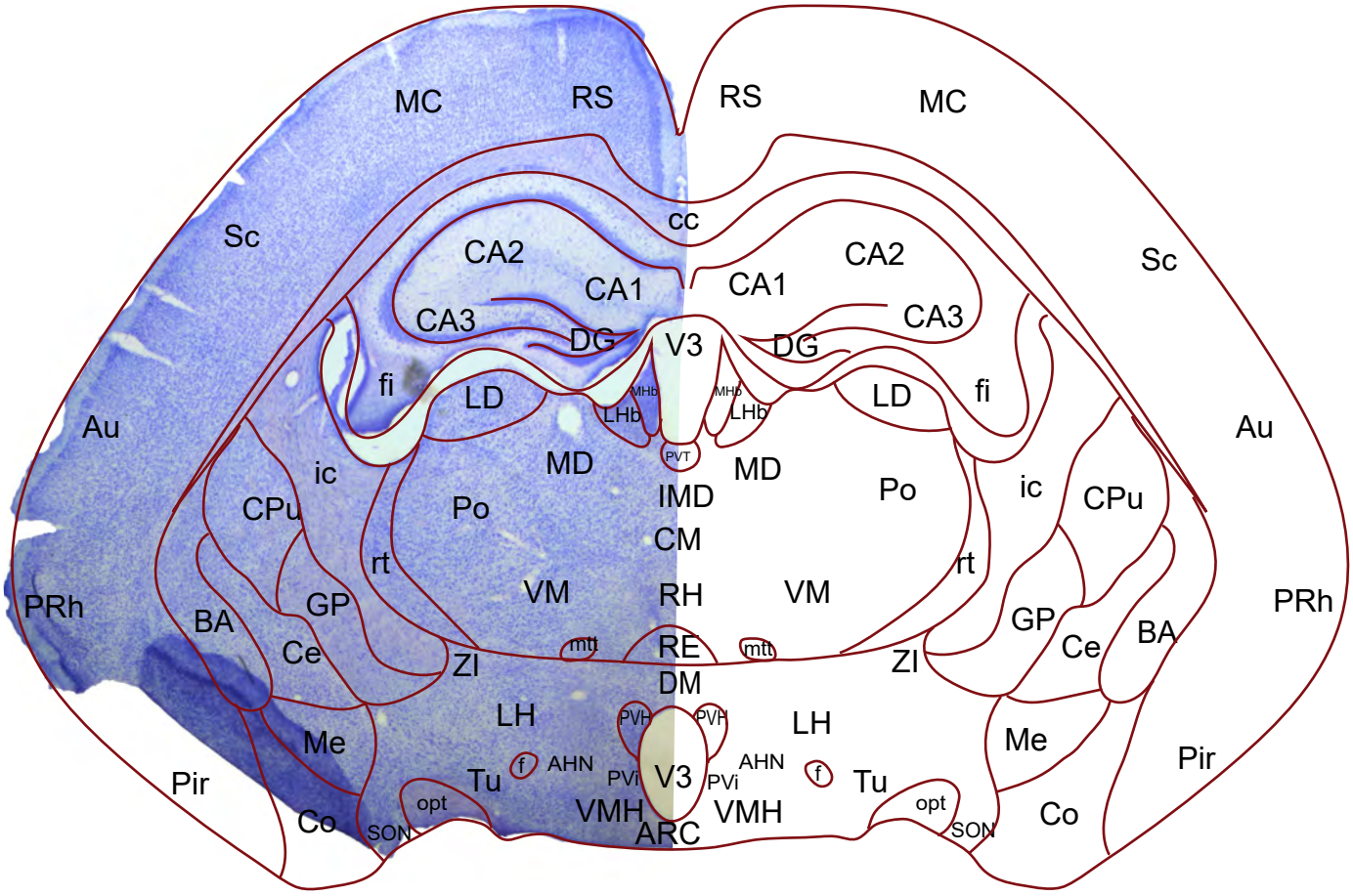

Set 25: OXT oc +1650µm

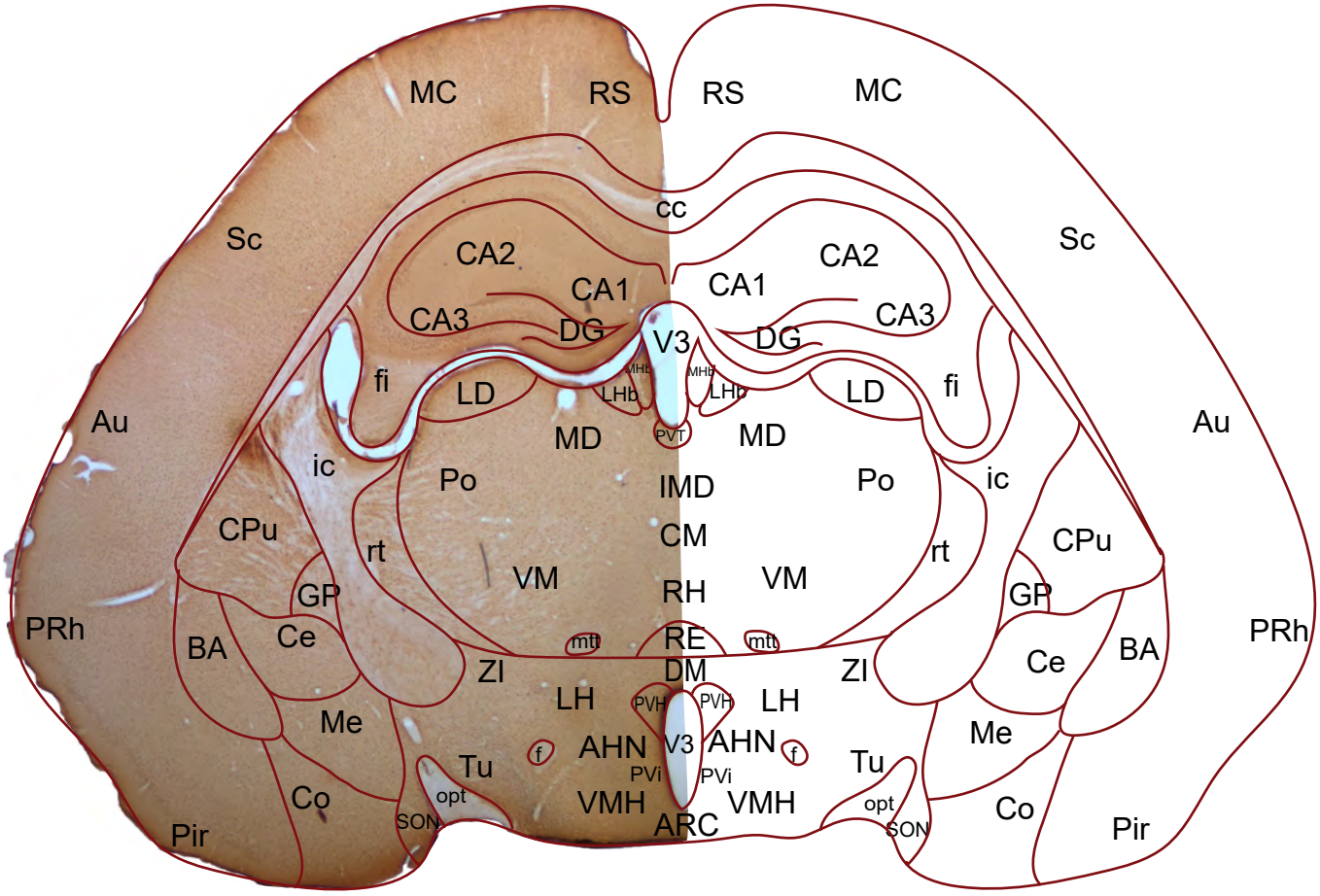

Set 25: Myelin oc +1700µm

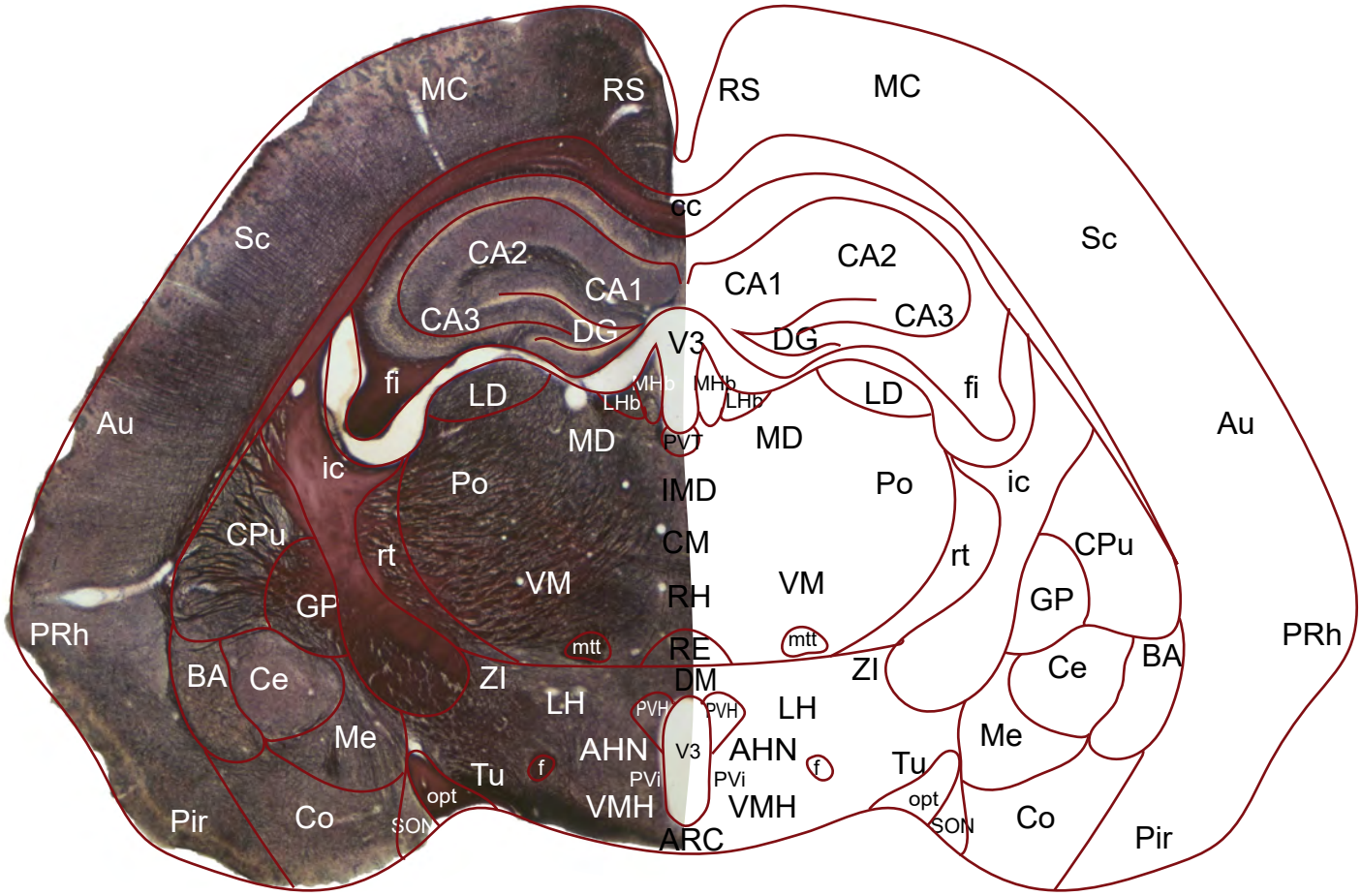

Set 26: OXT oc +1750µm

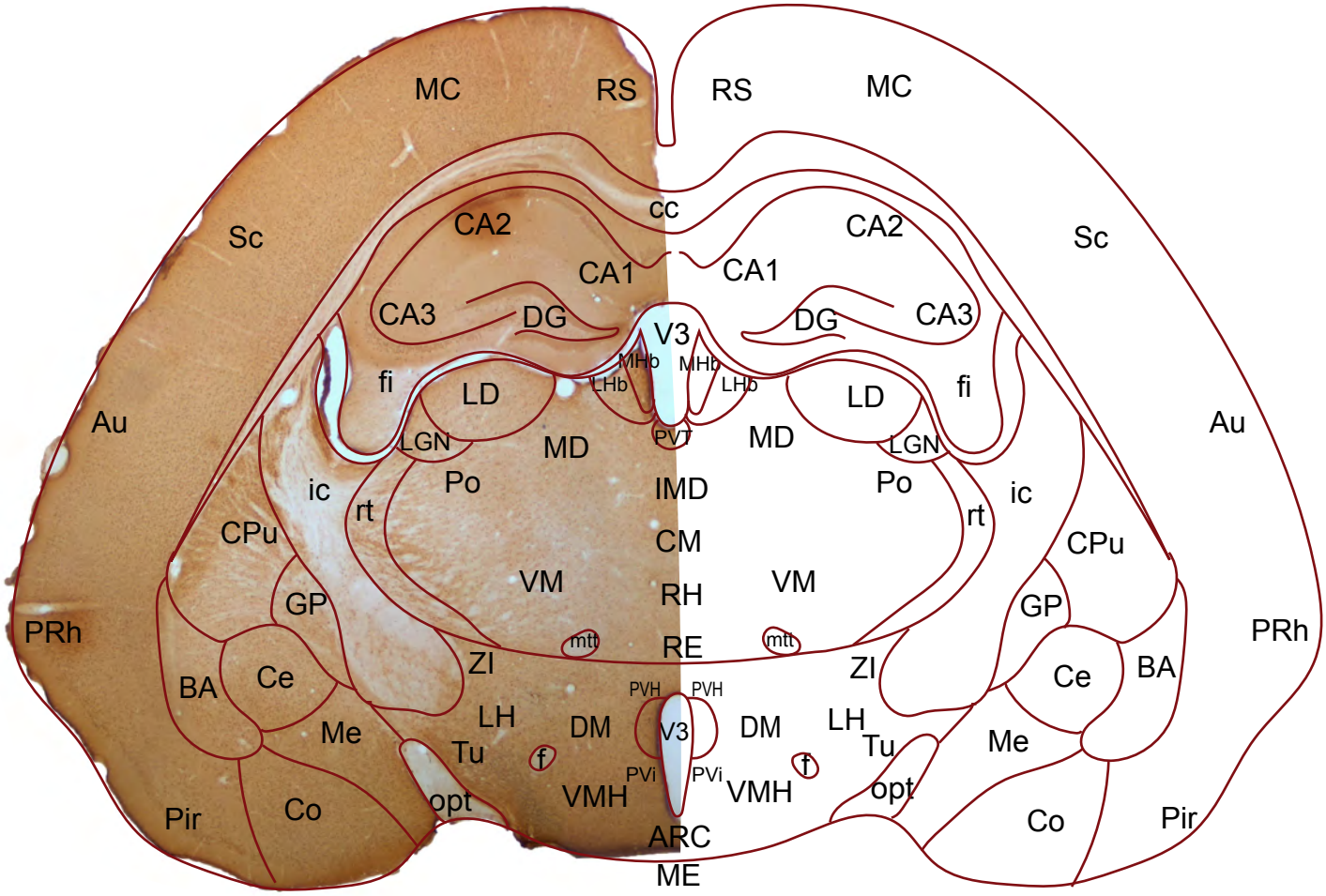

Set 26: Nissl oc +1800µm

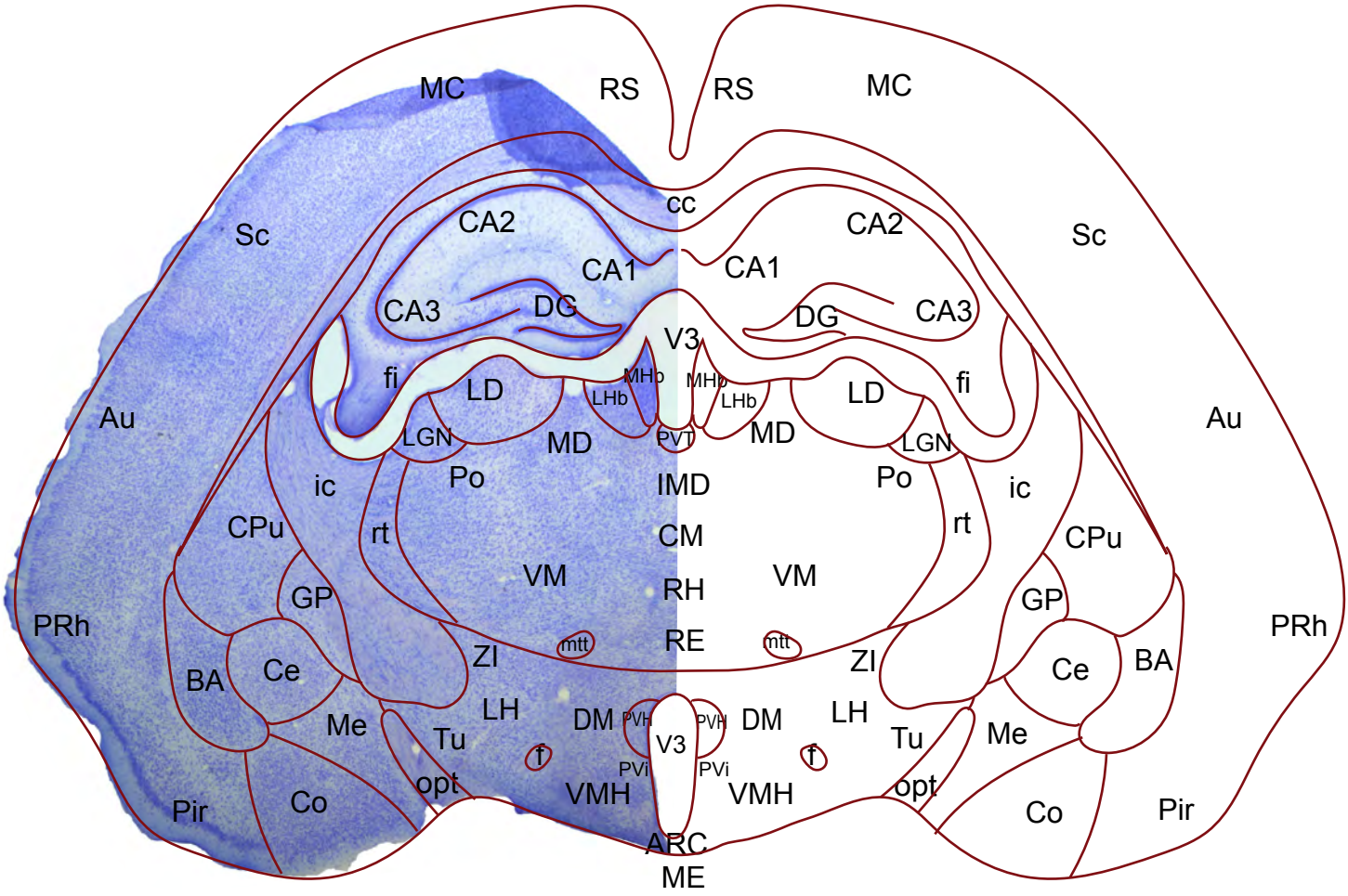

Set 26: OXT oc +1850µm

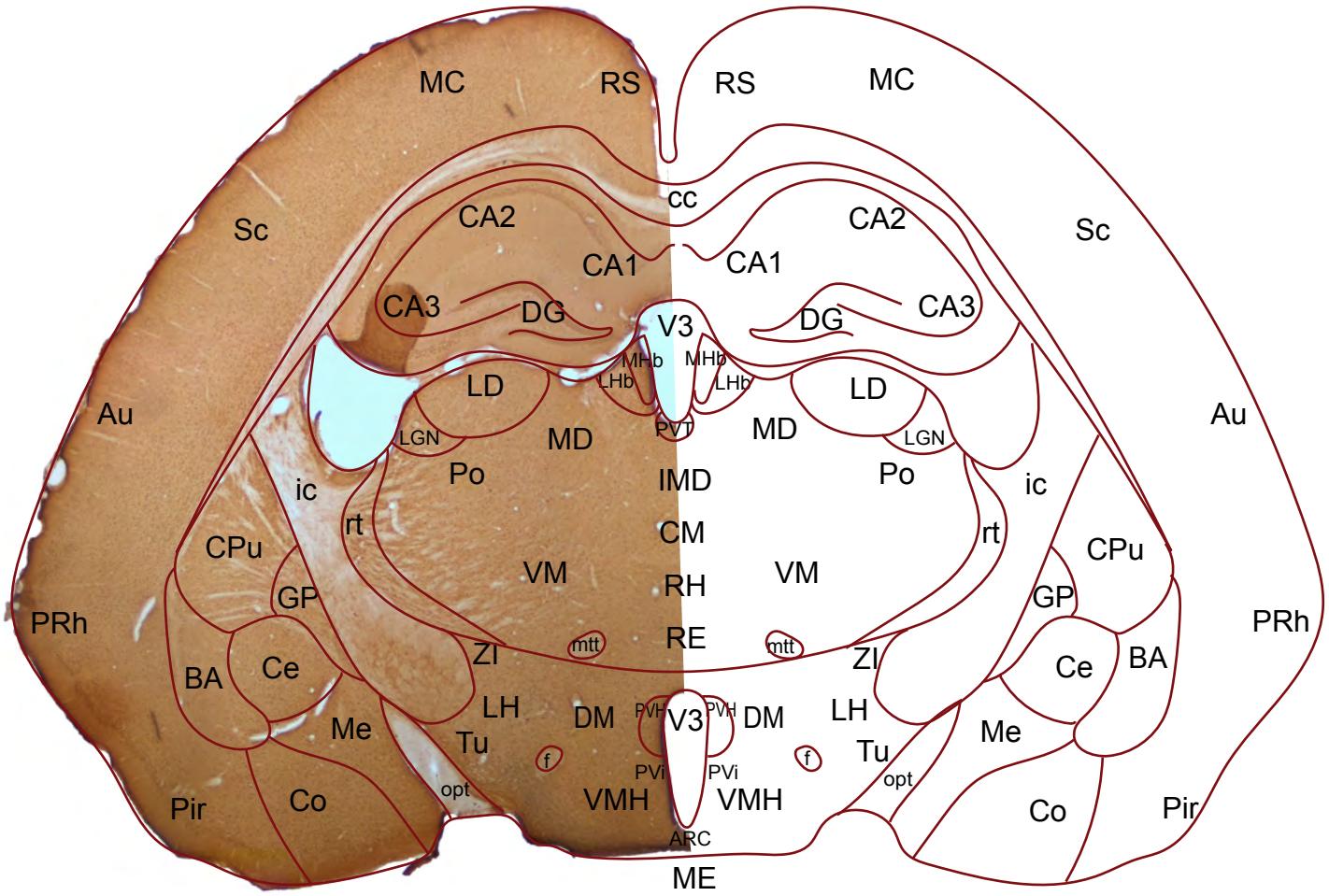

Set 26: Myelin oc +1900µm

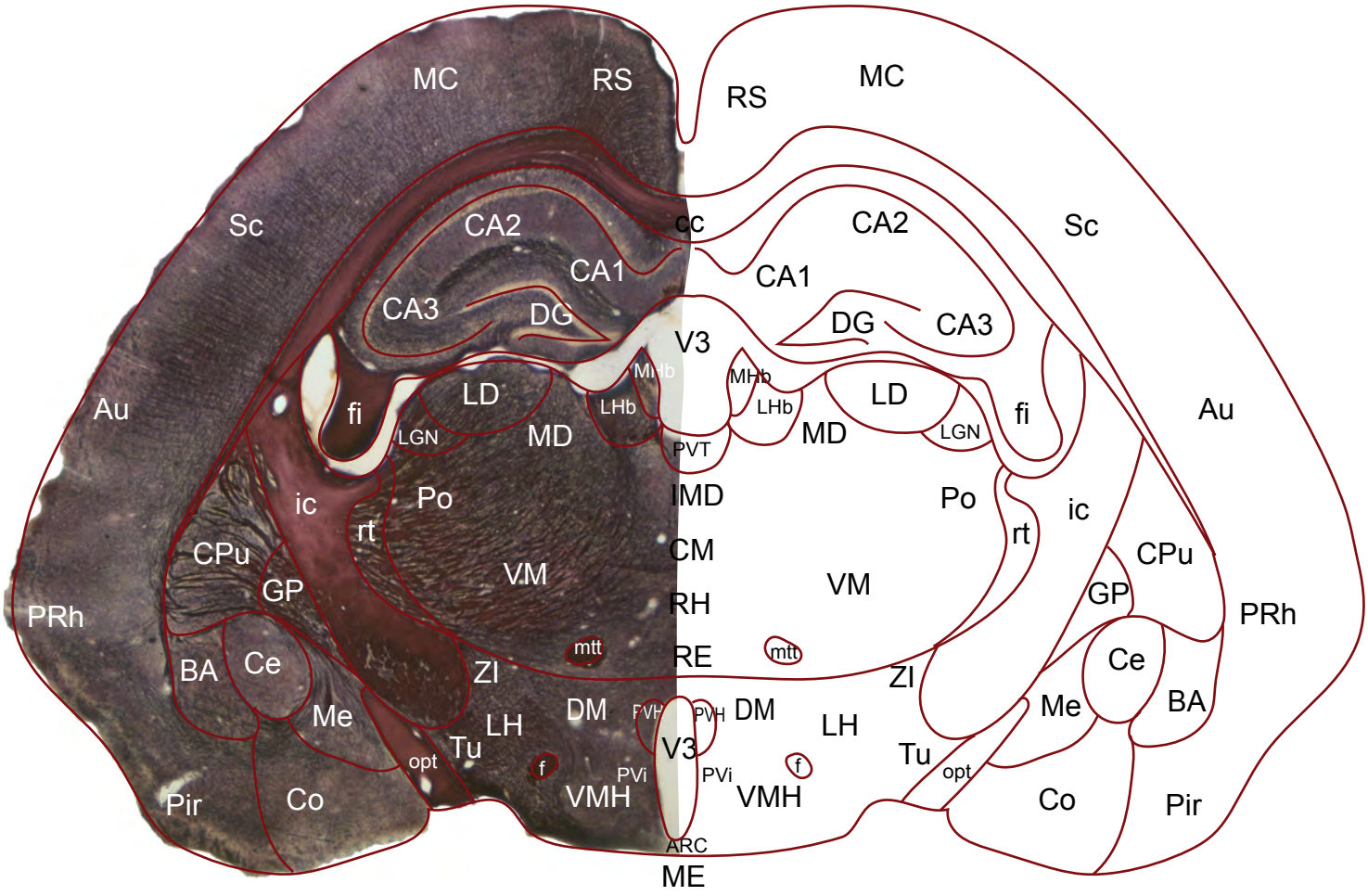

Set 27: OXT oc +1950µm

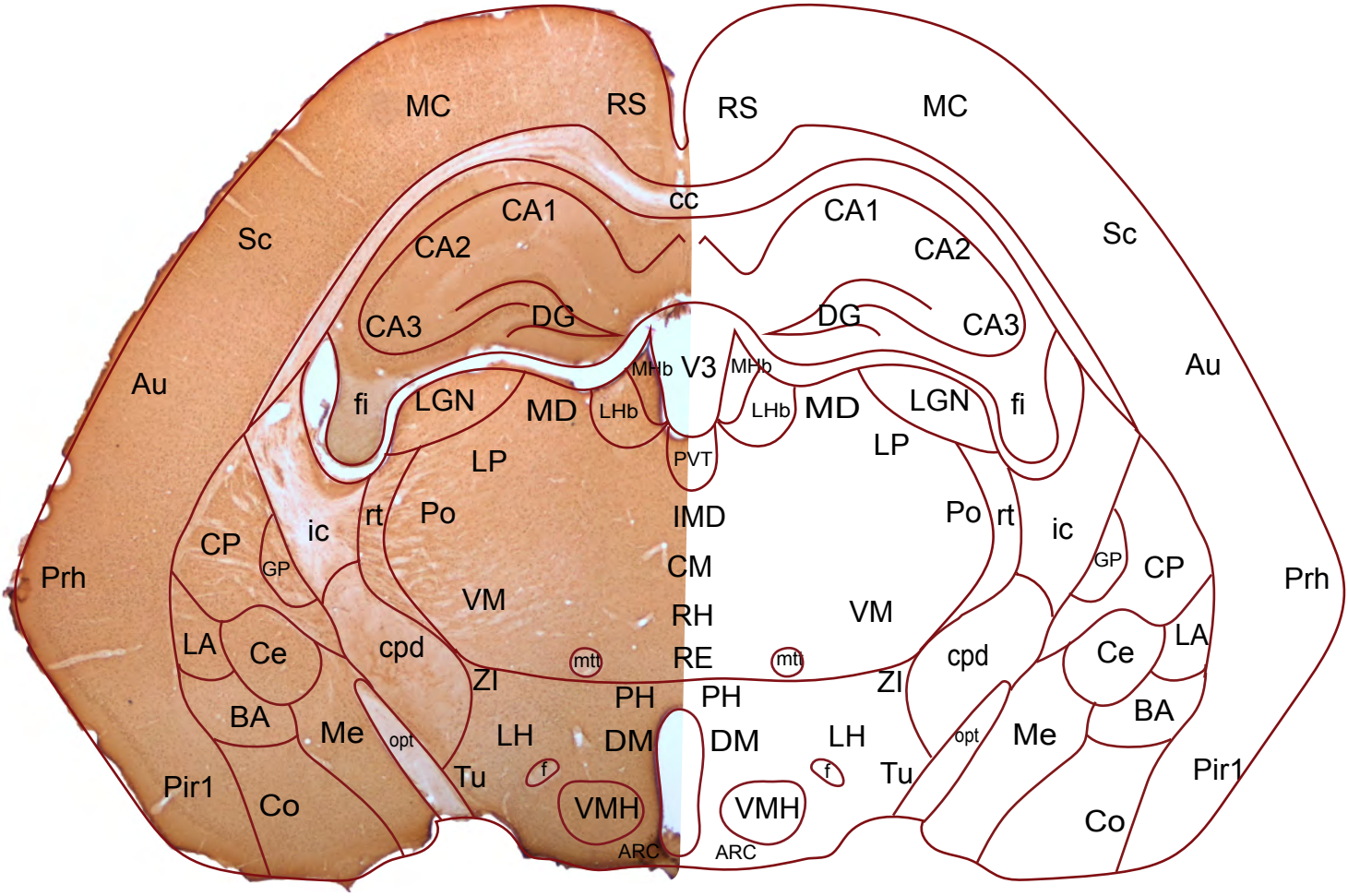

Set 27: Nissl oc +2000µm

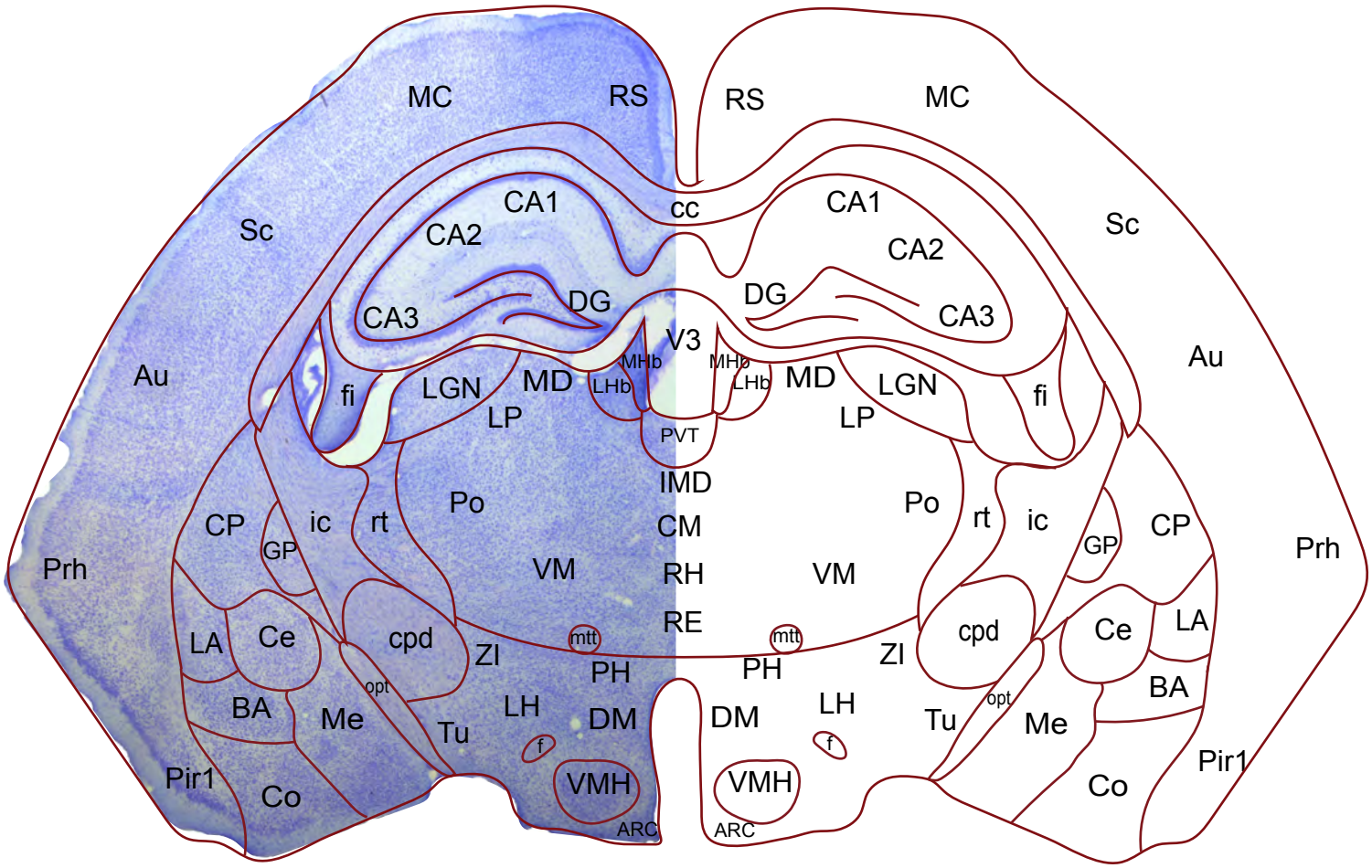

Set 27: OXT oc +2050µm

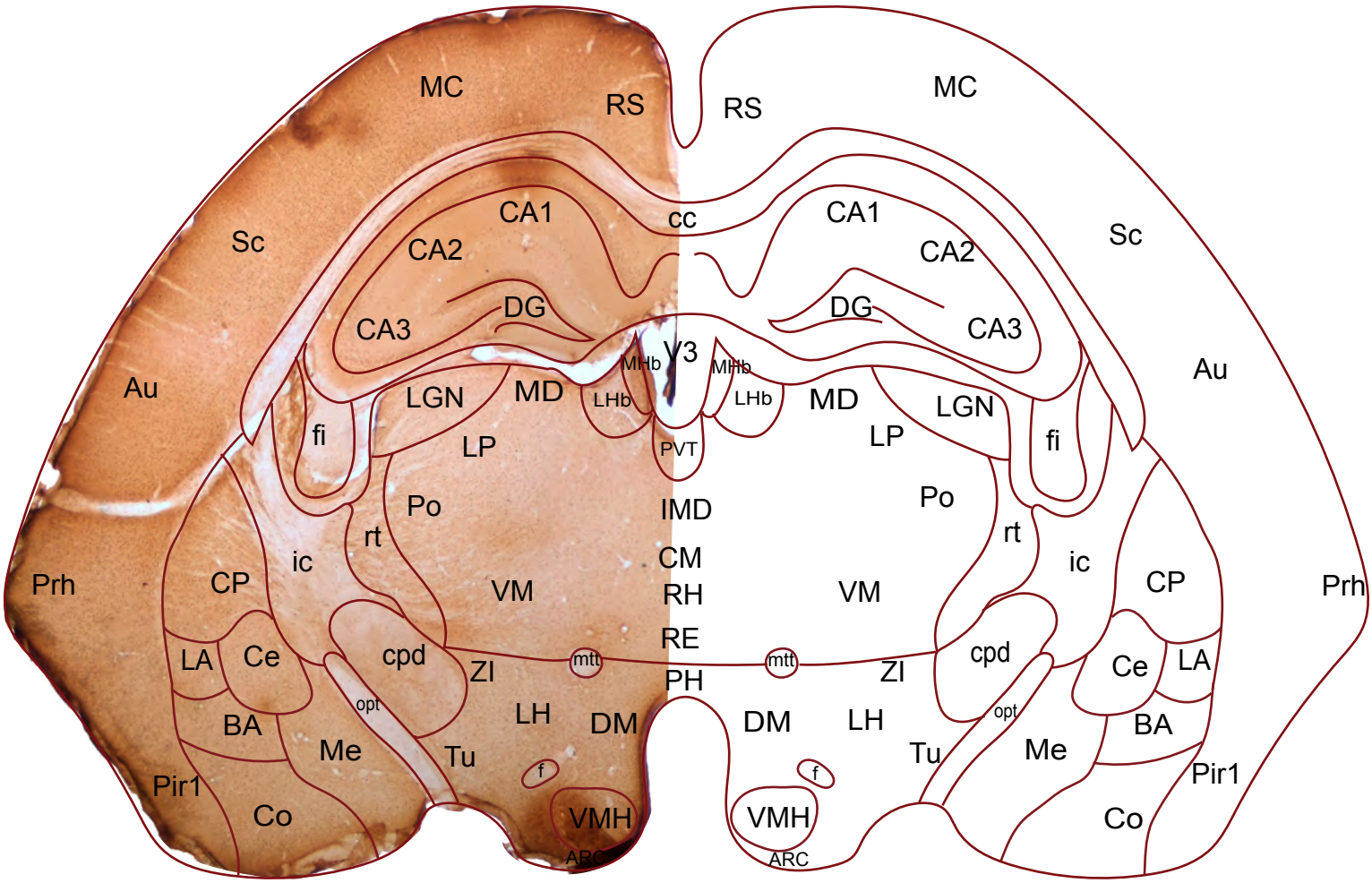

Set 27: Myelin oc +2100µm

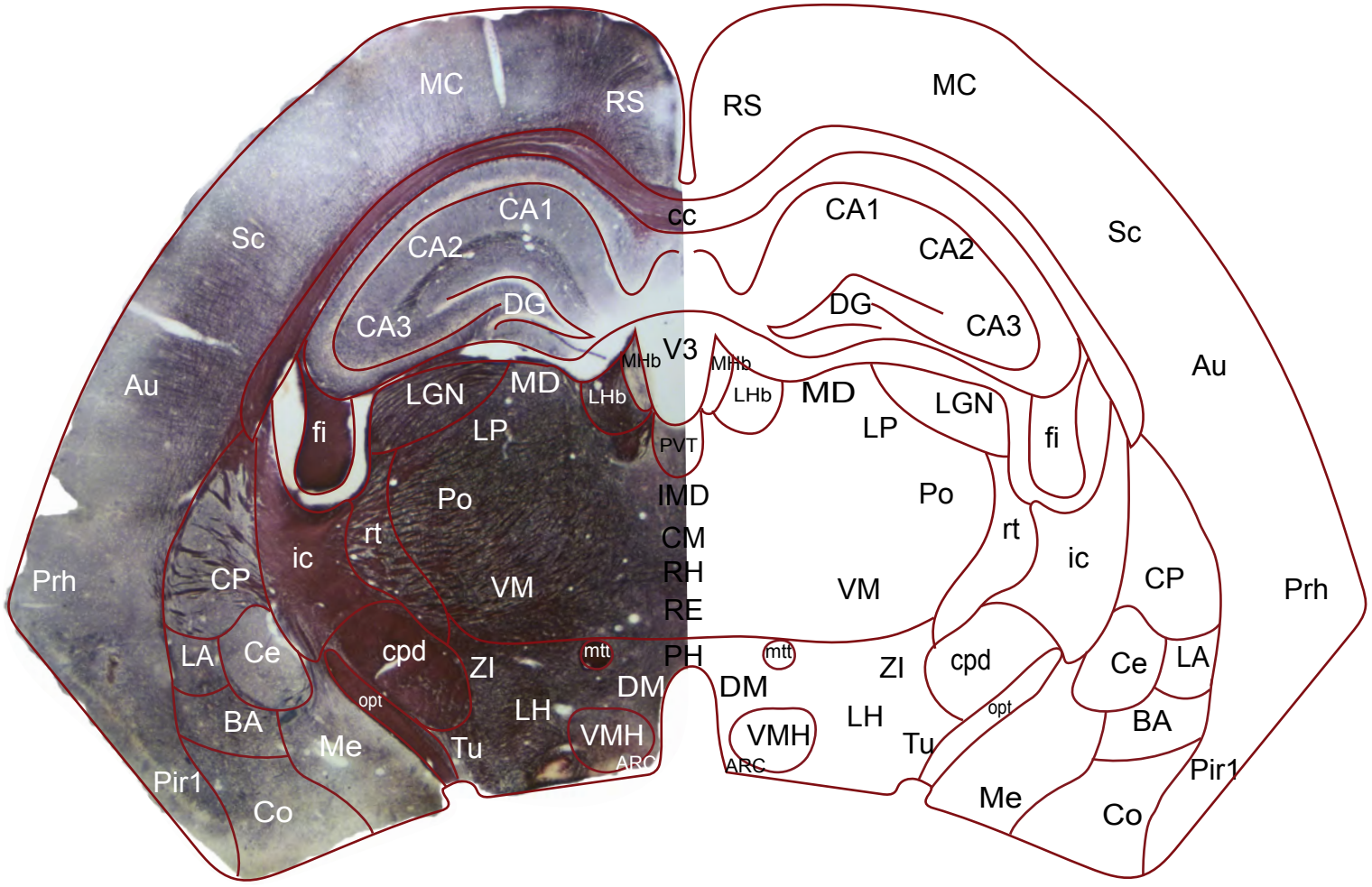

Set 28: OXT oc +2150µm

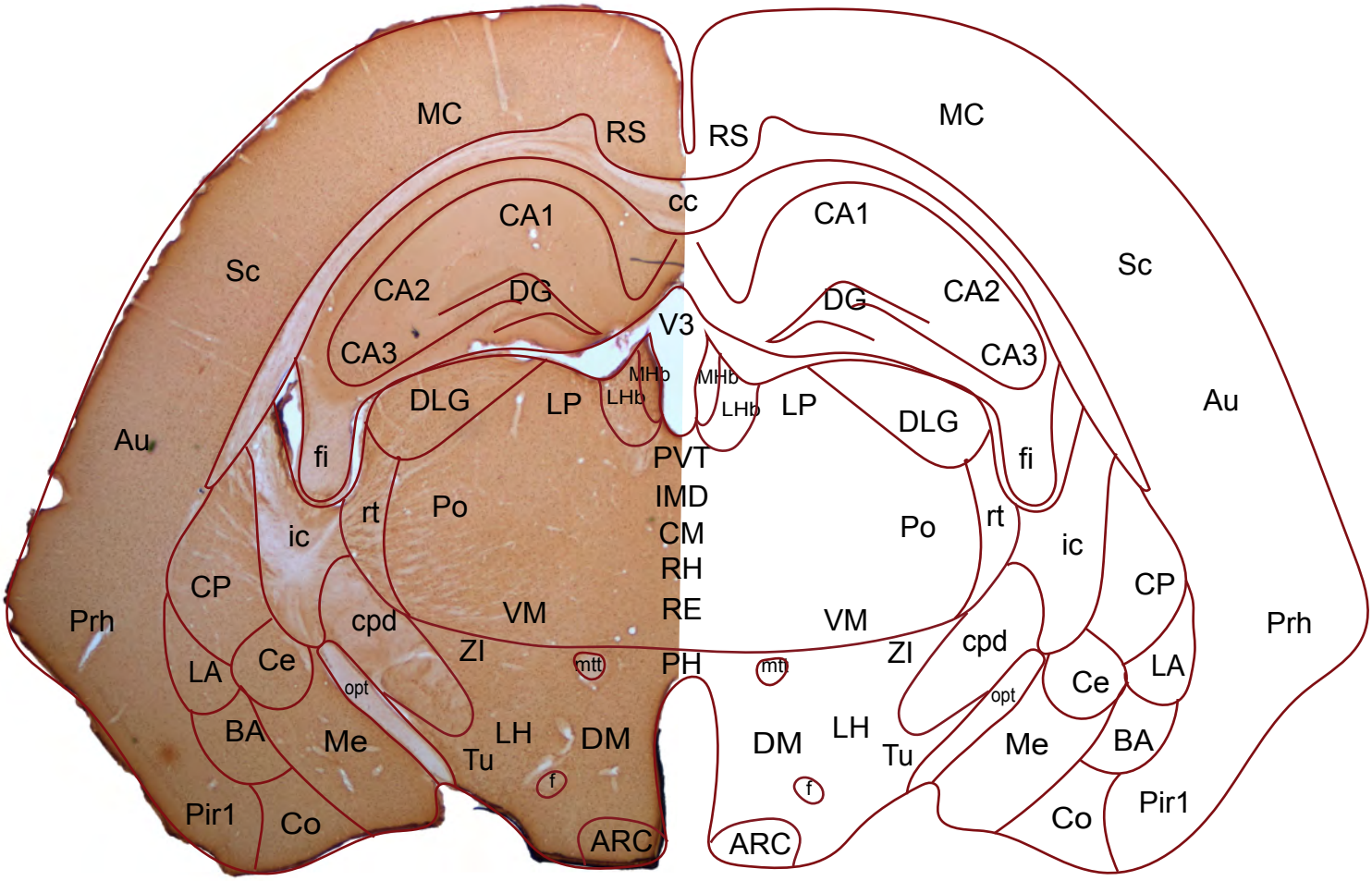

Set 28: Nissl oc +2200µm

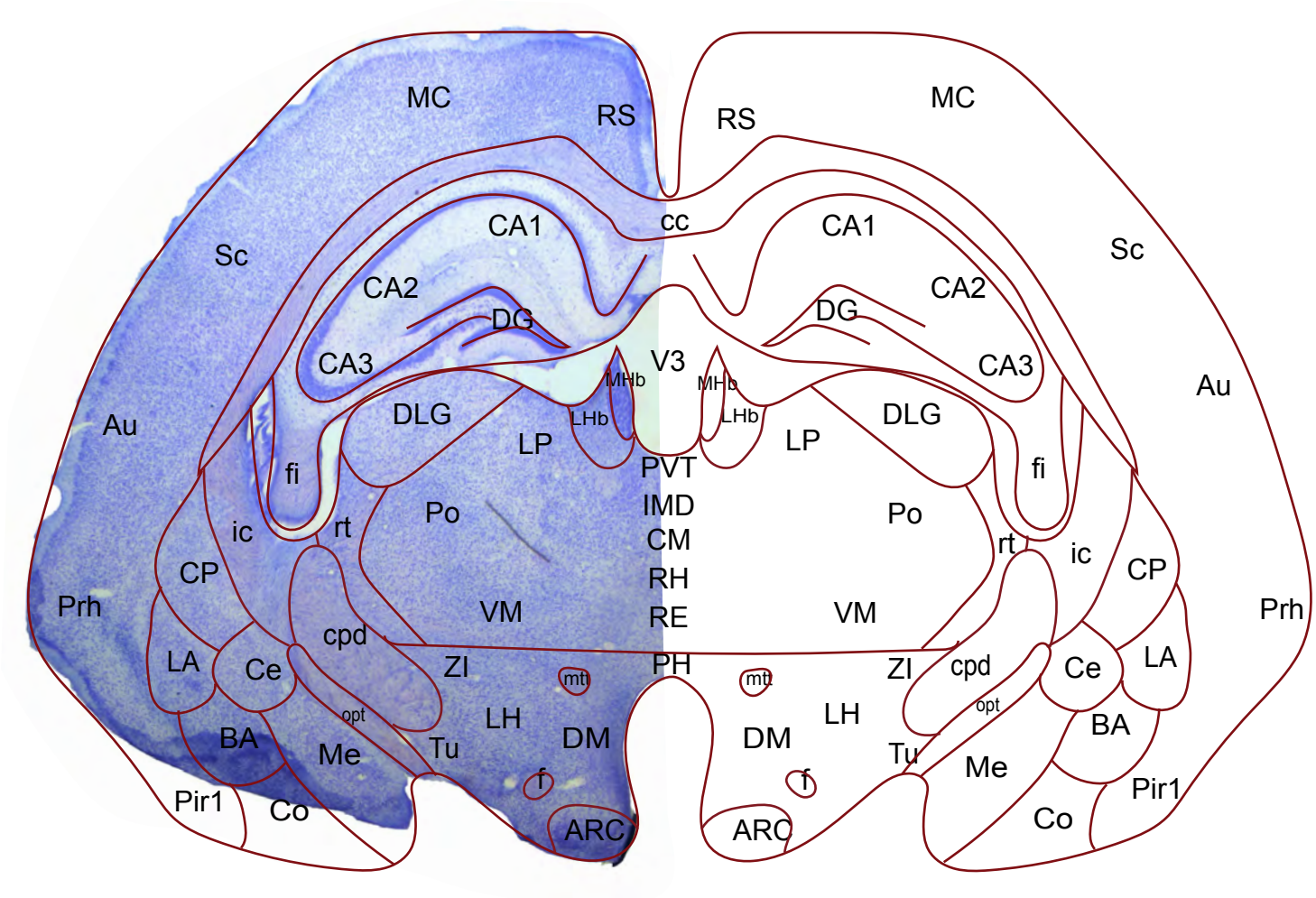

Set 28: OXT oc +2250µm

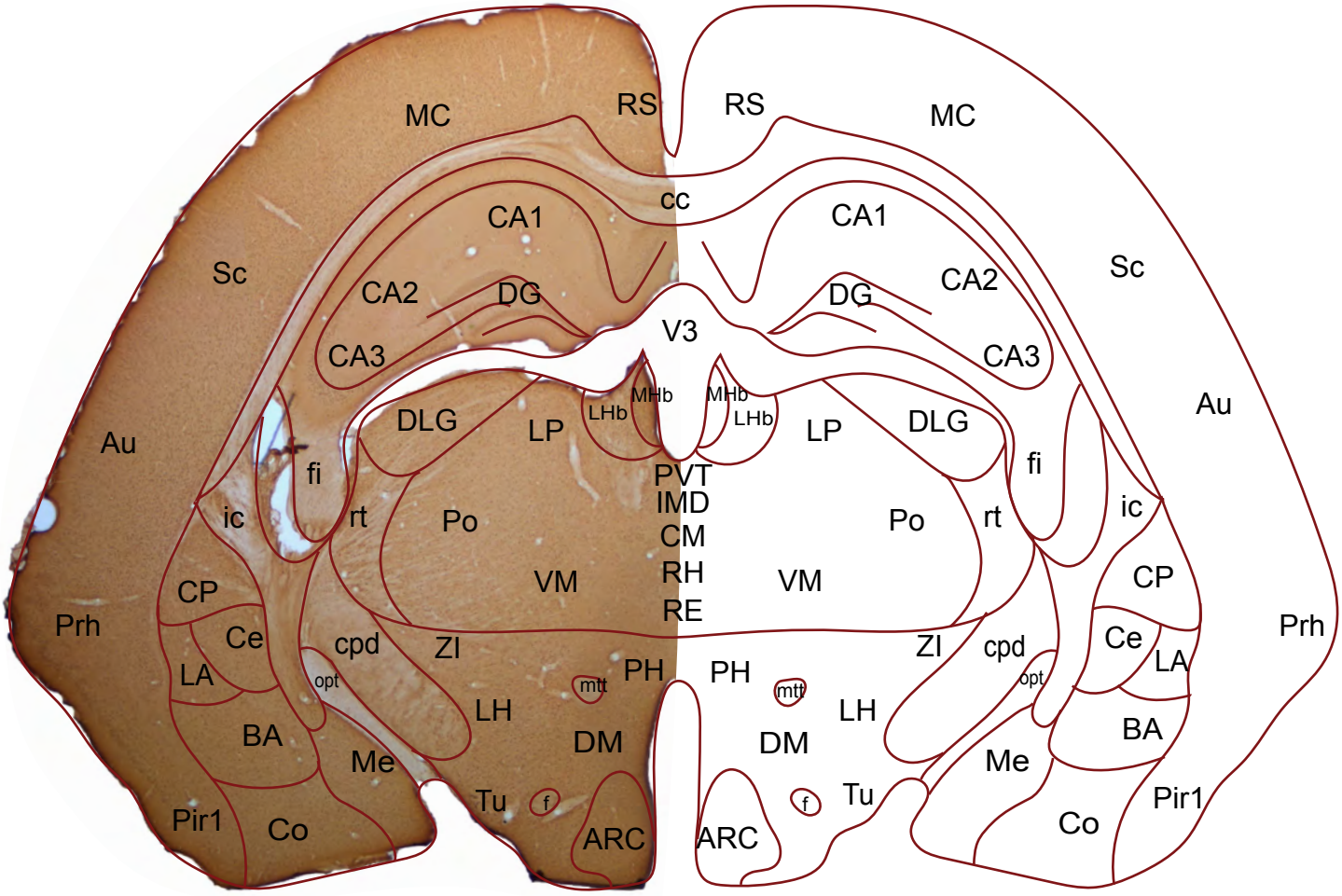

Set 28: Myelin oc +2300µm

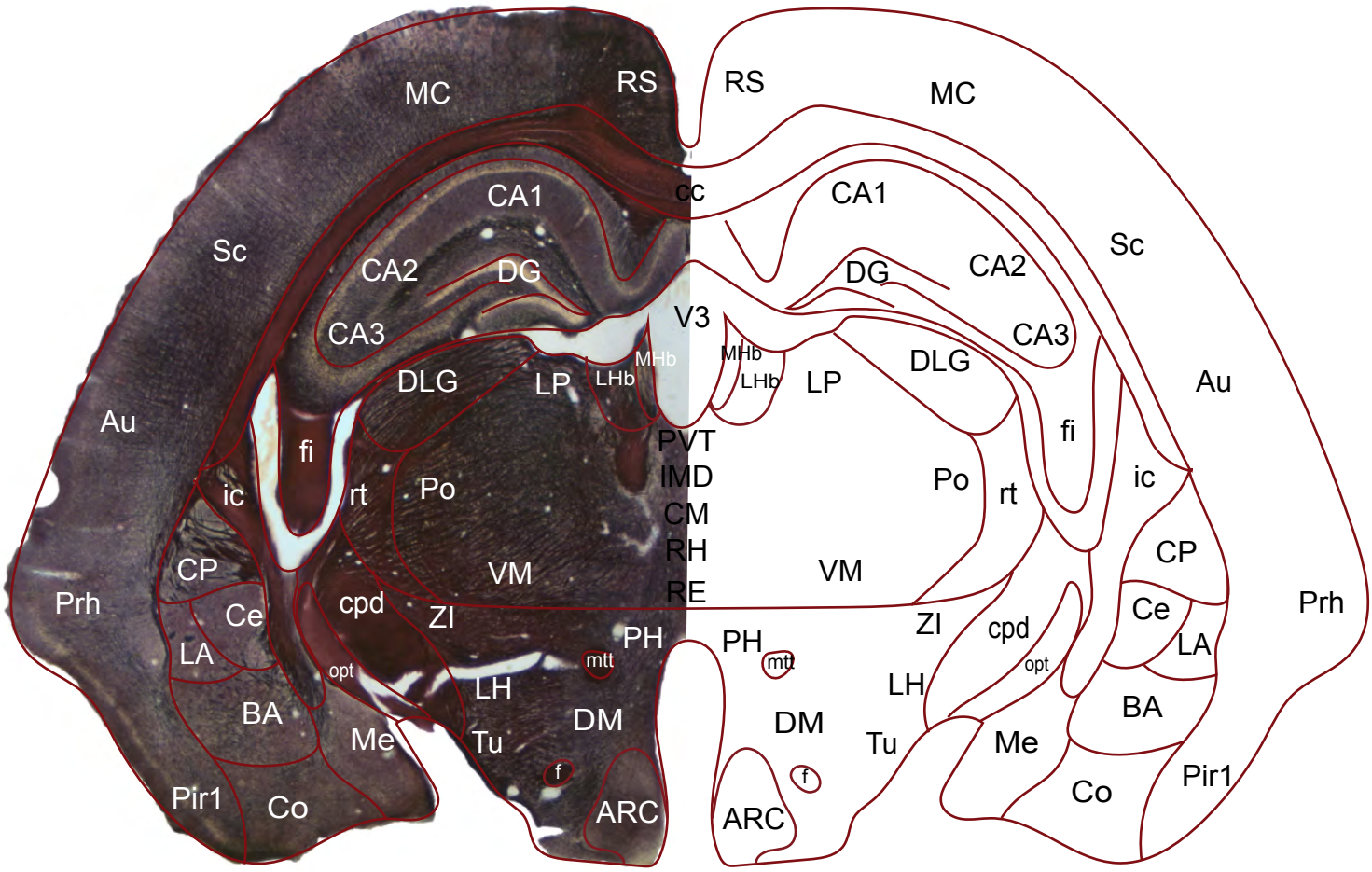

Set 29: OXT oc +2350µm

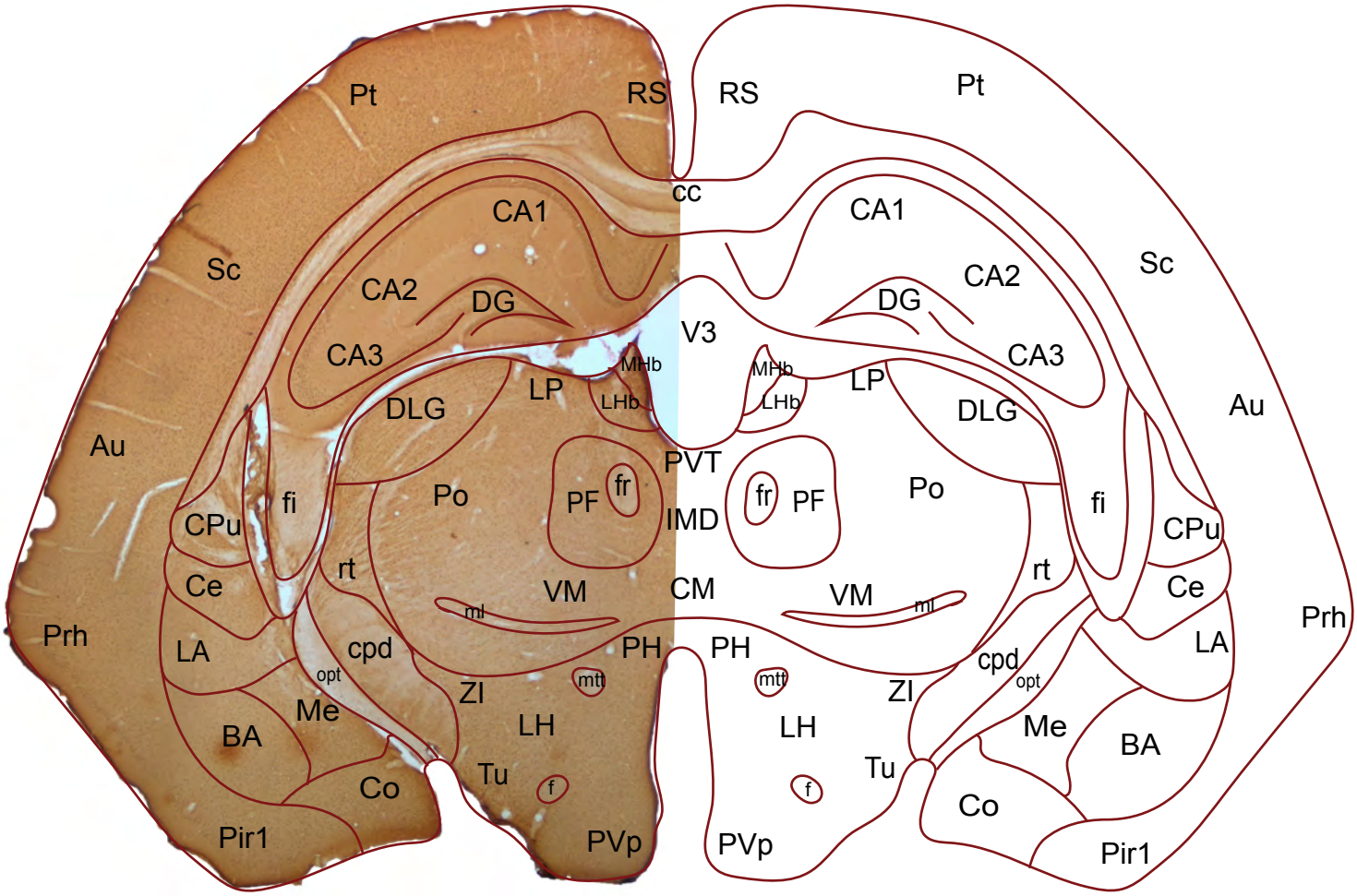

Set 29: Nissl oc +2400µm

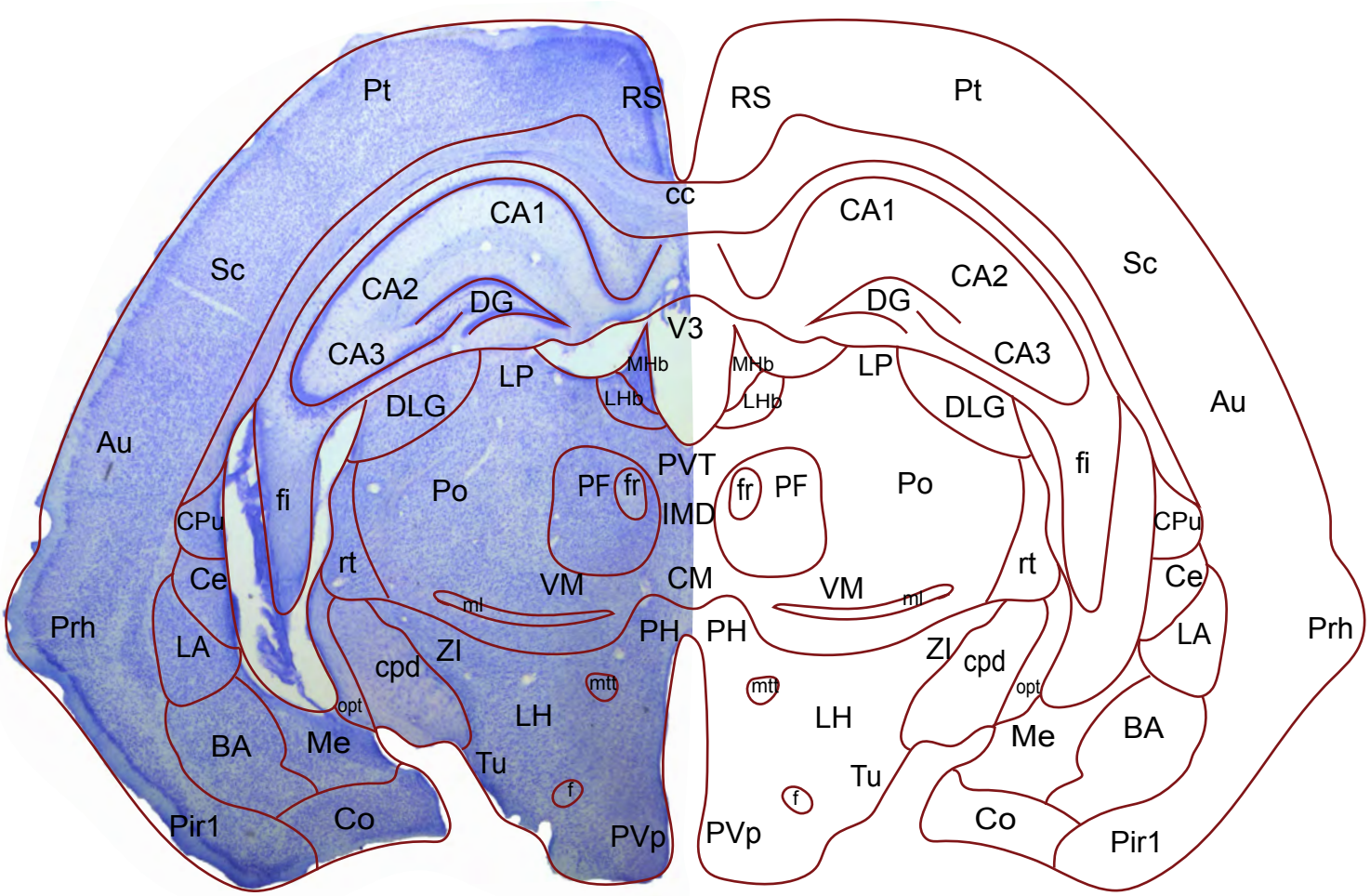

Set 29: OXT oc +2450µm

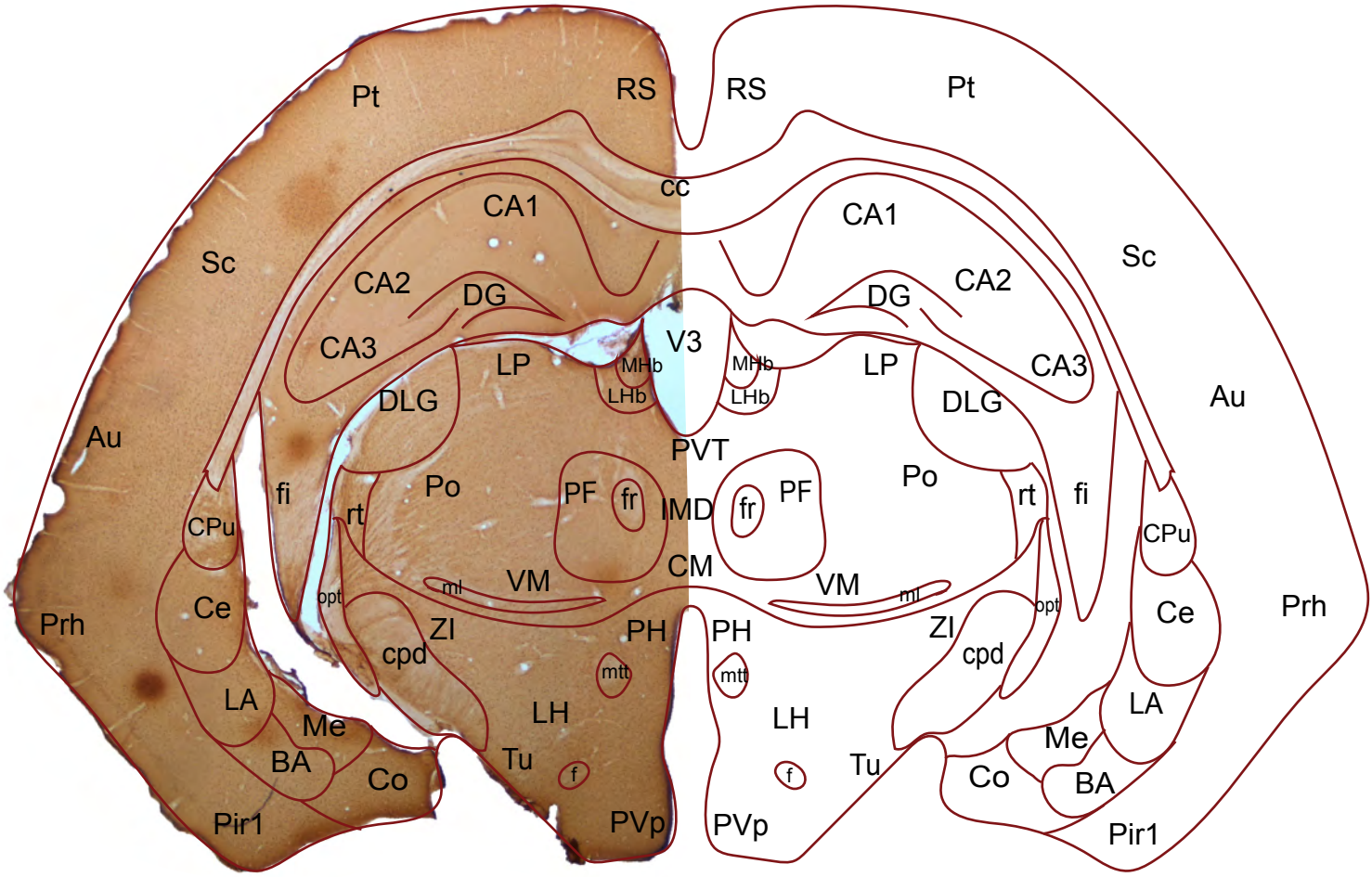

Set 29: Myelin oc +2500µm

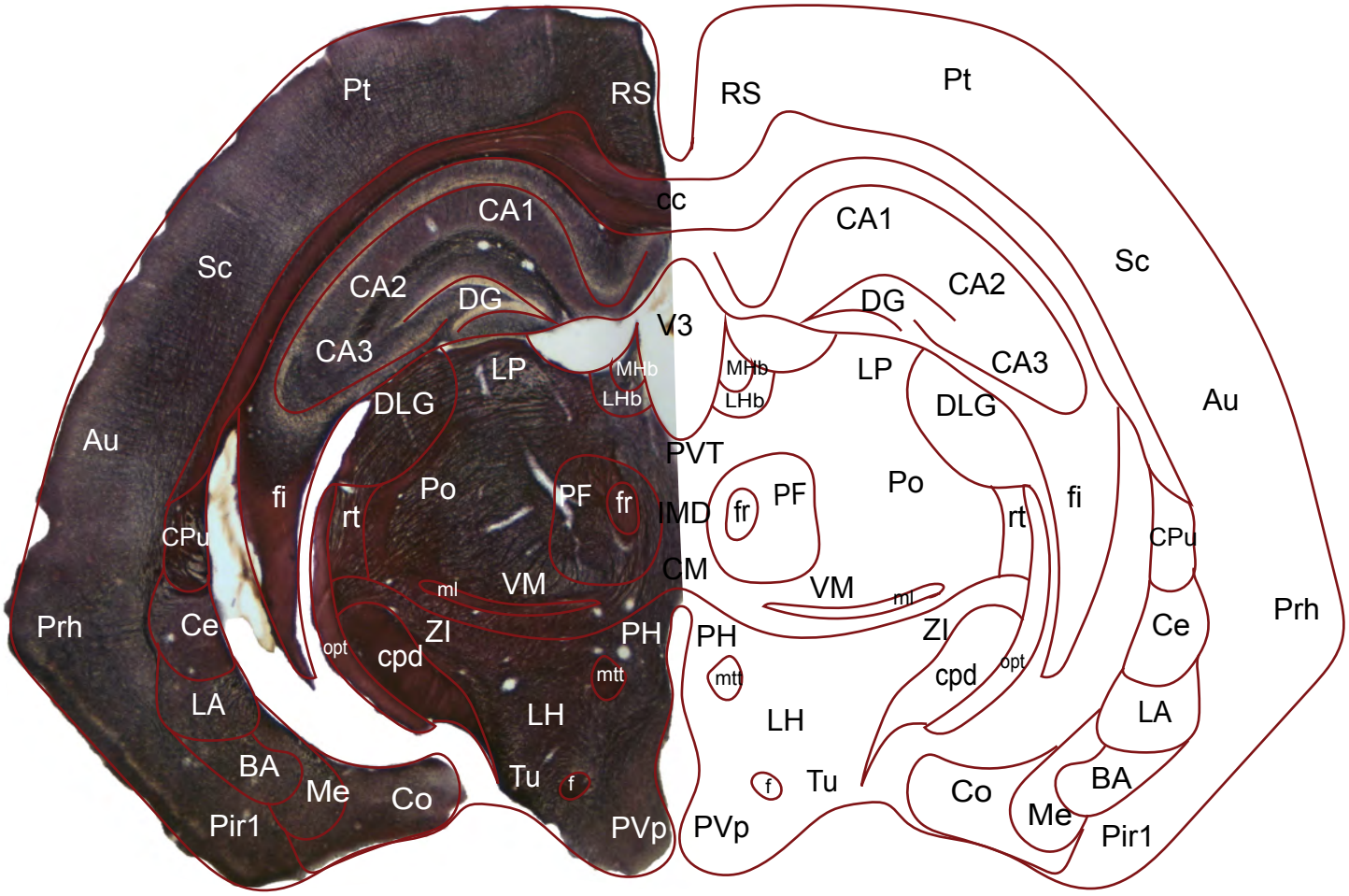

Set 30: OXT oc +2550µm

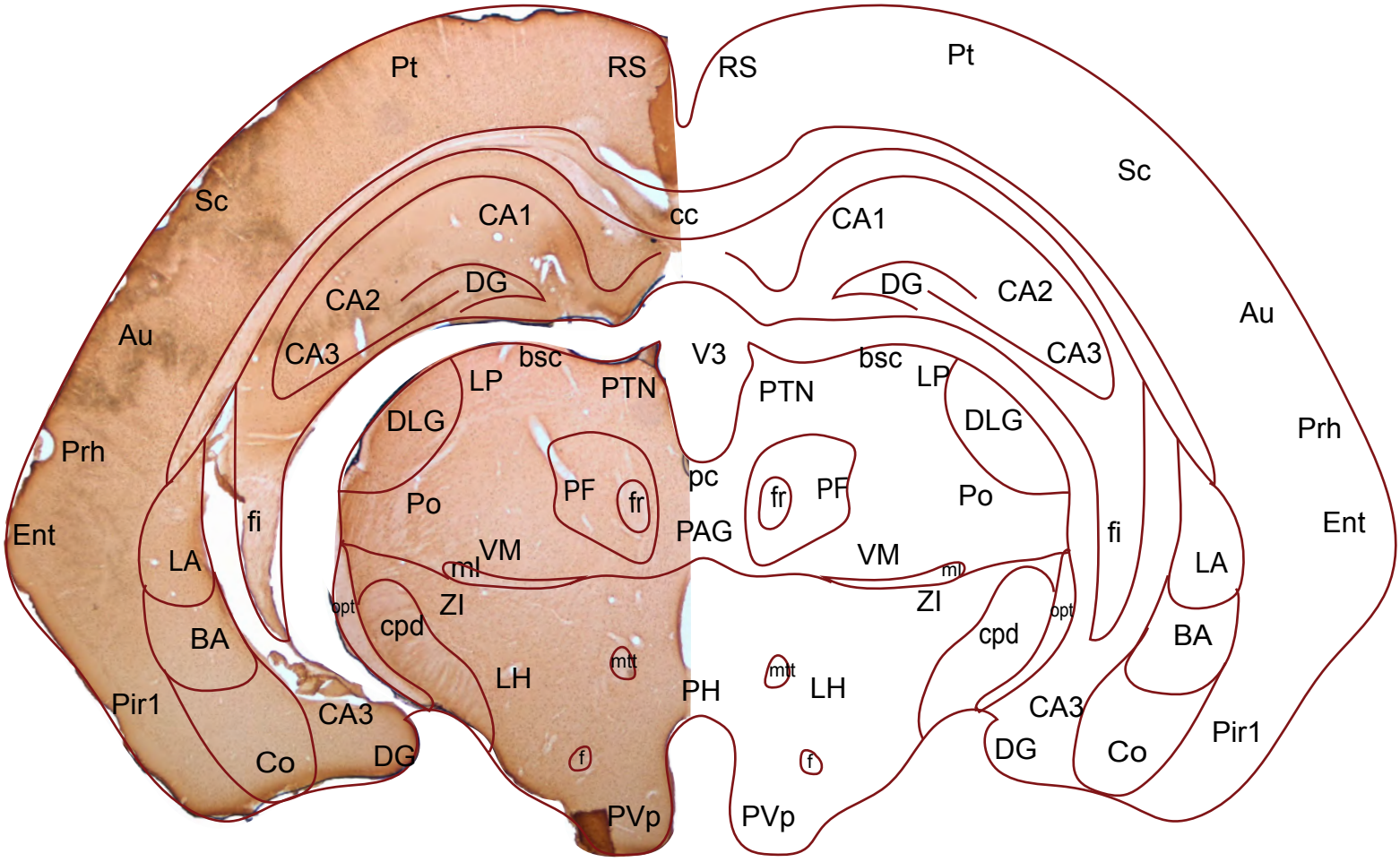

Set 30: Nissl oc +2600µm

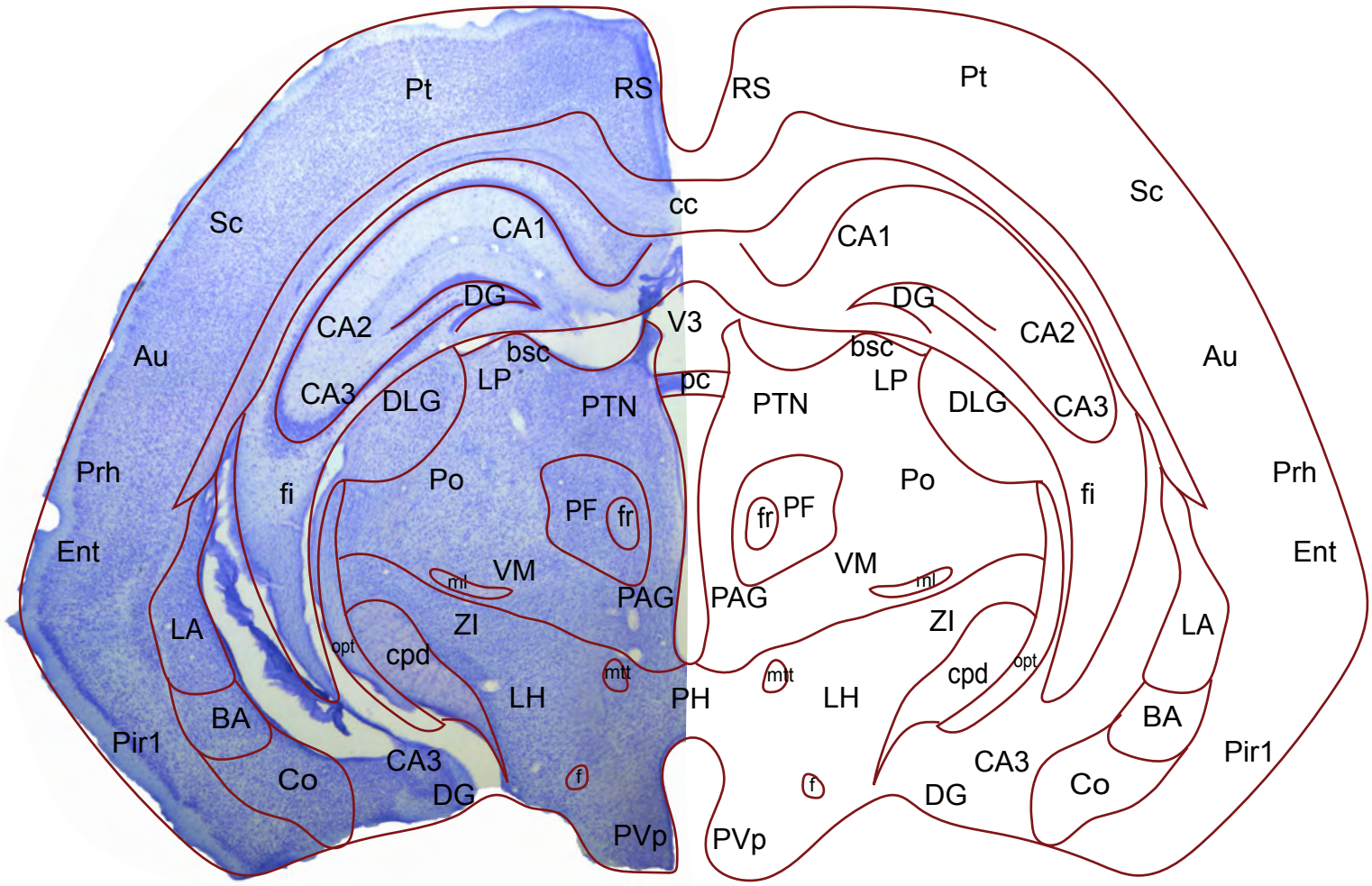

Set 30: OXT oc +2650µm

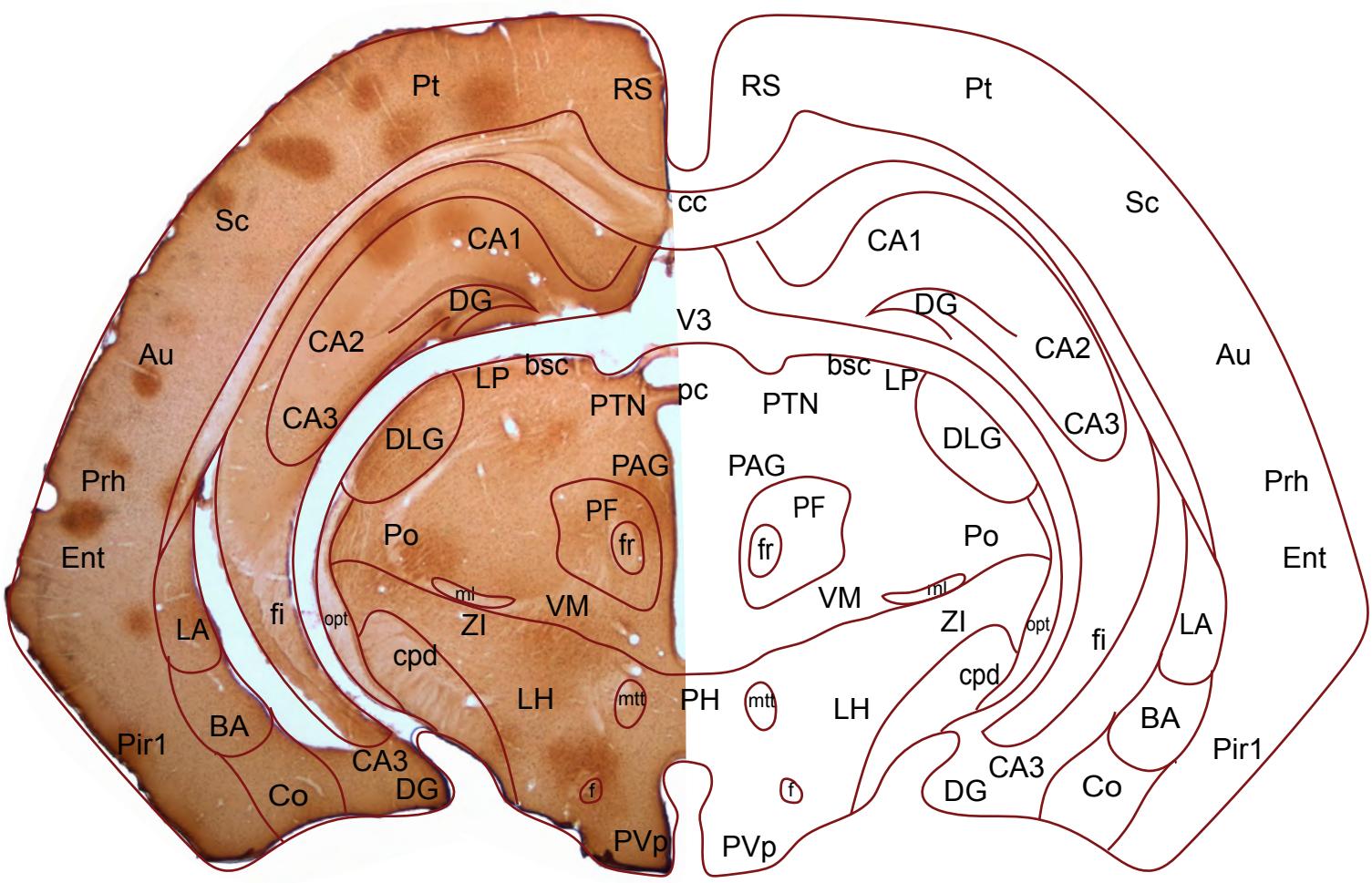

Set 30: Myelin oc +2700µm

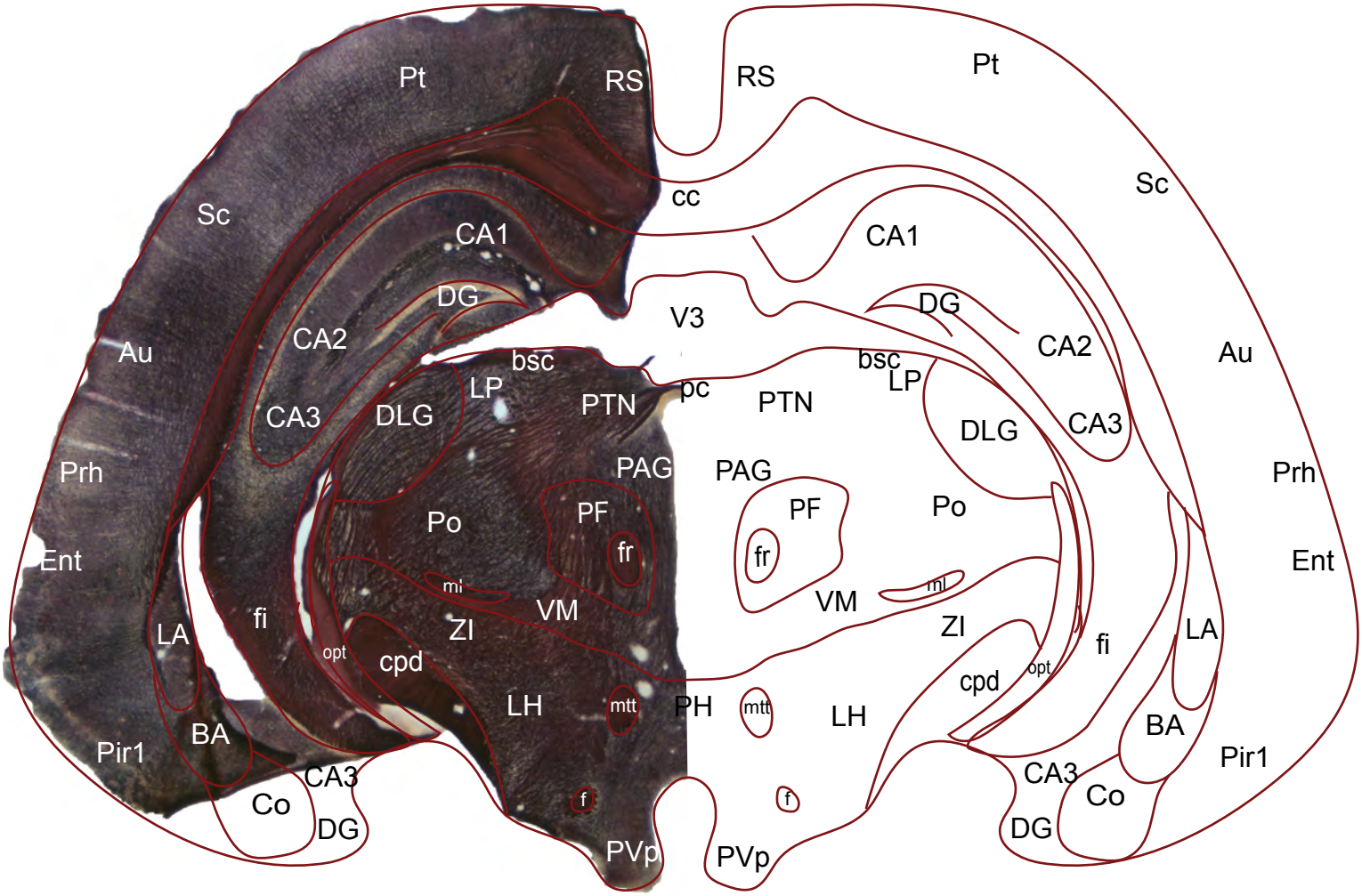

Set 31: OXT oc +2750µm

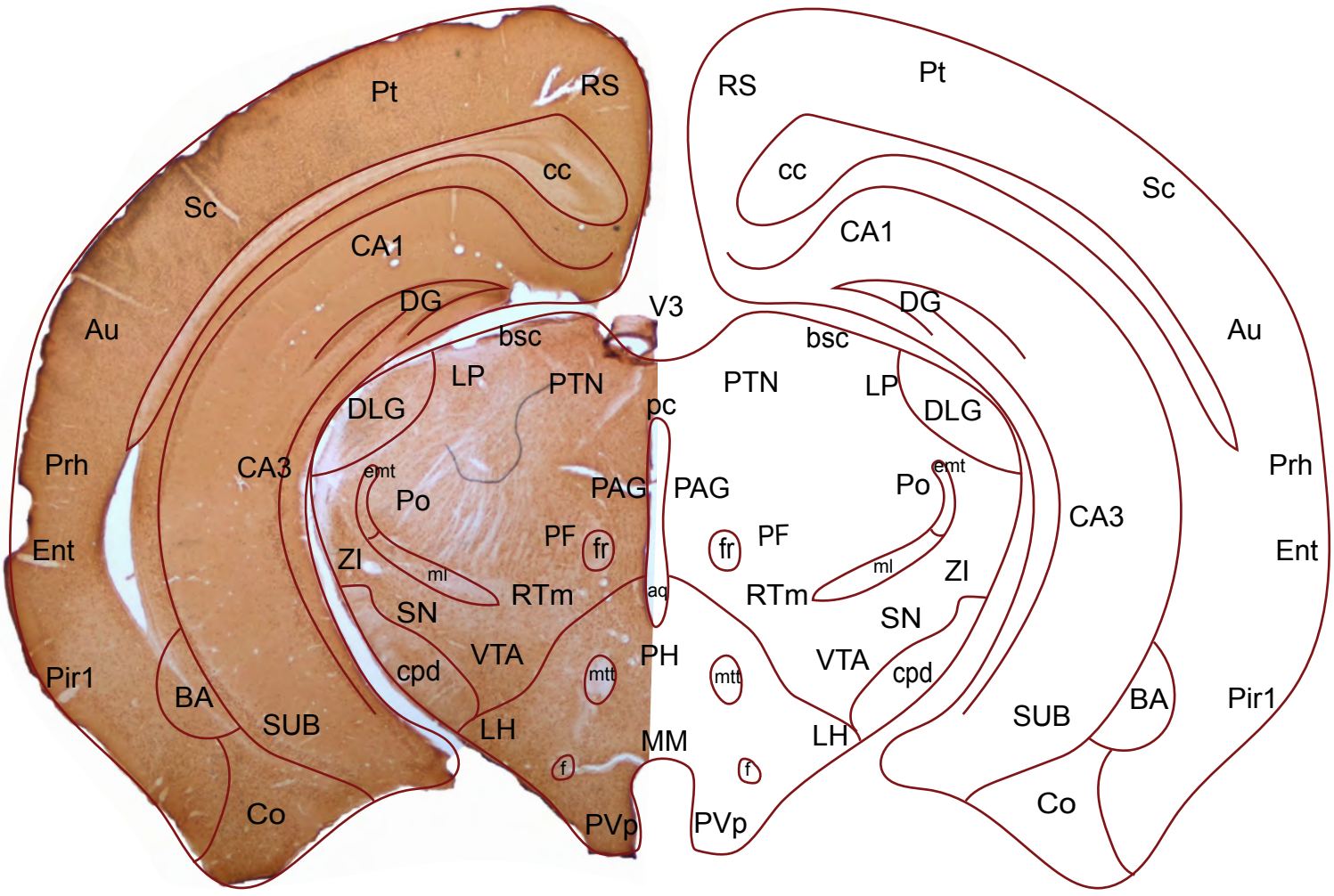

Set 31: Nissl oc +2800µm

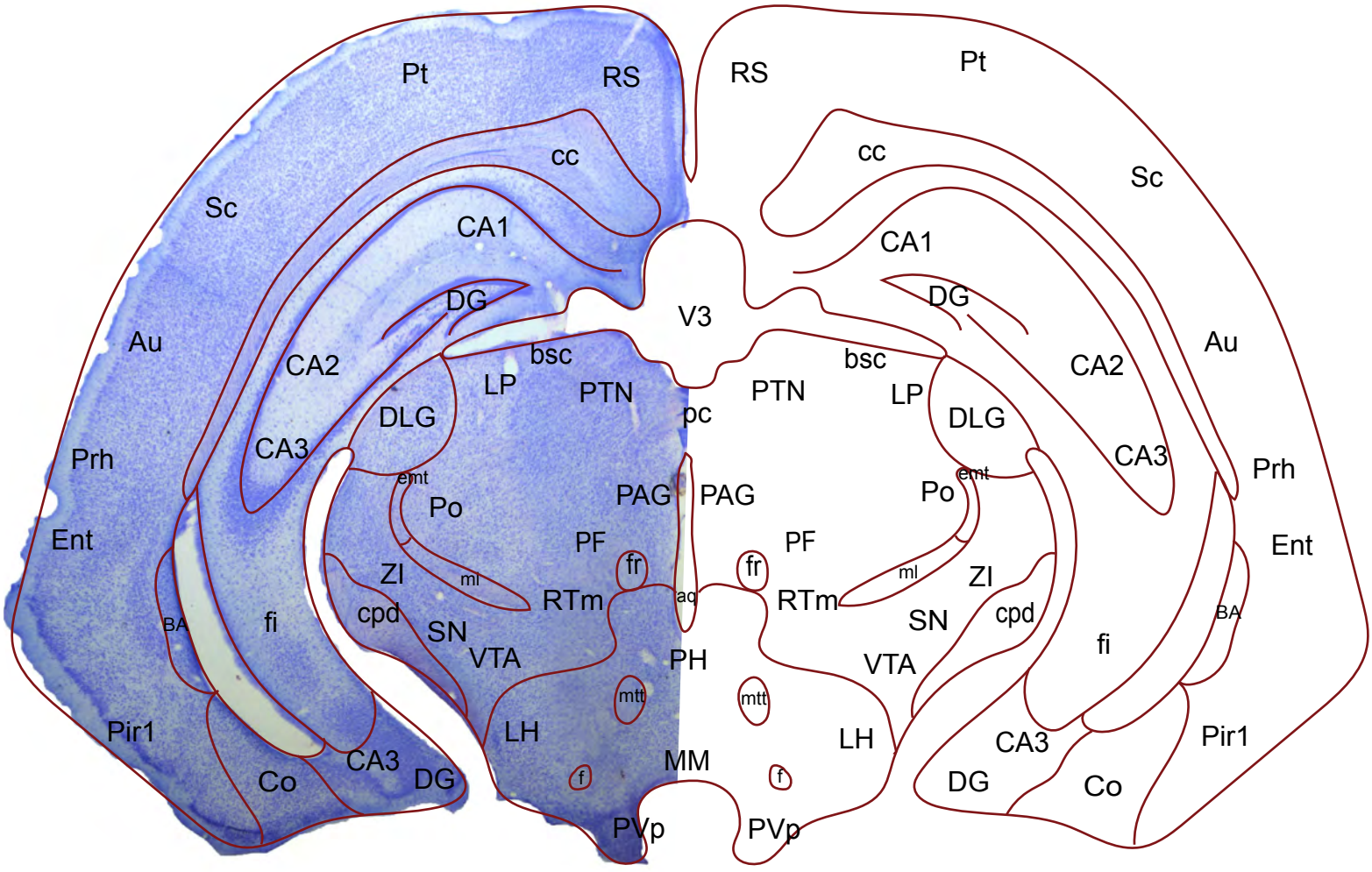

Set 31: OXT oc +2850µm

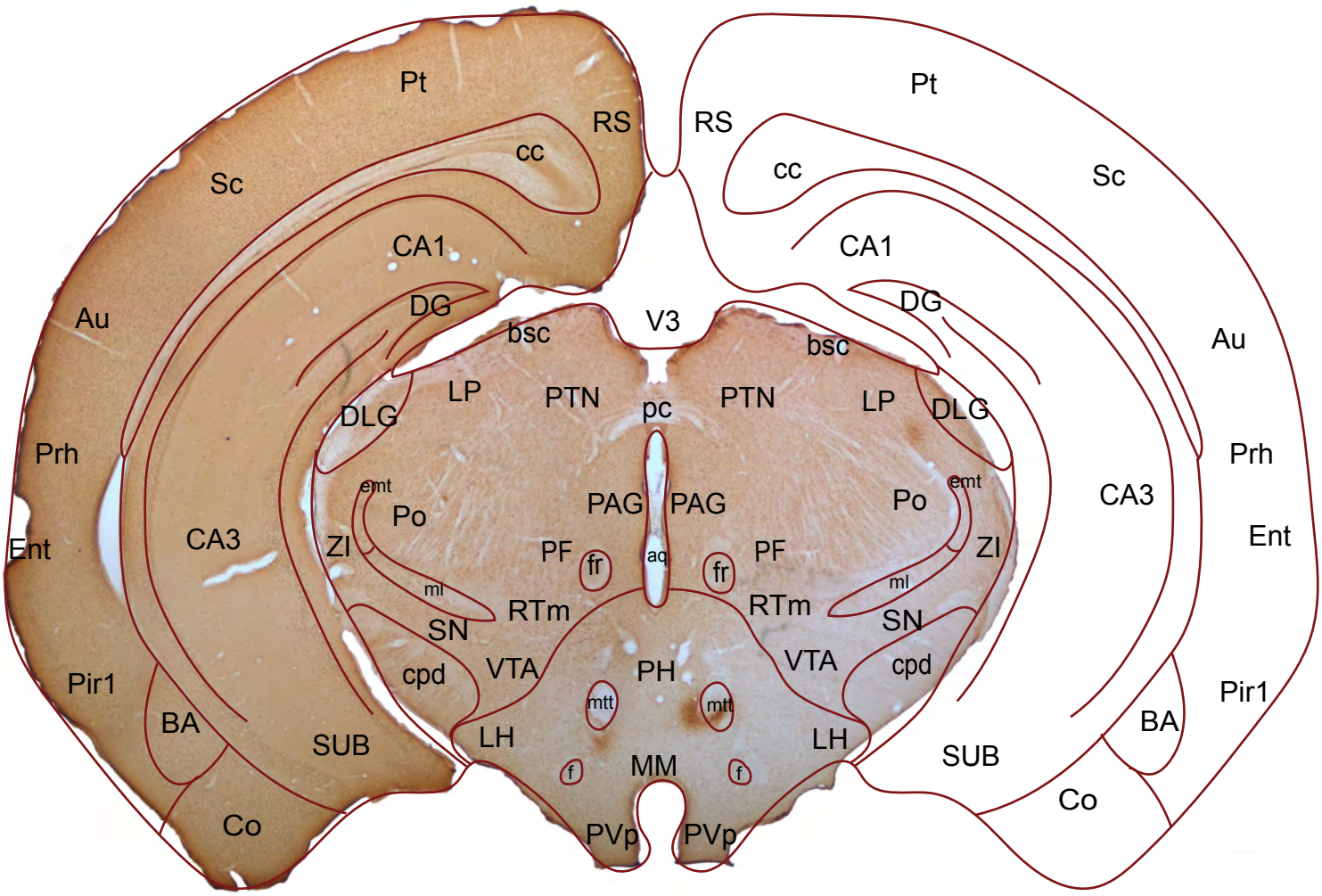

Set 31: Myelin oc +2900µm

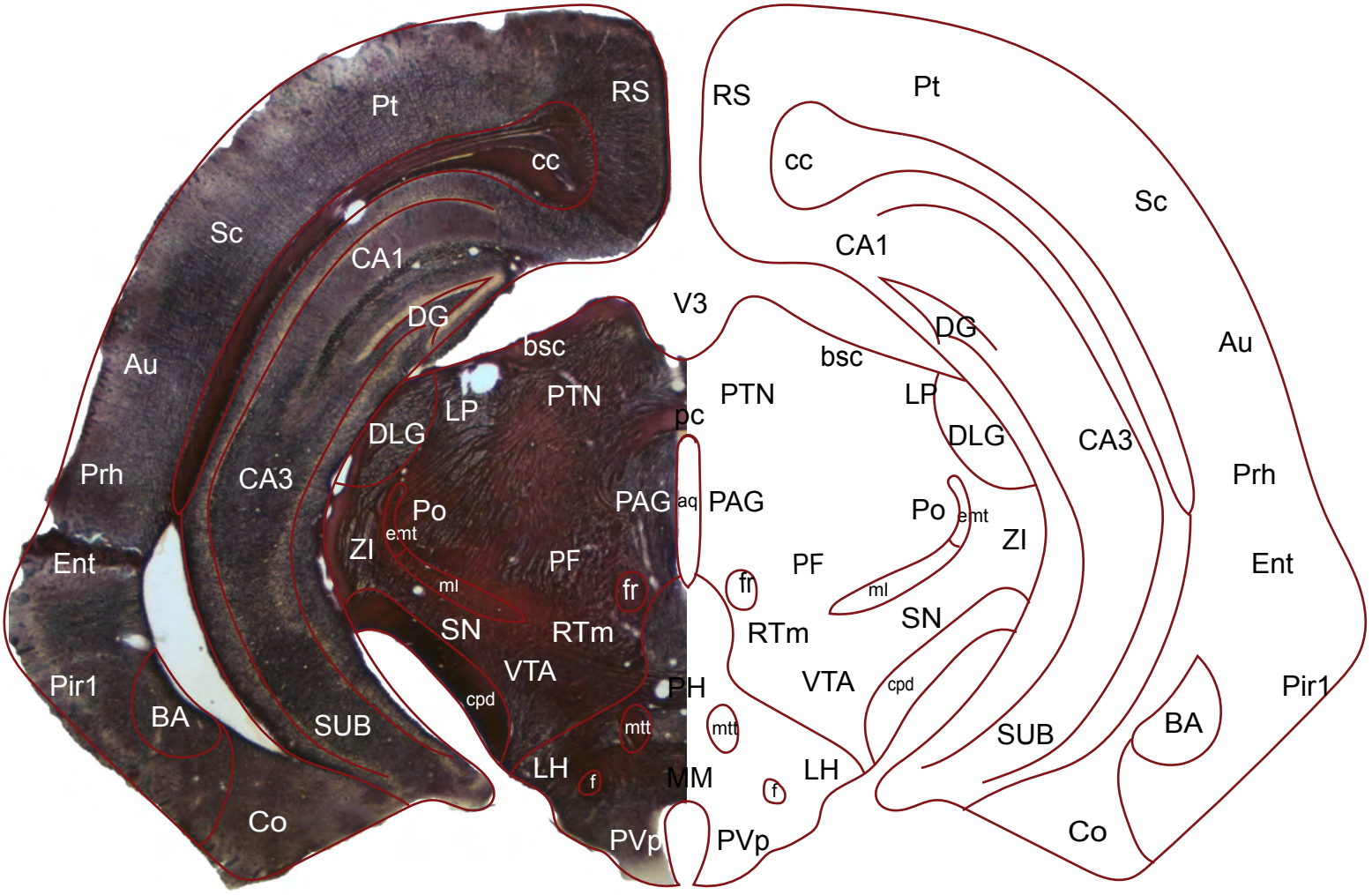

Set 32: OXT oc +2950µm

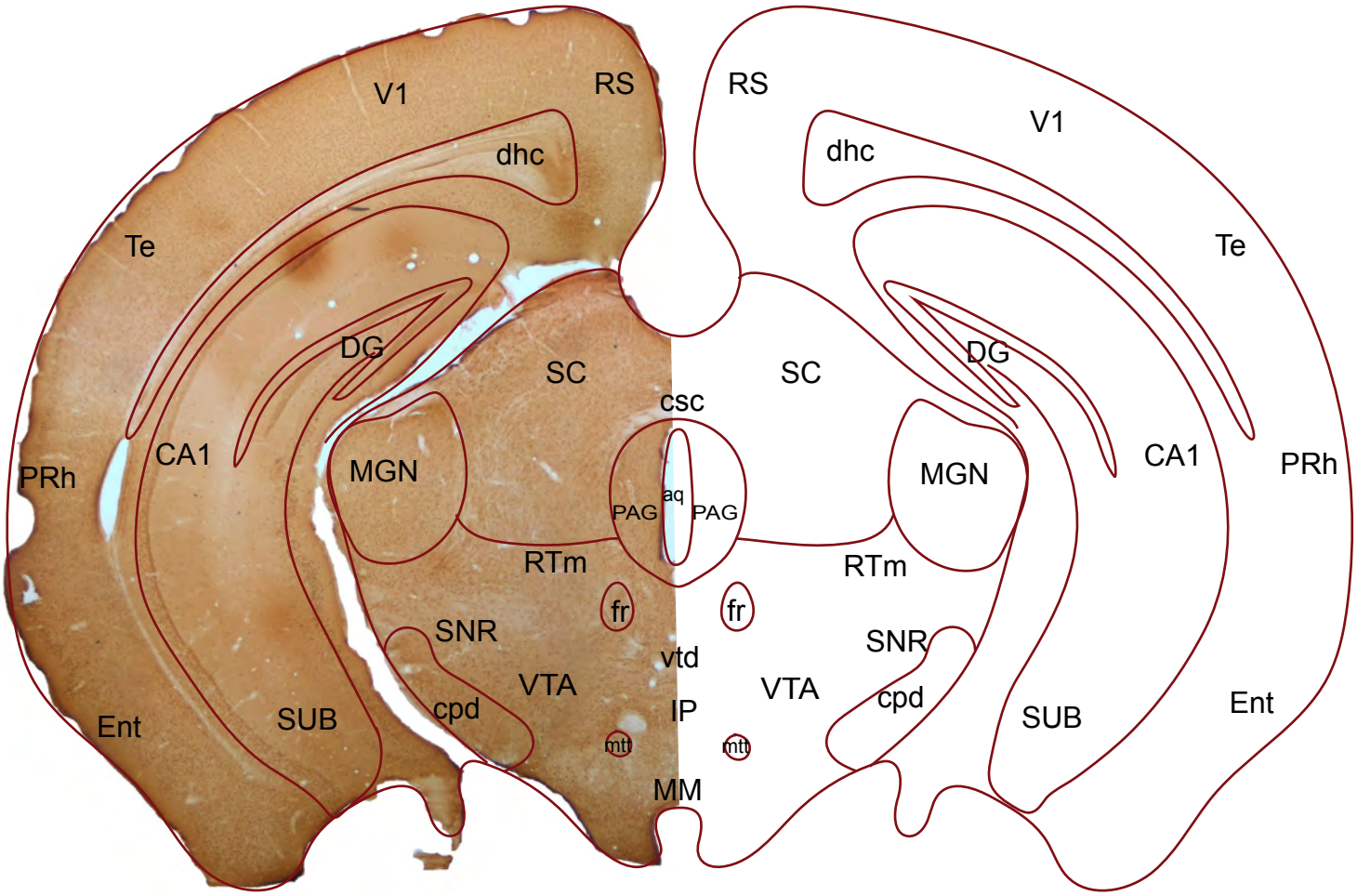

Set 32: Nissl oc +3000µm

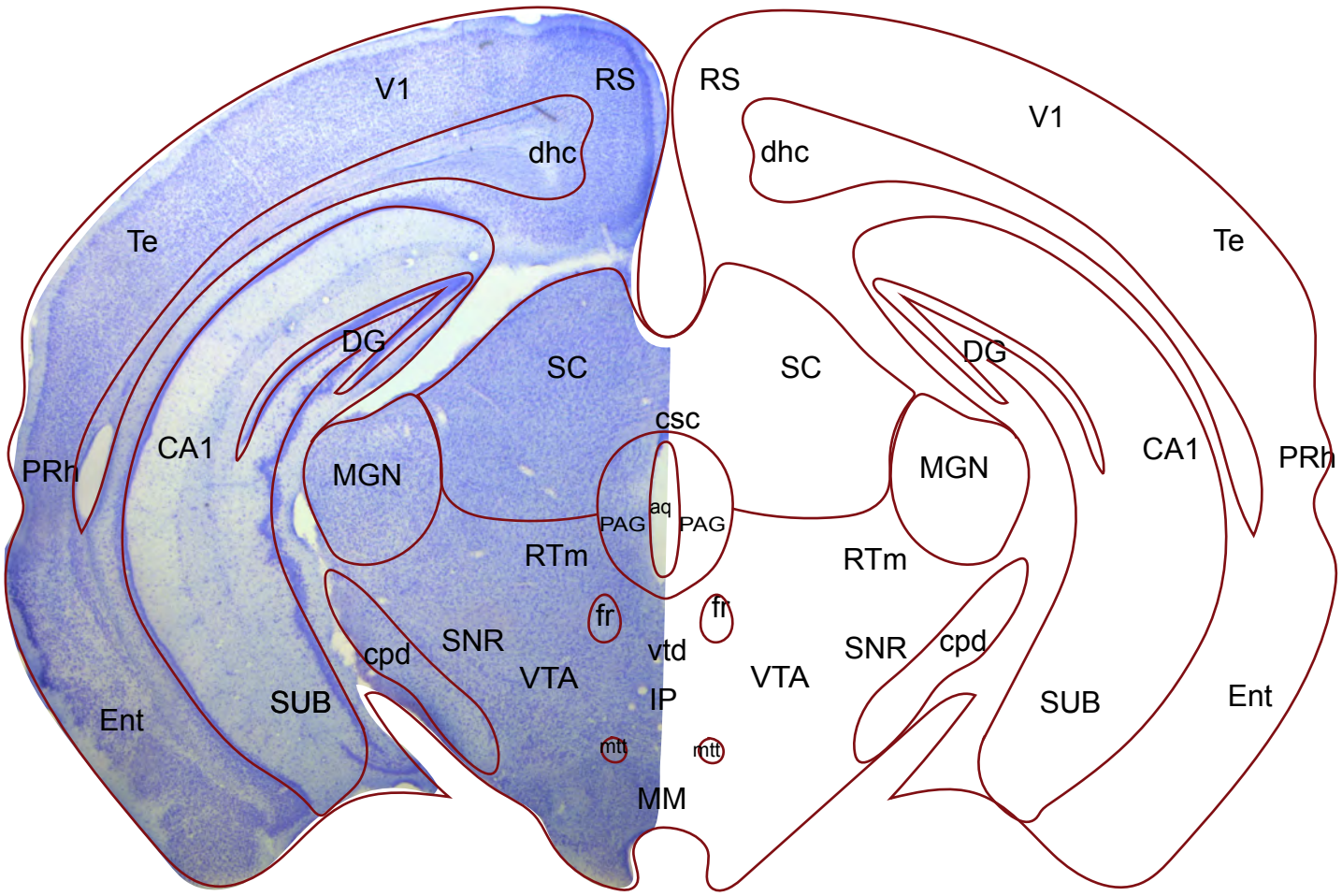

Set 32: OXT oc +3050µm

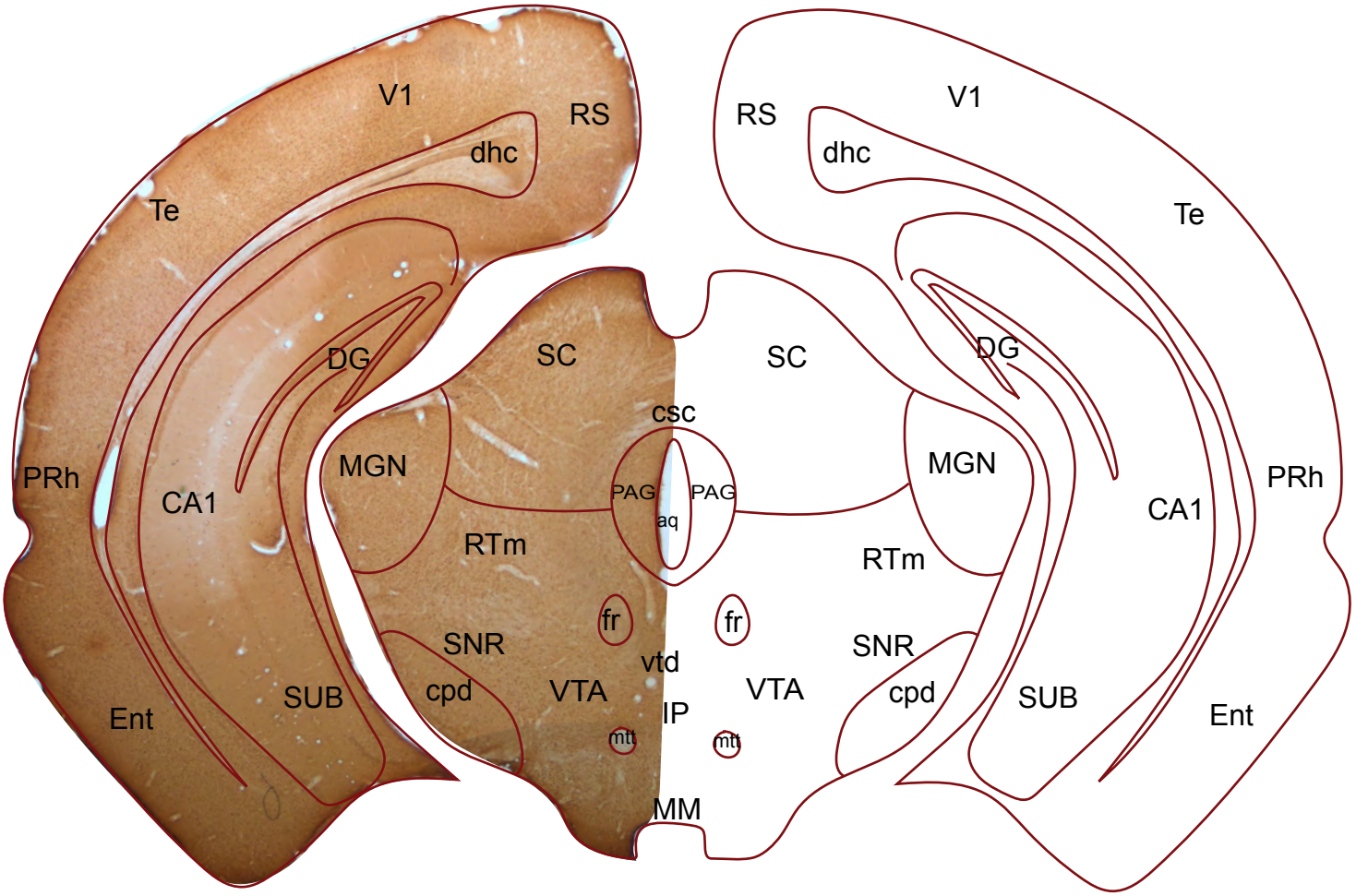

Set 32: Myelin oc +3100µm

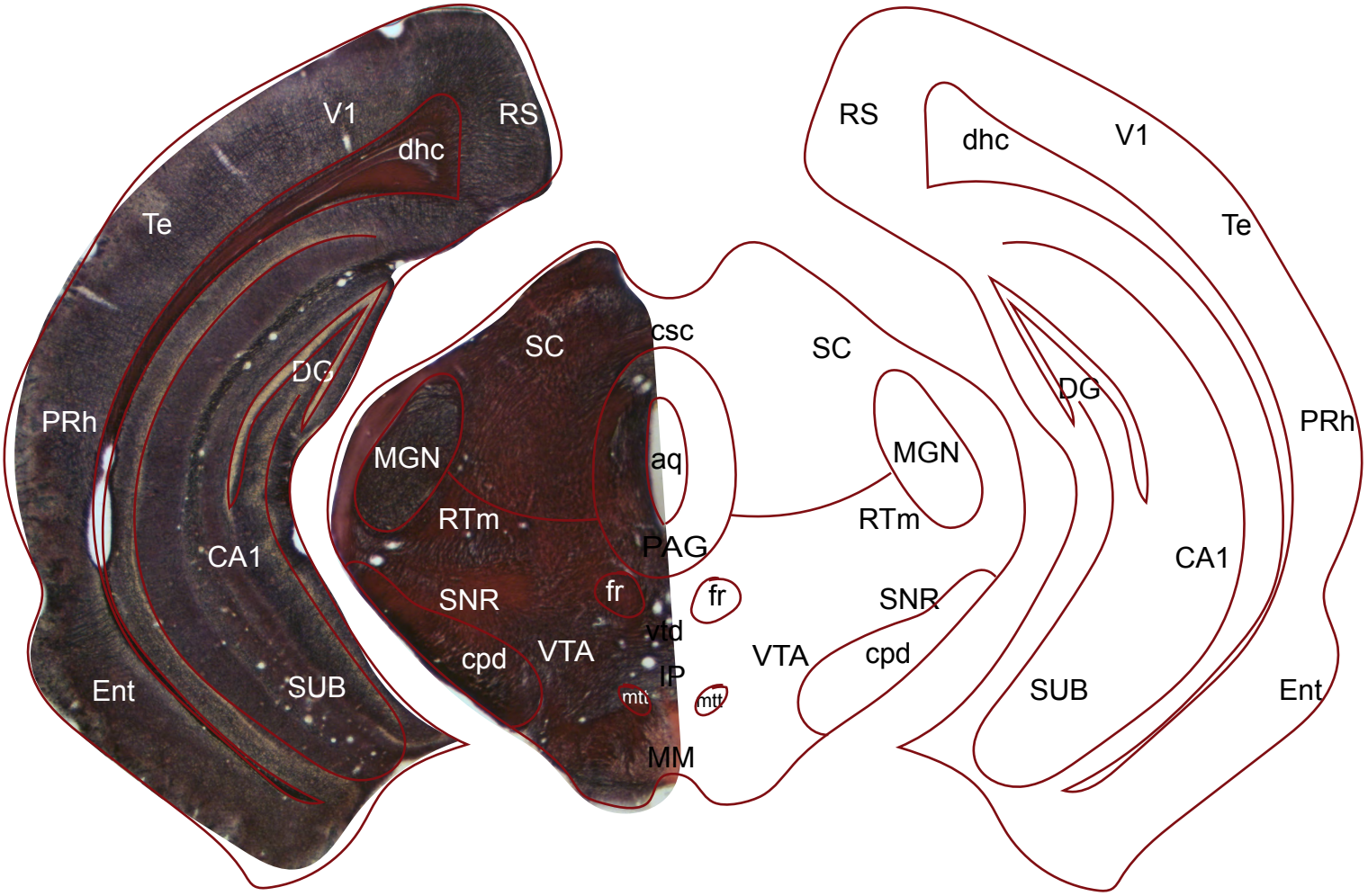

Set 33: OXT oc +3150µm

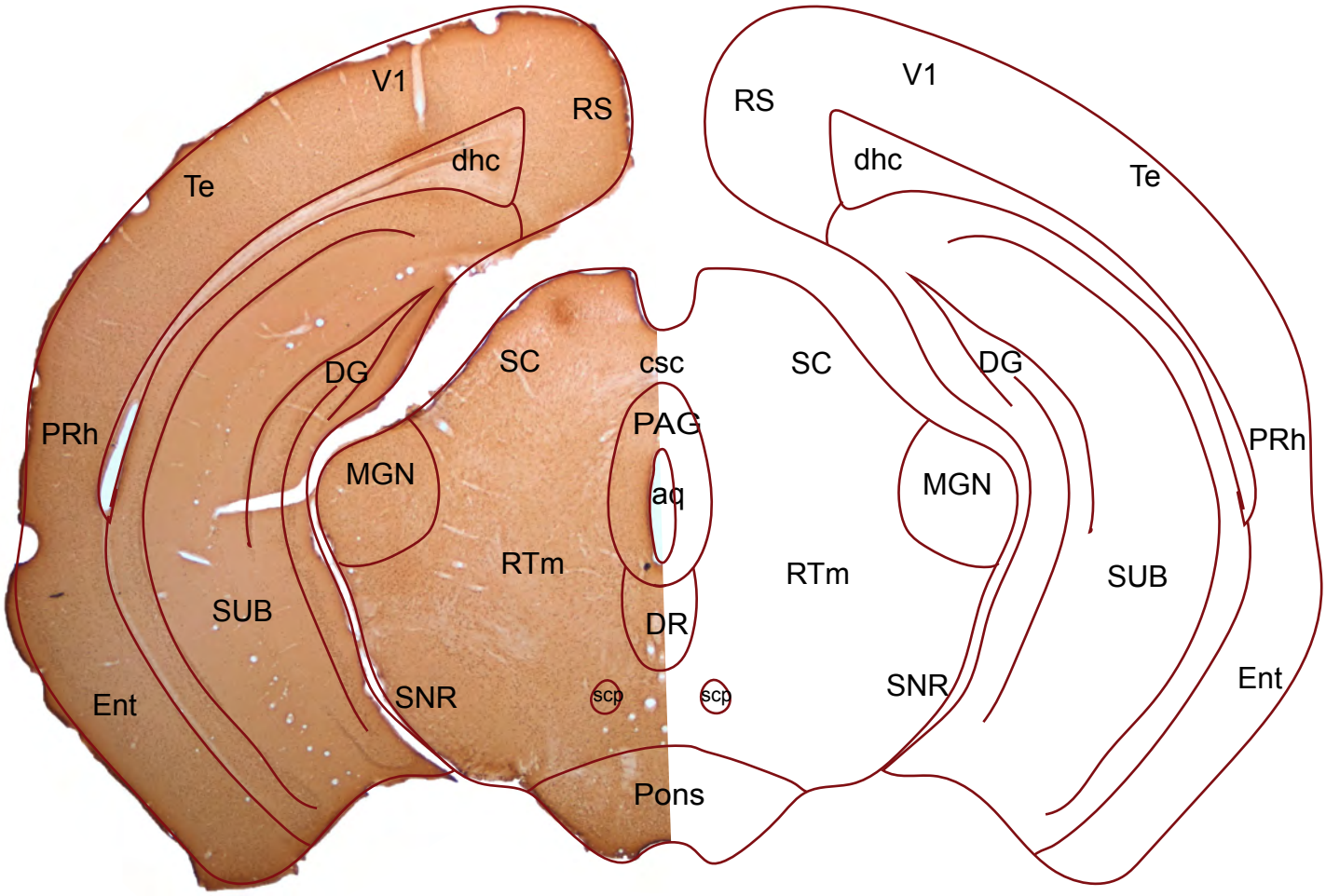

Set 33: Nissl oc +3200µm

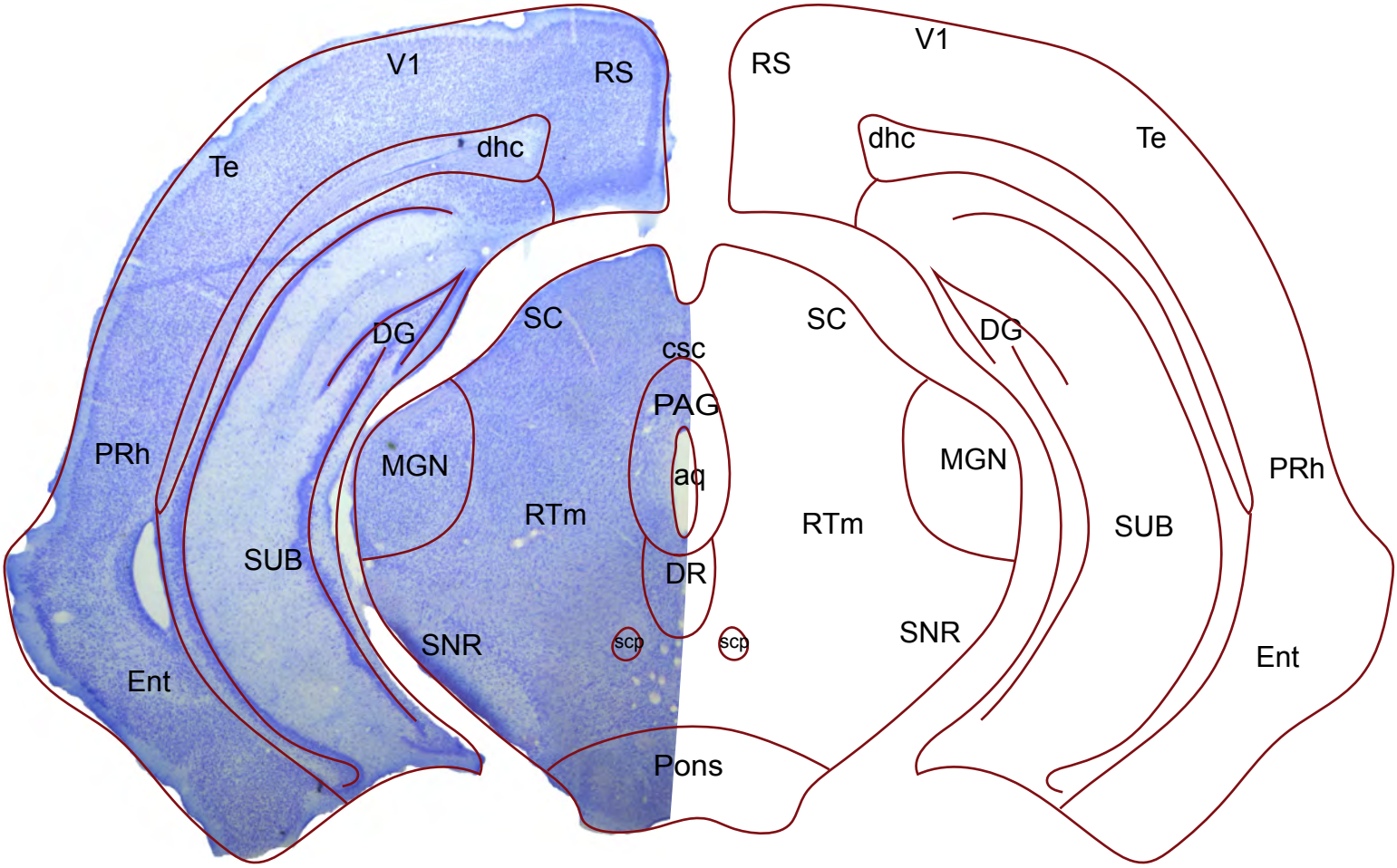

Set 33: OXT oc +3250µm

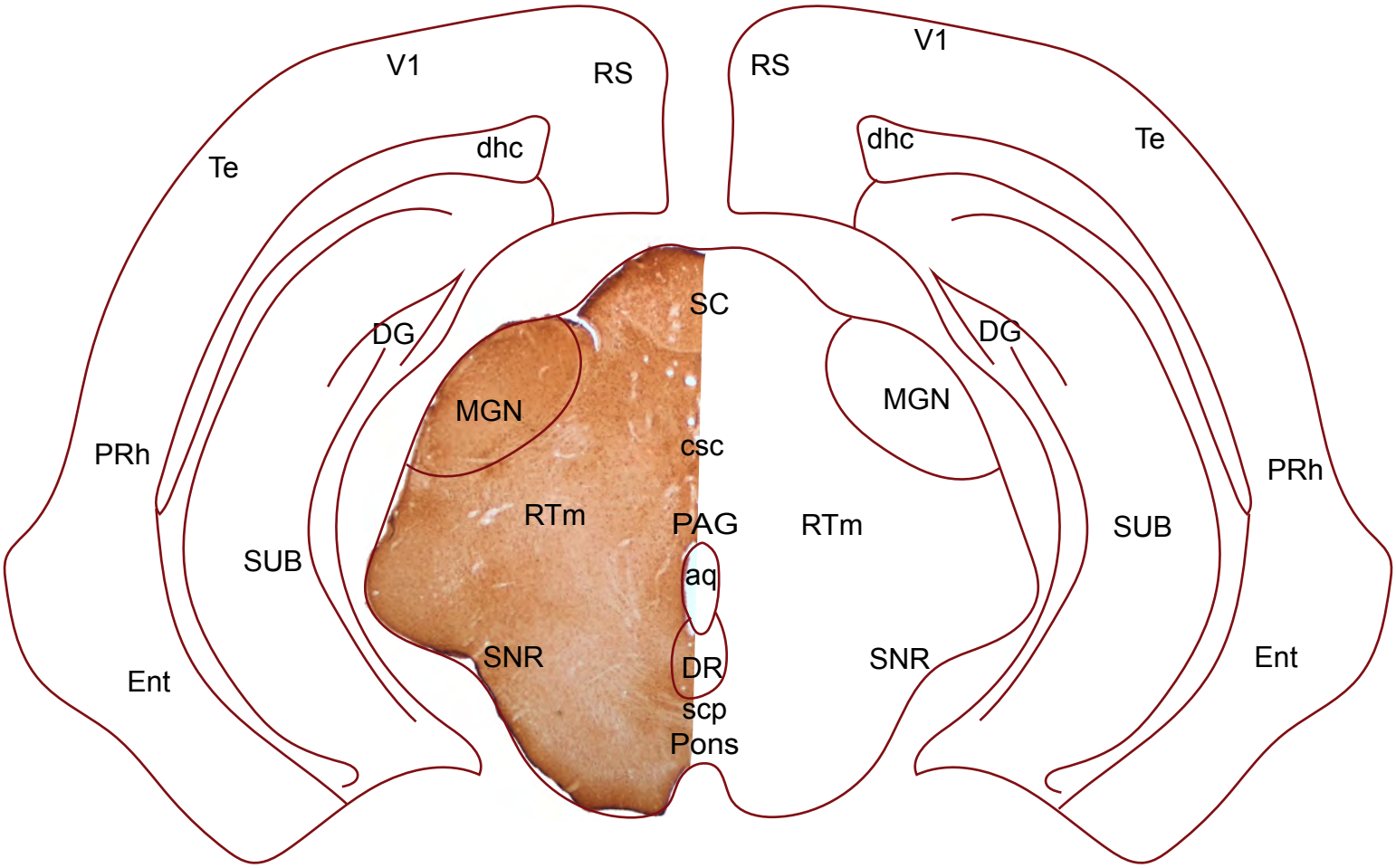

Set 33: Myelin oc +3300µm

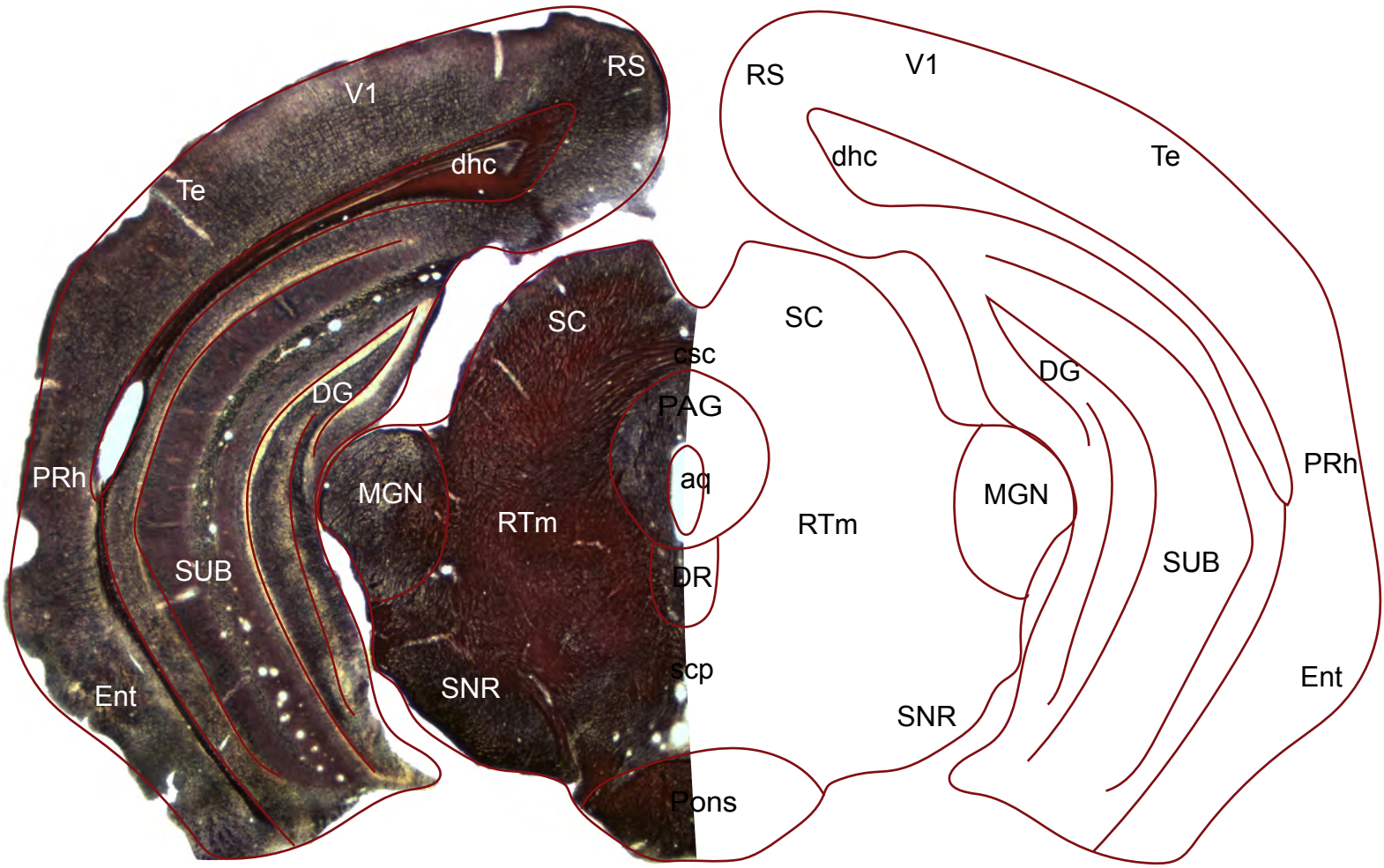

APPENDIX B:
Tables Related to Chapter 3

Supplemental Table 1

Staining density index scores for all OXT cell-body containing regions of each male and female subject. SDI was calculated as: (3N3+2N2+N1)/3NT, where N3, N2, and N1 are the number of sections with a +++, ++, or + score, and NT is the number of sections the region spans, including the sections with no cells. The values in this table were used for the analysis in Supplemental Figure 2(a). NA's indicate the region was not examined in the subsample of sections in that animal.

Abbreviation	Full Region Name	Male 1 SDI	Male 2 SDI	Male 3 SDI	Female 1 SDI	Female 2 SDI	Female 3 SDI
AHN	anterior hypothalamic nucleus	0.22	0.00	0.17	0.22	0.00	0.22
ARC	arcuate nucleus	0.17	0.00	0.00	NA	NA	0.00
AVPV	anteroventral periventricular nucleus	0.22	1.00	0.67	0.33	1.00	0.17
BNST	bed nucleus of the stria terminalis	0.28	0.33	0.00	0.33	0.83	0.25
DM	dorsal medial nucleus of the hypothalamus	0.08	0.33	NA	NA	0.00	0.33
LH	lateral hypothalamus	0.50	0.53	0.22	0.44	0.56	0.33
LPOA	lateral preoptic area	0.17	0.00	0.00	0.00	0.17	0.17
MEPO	median preoptic area	0.17	0.33	0.33	0.33	0.33	0.17
MPOA	medial preoptic area	0.44	0.33	0.00	0.67	0.33	0.33
PVH	paraventricular hypothalamic nucleus	1.00	1.00	1.00	0.89	1.00	1.00
PVi	periventricular hypothalamic nucleus-intermediate	0.11	0.17	0.17	0.33	0.00	0.08

PVpo	periventricular hypothalamic nucleus-preoptic part	0.67	0.33	0.00	0.33	0.33	0.56
RCH	retrochiasmatic nucleus	0.29	0.17	NA	0.67	1.00	0.33
SCH	suprachiasmatic nucleus	0.11	0.00	0.00	0.00	0.00	0.00
SON	supraoptic nucleus	0.97	1.00	1.00	1.00	1.00	1.00
Tu	(tuberal nucleus)	0.56	0.67	0.50	NA	0.67	0.78
VLPO	ventrolateral preoptic area	0.06	0.67	0.00	0.00	0.67	0.00
VMPO	ventromedial preoptic area	0.20	1.00	0.33	0.00	0.33	0.67

Supplemental Table 2

Staining Density Index scores for OXT axonal density in regions of each male and female subject. SDI was calculated as: (3N3+2N2+N1)/3NT, where N3, N2, and N1 are the number of sections with a +++, ++, or + score, and NT is the number of sections the region spans, including the sections with no cells. The values in this table were used for the analysis in Supplemental Figure 2(b). NA's indicate the region was not examined in the subsample of sections in that animal.

Abbreviation	Full Region Name	Male 1 SDI	Male 2 SDI	Male 3 SDI	Female 1 SDI	Female 2 SDI	Female 3 SDI
ac	anterior commissure	0.33	0.44	0.17	0.00	0.67	0.33
AcbC	nucleus accumbens core	0.48	0.78	1.00	0.00	0.50	0.67
AcbSh	nucleus accumbens shell	0.54	0.89	1.00	0.33	1.00	0.67
aco	anterior commissure, olfactory limb	0.19	0.08	0.00	0.00	0.00	0.06
act	anterior commissure, temporal limb	0.22	NA	NA	NA	NA	NA
AD	anterodorsal nucleus of the thalamus	0.00	0.00	0.00	0.00	0.00	0.00
AHN	anterior hypothalamic nucleus	0.78	0.89	0.67	1.00	1.00	1.00
AI	agranular insular area	0.06	0.00	0.07	0.00	0.00	0.00
AM	anteromedial nucleus of the thalamus	0.07	0.00	0.00	0.00	0.33	0.00
Amy	amygdala	0.23	0.50	0.44	0.22	0.78	0.38
AOB	accessory olfactory bulb	0.00	NA	NA	NA	NA	NA
AON	anterior olfactory nucleus	0.27	0.89	0.67	0.11	0.33	0.08
aq	cerebral aqueduct	0.67	0.00	0.00	0.00	0.00	NA
ARC	arcuate nucleus	0.67	1.00	1.00	NA	NA	1.00
Au	auditory cortex	0.02	0.00	0.11	NA	0.00	0.07
AV	anteroventral nucleus of the thalamus	0.11	0.00	0.00	0.00	0.00	0.00
AVPV	anteroventral periventricular nucleus	0.72	1.00	1.00	0.67	1.00	1.00
BNST	bed nucleus of the stria terminalis	0.61	1.00	1.00	0.67	1.00	0.83

bsc	brachium of superior colliculus	0.00	0.00	0.00	0.00	0.00	0.00
CA1	hippocampal area 1	0.02	0.00	0.00	0.00	0.00	0.00
CA2	hippocampal area 2	0.00	0.00	0.00	NA	0.00	0.00
CA3	hippocampal area 3	0.10	0.00	0.00	0.00	0.00	0.00
cc	corpus callosum	0.04	0.00	0.00	NA	0.00	0.03
cg	cingulum bundle	0.00	0.00	NA	0.00	0.00	0.00
Cg	cingulate cortex	0.02	0.08	0.00	0.00	0.00	0.00
Cga	cingulate area-anterior	0.07	0.00	0.00	0.00	NA	0.00
CLA	claustrum	0.08	0.00	0.00	0.00	0.00	0.00
CM	central medial thalamic nucleus	0.35	0.40	0.33	0.22	1.00	0.60
Co	cortical amygdaloid nucleus	0.08	0.00	NA	NA	0.00	0.00
cpd	cerebral peduncle	0.13	0.33	0.00	0.00	0.50	0.22
CPu	caudate putamen	0.20	0.11	0.17	0.06	0.11	0.06
csc	superior colliculus commmisure	0.61	0.33	0.67	0.00	1.00	0.33
DB	diagonal band of Broca	0.29	0.44	0.33	0.17	1.00	0.50
DG	dentate gyrus	0.02	0.00	0.00	0.00	0.00	0.00
dhc	dorsal hippocampal commissure	0.00	0.00	0.00	NA	0.00	0.00
DLGN	dorsal lateral geniculate nucleus	0.00	0.00	0.00	NA	NA	0.00
DM	dorsal medial nucleus of the hypothalamus	0.75	1.00	NA	NA	1.00	1.00
DR	dorsal raphe	0.50	0.67	NA	NA	NA	NA
ec	external capsule	0.00	0.00	NA	NA	NA	0.00
emt	external medullary lamina of the thalamus	0.00	0.00	0.00	NA	0.00	0.00
Ent	entorhinal cortex	0.00	0.00	0.00	0.00	0.00	0.00
EPd	endopiriform dorsal part	0.15	0.20	0.17	NA	0.00	0.00
f	fornix	0.39	0.92	0.83	0.67	0.80	0.80

fa	corpus callosum-anterior forceps	0.33	0.00	0.00	0.00	NA	0.67
fi	fimbria	0.04	0.00	0.00	0.00	0.00	0.17
fr	fasciculus retroflex	0.13	0.67	0.00	NA	0.67	0.11
FrA	frontal association cortex	0.10	0.00	NA	NA	0.33	NA
GL	glomerular layer of the olfactory bulb	0.00	NA	NA	NA	NA	NA
GP	globus pallidus	0.29	0.22	0.67	0.22	0.67	0.20
GrO	granular cell layer olfactory limb	0.17	NA	NA	0.00	0.17	0.00
Hb	habenula	0.15	0.00	0.33	0.00	0.00	0.00
IAM	interanteromedial nucleus of the thalamus	0.00	NA	NA	NA	NA	NA
ic	internal capsule	0.44	0.67	0.33	0.78	0.92	0.58
IL	infralimbic cortex	0.24	0.33	0.00	0.00	0.50	0.17
IMD	intermediodorsal nucleus of the thalamus	0.33	0.67	0.33	0.00	NA	0.67
IP	interpeduncular nucleus	0.33	1.00	NA	NA	1.00	1.00
islm	major island of Calleja	0.33	NA	NA	NA	NA	NA
LD	lateral dorsal thalamic nucleus	0.00	0.00	0.00	0.00	0.00	0.00
LGN	lateral geniculate nucleus	0.00	0.00	NA	NA	0.00	0.00
LH	lateral hypothalamic nucleus	0.98	1.00	1.00	1.00	1.00	1.00
LHb	lateral habenular nucleus	0.17	NA	NA	NA	NA	NA
lot	lateral olfactory tract	0.00	0.00	0.00	0.00	0.00	0.00
LP	lateral posterior thalamic nucleus	0.00	0.00	0.00	NA	NA	0.00
LPOA	lateral preoptic area	0.61	0.67	0.67	0.00	1.00	1.00
LS	lateral septum	0.37	0.83	0.33	0.17	0.67	0.67

LSd	lateral septum - dorsal	0.72	1.00	0.67	0.00	1.00	0.33
LSi	lateral septum - intermediate	0.67	NA	NA	NA	Na	0.67
LSv	lateral septum - ventral	0.56	1.00	0.33	0.33	1.00	0.67
LV	lateral ventricle	0.35	0.00	0.00	0.00	0.00	0.00
MC	motor cortex	0.01	0.00	0.00	0.00	0.00	0.00
MD	mediodorsal nucleus of the thalamus	0.03	0.00	0.00	0.00	0.00	0.00
ME	median eminence	1.00	1.00	NA	NA	NA	1.00
MEPO	median preoptic nucleus	0.83	1.00	1.00	1.00	1.00	0.83
MGN	medial geniculate nucleus	0.21	0.11	0.00	0.00	0.17	0.00
MHb	medial habenular nucleus	0.17	NA	NA	NA	NA	NA
ml	medial lemniscus	0.04	0.00	0.00	NA	0.00	0.00
MM	mammillary nucleus	0.78	1.00	1.00	NA	1.00	0.67
MPOA	medial preoptic area	0.69	1.00	1.00	NA	1.00	1.00
MS	medial septal nucleus	0.58	0.67	0.33	NA	1.00	0.83
mtt	mammillothalamic tract	0.14	0.22	0.00	NA	0.33	0.07
och	optic chiasm	0.19	NA	NA	NA	0.00	0.00
on	optic nerve	0.67	0.33	NA	NA	0.00	0.00
opt	optic tract	0.35	0.28	0.44	0.22	0.44	0.33
ORB	orbital area	0.30	0.33	0.00	0.00	0.08	0.13
OT	olfactory tubercle	0.27	0.47	0.33	0.11	0.78	0.40
PAG	periaqueductal gray	0.92	1.00	1.00	0.67	1.00	1.00
PF	parafascicular thalamic nucelus	0.17	0.00	0.00	NA	NA	0.00
PH	posterior hypothalamic nucleus	0.67	1.00	1.00	NA	1.00	1.00
Pir	piriform cortex	0.14	0.00	0.00	0.00	0.00	0.04
Po	posterior complex of the thalamus	0.00	0.00	0.00	0.00	0.00	0.00

Pons	Pons	0.58	1.00	1.00	1.00	1.00	NA
PRh	perirhinal cortex	0.02	0.00	0.00	0.00	0.00	0.00
PrL	prelimbic cortex	0.20	0.22	0.33	0.00	0.11	0.00
PT	parietal cortex	0.07	0.00	0.00	NA	NA	0.00
PTN	pretectal nucleus	0.25	0.00	NA	NA	0.67	0.00
PVH	paraventricular hypothalamic nucleus	0.95	1.00	1.00	1.00	1.00	1.00
PVi	periventricular hypothalamic nucleus - intermediate	0.64	0.92	0.83	1.00	0.33	0.92
PVpo	periventricular hypothalamic preoptic part	0.96	1.00	1.00	1.00	1.00	1.00
PVT	paraventricular nucleus of the thalamus	0.67	1.00	0.89	0.44	1.00	0.95
RCH	retrochiasmatic area	0.76	0.83	NA	0.67	1.00	1.00
RE	nucleus of reuniens	0.44	0.93	0.50	0.22	1.00	0.40
RH	rhomboid nucleus	0.17	0.33	NA	0.00	1.00	0.00
RS	retrosplineal area	0.00	0.00	0.00	0.00	0.00	0.00
rt	reticular nucleus of the thalamus	0.13	0.00	0.00	0.22	0.00	0.07
RTm	reticular nucleus - midbrain	0.50	0.67	1.00	0.00	0.33	0.33
Sc	somatosensory cortex	0.02	0.00	0.00	0.00	0.00	0.06
SC	superior colliculus	0.13	0.00	0.00	0.00	0.33	0.00
SCH	suprachiasmatic nucleus	0.33	0.67	0.67	0.50	1.00	0.67
scp	superior cerebelar peduncles	0.33	0.00	NA	NA	NA	NA
sm	stria medularis	0.33	0.50	1.00	0.00	0.33	0.22
SN	substantia nigra	0.75	1.00	NA	NA	1.00	1.00
SNR	substantia nigra reticular part	0.67	1.00	0.33	0.33	1.00	NA
SON	supraoptic nucleus	0.85	1.00	1.00	1.00	1.00	1.00

st	stria terminalis	0.22	0.00	NA	NA	NA	0.00
SUB	subiculum	0.00	0.00	0.00	NA	NA	0.00
Te	temporal cortex	0.00	0.00	NA	0.00	0.00	NA
TT	taenia tecta	0.56	0.58	0.83	0.11	0.83	0.42
Tu	tuberal nucleus	1.00	1.00	1.00	NA	1.00	1.00
V	visual cortical area 1	0.00	0.00	0.00	NA	NA	0.00
V1	visual 1 cortex	0.00	0.00	0.00	0.00	0.00	0.00
V2	visual 2 cortex	0.00	0.00	NA	NA	0.00	NA
V3	third ventricle	0.20	0.00	0.00	0.00	0.00	0.00
vhc	ventral hippocampal commissure	0.08	NA	NA	NA	NA	0.00
VLPO	ventrolateral preoptic area	0.44	0.67	0.67	0.33	1.00	0.67
VM	ventral medial thalamic nucleus	0.04	0.00	0.00	NA	0.00	0.00
VMH	ventromeidal hypothalamus	0.29	0.67	0.67	NA	1.00	0.83
VMPO	ventromedial preoptic area	0.93	1.00	1.00	0.33	1.00	1.00
VP	ventral pallidum	0.00	0.00	0.00	0.00	0.00	0.00
VTA	ventral tegmental area	0.61	0.78	NA	0.00	0.83	1.00
vtd	ventral tegmental decussation	0.17	0.00	NA	NA	1.00	NA
ZI	zona incerta	0.25	0.20	0.00	NA	0.17	0.20

Supplemental Table 3

Relationship between OXT fiber density and *Oxtr* transcript score from Inoue et al., 2022. OXT fiber SDI's are pooled SDI's across all male and female brains to account for the difference in number of sections analyzed. NA's indicate regions that have an OXT SDI score, but no corresponding *Oxtr* score.

Abbreviation	Full Region Name	Classified Region	OXT Fibers SDI	Oxtr transcript score
TT	Tenia Tecta	Cerebral cortex	0.54	4.00
AcbSh	Nucleus accumbens-shell	Striatum/Pallidum	0.67	4.00
AcbC	Nucleus accumbens-core	Striatum/Pallidum	0.53	4.00
LSd	Lateral septum-dorsal	Striatum/Pallidum	0.67	3.00
BNST	Bed nucleus of the stria terminalis	Striatum/Pallidum	0.73	3.17
MPOA	Medial preoptic area	Hypothalamus	0.81	3.00
VMH	Ventromedial hypothalamic nucleus	Hypothalamus	0.51	4.00
ARC	Arcuate hypothalamic nucleus	Hypothalamus	0.82	3.00
PH	Posterior hypothalamic nucleus	Hypothalamus	0.79	3.00
MM	Mammillary nucleus	Hypothalamus	0.83	3.00
PVT	Paraventricular nucleus of the thalamus	Thalamus	0.78	4.00
RE	Nucleus of reuniens	Thalamus	0.53	3.50
GrO	Granule cell layer olfactory limb	Cerebral cortex	0.14	4.00
AON	Anterior olfactory nucleus	Cerebral cortex	0.32	3.00
FrA	Frontal association cortex	Cerebral cortex	0.11	3.00
Cga	Cingulate area anterior	Cerebral cortex	0.03	3.33
Cg	Cingulate cortex	Cerebral cortex	0.05	3.00
RS	Retrosplineal area	Cerebral cortex	0.00	4.00
MC	Motor cortex	Cerebral cortex	0.01	3.00
AI	Agranular insular cortex	Cerebral cortex	0.03	3.00
PT	Parietal cortex	Cerebral cortex	0.03	2.67
PrH	Perirhinal cortex	Cerebral cortex	0.01	3.00
V2	Visual cortex	Cerebral cortex	0.00	3.00
Te	Temportal cortex	Cerebral cortex	0.00	3.00

OT	Olfactory tubercle	Striatum/Pallidum	0.41	4.00
CA2	Hippocampal area 2	Cerebral cortex	0.00	4.00
islm	Major island of Calleja	Striatum/Pallidum	0.33	4.00
CPu	Caudate putamen	Striatum/Pallidum	0.15	3.50
Amy	Amygdala	Cerebral cortex	0.14	3.00
Co	Cortical amygdaloid nucleus	Cerebral cortex	0.04	3.50
CM	Central medial thalamic nucleus	Thalamus	0.42	4.00
VM	Ventral medial thalamic nucleus	Thalamus	0.02	3.00
RH	Rhomboid nucleus	Thalamus	0.24	4.00
LSi	Lateral septum-intermediate	Striatum/Pallidum	0.67	2.00
LSv	Lateral septum-ventral	Striatum/Pallidum	0.64	2.00
AHN	Anterior hypothalamic nucleus	Hypothalamus	0.87	2.50
SCH	Suprachiasmatic nucleus	Hypothalamus	0.51	2.00
VLPO	Ventrolateral preoptic nucleus	Hypothalamus	0.55	1.00
SON	Supraoptic nucleus	Hypothalamus	0.93	1.00
PVH	Paraventricular hypothalamic nucleus	Hypothalamus	0.98	1.00
RCH	Retrochiasmatic area	Hypothalamus	0.81	1.00
ME	Median eminence	Hypothalamus	1.00	1.00
DM	Dorsomedial hypothalamus	Hypothalamus	0.96	1.33
LH	Lateral hypothalamus	Hypothalamus	0.99	2.00
VTA	Ventral tegmental area	Midbrain	0.67	1.00
SN	Substantia nigra	Midbrain	0.88	1.00
PAG	Periaqueductal gray	Midbrain	0.94	1.25
IP	Interpeduncular nucleus	Midbrain	0.67	1.00
DR	Dorsal raphe	Midbrain	0.56	2.00
RTm	Reticular nucleus of the midbrain	Midbrain	0.50	2.00
ORB	Orbital area	Cerebral cortex	0.21	1.00
Sc	Somatosensory cortex	Cerebral cortex	0.02	2.00
Pir	Piriform cortex	Cerebral cortex	0.07	2.50

Au	Auditory cortex	Cerebral cortex	0.03	2.00
Ent	Entorhinal cortex	Cerebral cortex	0.00	1.40
V1	Visual cortex	Cerebral cortex	0.00	2.00
EPd	Endopiriform cortex- dorsal	Cerebral cortex	0.11	2.00
DG	Dentate Gyrus	Cerebral cortex	0.01	2.00
CA1	Hippocampal area 1	Cerebral cortex	0.01	1.50
CA3	Hippocampal area 3	Cerebral cortex	0.05	1.00
SUB	Subiculum	Cerebral cortex	0.00	2.00
CLA	Claustrum	Cerebral cortex	0.04	2.00
DB	Diagonal band of Broca	Striatum/Pallidum	0.41	1.00
GP	Globus pallidus	Striatum/Pallidum	0.31	1.50
rt	Reticular nucleus of the thalamus	Thalamus	0.09	1.00
AM	Anteromedial nucleus of the thalamus	Thalamus	0.05	1.00
AD	Anterodorsal nucleus of the thalamus	Thalamus	0.00	1.00
ZI	Zona incerta	Hypothalamus	0.21	1.50
IAM	Interanteromedial nucleus of the thalamus	Thalamus	0.00	2.00
MHb	Medial habenular nucleus	Thalamus	0.17	2.00
LHb	Lateral habenular nucleus	Thalamus	0.17	1.00
LP	Lateral posterior thalamic nucleus	Thalamus	0.00	1.00
PTN	Pretectal nucleus	Midbrain	0.21	1.00
Regions with no *Oxtr* score				
PVpo	Periventricular hypothalamic preoptic part	Hypothalamus	0.98	NA
MEPO	Median preoptic nucleus	Hypothalamus	0.88	NA
VMPO	Ventromedial preoptic area	Hypothalamus	0.90	NA
AVPV	anteroventral periventricular nucleus	Hypothalamus	0.83	NA
PVi	periventricular hypothalamic nucleus - intermediate	Hypothalamus	0.74	NA
LPOA	lateral preoptic area	Hypothalamus	0.70	NA
Tu	tuberal nucleus	Hypothalamus	0.67	NA

f	fornix	Fiber tracts	0.60	NA
ic	internal capsule	Fiber tracts	0.55	NA
MS	medial septal nucleus	Striaum/Pallidum	0.63	NA
SNR	Substantia nigra reticular part	Midbrain	0.67	NA
csc	superior colliculus commmisure	Fiber tracts	0.53	NA
LS	lateral septum	Striatum/Pallidum	0.46	NA
opt	optic tract	Fiber tracts	0.34	NA
on	optic nerve	Fiber tracts	0.25	NA
vtd	ventral tegmental decussation	Fiber tracts	0.33	NA
ac	anterior commissure	Fiber tracts	0.31	NA
act	anterior commissure, temporal limb	Fiber tracts	0.22	NA
fr	fasciculus retroflex	Fiber tracts	0.25	NA
sm	stria medularis	Fiber tracts	0.32	NA
IMD	intermediodorsal nucleus of the thalamus	Thalamus	0.43	NA
LV	lateral ventricle	Ventricle	0.18	NA
3V	third ventricle	Ventricle	0.10	NA
Amy	amygdala	Cerebral cortex	0.33	NA
fa	corpus callosum- anterior forceps	Fiber tracts	0.23	NA
och	optic chiasm	Fiber tracts	0.13	NA
cpd	cerebral peduncle	Fiber tracts	0.21	NA
IL	infralimbic cortex	Cerebral cortex	0.24	NA
aco	anterior commissure, olfactory limb	Fiber tracts	0.11	NA
mtt	mammillothalamic tract	Fiber tracts	0.15	NA
SC	superior colliculus	Midbrain	0.09	NA
st	stria terminalis	Fiber tracts	0.15	NA
fi	fimbria	Fiber tracts	0.05	NA
ml	medial lemniscus	Fiber tracts	0.02	NA
LD	lateral dorsal thalamic nucleus	Thalamus	0.05	NA
Po	posterior complex of the thalamus	Thalamus	0.00	NA

aq	cerebral aqueduct	Ventricle	0.37	NA
scp	superior cerebelar peduncles	Fiber tracts	0.22	NA
MGN	medial geniculate nucleus	Thalamus	0.15	NA
PrL	prelimbic cortex	Cerebral cortex	0.14	NA
Hb	habenula	Thalamus	0.11	NA
PF	parafascicular thalamic nucelus	Thalamus	0.08	NA
vhc	ventral hippocampal commissure	Fiber tracts	0.07	NA
AV	anteroventral nucleus of the thalamus	Thalamus	0.04	NA
cc	corpus callosum	Fiber tracts	0.02	NA
AI	agranular insular area	Cerebral cortex	0.00	NA
AOB	accessory olfactory bulb	Cerebral cortex	0.00	NA
bsc	brachium of superior colliculus	Fiber tracts	0.00	NA
cg	cingulum bundle	Fiber tracts	0.00	NA
dhc	dorsal hippocampal commissure	Fiber tracts	0.00	NA
DLGN	dorsal lateral geniculate nucleus	Thalamus	0.00	NA
ec	external capsule	Fiber tracts	0.00	NA
emt	external medullary lamina of the thalamus	Fiber tracts	0.00	NA
GL	glomerular layer of the olfactory bulb	Cerebral cortex	0.00	NA
LD	lateral dorsal thalamic nucleus	Thalamus	0.00	NA
LGN	lateral geniculate nucleus	Thalamus	0.00	NA
lot	lateral olfactory tract	Fiber tracts	0.00	NA
MD	mediodorsal nucleus of the thalamus	Thalamus	0.01	NA

Appendix C:

Dopaminergic and Oxytocinergic Cells in the Nucleus Accumbens and Cingulate Cortex of the Prairie Vole

Introduction:

The dopaminergic and oxytocinergic systems of the prairie vole interact to modulate behavioral output (Liu and Wang 2003; Lee and Beery 2021). The nucleus accumbens shell (AcbSh) is a region intimately involved in driving maternal behavior (Champagne 2004) and alloparental behavior in virgin female prairie voles (Olazábal and Young 2006). Dopamine and oxytocin interact within the nucleus accumbens to drive motivated behaviors, but which medium spiny neurons (MSNs) oxytocin is primarily acting through to drive differences in behavior within the vole is unknown. There are 2 types of MSNs in the Acb, Type 1 or dopamine 1 receptor-expressing (D1r), and Type 2 or dopamine 2 receptor-expressing (D2r), these cells project through direct and indirect pathways, respectively. The output of the Acb and which cells are being modulated by OXT binding to OXTR, thus, would result in the modulation of different circuitries. This may potentially lead to individual differences in behavior. Further, the cingulate cortex is a region involved in the top-down control of the amygdala and will mediate aggressive behaviors (Van Heukelum et al. 2021). Here we examined the colocalization of the transcripts for dopamine and oxytocin receptors (*Drd1*, *Drd2*, and *Oxtr*) in the AcbSh, and Cg, and the Acb core (AcbC) as a control region.

Methods:

Using virgin adult (PND60-90) female prairie voles, we examined the colocalization of *Drd1*, *Drd2*, and *Oxtr* transcripts using RNAScope *in situ* hybridization.

Tissue preparation for RNAScope:

12 female prairie voles were anesthetized with an overdose of sodium pentobarbital. The brains were immediately extracted on dry ice and stored at -80°C until sectioning. For cryostat sectioning, the brains were acclimated at -20°C for at least 2 hours, sliced at 15μm thickness, and mounted onto Superfrost plus slides (Fisherbrand; Pittsburg, Pennsylvania), and stored in slide boxes at -80°C until fluorescent RNAScope staining.

Fluorescent RNAScope for visualizing Oxtr transcripts:

Slides containing 2 coronal sections of the forebrain, including nucleus accumbens (Acb) and the anterior cingulate cortex (Cg), and directly posterior to the genu of the corpus callosum were selected for RNAScope in situ hybridization for the mapping of *Drd1*, *Drd2*, and *Oxtr* transcripts. An RNAScope Multiplex Fluorescent Reagent Kit version 2 (Advanced Cell Diagnostics; Newark, California) was used for fluorescent staining of *Drd1*, *Drd2*, and *Oxtr* transcripts, according to the manufacturer's instructions. Briefly, slides were fixed in 4% paraformaldehyde in 4°C for 1 hour, and then dehydrated through a series of ethanol solutions of 50%, 70%, and two 100%, 5 minutes each. The slides were then stored for up to one week at -20°C. On day 2 of staining, the slides were blocked in hydrogen peroxide, incubated in protease reagents, the *Drd1* probe (CAT. No. 58861), *Drd2* probe (CAT. No. 534471), *Oxtr* probe (CAT. No. 500721), and three amplification reagents. The hybridized probes were visualized using, OPAL 520 (*Drd1*), OPAL 570 (*Drd2*), OPAL 690 (*Oxtr*) and counterstained using DAPI. Finally, slides were coverslipped with ProLong Gold Antifade Mountant (ThermoFisher Scientific; Waltham, Massachusetts). A negative, bacterial DapB (Cat. No. 320871), and a

positive, PPIB (Cat. No. 533491) control probes were run in parallel. For the negative control, there was no specific labeling, and for the positive, there were > 15 puncta per cell.

Imaging and Analysis of Drd1, Drd2, and Oxtr:

For RNAScope imaging of *Oxtr* transcripts, a STELLARIS 5 (Leica Microsystems) confocal microscope with a 10x objective was used for whole section fluorescence imaging, and a 40x objective for high-magnification z-stack imaging of sections containing the (2 images per hemisphere) Cg (**Fig 1A-B**) and Acb (a tiled region of 4 images) (**Fig 1C-D**). Identical settings of the gain and intensity were used for each brain and image. The publicly available software QuPath was used to calculate the percentage of cells and *Oxtr* puncta in the nucleus accumbens shell (AcbSh), core (AcbC), and cingulate cortex (Cg). The "Cell Detection" tool was used to outline all DAPI nuclei and further expanded by 5 µm to account for cytoplasm. All brains were analyzed using the same threshold parameters, and the subcellular detection tool was further used to automatically count the *Oxtr* puncta.

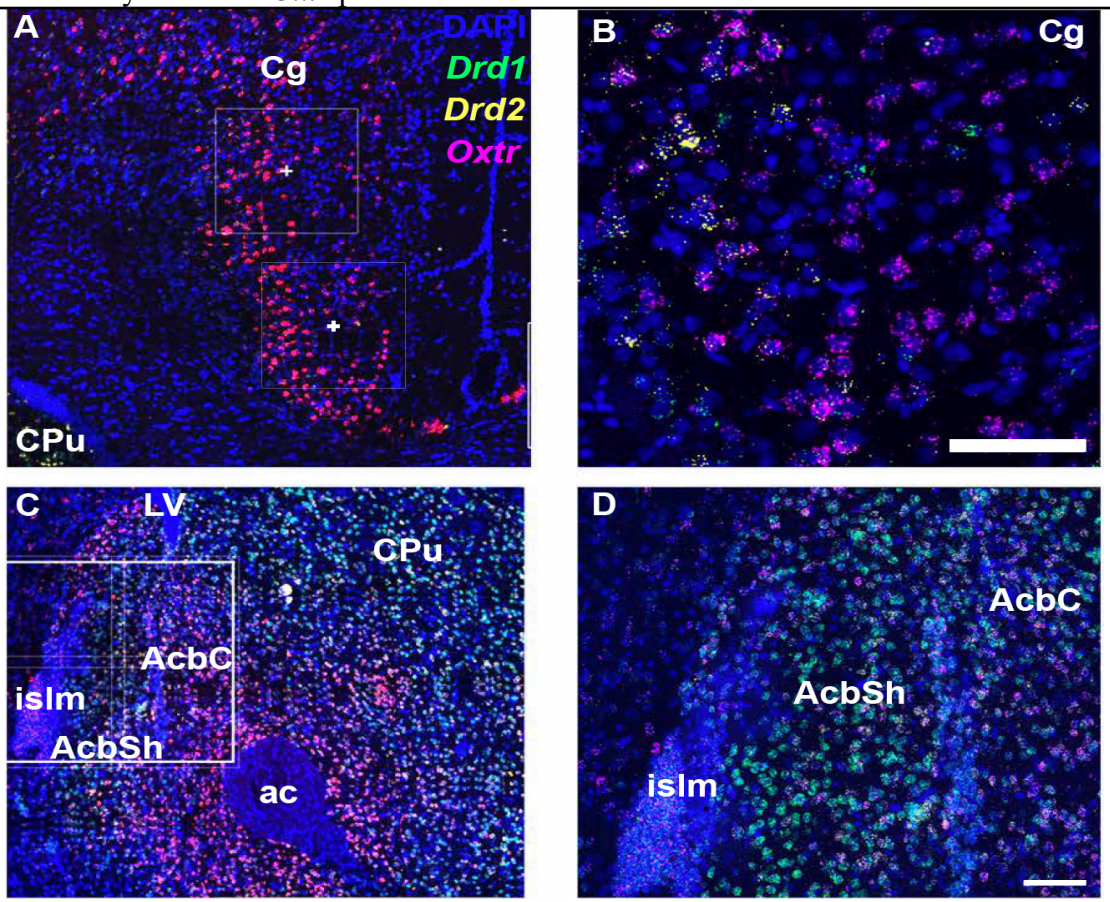

Figure 1: RNAScope in situ hybridization within the cingulate cortex and nucleus accumbens of the prairie vole brain, displaying the regions that were analyzed using QuPath. **A-D)** DAPI = blue, *Drd1* = green, *Drd2* = yellow, *Oxtr* = magenta **A**) Low magnification image displaying a representative image of the cingulate cortex, boxed regions are indicative of where the high magnification images were taken. **B**) High magnification image of the Cg shown in A, scale bar = 100 µm. **C)** Low magnification image of the Acb, all Acb images were four tiled squares spanning from the most ventral portion of the ventricle through the medial accumbens shell and core. **D**) High magnification image of the tiled region shown in C, scale bar = 100 µm. AcbC = nucleus accumbens core, AcbSh = nucleus accumbens shell, ac = anterior commissure, Cg = cingulate cortex, cc = corpus callosum, CPu = caudate putamen, islm = major island of Calleja, LV = lateral ventricle

Results:

The RNAScope visualization of *Drd1, Drd2,* and *Oxtr* in 24 sections from 12 animals revealed that of all cells in the AcbSh, 44.29% ± 4.78 are *Drd1*+, for *Drd2* cells 22.38% ± 3.62 are *Drd2*+, and 19.65% ± 9.28 are *Oxtr*+ (**Fig 2A**), note: *Oxtr*-expressing cells include *Drd1*, *Drd2*, and *Oxtr*-only expressing cells. The average *Oxtr* transcripts per cell on the co-expressing *Drd1/Oxtr* cells are 3.31 ± 1.23, *Drd2/Oxtr* cells are 3.84 ± 1.28, and on the *Oxtr*-only expressing cells are 2.41 ± 1.18 (**Fig 2B**).

Within the AcbC, 34.39% ± 4.61 are *Drd1*+, while 27.9% ± 4.88 are *Drd2*+, and 24.37% ± 11.2 are *Oxtr*+ cells (**Fig2C)**. Average Oxtr transcripts per cell on *Drd1/Oxtr* cells are 3.65 ± 1.76, *Drd2/Oxtr* cells are 3.68 ± 1.85, and on the *Oxtr*-only expressing cells are 2.52 ± 1.59 (**Fig2D**).

Within the Cg, 10.5% ± 5.05 are *Drd1*+, while only 4.37% ± 4.38 are *Drd2*+, and 18.8% ± 6.85 are *Oxtr*+ cells (**Fig2E**). Average *Oxtr* transcripts per cell on *Drd1/Oxtr* cells are 10.7 ± 2.17, *Drd2/Oxtr* cells are 7.73 ± 2.64, and on the *Oxtr*-only expressing cells are 7.12 ± 1.78 (**Fig2F**).

Discussion:

These data illustrate in control animals the percent of *Drd1*, *Drd2*, and *Oxtr*-expressing cells in the Acb and Cg, and the average number of Oxtr transcripts on each corresponding cell type. To start, it is important to examine the baseline number of each of these cell types. in these regions. Because OXTR expression on one of the two cell types would differentially modulate the output of the Acb, the potential shift in the *Oxtr* transcript expression will be an interesting avenue to examine in future studies. This data can be further expanded upon and examined in the context of different behavioral paradigms. Particularly, *Oxtr* expression on *Drd1* or *Drd2* expressing cells in the AcbSh may be shifted in animals who display differences in alloparental behavior or parental care. While in the Cg *Oxtr* expression could be shifted towards one cell type or another to impact stress responsiveness or aggression.

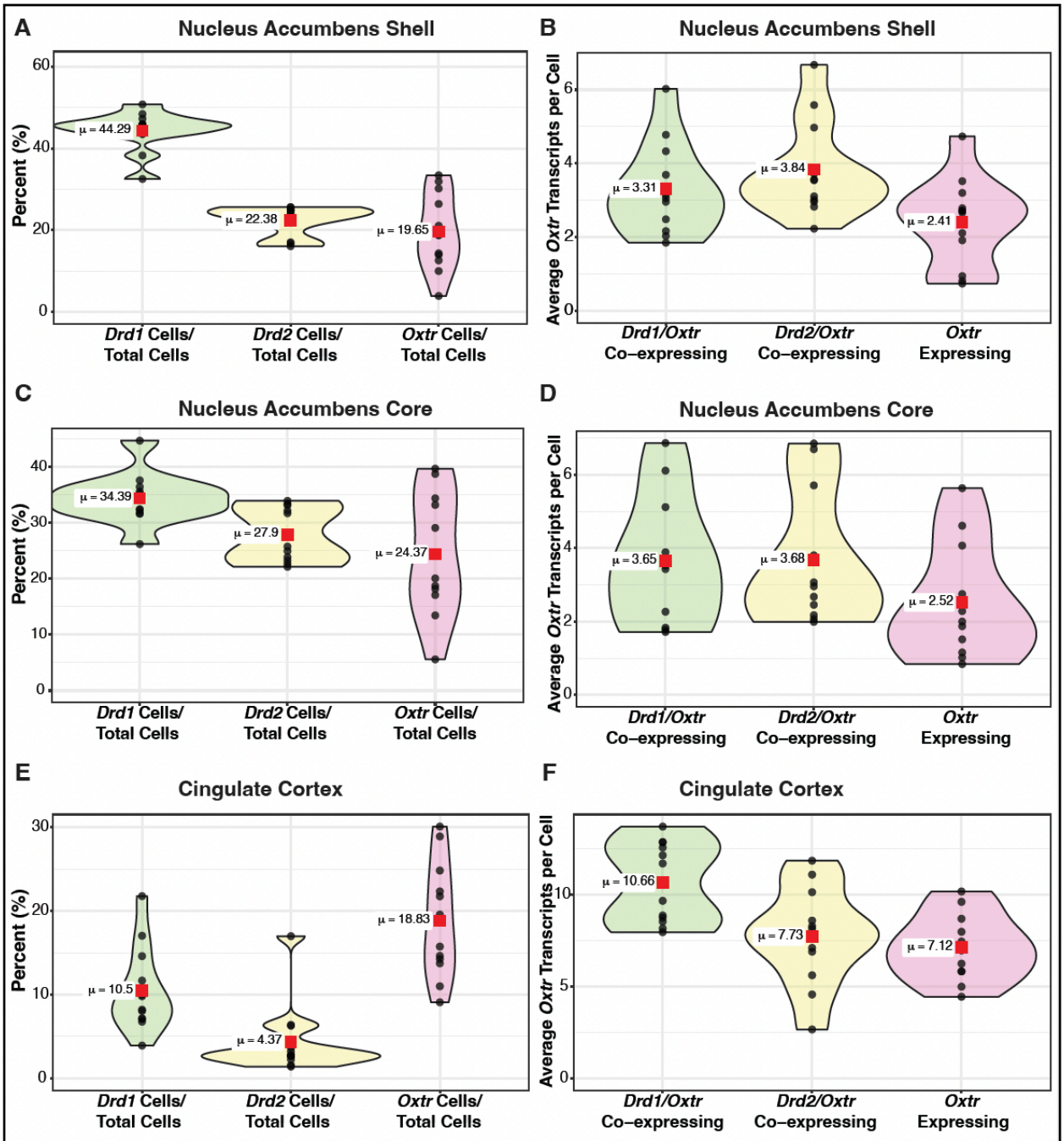

Figure 2: Graphical representations of the percent of cells in the Acb or Cg expressing *Drd1*, *Drd2*, *Oxtr*, and average number of *Oxtr* transcripts on *Oxtr* expressing cells. **A)** In the medial region of the AcbSh, 44.29% of cells are *Drd1* expressing, 22.38% are *Drd2* expressing, and 19.65% are *Oxtr* expressing. **B)** Of the 19.65% of *Oxtr* expressing cells, the co-expressing Drd1/Oxtr cells on average contain 3.31 transcripts, the co-expressing Drd2/Oxtr cells contain 3.84 transcripts, and the Oxtr-only expressing contain 2.41 transcripts. **C)** In the medial region of the AcbC, 34.39%, 27.9%, and 24.37% of cells are *Drd1*, *Drd2*, and *Oxtr*-expressing, respectively. **D)** Of the *Oxtr*-expressing cells in the core, each cell type averages 3.65, 3.68, and 2.52 *Oxtr* transcripts on *Drd1/Oxtr*, *Drd2/Oxtr*, and *Oxtr*-only expressing cells, respectively. **E)** In the Cg, 10.5%, 4.37%, and 18.83% of cells are *Drd1*, *Drd2*, and *Oxtr*-expressing, respectively. **F**) Of the *Oxtr*-expressing cells in the Cg, each cell type averages 10.66, 7.73, and 7.12 *Oxtr* transcripts on *Drd1/Oxtr, Drd2/Oxtr,* and *Oxtr*-only expressing cells, respectively.

References:

Champagne FA (2004) Variations in Nucleus Accumbens Dopamine Associated with Individual Differences in Maternal Behavior in the Rat. Journal of Neuroscience 24:4113–4123. https://doi.org/10.1523/JNEUROSCI.5322-03.2004

Lee NS, Beery AK (2021) The role of dopamine signaling in prairie vole peer relationships. Hormones and Behavior 127:104876. https://doi.org/10.1016/j.yhbeh.2020.104876

Liu Y, Wang ZX (2003) Nucleus accumbens oxytocin and dopamine interact to regulate pair bond formation in female prairie voles. Neuroscience 121:537–544. https://doi.org/10.1016/S0306-4522(03)00555-4

Olazábal DE, Young LJ (2006) Species and individual differences in juvenile female alloparental care are associated with oxytocin receptor density in the striatum and the lateral septum. Hormones and Behavior 49:681–687. https://doi.org/10.1016/j.yhbeh.2005.12.010

Van Heukelum S, Tulva K, Geers FE, et al (2021) A central role for anterior cingulate cortex in the control of pathological aggression. Current Biology 31:2321-2333.e5. https://doi.org/10.1016/j.cub.2021.03.062